GULF AND CARIBBEAN RESEARCH

Volume 27
2016
ISSN: 1528–0470

Published by

THE UNIVERSITY OF
SOUTHERN MISSISSIPPI

GULF COAST RESEARCH LABORATORY
Ocean Springs, Mississippi

Gulf and Caribbean Research

Volume 27 | Issue 1

2016

Introducing Ocean Reflections

Mark S. Peterson
University of Southern Mississippi, mark.peterson@usm.edu

Nancy J. Brown-Peterson
University of Southern Mississippi, nancy.brown-peterson@usm.edu

EDITORIAL

As with many other scientific journals, adjustments to content and format are inevitable. Thus, the editors of *Gulf and Caribbean Research (GCR)* are pleased to announce that starting in 2016 with Volume 27, we are adding a new section entitled 'Ocean Reflections.' The Editorial Advisory Board of GCR recently approved this new section which will highlight invited manuscripts from eminent senior scientists with a significant history of research in the Gulf of Mexico and Caribbean Sea regions. These invited contributors will address broad topics associated with the region and will discuss how their discipline has evolved during their career due to technological advances, changes in the discipline, or paradigm shifts. These invited contributions will be editor–reviewed, Open Access, and limited to 1–2 per volume (year). For Volume 27, the Mississippi-Alabama Sea Grant Consortium will support Open Access publication of the first Ocean Reflections article.

These invited articles will be advantageous for young scientists and undergraduate and graduate students alike as they will focus on the history and development of selected disciplines written by senior–level leaders in the field of study. A brief biography of the author will be included with each article. The Ocean Reflections section will highlight the development and changes in such diverse fields as deep sea research, coral reef ecology, harmful algal blooms and salt marsh ecology over the past 30–40 years. It is our hope that the GCR readership will gain an appreciation for the evolution of science and research through these Ocean Reflections articles.

Mark S. Peterson[1] and Nancy J. Brown–Peterson[2]
[1]Division of Coastal Sciences and the [2]Center for Fisheries Research and Development, School of Ocean Science and Technology, The University of Southern Mississippi, 703 East Beach Drive, Ocean Springs, MS 39564

Gulf and Caribbean Research

Volume 27 | Issue 1

2016

You Can't Catch a Fish with a Robot

R. Grant Gilmore Jr.
ECOS, rggilmorej@gmail.com

Gulf and Caribbean Research Vol 27, ii-xiv, 2016
DOI: 10.18785/gcr.2701.11

Manuscript received, November 25, 2016; accepted, December 4, 2016

OCEAN REFLECTIONS

YOU CAN'T CATCH A FISH WITH A ROBOT

R. Grant Gilmore, Jr.
Estuarine, Coastal and Ocean Science, Inc., 5920 First Street SW, Vero Beach, Florida 32968; email: rggilmorej@gmail.com

ABSTRACT: In this essay I will relate the challenges associated with deep sea ocean exploration as well as the advantages and disadvantages of today's ocean technologies based on experience with most of these systems. After nearly 5 decades using robotic vehicles (Remotely Operated Vehicles = ROVs and Autonomous Underwater Vehicles = AUVs) and manned submarines for fish research, I thought it would be appropriate to briefly describe a career spent using these technologies as they were developed. Deep sea ichthyologists cannot effectively catch a swimming fish with a robot even 40 years after the development of the first ROV for deep ocean science investigation, nor can most currently–available manned submarines. There is a continuing debate on the advantages of using robotic machines (cheaper, safer) versus manned machines (more expensive, dangerous) for ocean research. Appropriately designed and operated manned submarines can accomplish considerable ocean exploration that robotic vehicles cannot. Robotic vehicles have their own advantages and science missions that manned vehicles cannot accomplish, but there is a loss in capturing mobile specimens for study and recording important behaviors and ecologies that simply cannot be accomplished with robots. I have written this retrospective on deep ocean research capabilities as my profession, ichthyology, and the world, have lost a major technological asset that can easily be brought back once its value is realized.

KEY WORDS: Submarine, ROV, AUV, ichthyology, deep ocean, Johnson–Sea–Link

INTRODUCTION: THE OCEAN CHALLENGE

Sixty years ago, like many explorers of the past, we did not understand the immensity of the forces that challenged our success in exploring the deep sea. Most problems create valuable and helpful discoveries that aid in making dangerous explorations safer and successful. These discoveries, once understood, often reveal our initial ignorance of the forces that must be conquered, particularly for deep sea exploration. It takes naivety, imagination, fortitude and ingenuity to explore the unknown, particularly when it is a truly life or death endeavor. Often there are decisions to cure problems without truly knowing or understanding the problem. In my personal case it was the physiological impact of the deep sea on human health/survival. With appropriate technological advances, deep ocean machines can keep humans safe while diving to some of the greatest depths on Earth, while allowing unprecedented scientific progress.

The ocean was romanticized by one of its first routine human inhabitants, the inventor and ocean explorer, Jacques Ives Cousteau (Cousteau 1952; Cousteau and Dugan 1953; Cousteau and Dumas 1962; Cousteau and Schiefelbein 2007). He wrote many articles and books, and was one of the first to use cinema and television to reveal the ocean to the world audience with his global *Calypso* expeditions. Unfortunately, many of the most difficult problems, particularly those involving human physiology in pressure environments, were largely unknown when Cousteau was promoting his early ocean explorations in the 1950s and 60s. However, a contemporary of Cousteau, the ocean pioneer and inventor Edwin Link, was making some of the deepest and prolonged ocean dives at that time (Link 1958; 1963; 1964; 1973; Link and Littlehales 1965; van Hoek and Link 1993; Marden 1998). Detailed physiological research on humans in pressure chambers was just getting underway during the 1960s (Duke Center for Hyperbaric Medicine and Environmental Physiology, Duke University School of Medicine, http:www//anesthesiology.duke.edu/?page_id=828766; Wicklund 2011). To allow ocean exploration, new developments in materials as well as mechanical, hydraulic and electrical technology were necessary. In many ways, these challenges were considerably more difficult than those engineered for aerospace exploration. For example, humanity's interest in ocean exploration was far less than that for aerial and space exploration simply due to the universal visibility of air and space and the invisibility of the marvelous creatures below the ocean's surface. Out of sight, out of mind! In fact, the Chinese invented the rocket over 900 years ago, while Cousteau and Gagnon invented the first effective 'self–contained underwater breathing apparatus' (SCUBA) regulator in 1943.

People knew the surface of the ocean quite well. When looking out over the ocean from the deck of a ship, you are gazing upon a virtual desert with no visible forests, lush grasslands or animals except for the fortuitous sea bird or flying fish breaking the surface. The ocean's surface looks the same in the South China Sea as does in the Gulf of Mexico, or Caribbean Sea. I have always felt sorry for our predecessors (before 1950) in marine science trying to explore the ocean below the waves before the advent of SCUBA and research submarines. Marine science technology and hyperbaric phys-

iological understanding were literally in the dark ages when compared to space exploration (Kottler 1969; Brubach and Neuman 2003; Finlayson 2009) when I began my career in aquatic science. While large submarines carrying crews of humans have plied the seas for over a century, they had no windows. Tens of thousands of naval sailors swept pass trillions of unstudied, unclassified sea creatures without ever knowing they were there. Military submarines are still passing blindly through this rich 'living soup' over 100 years later while tiny manned research submarines are disappearing.

One eternal question that spurred the early ocean explorers during my career was: If living organisms can survive in the deep sea, can humanity survive there too? Additionally, many asked: If seals, dolphins and whales, mammals like us, can live continuously in the sea, why can't we? The popular movie of the early 1990s, *The Abyss* (Figure 1), presented these very questions. There were many reasons for the inability for humans to enter the sea. Many ocean exploration problems presented greater challenges than those that had to be solved before we could enter outer space, or go to the moon. Water is dense, heavy (30 cm of seawater depth = 0.445 psi), and absorbs light to the point that at 1,000 m (~3280 ft) below the surface there is no solar light under the most optimum conditions. It is totally dark beyond that depth except for biological light emanating from bioluminescent organisms. The darkness of the deep sea does not call us as the moon or Mars do since we cannot see it, know it, or understand it. There is one major reason for exploring the deep sea versus the moon and Mars —— the sea contains an abundance of living breathing organisms and we are dependent on a living sea for survival.

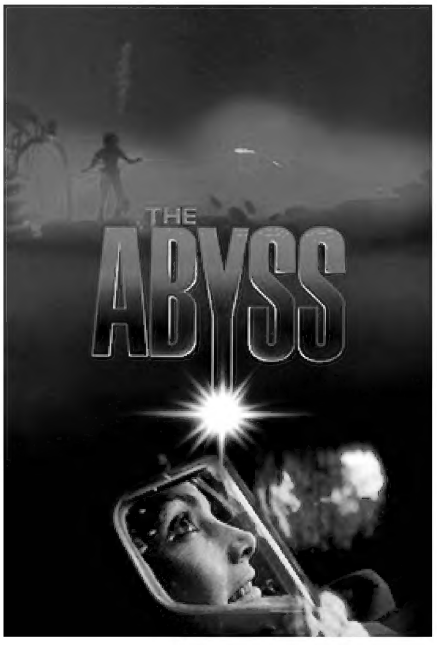

FIGURE 1. *Marquee from the 1990s movie,* The Abyss, *an unexplored physiologically alien environment illustrating the romantic concept of humans living within the deep ocean.*

After World War II (WWII), inventors around the globe created undersea habitats from the Black Sea to the Caribbean. Cousteau and Link were among these people who actually put people in undersea habitats for the first time (Stenuit 1964; van Hoek and Link 1993; Marden 1998; Cousteau and Schiefelbein 2007). I was in the generation who thought we could live in the deep sea. Many of my mentors and colleagues in marine science like Bruce Collette, Robert Jones, C. Lavett Smith, James Tyler, John McCosker, Sylvia Earle, and Eugenie Clark also shared the same dream. As a young naive marine scientist I, and my colleagues, agreed to live at 305 m (~1000 ft) depths with our bodies experiencing the pressure equal to about 445 psi (30 x surface atmospheric pressure at sea level) for prolonged periods of time even though it had never been done before. I also agreed to have a deep sea submarine transport me into the depths and 'burp' me out to conduct research and return even though it had never been done before. To that end, I agreed to live in an undersea habitat for a week or two and explore the ocean daily to 76 m (250 ft) on air (not helox, but air!).

These experiences were life—changing for me as they were for my colleagues. Most humans have not experienced deep sea organisms except through the public media, television, cell phones, and their computers. What is it like to be surrounded 360° by water with strange creatures that are curious about you? If you could, what would you do while there with these organisms that you could not do by dropping a baited hook and line, or net from the surface, as humans have been doing for millennia? Today there are literally thousands of robots dropped into the sea on a daily basis, although most not for scientific exploration. These robots typically take cameras with them that cable the images to the surface ship's control room. However, by using robots we are observing through a camera lens, which is not at all like being there within that lively deep remote environment.

What is the advantage in studying the ocean from within an acrylic bubble and making instantaneous decisions with a variety of tools? You are able to maneuver yourself as if you were a fish to make critical collections and observations. Manipulating a robot hundreds or thousands of feet away looking through a camera lens does not allow observation of an organism's entire environment and what it is doing in 3—dimensional space (i.e., mating, eating, sleeping, chasing, running away). However, while sitting comfortably and quietly in an air conditioned acrylic sphere at 350 m (~1150 ft) in crystal clear tropical waters (Figure 2) you are surrounded by the ocean universe and entertained by thousands of living organisms from minute glowing specks to giant sharks and squid. At the same time you are observing the reaction of the myriad of other creatures surrounding you. I know about the real—time interactions and observations, as I spent over 40 years and hundreds of hours using the undersea robots and staring through camera lenses, start-

FIGURE 2. Johnson-Sea-Link *manned submarine on bottom in Bahama Islands.*

ing with the very first one for scientific investigation, Link's 'Cabled Observation and Rescue Device' (CORD). This was among the first generation of undersea robots (e.g., Figure 3) now known collectively as 'remotely operated vehicles' (ROVs). I also spent thousands of hours in manned submarines starting as one of the first scientists to dive in the acrylic sphere of the *Johnson–Sea–Link–I* (*JSL–I*) submarine in 1971. The question in my mind during these early years was: "What if you wanted to capture that swimming fish and study its anatomy, physiology, and genetics?" How could a remotely tethered robot 350 m deep do that?

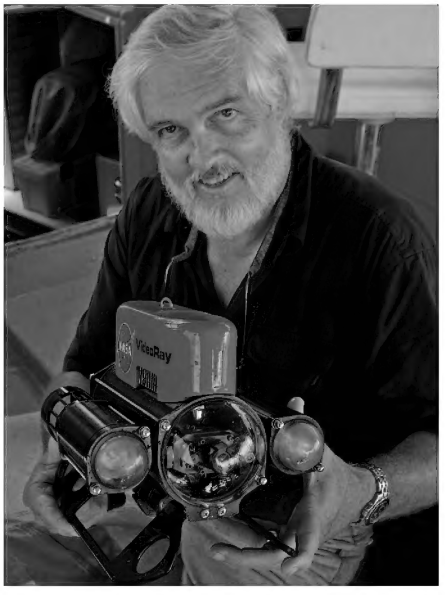

FIGURE 3. *The author with an early version of one of the most popular ROVs active today, the 'VideoRay.'*

Becoming a Scientist: Personal Experience and Decisions

While growing up around military aircraft and rocket launches I was always fascinated with aeronautics, the emerging space program, and being a pilot. Space and aeronautics were always in the headlines and in my personal experience! However, in parallel with these dreams and in a post–WWII environment of discovery, marine scientists were now able to enter the sea using SCUBA to at least 100 m (~328 ft) and they were making thousands of new discoveries in < 30 m (~98 ft), particularly around reef formations where trawls and dredges pulled by surface vessels were ineffective. It was at this time that Cousteau started his television and book series chronicling his undersea exploration of the world ocean (Cousteau and Schiefelbein 2007). The 1950s and 1960s were exciting years for youngsters interested in science careers. In my home town, Sarasota, Florida, the Cape Haze marine laboratory, founded by Dr. Eugenie Clark, sponsored an annual undersea science lecture series for children (Clark 1969) and across the state the federal space program at Cape Canaveral was open for public tours on weekends. These two fields of interest and study were in many ways similar and exciting. I went to school at the University of Florida to study aeronautical engineering, but I took two biology courses on living creatures as electives which changed my life and career. I transferred to the University of West Florida in Pensacola to study marine biology as an undergraduate and also completed my Master's degree there (see Biography). I never looked back!

Be Brave and Explore For A Job In Person: The Laboratory That Was Not Yet There evolved Into A Major Institution For Ocean Exploration

My career started when, while completing my Master's degree, I started looking for a research position at a marine laboratory. After a considerable number of applications were mailed (there was no internet then), it was personal contact with resume in hand that was the key for 4 job opportunities. I actually interviewed at a new marine laboratory that, in fact, was not even built yet! Through a college roommate, I heard about a new marine laboratory under construction in Fort Pierce, Florida and immediately drove to that location to make contacts and hopefully earn an interview. Again personal contacts are critical as I met an inebriated customer at a bar on the waterfront in Fort Pierce who had heard a rumor of a new marine research facility and offered to lead me there. We drove to a dirt road that appeared to lead to nowhere. I drove down the road passing what looked like a ship's bridge rusting in the sand, and after about a mile I came to a rustic metal Butler building. This did not look promising from the exterior but I was surprised when I opened the door, as in front of me was a gleaming aluminum and acrylic submarine. This was the *JSL–I* submarine that had just been completed that year and passed initial sea trials in winter and spring 1971 (Link 1973; van Hoek and Link 1993). It was a revolutionary design with an acrylic sphere for the occupants up front, and an aluminum diver lock out compartment in back (Figure 4). It was owned by the Smithsonian Institution with their logo across the ballast tanks. The sub's metal Butler building was on what appeared to be a channel in the mangroves extending out to a lagoon called the Indian River (see early work in Gilmore

1977a,b; Gilmore et al. 1978).

I met a lady behind a desk (Carolyn Zealand) in the next room and was introduced to Captain Smith, retired Navy, who was supervising the conversion of an old Coast Guard cutter, the *USS Yeaton*, into a research submarine tender (to be called the *R/V Johnson*). Captain Smith and I met in a drafting room and he kindly agreed to interview me and see what I was about. Apparently, I passed my first inspection. He later called Washington, D.C. to speak with Dr. I.E. Wallen of the Smithsonian Institution who met with me on one of his trips to east Florida and eventually gave me a job offer, though there was still no laboratory in which to work. I was then informed that I would be working for a newly established private non–profit entity called the Harbor Branch Foundation.

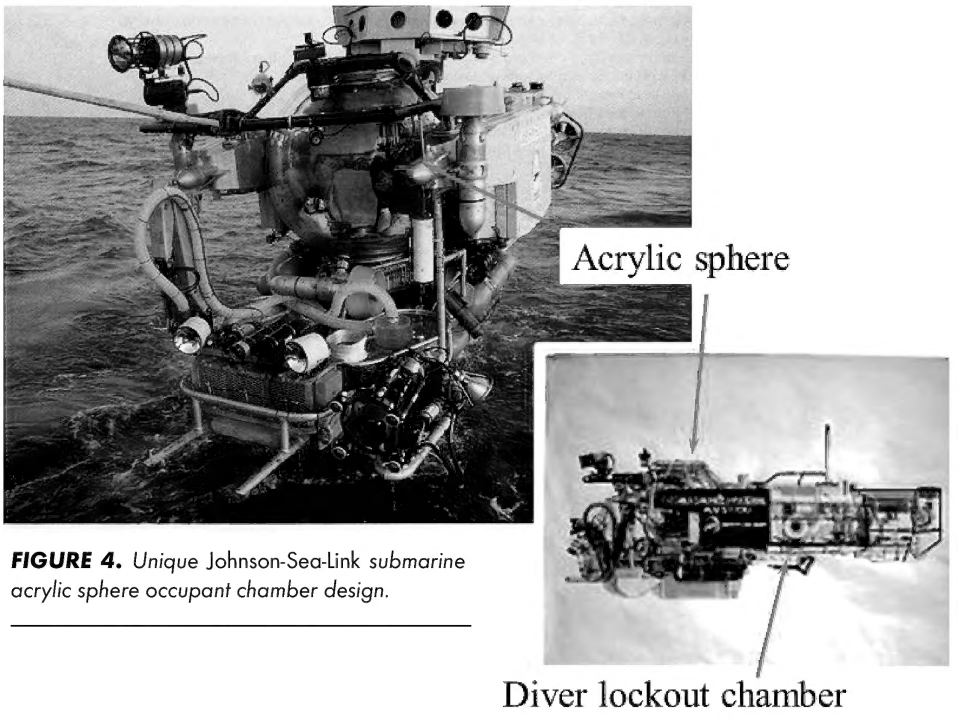

FIGURE 4. *Unique* Johnson-Sea-Link *submarine acrylic sphere occupant chamber design.*

Harbor Branch Foundation For Interdisciplinary Ocean Exploration And Technology Development: The History Of Marine Submarines At Harbor Branch Foundation

Mr. Seward Johnson, Sr. formed the Harbor Branch Foundation (HBF) in collaboration with Edwin Link for ocean exploration and marine ecological research. We had a credo up on the lab wall for years written by Mr. Johnson that expressed his desire to study everything in the ocean using the *JSL* submarines launched from the decks of the *R/V Johnson* and *R/V Sea Diver*. These ships were augmented with ocean trawling surface vessels, the *R/V Sea Hunter, R/V Joie de Vivre* and the *R/V Gosnold*, and by a fleet of small boats for inshore studies. They wanted to begin by classifying all marine organisms from the banks of the Indian River Lagoon to the depths of the ocean on the eastern side of the Bahama platform. They wanted all aquatic disciplines represented and within 7 years had hired chemists, geologists, oceanographers and a diverse array of marine biologists in phycology, phytoplankton, zooplankton, echinoderm biology, malacology, carcinology, polycheate reproduction, benthic ecology, deep sea physiology and comparative ecology (Young et al. 1974). In 1985, marine scientists from the HBF and the Smithsonian Institution joined with Ed Link's group of ocean engineers (first known as the Sea Diver Corporation), and this new endeavor was called the Harbor Branch Oceanographic Institution (HBOI). The first HBF employees (Gilmore, Williams, Putnam, Meek and Gore) had to agree to compress down to depths of 154 m (500 ft) and lock out of the *JSL* submarine to collect marine organisms in the deep sea that would be taken back to the laboratory in pressurized containers. I was one of the first HBF science employees (with Doug Putnam and Laverne (Coddy) Williams) to make the first dives in the *JSL–I* submarine, 1971–1972.

We had a laboratory–based steel pressure aquarium for physiological experiments on fish captured at depth by divers from the *JSL* deep sea submarine. To my knowledge this was the only research submarine capable of locking out divers to collect organisms at depths to 183 m (600 ft). Fish captured at depth could then be placed in pressurized transport vessels that were kept at ambient bottom pressure values and brought to the surface. The transport vessel carrying the fish was then mated to the steel pressurized aquarium back in the lab. Dr. Robert Meek conducted successful hyperbaric physiological studies on *Citharichthys* spp. flounders between 1972–73, until the tragic *JSL–I* submarine accident that killed Ed Link's son, Clay and Al Stover in June 1973. Dr. Meek left HBF after this fatal submarine accident and the pressure physiology program at HBF was never reinstated. Thereafter, with the exception of a few brief experiments by Dr. Robert Avent, the unique pressure aquarium was used only for testing and certifying deep sea instruments to be placed on the *JSL* submarines.

Clay Link and Al Stover did not die in vain. Due to the effort of Ed Link and his talented engineers, the following years saw major improvements in equipment and submarine operational procedures. New highly effective personnel created the safest deep sea research submarine operation on the planet. Submarine rescue ROV systems were developed at HBF and carried on the submarine mother ship. Launch and recovery operations were made under strict guidelines

and considerable time and effort was put into training new crews each year. Eventually another *Johnson–Sea–Link* submarine was built (*JSL– II*) as were additional submarine mother vessels. The HBF surface fleet from 1971 to 1990 consisted of the *R/V Sea Diver*, *R/V Johnson*, *R/V Seward Johnson* and the *R/V Edwin Link* carrying the *JSL–I and II* submarines and a Perry sub, the *Clelia*, with expeditions from the Mediterranean, to the Great Lakes, along the eastern seaboard from Canada to the Florida Keys, throughout the Caribbean Sea and into the eastern Pacific. Thousands of dives were made safely with hundreds of scientists from institutions around the world.

During the early 1970s, between deep sea field excursions and lock out dives from the *JSL* submarines, there was a series of hyperbaric duration trails using the hyperbaric chambers at the Center for Hyperbaric Medicine and Environmental Physiology, Duke University Medical Center, Durham, NC. All HBF employees were encouraged to participate in 228 m (750 ft) saturation living in the chambers for several days with 2 day excursions to 305 m (1,000 ft) depths. Some HBF employees saturated to 610 m depth pressures (= 2,000 ft seawater; 896 psi). It took several days to decompress from these saturation experiments. Though several scientists, engineers and divers from HBF participated in these dives between 1973 and 1975, enough physiological data were obtained to indicate that saturation at this level was not safe enough for human physiologies. I concurred after monitoring gases and divers in the first saturation dive series in January 1973 at the Duke hyperbaric chamber facility and reading extensively in their hyperbaric medical library.

Although I did not make a saturation chamber dive in that program, 2 years after the tragic 1973 submarine accident the *JSL* submarine saved my life during a NOAA sponsored saturation program. This program included living in the *Hydrolab* habitat and swimming deep excursions to 61 and 76 m (200 and 250 ft) to capture fish on a vertical wall using experimental rebreathers at Lucaya, Grand Bahama Island, Bahama Islands (Wicklund 2011). I lost consciousness at 42.7 m (140 ft) after convulsing from CO_2 poisoning, precipitated by O_2 toxicity, due to the failure of rebreather dissolved oxygen sensors. I was saved by a support diver, Mr. Robert Wicklund, who moved me to an undersea habitat (*Sub–Igloo)* where he gave me CPR (Wicklund 2011). The *JSL* submarine picked me up from there and mated to a decompression chamber below the O1 deck on the *R/V Johnson* which allowed a hyperbaric physician to lock in with me and start treatments for decompression, embolism and salt water consumption. I was eventually transferred to a critical care unit in a stateside hospital, although I nearly expired during the flight from the Bahamas to Miami in a plane that was delayed due to some faulty HBF administrative decisions (Wicklund 2011). We learned a lot about rebreathers, scientist capabilities in capturing fish on air to depths of 76 m (250 ft), and duration diving in the *Hydrolab* during these experiences. New species of fish were captured, but at great physical risk to the diving scientists, several suffering from narcosis, or becoming nauseous while working at 76 m (250 ft) depths on air.

How Can Ichthyologists Capture Deep Sea Fish Using Machines?

The overall objective of the HBF was to pursue aquatic science, and extend the knowledge of estuaries, coasts and the world's ocean. If you are investigating an unexplored ecosystem, the deep sea, and observing creatures never seen before, how can you know who, or what they are without examining them in hand, up close and personal? You cannot determine their reproductive status or stomach contents without examining them. How can you determine their genotype just by photographing them? In 1971 there was a global navy of deep sea "research" submarines but all were designed to observe, not capture, actively swimming marine organisms. Fish were not on the agenda and considered impossible to capture (Terry 1966; Oceanography in Florida 1970; Sweeney 1970; Piccard 1971; Limburg and Sweeney 1973). The exception was the *JSL–I* that was designed from the beginning for capturing fish with lock–out divers.

The logistics of deep sea exploration are challenging. Undersea exploration requires life support systems: air to breath, wastes to expel or modify, and living quarters for rest and work. Undersea vehicles must withstand immense pressure at the deepest location in the ocean, the Marianas Trench. The cold pressurized deep ocean is highly viscous, needing considerable energy and an efficient hydrodynamic design to maneuver within it. You must carry your own power source, reliable state–of–the–art batteries, in order to function. Military submarines use costly and dangerous nuclear energy. The only nuclear powered research submarine other than the Navy's *NR–1*, the *Benjamin Franklin*, was designed and built by a military contractor, Grumman Corporation, and successfully carried out the first long duration ocean exploration to a depth of 610 m (2,000 ft) for 30 days in 1969. Grumman had also built the *Lunar Excursion Module* (LEM) that took Neil Armstrong and Buzz Aldrin to the surface of the moon. They were on the moon when the *Ben Franklin* submerged to drift over 1,400 miles in the Gulf Stream, but no one remembers the *Ben Franklin* feat, only the lunar landing.

Unfortunately, the *Ben Franklin* was never used again for ocean exploration after its first major mission; the Navy's *NR–1* is also now retired. Unlike the *JSL* research submarine, all the other small research submarines built at the time, the *Perry* subs, *Alvin, Aluminaunt, Pisces I–IV, Deep-*

star–2000, Kuroshio II, NR–1, Nekton Alpha/Beta, Shinkai, Stars I & II, and *Trieste I & II*, were designed to observe the ocean through port holes, or glass hemispheres (Figure 5; Terry 1966; Oceanography in Florida 1970; Sweeney 1970; Piccard 1971; Limburg and Sweeney 1973; Penzias and Goodman 1973; Trillo 1979). Thus, these submarines had limited visibility. Most of them had a single large propeller for forward and backward motion, but not 'all axis' thrusters and maneuverability. Many had mechanical arms for picking up objects like rocks, but not for capturing living mobile creatures. When they were built the greatest concern was with geological resources (such as oil deposits) and military purposes, not biological and ecosystem understanding.

Fortunately, HBF had a unique submarine designed by Ed Link for high visibility with occupants in an acrylic sphere, and high maneuverability with multiple thrusters aligned on several axes (Figure 6A). The requirements of a manned fish capture machine are not too different from that of a manned aircraft used for fighting in aerial combat. So it is not too ironic that Edwin Link, inventor of the Link Trainer for aircraft pilots, designed and invented a submarine that had many of the capabilities of an aircraft, with emphasis on having high visibility and maneuverability. The rapidity of changing direction in all axes was created by placing stationary propeller thrusters facing in all compass directions both in the bow and along the sides.

From 1976 to 1989, HBF/HBOI engineers and biologists began work on fish capture devices that would eliminate the need for divers to saturate. The *JSL* submarines were being cleared for deeper diving, eventually allowing dives to 914 m (3,000 ft) and we had to develop a variety of fish capture systems. Original HBF biologists Dr. Robert Jones, John Miller, Dr. Marsh Youngbluth and I worked in collaboration with a group of talented HBF engineers, Chris Tietze, Doc Halliday, John Holt, Tony Wilson, Robert Tusting, Mike Camp, and Greg Kennedy to develop such tools. Machinists and vessel/submarine operations personnel, Roger Cooke, Tim Askew, Jeff Prentice, Dom Liberatore, Phil Santos, Jim Sullivan and

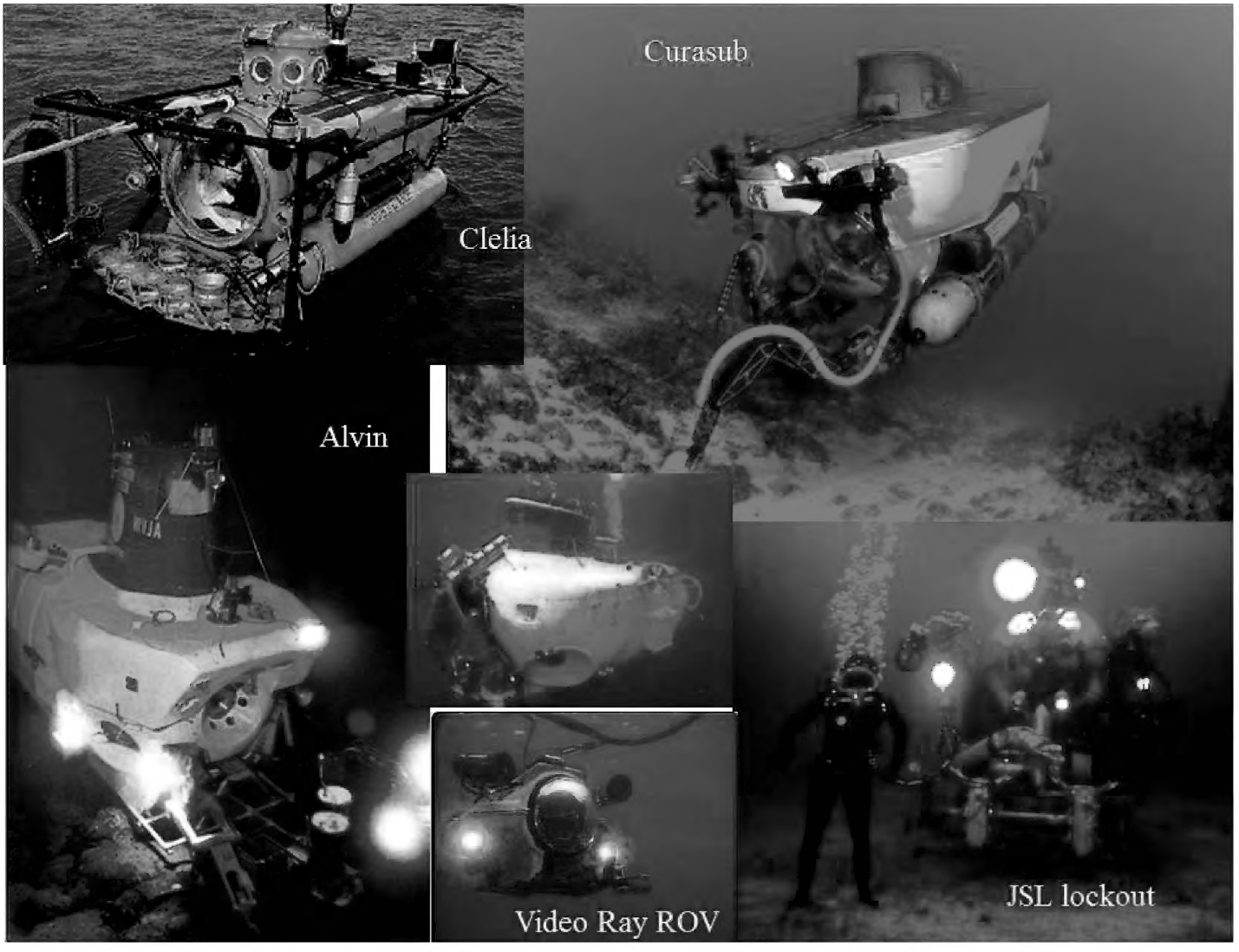

FIGURE 5. *Various deep sea research vehicle designs.*

others also helped to develop 7 major fish capture systems in addition to keeping manned submarine operations safe and efficient. These fish capture systems were:

1. Mechanical arm – This tool evolved over the years to be very proficient. Lights blinded new species of sharks and chimaeras while the arm captured the fish by grabbing it by the body. The rotenone injection system listed below was mounted on the mechanical arm as was the suction device so that they could be aimed and placed where fish were located (Figures 6B, 7 and 8).

2. Forward basket – This tool had a hydraulically operated cover and could be baited or unbaited. Large fish that had been captured with the spear system and hook and line listed below, or with the mechanical arm, could be placed here. This tool was responsible for capturing several rare and new fish species. It was responsible for capturing larger predaceous fishes such as groupers when baited (Figures 6B and 7).

3. Hydraulic grouper trap — This large rectangular trap was carried to the bottom and placed up to 10 m from the submarine as it settled on the bottom. It was operated with bait suspended in the center of the trap. Scientists could open and close doors on either end of the trap remotely. Up to 5 species of groupers were captured at one time during its operation at grouper aggregation and spawning sites.

4. Suction device with rotating bins – This system was used to suck up fish typically < 30 cm in length. Many new cryptic species were captured with this device. It was also used to suck up fish succumbing to rotenone. The plexiglass bins were numbered and on a rotating platform, so that collections for different depths and locations could be separated and recorded (Figure 6B, 7).

5. Rotenone injection system – Laboratory experiments with various rotenone mixtures, solvents, emulsifiers and quality of rotenone determined the mixture that was least toxic to invertebrates, but most effective in capturing fish (Gilmore et al. 1981). This unit ejected a stream of rotenone from a collapsible 20 liter container tie—wrapped inside the forward basket. Literally hundreds of fish were captured with this system (Figure 7, Gilmore et al. 1981).

6. Nine shot laser aimed spear/tagging system – A rotating arboreta spear system with hypodermic needle heads was developed that could inject any required agent into the targeted fish, or tag a fish with a streamer tag at depth. The spear was aimed using a laser pointer placed on top of the flat plate positioned above the rotating spears (Figure 8). We

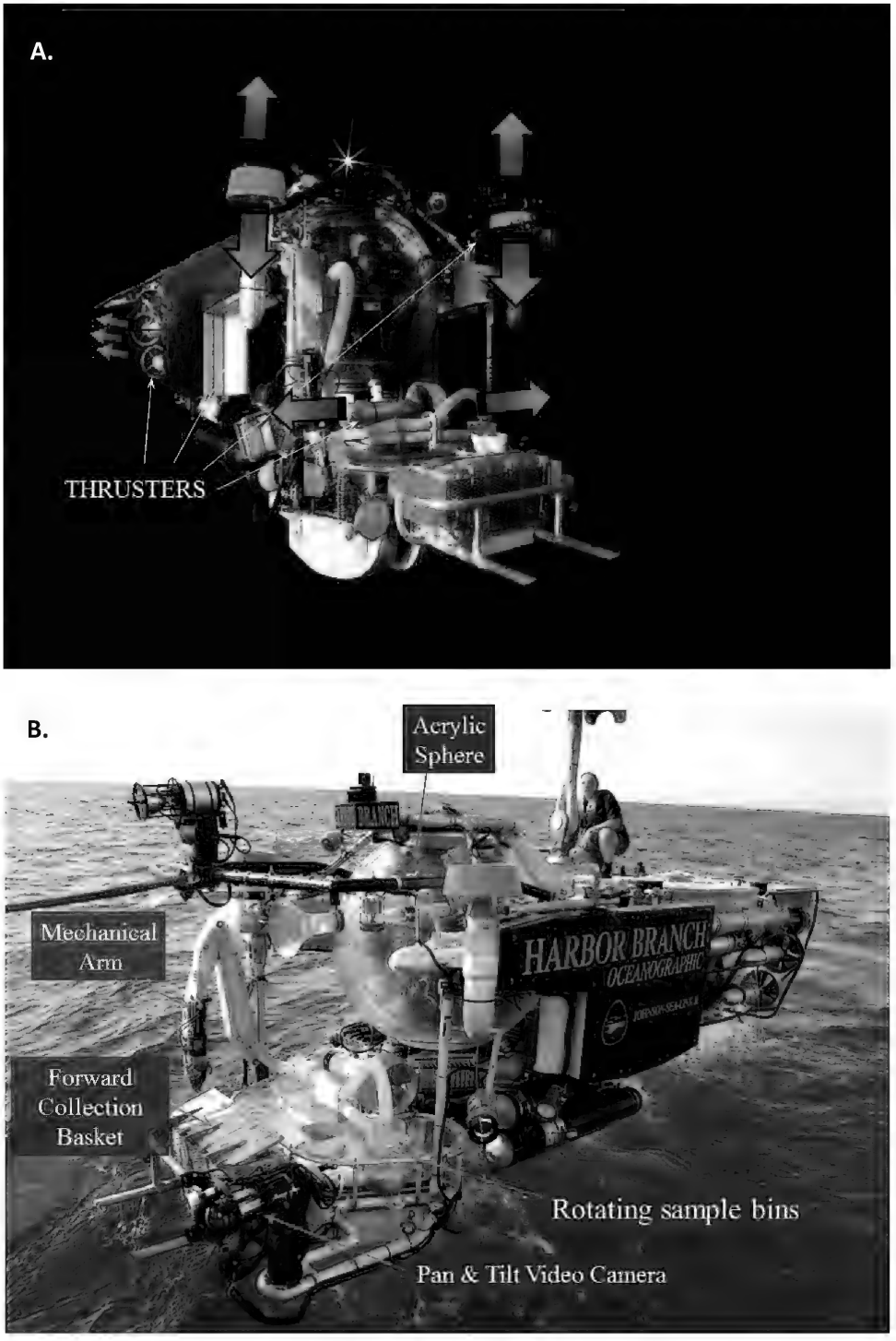

FIGURE 6. *The* Johnson-Sea-Link *submarine features that are critical for fish collections. A. Thruster arrangement for maximum maneuverability. B. Sample viewing and collection features.*

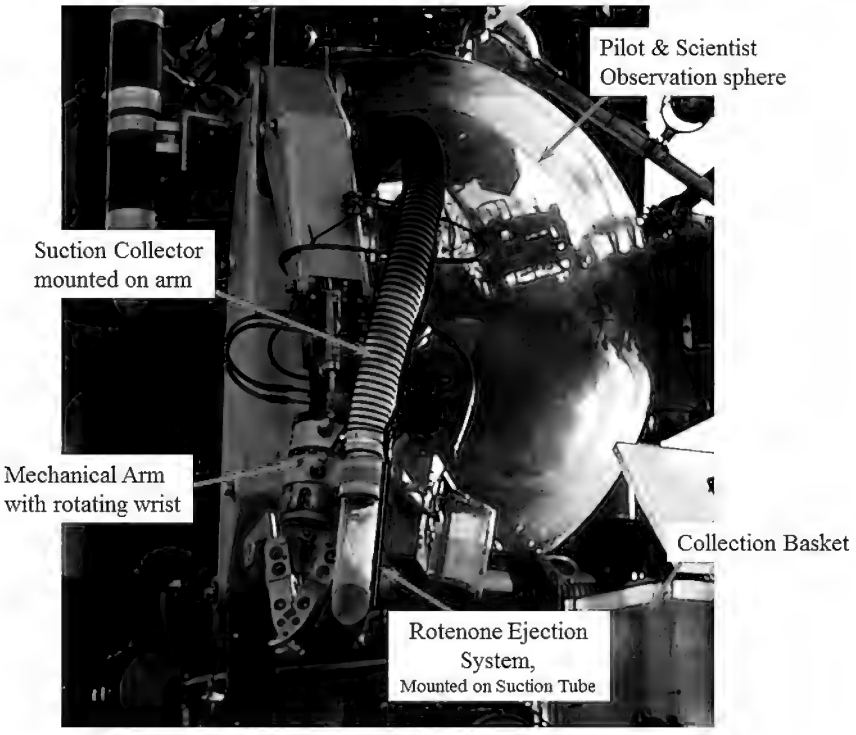

FIGURE 7. *Suction collector mounted on mechanical arm along with rotenone injection system on the* Johnson-Sea-Link *submarine.*

were able to successfully spear large fish with this system and place them in the front basket as well as tag several deep sea sharks with streamer tags.

7. *Short line float and baited hook* – This was an invention of the intrepid angler, Dr. John McCosker, California Academy of Sciences, on the 1995 Galapagos Islands expedition. A 1.0 m length of fishing line was tied to a small deep sea float (they do not collapse under pressure) and a 2–3 lb lead weight. A < 30 cm line is suspended between the float and weight with a baited fish hook. A new species of moray eel was captured on one of my submarine dives at 300 m with this system as well as a small scorpionfish, that was then eaten by a larger scorpionfish as it struggled, both being captured simultaneously.

Using all these systems required that the submarine choose a likely location for fish capture. The submarine would either settle at that location, or chase an active fish. Low illumination was necessary. High illumination typically caused fish to retreat to shelter. Fish capture is best without lights or major sounds produced by the submarine. The largely insolated 10.0 cm (4 inches) thick acrylic sphere of the *JSLs* did not allow sounds from the interior of the sphere to escape to the environment.

A variety of still and video camera systems were used in these studies, some with pan/tilt and zoom capability, color or black and white (Figure 6B). The most effective cameras for fish behavioral work were the SIT (Silicon Intensified) systems that produced black and white images under extremely low light conditions as most deep sea fish are sensitive to any light. Lighting was developed that included rheostat controls on red lights augmenting, and in some cases, precluding elaborate and diverse white light illumination. This is the opposite of the needs by coral and sponge collectors, or archaeologists as they usually want high illumination and then wonder why there are no fish around. Video and still cameras had laser aiming and measurement devices mounted on the cameras. The still camera photo would shut down the laser so that it did not show in the photos. A 15 m (50 ft) role of 35 mm Ektachrome film was loaded into an Edgerton submarine camera allowing at least 5,000 photos to be taken per 21–30 day expedition. This was extremely valuable in documenting *in–situ* fish color patterns and habitats.

Increased thruster power along with their placement along all axes allowed the *JSL* submarine to maneuver much like a helicopter, leaving the bottom within seconds to chase a lively fish in the water column. It is very important for the pilot

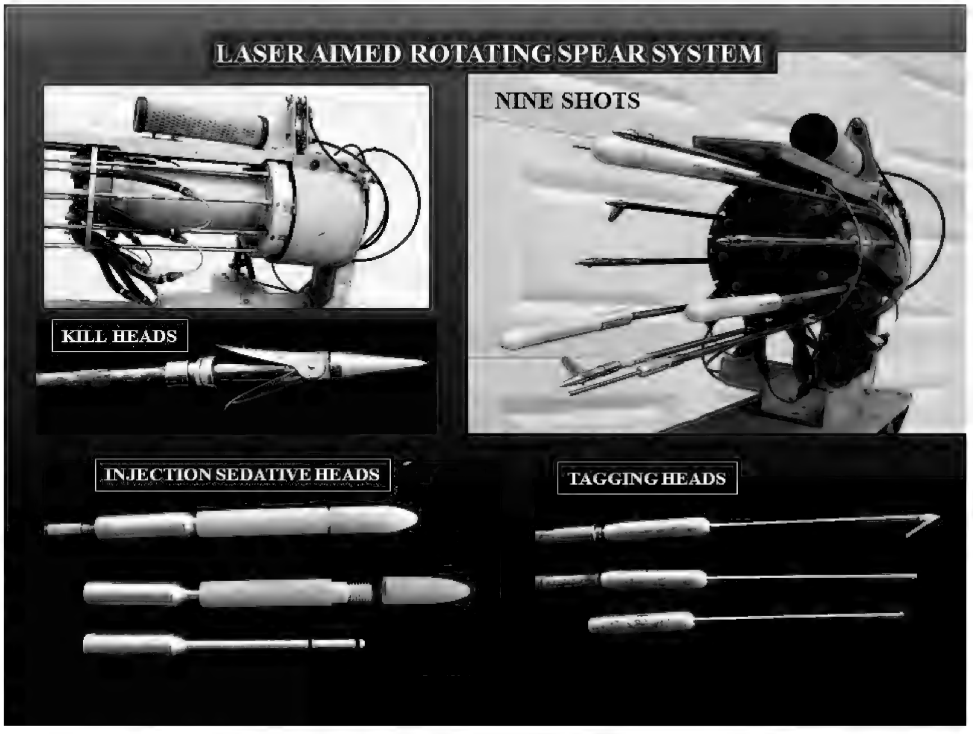

FIGURE 8. *Nine shot laser guided spear/tagging system on the* Johnson-Sea-Link *submarine.*

to be capable of quickly maneuvering the submarine along all axes to capture a mobile fish. The dexterity and visual capabilities of the pilot was most important in fish capture. Sponges, rocks, corals and other sessile invertebrates were easily picked up by any submarine fitted with a mechanical arm, but only the *JSL* submarine could effectively chase and capture fish attempting to swim away.

I personally used manned submarine and robotic vehicles to study fish for over 35 years, from 1971 to 2010, making over 350 dives to depths as great as 1,000 m (~3,280 ft). During this time we captured and described hundreds of fish specimens and their behaviors with the tools we developed at the HBOI, including 116 new species of fish never seen by human eyes (Gilmore 1979, 1980, 1983, 1986, 1991, 1993, 1995a, b, 1997, 2001; Gilmore et al.1981; Reed and Gilmore 1981; Gilmore et al. 1983a,b,c; Gilmore and Jones 1988, 1992; Gilmore and McCosker 1996; McCosker and Gilmore 1996; McCosker et al. 1997; Claro et al 2000; Belleville 2002, 2004; Gilmore et al. 2003; Gilmore et al. 2005; Messing et al. 2013; Tornabene et al. 2016). This was a dream fulfilled!

These tools were designed specifically for use on the *JSL* submarine, but were often copied and used by a variety of other manned vehicles elsewhere in the world. A new species of living organism cannot be described without a specimen in hand; a nice photo is unacceptable. The 1995 Galapagos expedition with John McCosker, Bruce Robinson, and David Stedman captured over 30 new fish species including 2 new sharks with the *JSL* submarine in 18 dives (Belleville 2004).

Despite the advantages of manned submarines, remotely operated vehicles (ROV) have resulted in many deep sea discoveries. The first ROV used for scientific investigations and ocean exploration was the CORD vehicle. This was developed by Edwin Link and his engineering team at HBF between 1973 and 1980. I had the opportunity to use this vehicle and several other ROVs for my own research programs. My own experience included extensive use of the *Mini–Rover*, *Hysub*, and the NOAA/NURP *Phantom* ROVs from 1986 to 1993 (including the *Super–Phantom*). I used these vehicles primarily for long term fish behavioral studies on reef formations from North Carolina to the northern Gulf of Mexico and the Galapagos Islands. They were used for recording shark and grouper mating behavior. We found both sharks and groupers would ignore the ROV vehicle (*SuperPhantom*, *VideoRay*, *Minirover*) swimming or sitting with them. While employed by Dynamac Inc. at the Kennedy Space Center (1999—2004), I used the NASA ROV, the *VideoRay*, for a variety of grouper behavior studies (Figures 3 and 5). ROVs and AUVs were also used in our fish acoustic research programs (Gilmore 2003; Gilmore et al. 2003). A U.S. Navy *REMUS* AUV made successful transects through spawning aggregations of Spotted Seatrout (*Cynoscion nebulosus*) within the Banana River Lagoon at the Kennedy Space Center in 2003 with no recorded change in fish choral displays in the presence of the AUV.

Sadly, in this age of robotics, many robotics experts have stated that manned vehicles are not necessary for ocean exploration. Apparently, none of these authors were interested in capturing actively swimming marine animals, such as fish. Even today, only appropriately designed manned submarine can capture an active marine organism, nearly 42 years after undersea unmanned robotic vehicles became practical research machines.

The only vehicles operational today that could be used for fish capture if mated with effective tools are the *Triton* submarines built by Triton Submarines, Inc. These submarines also benefit from great maneuverability and pilot/scientist visibility in an acrylic sphere (Figure 9). Unfortunately, I do not know of any *Triton* submarine being used in the United States for fish capture.

Conclusions

In 2016 are we progressing in developing tools with state—of—the—art manned submarine that can chase and capture new fish species in the deep sea? Forty—three years ago

FIGURE 9. *Triton submarine, the next generation of acrylic submarines yet to be used for active fish collection as they do not have the same* Johnson-Sea-Link *generation fish capture tools.Photo courtesy of Patrick Lahey, Triton Submarines, Inc.*

(1973), Edwin Link's wife, Marian C. Link wrote the following lines from her book *Windows in the Sea*:

> "Oceanography was coming—of—age at a dangerous moment in time, the peoples of the earth, weary of their polluted surroundings, were crying out for fresh territory. This combination could not help but generate a rapid surge forward in the exploitation of the oceans. It was indeed fortunate that until now the previously unconquerable seas guarded a precious two thirds of the globe. One can only hope that, his lesson learned, man would now assume responsibility for this valuable heritage and cherish it for the future. By the end of the decade (1970), Ed realized, what was now only a bit of experimentation here and there, would be commonplace. The oceans of the world would teem with vast programs of exploration and development made possible by the successors of this small bubble sub and the many other new devices now in the making."

Now, 45 years later, where are we in ocean exploration, particularly with the capability of capturing actively swimming marine organisms such as fish? The only fish capture operation that I am aware of in the tropical western Atlantic is that of Adrian "Dutch" Schrier, an entrepreneur who operates his own submarine "*Curasub*" for capturing fish sold to aquarists (Figure 10; http://www.substation—curacao.com/). He takes tourists on deep dives and most notably, rents the submarine to ichthyologists from the USNM, Smithsonian Institution (Drs. Carole Baldwin, Ross Robertson, and Luke Tornabene) for exploratory dives in both the Dutch West Indies (Curacao/Bonaire) and destinations further east. They have captured a number of new fish species in dives made over the past decade using quinaldene and suction systems (Baldwin and Johnson 2014; Baldwin and Robertson 2013, 2014, 2015; Baldwin et al. 2016a,b; Van Tassell et al. 2012; Tornabene et al. 2016a,b). The NOAA National Undersea Research Program no longer exists after supporting so many manned submarine operations in the past. HBOI no longer has operational submarine or surface vessels for ocean research. In fact, HBOI does not exist as a separate oceanographic laboratory any longer as it is owned by Florida Atlantic University and is principally dedicated to public education. The U.S. Navy's *Alvin* is still operational with Woods Hole Oceanographic Institution, but is limited to the study of rocks, wrecks and sessile invertebrates. ROVs and AUVs are everywhere.

I was fortunate to have been able to explore the ocean and study fish during a period of rapid technology development and discovery. It was also a period with mostly healthy seas and marine ecosystems. We were able to determine what human limitations were and what could be done to safely capture and observe active marine organisms. Yet, it is obvious that, if in my short career, I never came back to

FIGURE 10. *Curasub collecting fish with suction device on deep slope in Curacao, Dutch West Indies.Photo courtesy of Substation Curacao.*

the dock from a submarine expedition without capturing at least a few new fish species when operating at 305—914.4 m (1,000— 3,000 ft) depths, only a fraction of the mean ocean depth, there will be thousands of undescribed fish species waiting for the next generation of ocean explorers with new and superior tools.

Acknowledgments

I would like to acknowledge my late mother, Isabella Marshall Gilmore, for constant excitement and exposure to nature. She taught me to look at rainbows in a different light, read and learn as much as possible, and to keep an incurable curiosity about the natural world. Dr. I.E. Wallen gave me a chance to start a productive career. Dr. Robert Jones allowed my career to happen and was always encouraging me to pursue fish at any depth. I went to sea on several occasions with Mr. Edwin Link and Mr. Seward Johnson Sr. who had great vision for their oceanographic institution and exploration of the ocean from the beach to the deepest depths. Mr. Johnson's passion was to learn from the sea and use that knowledge to protect the ocean from human impacts. I would not have captured fish with a submarine if it were not for the unique design Mr. Link developed or without the talent and dexterity of sub pilots Roger Cooke, Tim Askew, Sr., Mike Adams, Phil Santos and Dominic Liberatore. Finally, I would not have been a research scientist if it were not for the encouragement of my intelligent, patient and beautiful wife of 47 years, Marilyn, for whom my first new species, the Orangebelly Goby, *Varicus marilynae,* was named.

Literature Cited

Baldwin, C.C. and G.D. Johnson. 2014. Connectivity across the Caribbean Sea: DNA barcoding and morphology unite an enigmatic fish larva from the Florida Straits with a new species of sea bass from deep reefs off Curaçao. PLoS ONE 9(5): e97661. doi:10.1371/journal.pone.0097661.

Baldwin, C.C. and D.R. Robertson. 2013. A new Haptoclinus blenny (Teleostei, Labrisomidae) from deep reefs off Curaçao, southern Caribbean, with comments on relationships of the genus. ZooKeys 306:71-81.

Baldwin C.C. and D.R. Robertson. 2014. A new Liopropoma sea bass (Serranidae: Epinephelinae: Liopropomini) from deep reefs off Curaçao, southern Caribbean, with comments on depth distributions of western Atlantic liopropomins. Zookeys 409:71-92 doi: 10.3897/zookeys.409.7249.

Baldwin, C.C. and D.R. Robertson. 2015. A new, mesophotic Coryphopterus goby (Teleostei, Gobiidae) from the southern Caribbean, with comments on relationships and depth distributions within the genus. Zookeys 513: 123-142, doi: 10.2897/zookeys.513.9998.

Baldwin, C.C., D.E. Pitassy, and D.R. Robertson. 2016a. A new deep-reef scorpionfish (Teleostei: Scorpaenidae: Scorpaenodes) from the southern Caribbean with comments on depth distributions and relationships of western Atlantic members of the genus. Zookeys 606:141-158, doi: 10.3897/zookeys.606.8590.

Baldwin, C.C., D.R. Robertson, A. Nonaka, and L. Tornabene. 2016b. Two new deep-reef basslets (Teleostei: Grammatidae: Lipogramma), with comments on the eco-evolutionary relationships of the genus. Zookeys 638:45-82. doi: 10.3897/zookeys.638.10455

Belleville, B. 2002. Deep Cuba: The Inside Story of an American Oceanographic Expedition. University of Georgia Press, Athens, GA, USA, 273 p.

Belleville, B. 2004. Sunken Cities, Sacred Cenotes, and Golden Sharks: Travels of a Water—Bound Adventurer. University of Georgia Press, Athens, GA, USA, 233 p.

Brubakk, A.O. and T.S. Neuman. 2003. Bennett and Elliott's Physiology and Medicine of Diving. Saunders Book Company, Collingwood, Ontario, Canada, 800 p.

Clark, E. 1969. Lady and the Sharks. Harper and Row Publishers, New York, NY, USA, 269 p.

Claro, R., R.G. Gilmore, C.R. Robins, and J.E. McCosker. 2000. Nuevos registros para la ictiofauna marina de Cuba. Avicennia12/13: 19—24.

Cousteau, J.Y 1952. Fish men explore a new world undersea. National Geographic 102:431—472.

Cousteau, J.Y. and J. Dugan. 1962. The Living Sea. Harper and Row, New York, NY, USA, 325 p.

Cousteau, J.Y and F. Dumas. 1953. The Silent World. Harper Brothers, New York, NY, USA, 266 p.

Cousteau, J.Y and S. Schiefelbein. 2007. The Human, the Orchid, and the Octopus: Exploring and Conserving our Natural World. Bloombury, New York, NY, USA, 305 p.

Finlayson, H.W. 2009. The Pathophysiology of Saturation Diving. Ph.D thesis. University of St. Andrews, St. Andrews, Scotland, UK, 73 p.

Gilmore, R.G. 1977a. Fishes of the Indian River lagoon and adjacent waters, Florida. Bulletin of the Florida State Museum 22:101—147.

Gilmore, R.G. 1977b. Notes on the opossum pipefish, *Oostethus lineatus* from the Indian River lagoon and vicinity, Florida. Copeia 1977:781—783.

Gilmore, R.G. 1979. *Varicus marilynae*, a new gobiid fish from Florida. Copeia 1979:126—128.

Gilmore, R.G. 1980. Color morphs and the classification of the *Epinephelus niveatus* complex. Book of Abstracts, Association of Southeastern Biologists, Tampa, FL, USA, 18—23 April 1980, p. 27.

Gilmore, R.G. 1983. Observations on the embryos of the longfin mako, *Isurus paucus* Guitart Manday and bigeye thresher shark, *Alopias superciliosus* (Lowe). Copeia 1983:375—382.

Gilmore, R.G. 1986. Reproductive strategies in lamnoid sharks. In: T. Uyeno, R. Arai, T. Taniuchi, and K. Matsuura, eds. Indo—Pacific Fish Biology: Proceedings of the Second International Conference on Indo—Pacific Fishes, Ichthyological Society of Japan, Tokyo National Museum, Ueno Park, Tokyo, 29 July—3 August 1985, p. 926—927.

Gilmore, R.G. 1991. Reproductive biology of Lamnoid sharks. In: S.H. Gruber, ed. Discovering Sharks: A Volume Honoring the Work of Stewart Springer. American Littoral Society, Highlands, NJ, USA, p. 64—67.

Gilmore, R.G. 1993. Reproductive strategies in Lamnoid sharks. Environmental Biology of Fishes 38:95—114. doi: 10.1007/BF00842907

Gilmore Jr., R.G. 1995a. Zoogeographic variation in Antillean and continental deep reef fish faunas at depths between 100 and 700 m in the Caribbean and Bahama Islands. Book of Abstracts, 75th Annual Meeting, American Society of Ichthyologists and Herpetology, Edmonton, Alberta, Canada (15—19 June 1995), p. 109.

Gilmore Jr., R.G. 1995b. Neotropical marine fish distribution, recruitment success and habitat limitation. Book of Abstracts, American Fisheries Society 125th Annual meeting, Tampa, FL, USA, 28—31 August 1995, p. 224.

Gilmore, R.G. 1995c. Environmental and biogeographic factors influencing ichthyofaunal diversity: Indian River Lagoon. Bulletin of Marine Science 57:153—170.

Gilmore, R.G. 1997. *Lipogramma robinsi*, a new grammatid fish from the tropical western Atlantic with descriptive and distributional notes on *L. flavescens* and *L. anabantoides*. Bulletin of Marine Science 60:782—788.

Gilmore, R.G. 2001. A comparative study of manned and unmanned submersible capabilities, generic sensor systems needs for the study of mobile marine fauna. Proceedings, Generic Sensor System Needs for Undersea Research Vehicles Symposium, Miami, FL, USA, 6 May 2001, p. 125—138.

Gilmore, R.G. 2003. Integrated environmental assessment: new technologies and systems for terrestrial, aquatic and extra—terrestrial applications. Emerging Technologies, Tools, and Techniques to Manage Our Coasts in the 21st Century, Technology Transfer Conference, Sponsored by the U.S. EPA Office of Water, Office of Wetlands, Oceans, and Watersheds, Oceans and Coastal Protection Division, Washington, D.C., USA, 28—31 January 2003, p. 41.

Gilmore, R.G and R.S. Jones. 1988. *Lipogramma flavescens*, a new grammid fish from the Bahama Islands with descriptive and distribution notes on *L. evides* and *L. anabantoides*. Bulletin of Marine Science 42:435—445.

Gilmore, R.G. and R.S. Jones. 1992. Color variation and associated behavior in the epinepheline groupers, *Mycteroperca microlepis* (Goode and Bean) and *M. phenax* Jordan and Swain. Bulletin of Marine Science 51:83—103.

Gilmore, R.G. and J.E. McCosker. 1996. Comparative submersible observations of epibathyal fish assemblages: Caribbean Sea and Galapagos Islands. Book of Abstracts, 76th Annual Meeting, American Society of Ichthyologists and Herpetologists, New Orleans, LA, USA, 13—19 June 1996, p. 154.

Gilmore, R.G., J.K. Holt, R.S. Jones, G.R. Kulczycki, L.G. MacDowell, III, and W.C. Magley. 1978. Portable tripod drop—net for estuarine fish studies. Fishery Bulletin 76:285—289.

Gilmore, R.G., P.A. Hastings, and G.R. Kulczycki. 1981. Crystalline rotenone as a reliable and effective fish toxin. Florida Scientist 44:193—203.

Gilmore, R.G., J.W. Dodrill, and P.A. Linley. 1983a. Embryonic development of the sand tiger shark *Odontaspis taurus* Rafinesque. Fishery Bulletin 81:201—225.

Gilmore, R.G., P.A. Hastings, and D.J. Herrema. 1983b. Ichthyofaunal additions to the Indian River lagoon and adjacent waters, east—central Florida. Florida Scientist 46:22—30.

Gilmore, R.G., A.M. Clark, and J. Cooke. 2003. Technologies for sustained biological resource observations with potential applications in coastal homeland security. Marine Technology Society Journal 37(3):134—141. doi: 10.4031/002533203787537159

Gilmore, R.G., O. Putz, and J.W. Dodrill. 2005. Oophagy, intrauterine cannibalism and reproductive strategy in lamnoid sharks. In: W. Hamlett, ed. Reproductive Biology and Phylogeny of Chondrichthyes. Science Publishers, Inc., Enfield, NH, USA. p. 435—462.

Kottler, C.F. 1969. Underwater systems within the scientific technological, and economic framework. Journal of Hydronautics 3:2—11. doi: 10.2514/3.62798

Limburg, P.R. and J.B. Sweeney. 1973. Vessels for Underwater Exploration. Crown Publishers, Inc., New York, NY, USA, 154 p.

Link, E.A. 1963. Our man in the sea project. National Geographic 123:713—717.

Link, E.A. 1964. Tomorrow on the deep frontier. National Geographic 125:778—802.

Link, E.A. and B. Littlehales. 1965. Outpost under the ocean. National Geographic 127:530—533.

Link, M.C. 1958. Sea Diver: A Quest for History Under the Sea. Holt, Rinehart and Winston, New York, NY, USA, 333 p.

Link, M.C. 1973. Windows in the Sea. Smithsonian Institution Press, Washington, D.C., USA, 198 p.

Marden, L. 1998. Master of the deep: Jacques—Yves Cousteau, 1910—1997. National Geographic 193:70—79.

McCosker, J.E. and R.G. Gilmore, Jr. 1996. Recent studies of the Galapagos ichthyofauna using SCUBA and submersible. Book of Abstracts, 76th Annual Meeting, American Society of Ichthyologists and Herpetologists, New Orleans, LA, 13—19 June 1999, p. 154.

McCosker, J.E., G. Merlen, D.J. Long, R.G. Gilmore, and C. Villon. 1997. Deep slope fishes collected during the 1995 eruption of Isla Fernandina, Galapagos. Noticias de Galapagos (May) 58: 22–26.

Messing, C.G., K. Stanley, J.K. Reed, and R.G. Gilmore. 2013. The first *in situ* habitat observations and images of the Caribbean roughshark, *Oxynotus caribbaeus* Cervigon, 1961 (Squaliformes: Oxynotidae). Proceedings of the Biological Society of Washington 126:234–239. doi:10.2988/0006–324X–126.3.234

Oceanography in Florida. 1970. R.E. Ring, and C. Ruis, eds. Florida Council of 100, Tampa, FL, USA, 262 p.

Penzias, W. and M.W. Goodman. 1973. Man Beneath the Sea: A Review of Underwater Ocean Engineering. Wiley–Interscience, New York, NY, USA, 831 p.

Piccard, J. 1971. The Sun Beneath the Sea. Charles Scribner's Sons, New York, NY, USA, 405 p.

Reed, J.K. and R.G. Gilmore. 1981. Inshore occurrence and nuptial behavior of the roughtail stingray, *Dasyatis centroura* (Dasyatidae), on the continental shelf, east–central Florida. Northeast Gulf Science 5:59–62.

Robertson D.R. and K.L. Cramer. 2014. Defining and dividing the Greater Caribbean: Insights from the biogeography of shorefishes. PLoS ONE 9(7): e102918. doi:10.1371/journal.pone.0102918

Stenuit, R. 1964. The deepest days. National Geographic 125:534–547.

Sweeney, J.B. 1970. A Pictorial History of Oceanographic Submersibles. Crown publishers, Inc., New York, NY, USA, 145 p.

Terry, R.D. 1966. The Deep Submersible. Western Periodicals Co., North Hollywood, CA, USA, 456 p.

Tornabene L, J.L Van Tassel, D.R. Robertson, and C.C. Baldwin. 2016a. Repeated invasions into the twilight zone: evolutionary origins of a novel assemblage of fishes from deep Caribbean reefs. Molecular Ecology. doi: 10.1111/mec.13704.

Tornabene, L., J.L. Van Tassell, R.G. Gilmore, D.R. Robertson, F. Young, and C.C. Baldwin. 2016b. Molecular phylogeny, analysis of character evolution, and submersible collections enable a new classification of a diverse group of gobies (Teleostei: Gobiidae: *Nes* subgroup), including nine new species and four new genera. Zoological Journal of the Linnean Society 177:764–812. doi:10.1111/zoj.12394

Trillo, R.L., ed. 1979. Jane's Ocean Technology, 4th edition, 1979–1980. Jane's Yearbooks, Franklin Watts Inc., New York, NY, USA, 824 p.

van Hoek, S. and M.C. Link. 1993. From Sky to Sea: A Story of Edwin A. Link. Best Publishing Co., Flagstaff, AZ, USA, 319 p.

Van Tassell, J.L., L. Tornabene, and P.L. Colin. 2012. Review of the western Atlantic species of *Bollmannia* (Teleostei: Gobiidae: Gobiosomatini) with the description of a new allied genus and species. Aqua, International Journal of Ichthyology 18:61–94.

Wicklund, R.I. 2011. Eyes in the Sea: Adventures of an Undersea Pioneer. Mariner Publishing, Buena Vista, VA, USA, 289 p.

Young, D.K., R.M. Avent, L.I. Briel, N.J. Eiseman, R.H. Gore, R.S. Jones, G.A. Kerr, H.H. Seibert, O. Von Zweck, and J.R. Wilcox. 1974. Harbor Branch Consortium: Indian River Study. Annual Report 1973–1974, Vol. 1–2. D.K. Young (ed.). Harbor Branch Foundation, Link Foundation, Smithsonian Institution, Woods Hole Oceanographic Institution, Fort Pierce, FL, USA, 385 p.

Open access of this article supported by the
Mississippi–Alabama Sea Grant Consortium.

Gulf and Caribbean Research

Volume 27 | Issue 1

2016

Phytoplankton pigment specific growth and losses due to microzooplankton grazing in a northern Gulf of Mexico estuary during winter/fall

Amanda M. McGehee
University of Southern Mississippi, amanda.mcgehee@usm.edu

Donald G. Redalje
University of Southern Mississippi, Donald.Redalje@usm.edu

Recommended Citation

McGehee, A. M. and D. G. Redalje. 2016. Phytoplankton pigment specific growth and losses due to microzooplankton grazing in a northern Gulf of Mexico estuary during winter/fall. Gulf and Caribbean Research 27 (1): 1-10.
Retrieved from https://aquila.usm.edu/gcr/vol27/iss1/1
DOI: https://doi.org/10.18785/gcr.2701.01

Gulf and Caribbean Research Vol 27, 1-10, 2016
DOI: 10.18785/gcr.2701.01
Manuscript received, November 12, 2015; accepted, March 11, 2016

PHYTOPLANKTON PIGMENT SPECIFIC GROWTH AND LOSSES DUE TO MICROZOOPLANKTON GRAZING IN A NORTHERN GULF OF MEXICO ESTUARY DURING WINTER/FALL

Amanda M. McGehee[1]* and Donald G. Redalje
*Department of Marine Science, University of Southern Mississippi, 1020 Balch Drive, Stennis Space Center, MS 39525, USA; [1]Current Address: Department of Coastal Sciences, University of Southern Mississippi, 703 East Beach Drive, Ocean Springs, MS 39564, USA; *Corresponding author, email: Amanda.Mcgehee@usm.edu*

ABSTRACT: Microzooplankton dilution grazing experiments were carried out on 6 dates, over a 3 month period at 2 locations in the Bay of St. Louis, MS (BSL) to determine phytoplankton pigment specific growth rates under natural (μ_0) and replete (μ_n) nutrient conditions and microzooplankton grazing. We hypothesized that diatoms would be the largest portion of the phytoplankton composition due to the winter/fall season and that these organisms would have the highest growth/grazing rates. We suspected that river flow from the Jourdan River would adversely affect growth and grazing rates of all phytoplankton classes. Growth rates of 5 phytoplankton accessory pigments (peridinin, fucoxanthin, alloxanthin, zeaxanthin, chlorophyll b) were identified. Intrinsic growth rates (μ_0) were often zero or negative (range: –0.46 to 0.56/d) at the location nearest the Jourdan River, particularly for alloxanthin (e.g., cryptophytes) and peridinin (e.g., dinoflagellates). Significant grazing of chlorophyll *a* was observed on 3 of 6 dates while grazing on marker pigments was variable. The phytoplankton community appeared nutrient limited during all but one experiment ($\mu_0<\mu_n$). Intrinsic growth and grazing rates were correlated ($p < 0.05$, Spearman Rank Order correlation). Peridinin and alloxanthin–based growth and grazing rates were positively correlated with salinity, suggesting a river influence on these 2 phytoplankton pigment classes. We conclude that in the BSL microzooplankton preferentially grazed on the phytoplankton class which had the highest intrinsic growth rate. We show that this is greatly affected by riverine input into the estuary and nutrient limitation.

KEY WORDS: Phytoplankton ecology, Subtropical Estuary, Dilution Technique, Grazing, Nutrient limitation

INTRODUCTION

The primary source of phytoplankton mortality in coastal and estuarine systems is grazing by microzooplankton (< 200 µm), which can represent an average loss of 60% of phytoplankton production (Calbet and Landry 2004). Grazing has been shown to control not only the abundance of phytoplankton in a population, but also the composition of the population through selective grazing on different phytoplankton classes (Porter 1977; Burkill et al. 1987; Strom and Welshmeyer 1991). The Landry and Hassett (1982) dilution technique is the most widely used method for the simultaneous estimation of phytoplankton growth and microzooplankton grazing rates in marine waters with minimal manipulation of the community. Application of this technique has enabled the examination of microzooplankton grazing and its impact on phytoplankton biomass and composition in a wide range of ocean systems (Calbet and Landry 2004; Schmoker et al. 2013).

The dilution technique was adapted by Burkhill et al. (1987) to give growth and grazing rates of individual phytoplankton taxa by coupling it with HPLC pigment analysis. Utilizing taxon–specific marker pigments, grazing and growth rates varied by phytoplankton taxa and were often significantly correlated, with faster growing phytoplankton classes grazed at the highest rates (Burkill et al.1987; Strom and Welschmeyer 1991; Latasa et al. 1997). There are limited data available on applications of the dilution technique in subtropical estuaries in comparison to other locations, thus representing a major knowledge gap (Schmoker et al. 2013).

Since estuaries are directly affected by urbanization, it is important to understand phytoplankton growth and losses, since nutrient loading can lead to an increase in biomass and/or blooms. Studies examining phytoplankton growth and microzooplankton grazing rates in subtropical estuaries have shown a strong top–down control of the phytoplankton community (Juhl and Murrell 2005; Palomares–García et al. 2006; Putland and Iverson 2007). In these studies, the rates of growth and grazing were of similar magnitude and microzooplankton proved to be major consumers of phytoplankton production. In other studies, growth rates were often greater than grazing rates, suggesting other factors controlled the population such as viral lysis, physical factors, and/or environmental conditions (Chevez et al. 1991; Landry et al. 1995; Murrell et al. 2002; Calbet et al. 2011; Ortmann et al. 2011).

The biological communities in the Bay of St. Louis (BSL) presented an opportunity to increase our understanding of the interaction between phytoplankton growth, microzooplankton grazing, and nutrient limitation. Recent studies indicate that the N/P ratio was lower than the Redfield ratio and given the low concentration of dissolved inorganic nitrogen (DIN), the BSL was considered nitrogen–deficient (Cai et al. 2012; Camacho et al. 2014). Dissolved inorganic nitrogen concentrations ranged from <1 µM to 12 µM and were highest during high river discharge (Sawant 2009; Cai et al. 2012; Camacho et al. 2014). Orthophosphate (PO_4^{3-}) concentrations were generally low with mean concentrations

of < 0.5 µM, and increase with increasing salinity (Phelps 1999; Sawant 2009; Cai et al. 2012).

The taxonomic composition of the phytoplankton assemblage and its relation to measured environmental parameters has been previously examined in the BSL (Holtermann 2001; Molina 2011). In Holtermann (2001), the phytoplankton was comprised of diatoms, cyanobacteria, and chlorophytes during summer and by diatoms during winter. During the winter, chlorophyll *a* (chl *a*) was dominated by diatoms. A bloom of dinoflagellates occurred during the spring and fall at the mouth of the Jourdan River (JR), while during the rest of the year dinoflagellates contributed little to total chl *a*. Molina (2011) examined one station near the mouth of the BSL, finding diatoms were the dominant taxa during the study period (September 2007 to November 2009) and there was no clear indication of any seasonal trends in composition.

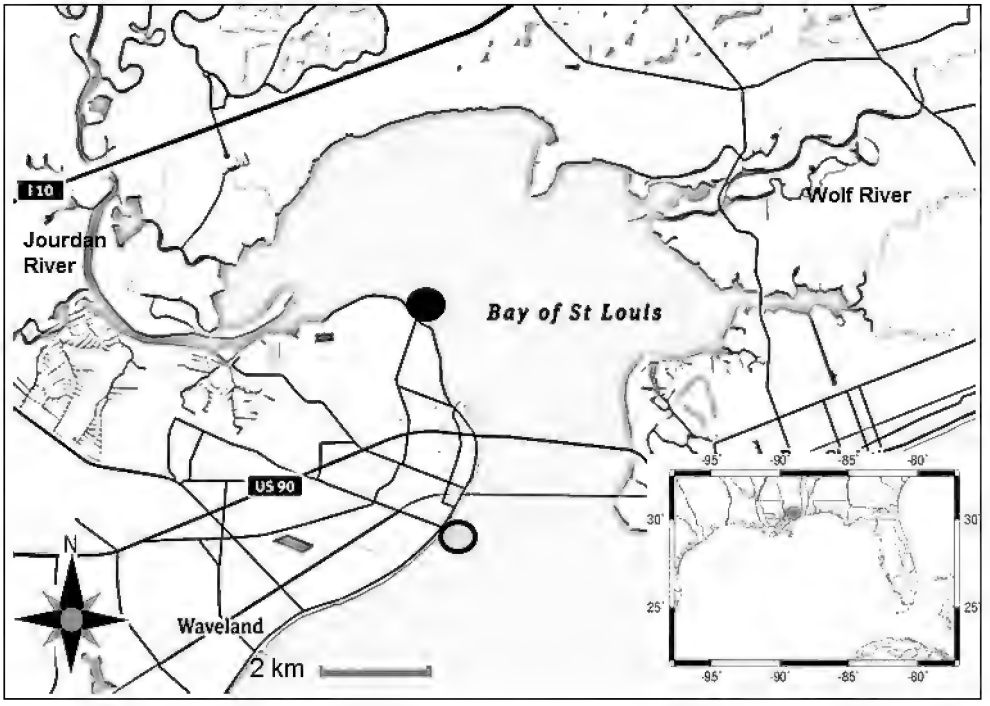

FIGURE 1. *Map of the Bay of St. Louis with the location of the Dunbar Street and Washington Street piers marked (solid and open circles, respectively). Inset: location of the sampling area along the northern Gulf of Mexico.*

No studies have investigated microzooplankton grazing on phytoplankton in the BSL. The purpose of this study was to fill a knowledge gap in phytoplankton ecology about the dynamics of phytoplankton growth and microzooplankton grazing in this nutrient limited subtropical estuary. We hypothesized that diatoms would be the most prevalent species during winter samplings, and that they would have high growth rates and therefore high grazing rates in the BSL. We also believe that environmental factors, particularly salinity, will affect the growth and grazing rates of all phytoplankton pigment classes.

Materials and Methods

Site Description

The BSL is a small (area = 40 km^2; Eleuterius 1984), shallow (~1.5 m mean depth) semi—enclosed estuary located on the Gulf of Mexico coast of Mississippi (MS) connected to the Mississippi Sound (a large barrier island estuary that spans 145 km between MS and Alabama (AL)) through an inlet that is about 3 km wide and 300 m long (Figure 1). Two rivers provide freshwater input to the BSL: the JR to the west (historical mean discharge rate: 23.5 m^3/s) and the Wolf River (WR) to the east (historical mean discharge rate: 20 m^3/s; Eleuterius, 1984). The range of salinity in the BSL is 0—26 and is lower in the winter due to increased river runoff (Phelps 1999; Sawant 2009; Cai et al. 2012). Water temperature ranges from 9.9—33.2°C annually (Phelps 1999; Sawant 2009; Cai et al. 2012). Annual chl *a* concentration ranges from 0.12—56.08 µg/L (Sawant 2009).

Sample Collection and Processing

Samples were collected from the Washington Street (WS) pier located near the mouth of the bay and the Dunbar Street (DS) pier located near the mouth of the JR (Figure 1). Sampling was conducted once monthly for 3 months (November 2013 through January 2014) at each location. The WS location was sampled and processed first, the DS location was sampled 2 days later.

All incubation bottles, filtration flask, and filter holders used in the study were washed with 10% HCl and triple rinsed with nanopure water. Sampling carboys were triple rinsed with BSL water prior to filling. On sampling days, 50 L of surface water was collected and environmental parameters (temperature (°C), salinity, turbidity (formazine turbidity units, FTU)) were measured using an In—Situ® Multi—Parameter Troll 9500 WQP—100 (In—Situ Inc.) profiling device. After returning to the laboratory, the water sample was filtered through 200 µm mesh to remove the larger zooplankton and detritus.

Initial samples were taken from the carboy for analysis of pigment composition (µg/L), nutrient concentrations (µM), particulate organic carbon (POC; mg/L), and particulate nitrogen (PN; mg/L). Triplicate whole seawater samples (WSW) were prepared in 2 L trace metal—clean polycarbonate bottles (Fitzwater et al. 1982). The bottles were soaked in Micro—90 cleaning solution (Sigma Chemical Company)

for a total of 5 days, rinsed with nanopure water, soaked for 2 days in nanopure water, and finally soaked in 10% HCL to ensure removal of trace metals. A carboy containing 26 L of WSW was spiked with nutrients to a final concentration of 16 µM NO_3^- and1.6 µM PO_4^-. Particle free seawater (PFSW) was prepared by filtering half the spiked sample through a 142 mm diameter Gelman A/E glass fiber filter followed by filtration through a 0.2 µm Whatman POLYCAP TC filter capsule to ensure removal of all organisms (Li and Dickie 1985). The dilution series included triplicates of 100%, 70%, 40%, and 10% WSW diluted with PFSW. The bottles were incubated for 24 h at *in situ* temperature in a Sanyo MLR–351H plant growth chamber using a 12:12 light:dark cycle. The light levels in the incubators were measured to be about 300 micromoles quanta/m^2/sec using a Biospherical Instruments, Inc. QSL–100 Quantum Scalar Photosynthetically Available Radiation (PAR) Irradiance Sensor. Incubator conditions were monitored throughout the experiment using an Onset HOBO Data Logger with temperature and PAR sensors.

HPLC Analysis

For pigment analysis, about 350–1600 mL of sample was filtered onto 47 mm Whatman GF/F filters, then placed into a cryotube, and stored in liquid nitrogen until HPLC analysis. Prior to HPLC analysis, samples were freeze dried to remove excess water, which allowed for better extraction of the pigments (Hagerthey et al. 2006). Pigments were then extracted from the filters overnight in 90% acetone and filtered through a 0.2 µm PTFE syringe filter to remove particles. A 1:1 mixture of extracted sample and ion pairing agent (IPA: 0.5 M Ammonium Acetate at pH 7.2) was prepared for injection. The HPLC method of Wright et al. (1991) was used for detection of pigments using an Alltech Alltima High Purity C–18 column on a Waters 600 Controller and Pump HPLC connected to a Waters 2996 Photodiode Array Detector. The method was modified as follows: solvent B was changed to 100% acetonitrile with 0.01% 2,6–di–*tert*–butyl–4–methylphenol. The external standard equation of Mantoura and Repeta (1997) was used to calculate pigment concentration of the sample.

Particulate Organic Carbon and Nitrogen Analysis

About 50 mL of WSW was filtered onto a combusted (450°C, 6 h) 21 mm Whatman GF/F filter for the determination of POC and PN. The samples were dried (60°C, 24 h), folded and placed into tin boats, and analyzed using a Costech ECS 4010 elemental analyzer. The concentration of the sample was determined from a standard linear regression using acetanilide constructed for each run of 3 runs (r^2 ranged from 0.998–0.999 for N and 0.999–1.00 for C).

Nutrient Analysis

About 50 mL of sample were filtered through a pre–rinsed Whatman 25 mm GF/F filter for nutrient analysis. The filtrate was stored frozen (–4°C) in acid cleaned (10% HCL) 250 mL polyethylene sample bottles until analysis. Samples were analyzed fluorometrically (nitrogen species) and colormetrically (PO_4^- and $Si(OH)_4$) using an Astoria Pacifica A2+2 nutrient auto–analyzer (Method #A179, A027, A205, and A221; Astoria–Pacific International, Oregon USA).

Calculations

Growth and grazing rates (/d) of pigments were calculated based on the method of Landry et al. (1995). The apparent growth rate (k) is defined as growth in the incubation bottles in the presence of grazing pressure and calculated by: $k = (1/t)\ln[N_t/(N_o \times D)]$, where N_t and N_o are the final and initial pigment concentrations (µg/L), respectively, D is the proportion of WSW, and t is duration of incubation (h). The grazing rate (m) was calculated as the slope of the model II regression between k and dilution factor; if the slope was not significantly different from zero ($p > 0.05$), then m was assumed zero (0/d). The intrinsic growth rate (μ_o), growth in the absence of added nutrients and grazing, was calculated as k in non–diluted, non–nutrient amended bottles plus grazing rate ($\mu_o = k + m$). The nutrient–replete growth rate (μ_n, defined as growth in the presence of added nutrients and absence of grazing) was estimated as the Y–axis intercept of the linear regression (model II) between k (y axis) and dilution factor (D), for cases when the slope of the regression was significantly different from zero ($p < 0.05$). When the slope of the regression was not significantly different from zero, μ_n was calculated as the mean k of all nutrient–replete dilutions.

Nutrient limitation was explored using the Nutrient Limitation Index (NLI; Landry et al. 1998). This metric is the ratio of the growth rate in the absence of nutrients (μ_o) to the growth rate in the presence of nutrients (μ_n). When NLI is <1, the phytoplankton class is considered to be nutrient limited during the incubation.

Statistics

Significance and the 95% confidence interval of the model II (standard major axis: SMA; one–tailed; 99 permutations) regression were determined using the lmodel2 package in the statistical program R (Legendre 2008; R Core Team 2013). To compare growth and grazing rates to selected measured environmental parameters, a Spearman correlation (r_s, two–tailed; H0: There is no association between the two variables) was performed using SPSS v22.

Results

Conditions in the Bay

Temperature at all sampling locations ranged from 4.8–15.4°C, while salinity ranged from 10.9–23.1 (Table 1). Inorganic nitrogens (NO_2, NO_3, and NH_4) were low during all samplings (< 2 µM). Chlorophyll *a* ranged from 4.2–9.7

TABLE 1. *Measured environmental conditions (mean ± sd) at the Washington St. (WS) location and the Dunbar St. (DS) location. FTU = formazine turbidity units.*

Site	Date	Temp (°C)	Salinity	Turbidity (FTU)	C:N	NO_2 (µM)	NO_3 (µM)	NH_4 (µM)	PO_4 (µM)	SiO_4 (µM)	Chl *a* (µg/L)
WS	11 Nov 2013	15.4	18.7	7	7.7 ± 0.4	0.03	0.17	0.23	0.71	37.55	4.25 ± 0.08
	10 Dec 2013	12.5	23.1	2.9	6.5 ± 0.3	0.05	0.35	1.77	0.52	28.62	5.1 ± 0.07
	09 Jan 2014	4.8	13.6	6.6	11.4 ± 1.5	0.04	0.25	1.60	1.02	50.33	7.2 ± 0.15
DS	14 Nov 2013	10.8	17.6	25.8	9.5 ± 0.2	0.02	0.19	0.31	0.70	39.94	7.0 ± 0.1
	12 Dec 2013	10.8	10.9	19.7	9.2 ± 1.2	0.07	1.27	0.56	0.11	60.54	9.7 ± 0.17
	13 Jan 2014	10.7	10.9	2	8.4 ± 0.8	0.09	0.61	0.63	0.88	66.78	5.0 ± 0.19

µg/L, being highest on 12 December 2013 and lowest on 11 November 2013.

A total of 6 marker pigments were identified in the samples (Table 2). Fucoxanthin was found at the highest concentration indicating the bay was diatom dominated (Figure 2). Peridinin and alloxanthin were also prevalent, indicative of dinoflagellates and cryptophytes. Chlorophyll *b* was found in low concentrations (range 0–0.71 µg/L), whereas lutein and prasinoxanthin were often present at very low concentrations (< 0.13 µg/L). This made it impossible to examine chlorophytes and prasinophytes separately and they were therefore grouped as green algae. Zeaxanthin was detected during November indicating the presence of cyanobacteria.

TABLE 2. *Diagnostic pigments used in this study.*

Pigment	Abbreviation	Taxonomic Group
Peridinin	Per	Dinoflagellates
Fucoxanthin	Fuc	Diatoms
Zeaxanthin	Zea	Cyanobacteria
Alloxanthin	Alx	Cryptophytes
Chlorophyll *b*	Chl *b*	Green Algae
Chlorophyll *a*	Chl *a*	All photosynthetic groups

Growth and grazing rates

The phytoplankton community (measured as chl *a*) had nutrient–replete growth rates (μ_n) that ranged from 0.14–0.79/d (Tables 3 and 4). The intrinsic community growth rates (μ_0) ranged from –0.11 to 0.44/d and were always lower than or similar to the nutrient replete growth rates (μ_n). The lowest growth rates (μ_0 and μ_n) were observed on 14 November 2013 and the highest were observed on 11 November 2013. Significant grazing (m) at the community level (chl *a*) was observed only during three of the samplings (Tables 3 and 4; range 0–0.49/d). During the three samplings in which significant grazing on the community (chl *a*) was observed, grazing rates were lower than or similar to nutrient–replete growth rates (μ_n).

The nutrient–replete growth rate (μ_n) for marker pigment classes at the WS location ranged from 0–1.0/d (Table 3). Diatoms (fucoxanthin) had the highest growth rates (μ_n) in November and December (1.01 and 0.93/d, respectively); while in January diatoms and green algae had similar rates (0.36 and 0.33/d, respectively). The intrinsic growth rates (μ_0), estimated using marker pigments, ranged from 0–0.73/d and varied for all pigment classes (Table 3). The intrinsic growth rates (μ_0) were less than or similar to the nutrient replete growth rates, except for alloxanthin during December, when μ_0 (0.73/d) was greater than μ_n (0.58/d).

The growth rates observed at the DS location often showed extreme nutrient limitation (NLI < 1), which varied by pigment class. The nutrient–replete growth rate (μ_n) ranged from 0–0.67/d at the DS location (Table 4). Large negative intrinsic growth rates were observed for peridinin and alloxanthin (–0.46 and –0.32/d, respectively) in December due to nutrient limitation within the incubation bottle.

Grazing rates (m) for marker pigment classes ranged from 0–0.88/d during the study (Tables 3 and 4). Selective grazing on specific pigments was observed in 5 out of 6 experiments. In one experiment significant grazing was observed for all marker pigment classes (11 November 2013 sampling, WS). In another experiment (12 December 2013; DS) no significant grazing was observed for any marker pigment.

Possible Controls on Phytoplankton Growth and Microzooplankton Grazing

Three possible controls of phytoplankton growth and microzooplankton grazing were explored to gain an understanding of these processes: nutrient limitation during the incubation, coupling between growth and grazing rates, and correlations with measured environmental variables. Nutrient limitation during the incubation was observed during all experiments based on the NLI (Tables 3 and 4). The large values in the table are due to nutrient–replete growth rates (μ_n) close to 0/d and large negative values for μ_0. Alloxanthin in January at the WS location had no NLI value due to μ_n = 0/d.

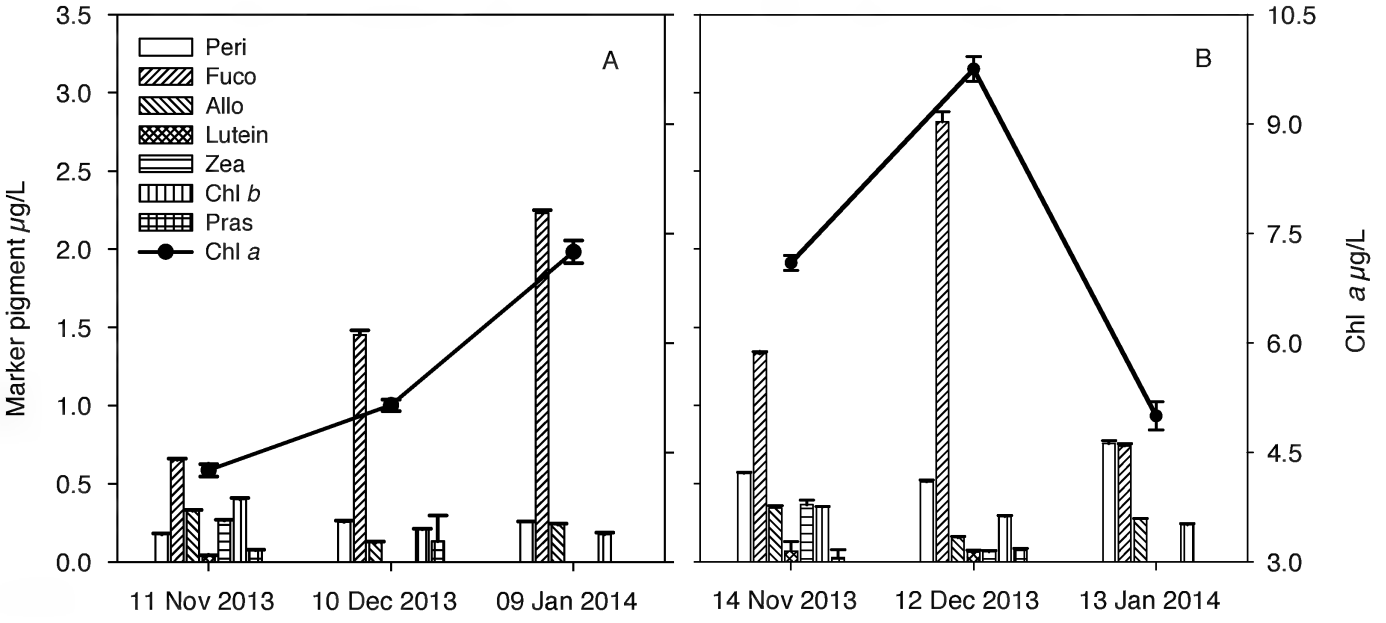

FIGURE 2. *Mean (± sd) marker pigment and chl a concentrations of the Bay of St. Louis for the Washington Street (A) and Dunbar Street (B) sampling locations during all sampling periods. Per = peridinin, Fuc = fucoxanthin, alx = alloxanthin, Zea = zeaxanthin, Chl* b *= chlorophyll* b*, Pras = prasinoxanthin, Chl* a *= chlorophyll* a*.*

A reported mechanism to explain selective grazing of microzooplankton on the phytoplankton community is that microzooplankton selectively graze on the phytoplankton classes which demonstrate the highest growth rates. The intrinsic growth rate (μ_o) was significantly correlated to grazing rates at the WS location (r_s = 0.698, p = 0.003) and the DS location (r_s = 0.773, p < 0.001; Figure 3). The nutrient–replete growth rate was not correlated with the grazing rates at either location. To determine if microzooplankton grazed on phytoplankton classes that experienced the least amount of nutrient limitation, grazing rates were compared to NLI. The NLI was correlated to grazing rates only at the DS location (r_s= 0.873, p = 0.001; Figure 3B). The negative values obtained for the nutrient limitation index were removed from this analysis since they were a product of the calculation and are not an accurate measure of the phytoplankton dynamics. A comparison of biomass (µg/L of pigment) and grazing rates showed no correlation (p > 0.05) indicating that phytoplankton classes were not selectively grazed due to high abundance.

Measured environmental conditions at the time of sampling were correlated to some phytoplankton pigment classes. Peridinin and alloxanthin growth and grazing rates were shown to be correlated significantly with salinity of the bay (Table 5; for peridinin r_s = 0.899 for μ_o, r_s = 0.841 for μ_n and r_s = 0.941 for m; for alloxanthin r_s = 0.986 for μ_o and 0.955 for m; all p < 0.05). The correlation analysis also showed that silicate was correlated inversely to salinity within the BSL (r_s = –0.986, p < 0.01 data not shown). Nutrient–replete growth rates and grazing rates for alloxanthin were also correlated significantly with temperature (Table 5, r_s = 0.899 for μ_n and 0.832 for m; both p < 0.05). Fucoxanthin and chl *a* nutrient–replete growth rates were correlated inversely (r_s = –0.829, p < 0.05) to the C:N ratio of particulate organic matter at the time of sampling.

Discussion

This study demonstrated that microzooplankton grazing and environmental conditions may play an important role in controlling phytoplankton composition in the BSL. Nutrient limitation was observed during 5 out of 6 of the samplings, as evident by higher growth rates in nutrient replete incubation bottles and the low observed nutrient concentrations. Microzooplankton grazers selected the phytoplankton classes that had the highest intrinsic growth rate, therefore exerting a degree of control on phytoplankton composition. Growth and grazing rates of cryptophytes (alloxanthin) and dinoflagellates (peridinin) were correlated with measured environmental parameters (e.g. salinity, silicate, and temperature) indicating the importance of fresh water inflow in controlling phytoplankton composition.

The community growth rates (chl *a*) were similar to rates measured in other Gulf of Mexico estuaries: the Suwannee River estuary in Florida (Jett 2004) and Mobile Bay in Alabama (Lehrter et al. 1999; Ortmann et al. 2011). The growth rates were also similar to those found in estuaries in other regions (Murrell and Hollibaugh 1998; Calbet and Landry 2004; York et al. 2010). Calbet and Landry (2004) summarized results from dilution experiments in 66 studies from coastal, oceanic, and estuarine habitats and found that

in estuarine systems the mean community (chl *a*) growth rate was 0.97 ± 0.07/d and the mean grazing rate was 0.53 ± 0.04/d (n=136). The rates measured during the current study only included winter samplings, which may explain why the rates observed were lower than those observed in other studies. It is expected that summer growth and grazing rates would be higher than winter rates due to seasonal factors; this has been shown in other studies at multiple locations (Strom et al. 2001; Gutierrez–Rodriguez et al. 2011; Lawrence and Menden–Deuer 2012). The low ambient nutrient concentration in the BSL is likely also a factor in the low rates observed where nitrogen limitation was suggested.

Even though fucoxanthin was always the dominant pigment, it was not always the pigment with the highest growth rate. This finding indicates that some mechanism controls the biomass of the fastest growing classes, which in this study was shown to be selective grazing by microzooplankton and environmental factors (e.g. salinity, silicate, and temperature). The strong correlation between intrinsic growth and grazing rates suggested that microzooplankton play a large role in controlling phytoplankton biomass, but only for certain phytoplankton classes. This correlation between rates demonstrates the strong ecological coupling between these two groups of organisms and has been demonstrated in numerous studies, including this one (Burkill et al. 1987; Strom and Welschmeyer 1991; Latasa et al. 1997; Murrell et al. 2002). When the phytoplankton in this study were supplemented with nutrients this ecological coupling appeared to break down as evidenced by the lack of correlation between nutrient replete growth rates and microzooplankton grazing rates.

The connection between top–down and bottom–up controls on phytoplankton biomass was previously noted in Pensacola Bay, FL, another Gulf of Mexico estuary (Juhl and Murrell 2005). In Pensacola Bay, the intrinsic growth rates (μ_o) of the phytoplankton were matched by equal grazing rates due to nutrient limitation of the phytoplankton community. In the BSL, grazing rates were higher than intrinsic growth rates (μ_0) for 38.4% of pigments tested. Nutrient–replete growth rates (μ_n) proved to be variable in relation to grazing rates. Negative and zero μ_o were observed when grazing rates were 0/d during 66.6% of the experiments; this was also observed in Long Island

TABLE 3. *Pigment specific regression statistics, growth/grazing rate, and nutrient limitation index (NLI; μ_o/μ_n) for the Washington Street location.*

	Pigment	Model r^2	m/d (95% CI)	μ_n/d (95% CI)	μ_o/d	NLI
11 Nov 13	Chlorophyll a	0.72**	0.49 (0.34, 0.70)	0.79 (0.71, 0.91)	0.35	0.44
	Peridinin	0.73**	0.61 (0.43, 0.87)	0.60 (0.50, 0.74)	0.23	0.39
	Fucoxanthin	0.50**	0.52 (0.31, 0.83)	1.01 (0.89, 1.17)	0.53	0.53
	Zeaxanthin	0.58**	0.32 (0.20, 0.49)	0.81 (0.74, 0.91)	0.73	0.9
	Alloxanthin	0.87**	0.65 (0.51, 0.83)	0.70 (0.62, 0.80)	0.34	0.49
	Chlorophyll b	0.67**	0.53 (0.36, 0.79)	0.87 (0.77, 1.01)	0.52	0.59
10 Dec 13	Chlorophyll a	0.09	0	0.69 (0.61, 0.77)	0.11	0.16
	Peridinin	0.49**	0.37 (0.23, 0.60)	0.44 (0.36, 0.57)	0.24	0.56
	Fucoxanthin	0.13	0	0.93 (0.84, 1.01)	0.32	0.35
	Zeaxanthin	–	–	–	–	–
	Alloxanthin	0.40*	0.88(0.52, 1.48)	0.58 (0.38, 0.91)	0.73	1.26
	Chlorophyll b	0.08	0	0.57 (0.47, 0.67)	0.13	0.24
09 Jan 14	Chlorophyll a	0.32*	0.21 (0.06, 0.93)	0.25 (0.23, 0.37)	0.21	0.77
	Peridinin	0.52**	0.13 (0.08, 0.21)	0.07 (0.04, 0.11)	0.02	0.4
	Fucoxanthin	0.44**	0.28 (0.17, 0.47)	0.36 (0.30, 0.46)	0.31	0.87
	Zeaxanthin	–	–	–	–	
	Alloxanthin	0	0	0	–0.06	
	Chlorophyll b	0.63*	0.47 (0.31, 0.71)	0.33 (0.24, 0.46)	0.33	1.01

*Modell II regression, ** shows significance at p < 0.01, * shows significance at p < 0.05. m = grazing rate, μ_n = nutrient replete growth rate, μ_o= apparent growth rates, CI =Confidence Interval*

TABLE 4. *Pigment specific regression statistics, growth/grazing rate, and nutrient limitation index (NLI; μ_o/μ_n) for the Dunbar Street location.*

	Pigment	Model r^2	m/d (95% CI)	μ_n/d (95% CI)	μ_o/d	NLI
14 Nov 13	Chlorophyll *a*	0.08	0	0.14 (0.10, 0.18)	–0.11	–0.8
	Peridinin	0.37*	0.34 (0.20, 0.58)	0.27 (0.19, 0.40)	0.21	0.77
	Fucoxanthin	0.05	0	0.19 (0.15, 0.23)	–0.01	–0.07
	Zeaxanthin	0.01	0	0.12 (0.08, 0.15)	0.03	0.26
	Alloxanthin	0.56*	0.35 (0.22, 0.54)	0.39 (0.32, 0.50)	0.16	0.41
	Chlorophyll *b*	0.05	0	0.23 (0.17, 0.28)	–0.04	–0.17
12 Dec 13	Chlorophyll *a*	0.17	0	0.50 (0.45, 0.59)	0.13	0.27
	Peridinin	0.14	0	–0.01 (–0.08, 0.05)	–0.46	36.27
	Fucoxanthin	0.09	0	0.67 (0.59, 0.76)	0.34	0.51
	Zeaxanthin	–	–	–	–	
	Alloxanthin	0	0	0.02 (–0.06, 0.10)	–0.32	–15.89
	Chlorophyll *b*	0.14	0	0.46 (0.38, 0.54)	0.07	0.15
13 Jan 14	Chlorophyll *a*	0.45**	0.49 (0.30, 0.82)	0.47 (0.36, 0.65)	0.44	0.94
	Peridinin	0.24	0	0.25 (0.17, 0.33)	0.07	0.31
	Fucoxanthin	0.58**	0.53 (0.34, 0.82)	0.54 (0.44, 0.70)	0.52	0.97
	Zeaxanthin	–	–	–	–	
	Alloxanthin	0.08	0	0.25 (0.07, 0.43)	–0.11	–0.44
	Chlorophyll *b*	0.53**	0.59 (0.37, 0.94)	0.57 (0.45, 0.76)	0.56	0.99

*Modell II regression, ** shows significance at p < 0.01, * shows significance at p < 0.05. m = grazing rate, μ_n = nutrient replete growth rate, μ_o= apparent growth rates, CI = confidence interval*

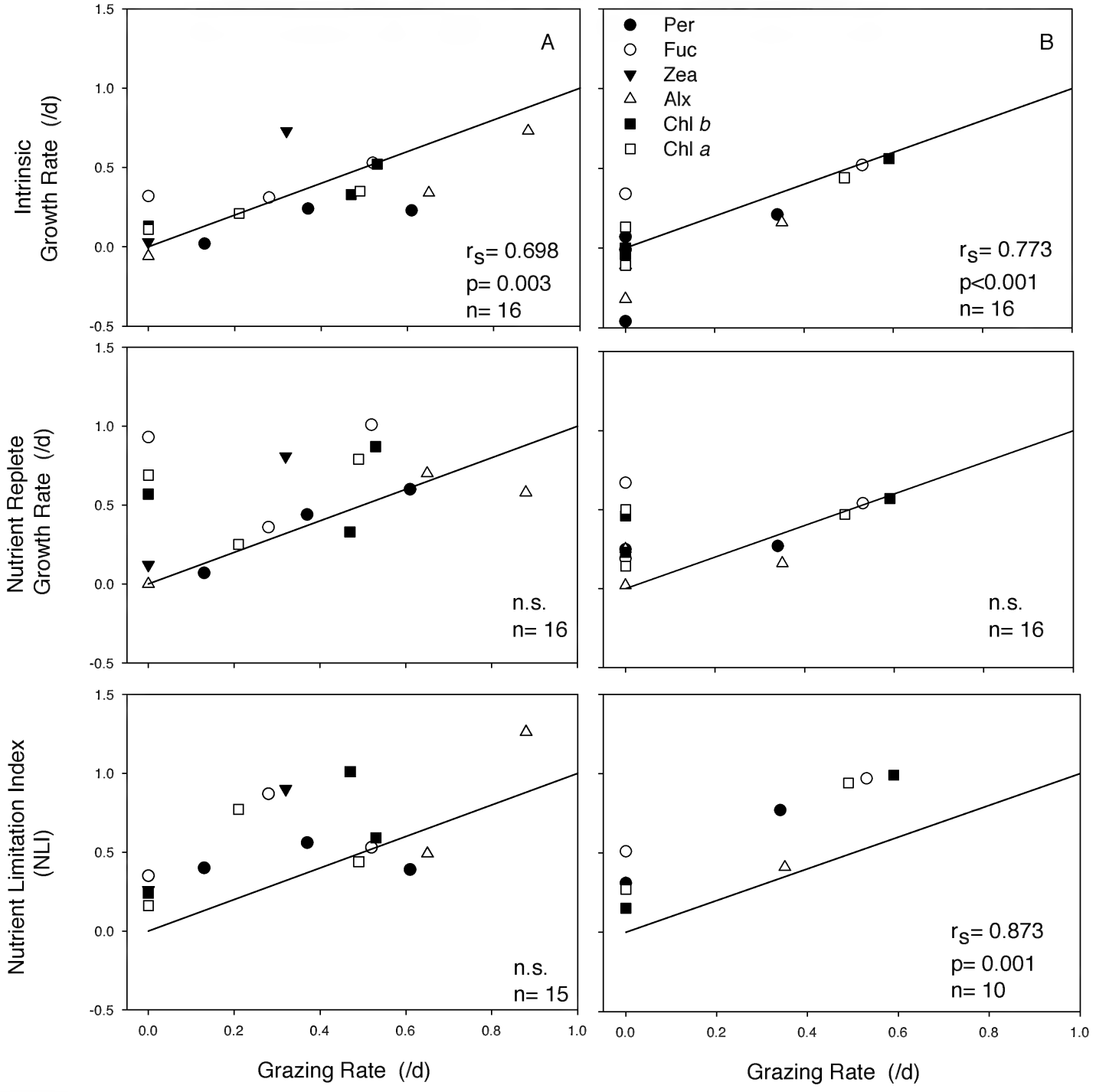

FIGURE 3. *Relationship between grazing rates and intrinsic growth rates (μo), nutrient replete growth rates (μn), and nutrient limitation index (NLI) at the Washington Street (A) and Dunbar Street (B) locations. Per = peridinin, Fuc = fucoxanthin, alx = alloxanthin, Zea = zeaxanthin, Chl* b *= chlorophyll* b*, Pras = prasinoxanthin, Chl* a *= chlorophyll* a*.* r_s*, Spearman Rank Order Correlation.*

Sound, New York and Tuggerah Lake, Australia (York et al. 2010; Sanderson et al. 2012). When nutrient limitation was minimal in the BSL, growth and grazing rates became more similar to one another, suggesting that nutrient limitation played a large role in controlling phytoplankton composition. Non–significant grazing was also more frequently observed at the DS location (69.2% vs. 23% of test), which suggests that the Jourdan River may decouple microzooplankton from their phytoplankton prey. This may be due to the hydrodynamics of the river mouth, lowered salinity, low residence time, and/or higher turbidity.

The correlations between salinity and growth/grazing rates for peridinin and alloxanthin suggested that river flow was a factor in controlling the dynamics of these two phytoplankton classes. The data in this study suggest that during times of low river flow (high salinity) or when sampling further from the JR, dinoflagellates and cryptophytes grew faster and were grazed at a higher rate than the other

TABLE 5. *Significant correlations (r_s, Spearman Rank Order Correlation; $p < 0.05$) between growth rate (μ) or grazing rate (m) with measured environmental parameters (n=6).*

Pigment	Rate	Environmental Parameter	r_s
Peridinin	m	Salinity	0.941
	μ_o	Salinity	0.899
	μ_n	Salinity	0.841
Alloxanthin	m	Temperature	0.832
	m	Salinity	0.955
	μ_o	Salinity	0.986
	μ_n	Temperature	0.899
Fucoxanthin	μ_n	C:N	−0.829
Chl *b*	μ_n	Chl *a* (µg/L)	−0.829
	μ_o	Chl *a* (µg/L)	−0.829
Chl *a*	μ_n	C:N	−0.829

phytoplankton taxa. In Galveston Bay a greater biomass of diatoms was observed near the riverine inputs while dinoflagellates were found in areas of the bay where hydrologic displacement or nutrient loading from the river were not important (Dorado et al. 2015). Previous studies in the BSL have shown that the DIN concentrations were highest during times of high river flow (Sawant 2009; Cai et al. 2012; Camacho et al. 2014). As discussed by Dorado et al. (2015), it is possible that diatoms utilize these nutrient inputs, while they may be unimportant to dinoflagellates and cryptophytes since these organisms may be able to utilize alternative methods to acquire nutrients (i.e., mixotrophy, phagotrophy). Mesocosm studies of estuarine phytoplankton communities have shown that phytoflagellates were more abundant in static waters than waters which were being actively mixed, supporting hydrologic displacement as a factor adversely affecting cryptophytes and dinoflagellates (Pinckney et al. 1999). Further studies are needed in the BSL to further understand the correlation between river flow and growth/grazing rates.

The lack of correlation between ambient nutrient concentrations and phytoplankton growth during the current study is interesting, but not surprising, given the small sample number (n=6). Given the low ambient nutrient concentrations in the BSL it is likely that any new nutrients put into the system will be readily taken up by the phytoplankton community. Therefore, ambient nutrient concentration may be a misleading parameter for relating nutrients to phytoplankton growth. It may be more important to measure nutrient concentrations entering the system (i.e. from the Jourdan River). The difference in growth rates between the intrinsic and nutrient–replete growth rates supports that the community was most likely nutrient deficient and gives a better idea of the effects of nutrients on this population.

Many of the experiments in this study had slopes of apparent growth rate vs. dilution factor regressions that were not different significantly than zero, indicating no measurable grazing. This result has been observed in many studies using the dilution method in a variety of environments (Landry and Hassett 1982; Landry et al. 1984; Paranjape 1987; Gifford 1988; Kamiyama 1994; Murrell and Hollibaugh, 1998; Kim et al. 2007; York et al. 2010). Non–significant grazing has been attributed to high variability in the method due to the small sample number used in the dilution series (Schmoker et al. 2013). It has been suggested that the high variability masks low grazing rates. The data from the current study suggested that the 0/d grazing rates were the result of a decoupling between phytoplankton growth and microzooplankton grazing, possibly due to environmental factors such as temperature and/or river flow affecting the growth of the phytoplankton. It has been suggested that when phytoplankton lack the nutritional compounds required for grazers, growth and grazing can become uncoupled since the phytoplankton are no longer a viable food source for the microzooplankton (Murrell and Hollibaugh 1998; Strom 2002). Given the small sample number in the current study, more information is needed to further examine the effect of environmental parameters on grazing rates.

In summary, this study investigated how phytoplankton growth rates, microzooplankton grazing rates, and environmental conditions affected phytoplankton composition in the BSL, MS, in the northern Gulf of Mexico. We observed very low and often negative intrinsic growth rates (μ_0), selective grazing (m) by the microzooplankton community, and extensive nutrient limitation of the phytoplankton community. The low growth rates observed are likely attributable to the season which the study was conducted (winter/fall). Even though fucoxanthin was the most abundant pigment, microzooplankton grazed on the phytoplankton pigment classes which had the highest intrinsic growth rate in the BSL at the time of sampling. We also observed salinity influence on growth and microzooplankton grazing rates on only two pigment classes of dinoflagellates (peridinin) and cryptophytes (alloxanthin). These factors together have been shown to influence the composition of the phytoplankton community in the BSL.

Acknowledgments

We thank M. Tuel and T. Pittman for their assistance in sampling. We also thank the editors and two anonymous reviewers for their wisdom and constructive comments. Funding for this project was provided by The University of Southern Mississippi, Department of Marine Science.

Literature Cited

Burkill, P.H., R.F.C. Mantoura, C.A. Llewellyn, and N.J.P. Owens. 1987. Microzooplankton grazing and selectivity of phytoplankton in coastal waters. Marine Biology 93:581–590. doi:10.1007/BF00392796

Calbet, A. and M.R. Landry. 2004. Phytoplankton growth, microzooplankton grazing, and carbon cycling in marine systems. Limnology and Oceanography 49:51–57. doi:10.4319/lo.2004.49.1.0051

Calbet, A., E. Saiz, R. Almeda, J.I. Movilla, and M. Alcaraz. 2011. Low microzooplankton grazing rates in the Arctic Ocean during a *Phaeocystis pouchetii* bloom (Summer 2007): fact or artifact of the dilution technique? Journal of Plankton Research 33:687–701. doi:10.1093/plankt/fbq142

Cai, Y., L. Guo, X. Wang, A.K. Mojzis, and D.G. Redalje. 2012. The source and distribution of dissolved and particulate organic matter in the Bay of St. Louis, northern Gulf of Mexico. Estuarine, Coastal and Shelf Science 96:96–104. doi:10.1016/j.ecss.2011.10.017

Camacho, R.A., J.L. Martin, B. Watson, M.J. Paul, L. Zheng, and J.B. Stribling. 2014. Modeling the factors controlling phytoplankton in the St. Louis Bay estuary, Mississippi and evaluating estuarine responses to nutrient load modifications. Journal of Environmental Engineering 141:04014067. doi:10.1061/(ASCE)EE.1943–7870.0000892

Chevez, F.P., K.R. Buck, K.H. Coale, J.H. Martin, G.R. DiTullio, N.A. Welschmeyer, A.C. Jacobson, and R.T. Barber. 1991. Growth rates, grazing, sinking, and iron limitation of equatorial Pacific phytoplankton. Limnology and Oceanography 36:1816–1833. doi:10.4319/lo.1991.36.8.1816

Dorado, S., T. Booe, J. Steichen, A.S. McInnes, R. Windham, A. Shepard, A.E.B. Lucchese, H. Preischel, J.L. Pinckney, S.E. Davis, D.L. Roelke, and A. Quigg. 2015. Towards an understanding of the interactions between freshwater inflows and phytoplankton communities in a subtropical estuary in the Gulf of Mexico. PLoS One 10:e0130931. doi:10.1371/journal.pone.0130931

Eleuterius, C.K. 1984. Application of a hydrodynamic–numerical model to the tides of St. Louis Bay, Mississippi. Journal of the Mississippi Academy of Sciences 29:37–46.

Fitzwater, S.E., G.A. Knauer, and J.H. Martin. 1982. Metal contamination and its effect on primary production measurements. Limnology and Oceanography 27:544–551. doi:10.4319/lo.1982.27.3.0544

Gifford, D.J. 1988. Impact of grazing by microzooplankton in the northwest arm of Halifax Harbour, Nova Scotia. Marine Ecology Progress Series 47:249–258. doi:10.3354/meps047249

Gutierrez–Rodriguez, A., M. Latasa, R. Scharek, R. Massana, G. Vila, and J.M. Gasol. 2011. Growth and grazing rate dynamics of major phytoplankton groups in an oligotrophic coastal site. Estuarine, Coastal and Shelf Science 95:77–87. doi:10.1016/j.ecss.2011.08.008

Hagerthey, S.E., J.W. Louda, and P. Mongkronsri. 2006. Evaluation of pigment extraction methods and a recommended protocol for periphyton chlorophyll *a* determination and chemotaxonomic assessment. Journal of Phycology 42:1125–1136. doi:10.1111/j.1529–8817.2006.00257.x

Holtermann, K.E. 2001. Phytoplankton pigments in relation to environmental parameters in the Bay of St. Louis and Mississippi Sound. MS thesis. University of Southern Mississippi, Hattiesburg, MS, USA, 144 p.

Jett, C. 2004. Estimation of microzooplankton grazing in the Suwannee River Estuary, Florida, USA. MS thesis. University of Florida, Gainesville, FL, USA, 46 p.

Juhl, A.R. and M.C. Murrell. 2005. Interactions between nutrients, phytoplankton growth, and microzooplankton grazing in a Gulf of Mexico estuary. Aquatic Microbial Ecology 38:147–156. doi:10.3354/ame038147

Kamiyama, T. 1994. The impact of grazing by microzooplankton in northern Hiroshima Bay, the Seto Inland Seam, Japan. Marine Biology 119:77–88. doi:10.1007/BF00350109

Kim, S., M.G. Park, C. Moon, K. Shin, and M. Chang. 2007. Seasonal variations in phytoplankton growth and microzooplankton grazing in temperate coastal embayment, Korea. Estuarine, Coastal and Shelf Science 71:159–169. doi:10.1016/j.ecss.2006.07.011

Landry, M.R. and R.P. Hassett. 1982. Estimating the grazing impact of marine microzooplankton. Marine Biology 67:283–288. doi:10.1007/BF00397668

Landry, M.R., L.W. Haas, and V.L. Fagerness. 1984. Dynamics of microbial plankton communities: experiments in Kaneohe Bay, Hawaii. Marine Ecology Progress Series 16:127–133. doi:10.3354/meps016127

Landry, M.R., J. Constantinou, and J. Kirshtein. 1995. Microzooplankton grazing in the central equatorial Pacific during February and August. 1992. Deep–Sea Research II 42:657–671. doi:10.1016/0967–0645(95)00024–K

Landry, M.R., S.L. Brown, L. Campbell, J. Constantinou, and H. Liu. 1998. Spatial patterns in phytoplankton growth and microzooplankton grazing in the Arabian Sea during monsoon forcing. Deep–Sea Research II 45:2353–2368. doi:10.1016/S0967–0645(98)00074–5

Latasa, M., M.R. Landry, L. Schluter, and R.R. Bidigare. 1997. Pigment–specific growth and grazing rates of phytoplankton in the central equatorial Pacific. Limnology and Oceanography 42:289–298. doi:10.4319/lo.1997.42.2.0289

Lawrence, C. and S. Menden–Deuer. 2012. Drivers of protistan grazing pressure: seasonal signals of plankton community composition and environmental conditions. Marine Ecology Progress Series 459:39–52. doi:10.3354/meps09771

Legendre, P. 2008 lmodel2: model II regression. http://cran.r–project.org/web/packages /l?model2/index.html. (viewed on 1/20/2014).

Lehrter, J.C., J.R. Pennock, and G.B. McManus. 1999. Microzooplanktong grazing and nitrogen excretion across a surface estuarine—coastal interface. Estuaries 22:113— 125. doi:10.2307/1352932

Li, W.K.W. and P.M. Dickie. 1985. Growth of bacteria in seawater filtered through 0.2 µm Nuclepore membranes: implications for dilution experiments. Marine Ecology Progress Series 26:245—252. doi:10.3354/meps026245

Mantoura, R.F.C. and D.J. Repeta. 1997. Calibration methods for HPLC. In S.W. Jeffrey, R.F.C. Mantoura, and S.W. Wright, eds. Phytoplankton pigments in oceanography. UNESCO, Paris, France, p. 407—428

Molina, L.K. 2011. Phytoplankton abundance and species composition in relation to environmental parameter in coastal Mississippi waters. MS thesis. University of Southern Mississippi, Hattiesburg, MS, USA, 121 p.

Murrell, M.C. and J.T. Hollibaugh. 1998. Microzooplankton grazing in northern San Francisco Bay measured by the dilution method. Aquatic Microbial Ecology 15:53—63. doi:10.3354/ame015053

Murrell, M.C., R.S. Stanley, E.M. Lores, G.R. DiDonato, and D.A. Flemer. 2002. Linkage between microzooplankton grazing and phytoplankton growth in a Gulf of Mexico estuary. Estuaries 25:19—29. doi:10.1007/BF02696046

Ortmann, A.C., R.C. Metzger, J.D. Liefer, and L. Novoveska. 2011. Grazing and viral lysis vary for different components of the microbial community across an estuarine gradient. Aquatic Microbial Ecology 65:143—157. doi:10.3354/ame01544

Palomares—Garcia, R., J.J. Bustillos—Guzman, and D. Lopez—Cortes. 2006. Pigment specific rates of phytoplankton growth and microzooplankton grazing in a subtropical lagoon. Journal of Plankton Research 28:1217—1232. doi:10.1093/plankt/fbl051

Paranjape, M.A. 1987. Grazing by microzooplankton in the eastern Canadian arctic in summer 1983. Marine Ecology Progress Series 40:239—246. doi:10.3354/meps040239

Phelps, E. I. 1999. Environmental quality of Saint Louis Bay, Mississippi. MS thesis. University of Southern Mississippi, Hattiesburg, MS, USA, 62 p.

Pinckney, J.L., H.W. Paerl, and M.B. Harrington. 1999. Responses of the phytoplankton community growth rate to nutrient pulses in variable estuarine environments. Journal of Phycology 35:1455—1463. doi:10.1046/j.1529—8817.1999.3561455.x

Porter, K.G. 1977. The plant—animal interface in freshwater ecosystems: microscopic grazers feed differentially on planktonic algae and can influence their community structure and succession in ways that are analogous to the effects of herbivores on terrestrial plant communities. American Scientist 65:159—170. doi:10.2307/27847715

Putland, J.N. and R.L. Iverson. 2007. Microzooplankton: major herbivores in an estuarine planktonic food web. Marine Ecology Progress Series 345:63—73. doi:10.3354/meps06841

R Core Team. 2013. R: A language and environment for statistical computing. R Foundation for Statistical Computing, Vienna, Austria. ISBN 3—900051—07—0. http://www.R—project.org/.

Sanderson, B., A.M. Redden, and K. Evans. 2012. Grazing constants are not constant: microzooplankton grazing is a function of phytoplankton production in an Australian Lagoon. Estuaries and Coasts 35:1270—1284. doi:10.1007/s12237—012—9524—9

Sawant, P.A. 2009. Factors influencing the environmental quality of the Bay of Saint Louis, Mississippi and implications for evolving coastal management policies. Ph.D. dissertation. University of Southern Mississippi, Hattiesburg, MS, USA, 222 p.

Schmoker, C., S. Hernandez—Leon, and A. Calbet. 2013. Microzooplankton grazing in the oceans: impacts, data variability, knowledge gaps and future directions. Journal of Plankton Research 35:691—706. doi:10.1093/plankt/fbt023

Strom, S. 2002. Novel interactions between phytoplankton and microzooplankton; their influence on the coupling between growth and grazing rates in the sea. Hydrobiologia 480:41—54. doi:10.1023/A:1021224832646

Strom, S.L. and N.A. Welschmeyer. 1991. Pigment—specific rates of phytoplankton growth and microzooplankton grazing in the open subarctic Pacific Ocean. Limnology and Oceanography 36:50—63. doi:10.4319/lo.1991.36.1.0050

Strom, S.L., M.A. Brainard, J.L. Holmes, and M.B. Olson. 2001. Phytoplankton blooms are strongly impacted by microzooplankton grazing in coastal North Pacific waters. Marine Biology 138:355—368. doi:10.1007/s002270000461

Wright, S.W., S.W. Jeffrey, R.F.C. Mantoura, C.A. Llewellyn, T. Bjornland, D. Repeta, and N. Weschmeyer. 1991. Improved HPLC method for the analysis of chlorophylls and carotenoids from marine phytoplankton. Marine Ecology Progress Series 77:183—196. doi:10.3354/meps077183

York, J.K., B.A. Costas, and G.B. McManus. 2010. Microzooplankton grazing in green water — results from two contrasting estuaries. Estuaries and Coasts 34:373—385. doi:10.1007/s12237—010—9336—8

Gulf and Caribbean Research

Volume 27 | Issue 1

2016

Endohelminth parasites of some midwater and benthopelagic stomiiform fishes from the northern Gulf of Mexico

Michael J. Andres
University of Southern Mississippi, michael.andres@usm.edu

Mark S. Peterson
University of Southern Mississippi, mark.peterson@usm.edu

Robin M. Overstreet
University of Southern Mississippi, robin.overstreet@usm.edu

Gulf and Caribbean Research Vol 27, 11-19, 2016
DOI: 10.18785/gcr.2701.02
Manuscript received, January 21, 2016; accepted, April 25, 2016

ENDOHELMINTH PARASITES OF SOME MIDWATER AND BENTHOPELAGIC STOMIIFORM FISHES FROM THE NORTHERN GULF OF MEXICO

Michael J. Andres*, Mark S. Peterson, and Robin M. Overstreet
*The University of Southern Mississippi, Department of Coastal Sciences, 703 East Beach Drive, Ocean Springs, MS 39564; *Corresponding author, email: michael.andres@usm.edu*

ABSTRACT: Mesopelagic fishes represent significant ecological links between mesozooplankton and the larger pelagic squids, fishes, and marine mammals. As such, these fishes also play a significant role as intermediate or paratenic hosts for parasites that require a crustacean intermediate host and mature in marine mammals or pelagic fishes. We examined a total of 208 individuals representing 5 species of Sternoptychidae and 88 individuals representing 2 species of Phosichthyidae from 20 locations in the northern Gulf of Mexico (nGOM). Six of the 7 species we examined are mesopelagic and one species was benthopelagic. We found the larval stages of *Anisakis brevispiculata, Anisakis typica, Hysterothylacium fortalezae* (all Nematoda: Ascaridoidea); *Bolbosoma* sp. (Acanthocephala: Polymorphidae); and Tetraphyllidea (Cestoda) plus an immature specimen of *Brachyphallus* sp. (Digenea). Molecular sequencing was used to identify the ascaridoids and *Bolbosoma* sp. and to confirm the identification of 3 host sternoptychid species. The mesopelagic fishes hosted *Anisakis brevispiculata* (that matures in pygmy and dwarf sperm whales) and *Hysterothylacium fortalezae* (that matures in pelagic fishes, primarily mackerels), whereas the benthopelagic species was parasitized by *Anisakis typica* (that matures in dolphins). We suggest this pattern of infection indicates a pelagic life–cycle for *Anisakis brevispiculata* and *Hysterothylacium fortalezae* and a demersal life–cycle for *Anisakis typica*. Our study represents the first published sequences from the nGOM for the fishes *Argyropelecus aculeatus, Maurolicus weitzmani*, and *Polyipnus clarus* and the first molecular identification of larval ascaridoids from mesopelagic fishes in the nGOM.

KEYWORDS: *Anisakis, Hysterothylacium,* marine mammals, Phosichthyidae, Sternoptychidae

INTRODUCTION

Mesopelagic fishes represent significant ecological links between mesozooplankton and the larger pelagic squids, fishes, and marine mammals (e.g., Pauly et al. 1998, Choy et al. 2013, Young et al. 2015). Members of the orders Stomiiformes and Myctophiformes account for the vast majority of such fishes (Bernal et al. 2015). Most parasitological studies of midwater fishes have revealed larval or juvenile stages of helminths that mature in large pelagic fishes and marine mammals rather than adult helminths (e.g., Noble and Collard 1970, Gartner and Zwerner 1989, Mateu et al. 2015). Typically, larval or juvenile stages of trematodes (that mature in fishes), cestodes (that mature in elasmobranchs), acanthocephalans (that mature in fishes and marine mammals), and nematodes, especially ascaridoids, have been reported (e.g., Noble and Collard 1970, Gartner and Zwerner 1989, Klimpel et al. 2006, 2010, Mateu et al. 2015).

The life–cycle of marine ascaridoids involves a crustacean first intermediate host and a vertebrate final host. Typically, members of the Raphidascarididae mature in teleosts, whereas those of Anisakidae mature in marine mammals. The crustacean first intermediate host is generally a copepod, but euphasiids serve as important intermediate hosts for species of *Anisakis* (see Smith and Wooten 1978). Larval ascaridoids commonly infect fishes and invertebrates that serve as paratenic, or transfer hosts (hosts that are not required for the development of the parasite). The use of these paratenic hosts acts as an adaptation to overcome the challenges of reaching appropriate final hosts in oceanic environments (Marcogliese 1995), and has led to the utility of ascaridoids as biological tags for fishes (Mattiucci et al. 2008) and trophic interactions (Palm and Klimpel 2008). The use of paratenic hosts also has public health implications for certain fisheries products because of the zoonotic (can be passed from animal to human) potential of some ascaridoids, especially those that mature in marine mammals (species of *Anisakis* and *Pseudoterranova*; see Sakanari and McKerrow 1989), but also some that mature in fishes (Overstreet and Meyer 1981, Overstreet 2012).

Despite the potential human health risk associated with some ascaridoids, the Gulf of Mexico (GOM) is poorly characterized with respect to the intermediate and paratenic host use patterns of those nematodes. Kuhn et al. (2011) modeled the geographic range of 9 species of *Anisakis* but did not include data for the GOM presumably because species of *Anisakis* were reported under junior synonyms, incomplete larval names, misidentifications, or they lacked molecular data (e.g., Gunter and Overstreet 1974). Cavallero et al. (2011) surveyed stranded cetacean hosts from the eastern GOM (eGOM), southeastern U.S. Atlantic coast, and Caribbean Sea and reported the presence of 7 species of *Anisakis*, *Pseudoterranova ceticola*, and larvae of *Contracaecum multipapillatum* (exclusively from inshore populations of the common bottlenose dolphin, *Tursiops truncatus*). However, the highly migratory nature of most marine cetaceans and the varied geographic stranding localities examined by Cavallero et al. (2011) do not provide a clear picture of the richness of *Anisakis* species in the northern GOM (nGOM).

The purpose of this study was to document larval ascaridoids as well as other endohelminths in stomiiform fishes

that were incidentally caught in bottom trawl surveys along the nGOM outer continental shelf and continental slope. We examined 5 mesopelagic species (the Atlantic Sliver Hatchetfish, *Argyropelecus aculeatus*; the Silvery Hatchetfish, *Argyropelecus sladeni*; the Atlantic Pearlside, *Maurolicus weitzmani*; the Slope Hatchetfish, *Polyipnus clarus* (all Sternoptychidae); and the Stareye Lightfish, *Pollichthys mauli* (Phosichthyidae)) and one benthopelagic species (the Rendezvous Fish, *Polymetme corythaeola* (Phosichthyidae)) for helminths. Morphological identification of larval ascaridoids to species level is generally problematic (e.g., Zhu et al. 1998, Mattiucci and Nascetti 2006, Mattiucci et al. 2014); therefore, we molecularly genotyped the 28S and internal transcribed spacer region (ITS; = ITS1, 5.8S, and ITS2) ribosomal DNA (rDNA) regions to confirm identifications.

Materials and Methods

Sample collection

Representative stomiiform fishes were collected from the nGOM by bottom trawl as a part of the NOAA–Fisheries Southeast Small Pelagic Survey in 2011–2012. Trawls were towed for 30 min and depths (m) at the end of trawl were recorded. Following capture of fishes, we identified and froze them at –20°C while on ship. We examined 208 individuals representing 5 species of Sternoptychidae and 88 individuals representing 2 species of Phosichthyidae from 20 locations (Figure 1A). In the laboratory, hosts were defrosted at 1–3°C, identifications confirmed using the keys developed by McEachran and Fechhelm (1998), measured (nearest mm SL), weighed (nearest 0.01 g), and sexed. The visceral organs and gastrointestinal tract of all fish were placed in a small amount of physiological saline and examined for helminths under a stereomicroscope. An initial subsample of 20 individuals each of *Maurolicus weitzmani*, *Pollichthys mauli*, *Polypinus clarus*, and *Polymetme corythaeola*, and all specimens of *Argyropelecus aculeatus* and *Argyropelecus sladeni*, were examined for larval helminths in the musculature by candling. Candling was conducted by putting fillets between two glass slides and examining them by stereomicroscope; however, no larvae were found in the musculature of any of the fishes examined, and the process was discontinued. Parasite specimens were fixed in 70% ethanol for morphological and molecular analyses. Nematodes were cleared in 95 parts 70% ethanol + 5 parts gylcerol for morphological examination. A single acanthocephalan and a single digenean were stained, cleared, and mounted according to the procedures in Andres and Overstreet (2013). Voucher specimens were deposited in the Gulf Coast Research Laboratory Museum (GCRLM), Ocean Springs, Mississippi (see Table 1 for accession numbers).

Ecological parasitology terms follow those defined by Bush et al. (1997): prevalence as the percentage of fish infected and mean intensity of infection as the mean number of parasites per infected fish. The 95% confidence interval for prevalence was calculated using the Clopper–Pearson exact CI (exactci) package found in the PropCIs library of R v. 2.15.2 (R Core Team, 2012).

Molecular analyses

Genomic DNA was extracted from a middle portion of 36 individual ascaridoids, a section of the posterior portion from the acanthocephalan, and a piece of muscle from a single individual of each sternoptychid species (with the exception of *Argyropelecus sladeni*; n = 4) using Qiagen DNAeasy tissue kit (Qiagen, Inc., Valencia, CA, USA) following the instructions provided. For ascaridoids, DNA fragments of ca. 1,020 base pairs (bp) long for the 28S ribosomal DNA (rDNA) gene and 800 bp long comprising the ITS rDNA gene were amplified from the extracted DNA by polymerase chain reaction (PCR) following the procedures of Nadler et al. (2000) and Zhu et al. (1998), respectively. For the acanthocephalan, a 668 bp partial portion of the mitochondrial cytochrome c oxidase 1 (*cox1*) was amplified following García–Varela and Nadler (2006) and for sternoptychids, ca. 640 bp partial portion of the *cox1* was amplified following Ward et al. (2005). See Table 2 for the list of primers used and their corresponding references. The resulting PCR products were excised from PCR gel using QIAquick Gel Extraction Kit (Qiagen, Inc., Valencia,

TABLE 1. *Gulf Coast Research Laboratory museum (GCRLM) and GenBank accession numbers for vouchers treated in this study.*

Taxon	GCRLM No.	GenBank Accession No. ITS	28S	cox1
Platyhelminthes				
Brachyphallus sp.	06551	–	–	–
Acanthocephala				
Bolbosoma sp.	06552	–	–	KX098556
Nematoda				
Anisakis brevispiculata	06553–5	KX098557–9	KX098560	–
Anisakis typica	06556	KX098561	KX098562	–
Hysterothylacium fortalezae	06557	KX098563	KX098564	–
Chordata				
Argyropelecus aculeatus	36551	–	–	KX098553
Maurolicus weitzmani	36552	–	–	KX098554
Polyipnus clarus	36553	–	–	KX098555

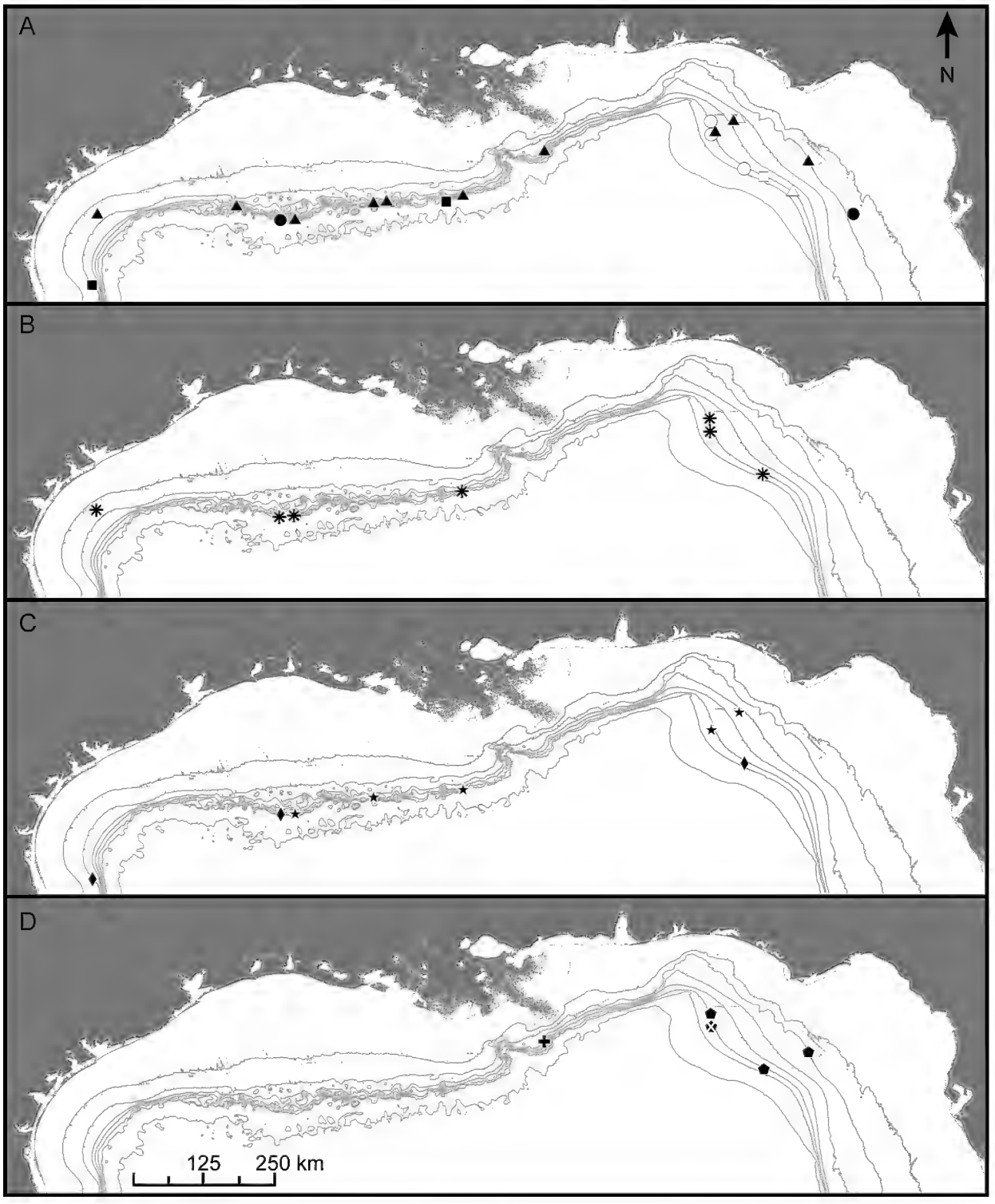

FIGURE 1. *Sampling localities in the northern Gulf of Mexico. A. Localities of sternoptychids (triangles), phosichthyids (squares), or both (circles) from 2011 (filled symbols) and (2012) (open symbols). B. Locations from which* Anisakis brevispiculata *were collected. C. Locations from which* Anisakis typica *(diamonds) and* Hysterothylacium fortalezae *(stars) were collected. D. Locations from which tetraphyllideans (pentagons),* Bolbosoma *sp. (+), and* Brachyphallus *sp. (white "X" overlaid a pentagon) were collected. Bathymetric contour lines represent 50 m, 100 m, 200 m, 300 m, 500 m, and 1,000 m.*

CA, USA) following kit instructions. They then were cycle–sequenced using ABI BigDye™ chemistry (Applied Biosystems, Inc., Carlsbad, CA, USA), ethanol–precipitated, and processed on an ABI 3130 Genetic Analyzer™. Sequences used for pairwise comparison were aligned using MAFFT version 6.611b (Katoh et al. 2005) with 1,000 cycles of iterative refinement and the *genafpair* algorithm.

TABLE 2. *PCR primers used for the various taxonomic groups and regions in this study.*

Group	Region	Primer	Direction	Annealing Temp.	Reference
Acanthocephala	cox1	5′–AGTTCTAATCATAARGATATYGG–3′	Forward	40°C	Folmer et al. 1994
		5′–TAAACTTCAGGGTGACCAAAAAATCA–3′	Reverse		
Ascaridoidea	28S	391: 5′–AGCGGAGGAAAAGAAACTAA–3′	Forward	55°C	Nadler et al. (2000)
		501: 5′–TCGGAAGGAACCAGCTA-CTA–3′	Reverse		
	ITS	NC5: 5′–GTAGGTGAACCTGCGGAAGGATCATT–3′	Forward	60°C	Zhu et al. (1998)
		NC2: 5′–TTAGTTTCTTTTCCTCCGCT–3′	Reverse		
Sternoptychidae	cox1	FishF1: 5′–TCAACCAACCACAAAGACATTGGCAC–3′	Forward	54°C	Ward et al. (2005)
		FishF2: 5′–ACTTCAGGGTGACCGAAGAATCAGAA–3′	Reverse		

Results

Host data

Of the 5 midwater species collected, *Polyipnus clarus* was the most common (n = 156 from 11 stations) followed by the phosichthyid *Pollichthys mauli* (n = 35 from 3 stations) whereas 53 individuals of the benthopelagic *Polymetme corythaeola* were collected from 4 stations. Individuals of *Argyropelecus aculeatus* and *Polymetme corythaeola* were collected from the deepest depths as well as the largest depth range (see Table 3). Individuals of both phosichthyid species tended to be longer and heavier than the sternoptychid species (Table 3). The *cox1* sequence of *Argyropelecus aculeatus* and *Maurolicus weitzmani* was identical to that of the unpublished sequence of *Argyropelecus aculeatus* (KF929623) collected from the slope water off Cape Hatteras and the sequence of *Maurolicus weitzmani* (KJ190037) from the Mid–Atlantic Bight (Davis et al. 2014), respectively. The *cox1* sequence of *Polyipnus clarus* differed from that of the *Polyipnus clarus* sequence FJ918932 collected from the slope water of southern New England (DeVaney 2008) by a single purine transition.

Genetic identification

Three ascaridoid species were found; *Anisakis brevispiculata* (Anisakidae), *Anisakis typica*, and *Hysterothylacium fortalezae* (Raphidascarididae). Of the 20 individuals of *Anisakis brevispiculata* sequenced, one 28S genotype and 3 ITS genotypes were found. All differences in those genotypes occurred at position 177 in the ITS2, with 15 individuals having a guanine; 4 individuals having an adenine, and one individual having an ambiguous purine. The most common ITS genotype (KX098557) was identical to the sequence of *Anisakis brevispiculata* AY826719 of Cavallero et al. (2011). No intraspecific variation occurred in either gene region of the 6 individuals of *Anisakis typica*. The ITS sequences we generated for *Anisakis typica* were identical to EU327688 (Iñiguez et al. 2009) and JQ912690 (Mattiucci et al. 2014) for *Anisakis typica* , but they differed from sequence AY826724 by Cavallero et al. (2011) that had 3 single bp indels in the ITS1 at positions 125, 131, and 161. No intraspecific variation occurred in either gene region of the 11 individuals of *Hysterothylacium fortalezae*. The 28S sequences we generated for *Hysterothylacium fortalezae* differed from the GenBank sequence U94760 (provided by RMO to Nadler and Hudspeth 1998) by a single bp indel at position 436.

The *cox1* sequence generated from the acanthocephalan was 88% similar to sequence JQ040303 for *Bolbosoma balaenae* (Gregori et al. 2012); 66% similar to sequence JX442190 for *Bolbosoma* sp. (García–Varela et al. 2013); and 65% similar to sequence JX442189 for *Bolbosoma turbinella* (García–Varela et al. 2013). The *cox1* sequences of the latter 2 species were 84% similar, suggesting that the acanthocephalan we collected was a species of *Bolbosoma* (Polymorphidae). Morphologically, the proboscis of our specimen was not everted; however, it did poses a funnel–shaped bulb in the foretrunk.

TABLE 3. *Host information for the species examined in this study. SL = Standard length in mm; g = grams; m = depth; Stations = number of stations that hosts were obtained from; + = number of stations that had parasitized fish.*

Taxonomic group	n	SL range	g	m	Stations	
					n	+
Phosichthyidae						
Pollichthys mauli	35	61–154	1.00–17.79	396–419	3	3
Polymetme corythaeola	53	91–184	3.08–36.87	76–468	5	3
Sternoptychidae						
Argyropelecus aculeatus	16	45–66	1.18–9.13	76–468	4	2
Argyropelecus sladeni	6	25–43	0.51–2.83	336	1	0
Maurolicus weitzmani	30	30–47	0.36–1.21	102–396	5	4
Polyipnus clarus	156	21–57	0.33–3.85	66–430	11	4

Parasitological data

The prevalence of helminths was relatively low (Table 4). No individual of *Argyropelecus sladeni* was infected with any helminth. Individuals of *Anisakis brevispiculata* were identified from all other midwater fish with the

exception of *Maurolicus weitzmani*. *Anisakis typica* was the only helminth found to infect *Polymetme corythaeola*, and was found to parasitize that host only. *Maurolicus weitzmani* had the highest prevalence of *Hysterothylacium fortalezae* because a single location in the western GOM (wGOM) had 5 infected individuals. The site of infection for individuals of *Anisakis brevispiculata* was in the mesenteric lining associated with the gonads, with the exception of 2 individuals in a single *Polypinus clarus*, where one individual occurred near the gonads and the other near the liver. Likewise, all individuals of *Anisakis typica* occurred in the mesenteric lining around the gonads, even in the single fish with an intensity of 2. All individuals of *Hysterothylacium fortalezae* were found in the mesenteric lining of the liver. None of the fish examined from the 2011 eGOM locations (east of Mobile Bay, AL; see Figure 1A) were infected with ascaridoids, whereas all of the 2012 sampling locations occurred in the eGOM, and only the southernmost location exhibited uninfected fish. All three ascaridoid species were found across the nGOM (Figure 1B–C). The depth range of fish infected with ascaridoids was 66–468 m for *Anisakis brevispiculata*, 98–468 m for *A. typica*, and 212–419 m for *Hysterothylacium fortalezae*, and all but the shallowest two locations (both of which occurred over the Texas shelf) occurred in > 200 m of depth.

The mean intensity (Table 4) for all helminths, with the exception of larval tetraphyllideans (Cestoda) from *Polypinus clarus*, was between 1.0–1.2. Tetraphyllideans were not identified past order, but were found in only mesopelagic fishes from the eGOM (Figure 1D) ranging from a depth of 102–419 m. The single specimen of *Bolbosoma* sp. was found in the proximal portion of the intestinal tract of *Maurolicus weitzmani* from the wGOM (Figure 1D) at a depth of 186 m. A single immature (based on possessing adult characters but not being mature) specimen of *Brachyphallus* sp. (Digenea: Hemiuridae) infected the stomach of *Polypinus clarus* from the eGOM (Figure 1D) at a depth of 419 m.

Discussion

We provide the first molecular identification of anisakids and a species of *Bolbosoma* from fish in the nGOM, the first parasitological survey of 4 sternoptychid species and 2 phosichthyid species in the nGOM, and provide the first *cox1* sequences for sternoptychids from the GOM. We found the larval stages of 5 helminth taxa (*Anisakis brevispiculata*, *Anisakis typica*, *Hysterothylacium fortalezae*, *Bolbosoma* sp., and Tetraphyllidea) and an immature species of *Brachyphallus*. The presence of generalist parasite taxa in the hosts that we examined is similar to the findings of previous authors who examined midwater fishes (e.g., Noble and Collard 1970, Gartner and Zwerner 1989, Klimpel et al. 2007, 2008, 2010, Mateu et al. 2015). We found an overall low prevalence and mean intensity of all parasitic taxa across all host species examined. *Polyipnus clarus* had the largest number of recovered helminth taxa (4), but it also had the highest sample size (156). *Argyropelecus sladeni* was not infected with any helminths, but only 6 individuals were examined, and, consequently, we do not include it in the following discussion.

All midwater species were parasitized by *Hysterothylacium fortalezae*, with *Maurolicus weitzmani* having the highest prevalence of infection (20%) for any host–parasite pair. *Hysterothylacium fortalezae* primarily parasitizes pelagic, piscivorous fishes (e.g., species of *Scomberomorous* as well as the Leatherjacket, *Oligoplites saurus*; Deardorff and Overstreet 1980), but those authors also reported adults from the Black Grouper, *Mycteroperca bonaci*. Our finding of *Hysterothylacium fortalezae* parasitizing midwater fishes rather than the benthopelagic *Polymetme corythaeola* is likely indicative of those fishes acquiring an infection while feeding on epipelagic crustaceans. Deardorff and Overstreet (1981) described larvae that they attributed to *Hysterothylacium fortalezae* from the viscera of coastal and offshore pelagic fishes (3 species of *Anchoa*, 2 species of *Peprilus*, and the Atlantic Cutlassfish, *Trichiurus lepturus*) but also from a penaeid shrimp and the structure–associated Black Sea Bass, *Centropristis striata* (as *C. melana*). However, the demersal species they found to be infected with *Hysterothylacium fortalezae* larvae have pelagic life–history stages that could have allowed those species to acquire their infection before settling. Most of the locations Overstreet and Deardorff (1981) sampled occurred in shal-

TABLE 4. *Percent prevalence (P) with 95% confidence interval and mean intensity of infection (I; ± SE) for the parasitic taxa of the 4 mesopelagic (M) hosts and one benthopelagic (B) host.*

Host	Zone	*Tetraphyllidea*		*Anisakis brevispiculata*		*Anisakis typica*		*Hysterothylacium fortalezae*	
		P	I	P	I	P	I	P	I
Pollichthys mauli	M	6 (0.7–19.2)	1	14 (4.8–30.3)	1	0	–	3 (0.1–14.9)	1
Polymetme corythaeola	B	0	–	0	–	9 (3.1–20.7)	1.2 ± 0.2	0	–
Argyropelecus aculeatus	M	0	–	13 (1.6–38.3)	1	0	–	6 (0.2–30.2)	1
Maurolicus weitzmani	M	5 (0.1–24.9)	1	0	–	0	–	20 (7.8–38.6)	1.2 ± 0.2
Polyipnus clarus	M	2 (0.4–5.2)	7 ± 1.9	8 (4.0–13.1)	1.1 ± 0.1	0	–	1 (0.2–4.6)	1

low water where trophic interactions between demersal and pelagic organisms are more likely to have occurred.

Anisakis brevispiculata parasitized all midwater fish species with the exception of *Mycteroperca weitzmani* and was the most numerous of all examined nematodes. One individual each of *Argyropelecus aculeatus* and *Polypinus clarus* had a co–infection of *Hysterothylacium fortalezae* and *Anisakis brevispiculata*. Pygmy and dwarf sperm whales (Kogiidae) serve as the final hosts for *Anisakis brevispiculata* (Mattiucci et al. 2001, Cavallero et al. 2011) and feed primarily on squids and to a lesser degree on mesopelagic fishes (Pauly et al. 1998). However, Mattiucci et al. (2001) reported that the demersal *Merluccius merluccius* (Macrouridae) served as a paratenic host in the central–eastern Atlantic Ocean; demersal fishes have been known to feed on midwater fishes, especially along continental slopes and seamounts (Pusch et al. 2004, Gartner et al. 2008), and this is reflected in their parasite fauna (e.g., Klimpel et al. 2008, Palm and Klimpel 2008). Therefore, we believe that *Anisakis brevispiculata* has a pelagic life–cycle in the nGOM but that additional midwater fish (especially myctophids) and squid species from the GOM should be studied to confirm this.

Anisakis typica parasitized *Polymetme corythaeola*, the only benthopelagic species examined. Palm et al. (2008) suggested a pelagic life–cycle for *Anisakis typica* off Indonesia based on their finding of larvae in scombrid and carangid fishes, but our findings suggest a demersal cycle in the nGOM. Cavallero et al. (2011) found that *Anisakis typica* was the dominant anisakid in offshore delphinids that had stranded along the coasts of the GOM, southeastern U.S., and Caribbean Sea. Our finding of *Anisakis typica* in the benthopelagic species only was surprising, considering that the diets of most oceanic delphinids consist of squid and epipelagic and mesopelagic fishes (e.g., Fiedler et al. 1998, Pauly et al. 1998, Davis et al. 2002). Therefore, additional paratenic hosts are likely necessary to transfer *Anisakis typica* to its final hosts. Additional benthopleagic and demersal fishes along the outer continental shelf and slope should be examined to further establish the life–cycle patterns of *Anisakis typica* in the nGOM.

The current underrepresentation of parasitological data for species of *Anisakis* in the nGOM is likely an artifact of the bathymetry of the GOM. The continental shelf is shallow and wide across most of the commercial and recreational fishing grounds, and the majority of ichthyoparasitological examinations in the region for ascaridoids (e.g., Overstreet 1978, Deardorff and Overstreet 1980, 1981) have focused on host species that occur in coastal waters or over the continental shelf. Likely reasons why anisakids are not commonly encountered in fisheries products from the GOM are the lack of surveys using molecular tools, the importance that oceanic euphasiids may play in the life–cycles of species of *Anisakis* (Smith and Wooten 1978), and the diversity of marine mammals associated with the bathymetric features (e.g., salt domes and diapirs) of the nGOM continental slope (Davis et al. 2002).

In the GOM, the only species of *Bolbosoma* reported is *Bolbosoma vasculosum* from Blainville's beaked whale, *Mesoplodon densirostris*, (Salgado–Maldonado and Amin 2009) However, in the Caribbean Sea, *Bolbosoma vasculosum* has been reported from both the pygmy killer whale, *Feresa attenuata*, and the Atlantic spotted dolphin, *Stenella frontalis*; another species, *Bolbosoma capitatum*, has been reported from the short–finned pilot whale, *Globicephala macrorhynchus*, and an unidentified species of *Bolbosoma* infected the pygmy sperm whale, *Kogia breviceps* (see Mignucci–Giannoni et al. 1998). Unfortunately, the freezing and subsequent thawing of the single specimen that we attribute to *Bolbosoma* sp. was based on molecular sequencing of the *cox1* gene and did not allow for morphological identification to species level. Species of *Bolbosoma* are one of the two acanthocephalan genera known to parasitize marine mammals (Raga et al. 2009). Euphasiids and copepods act as first intermediate hosts (Hoberg et al. 1993, Gregori et al. 2012), and fishes act as paratenic or transport hosts (Raga et al. 2009).

Likewise, tetraphyllideans use crustacean and fish intermediate hosts, mature in elasmobranchs, and the larvae are commonly found in marine fishes (e.g., Jensen and Bullard 2009). We attempted to amplify the 28S from the extracted DNA of 3 individual larvae but were unsuccessful. Jensen and Bullard (2009) provided a key to 15 larval types that they identified but our specimens could not clearly be assigned to any of them, most likely because of the freezing and thawing of hosts. The only species of *Brachyphallus* reported from the GOM by Overstreet et al. (2009) is *Brachyphallus parvum* (as *Lecithochirium parvum*). *Brachyphallus parvum* has been reported from 27 teleost species in the GOM, 5 of which are pelagic. The life–cycle of the congener *Brachyphallus crenatus* involves an opisthobranch snail, calanoid copepods, matures in teleosts, and can include chaetognaths and ctenophores as paratenic hosts (Køie 1992); therefore, the finding of an immature species in *Polypinus clarus* is not necessarily unexpected.

Few other studies on the parasites of midwater fishes have included sternoptychids or phosichthyids as hosts. Gartner and Zwerner (1989) examined *Argyropelecus aculeatus* and *Sternoptyx diaphana* from the western North Atlantic; Klimpel et al. (2004, 2007) examined *Maurolicus muelleri* from the Norwegian Deep and Mid–Atlantic Ridge; and Bray and Gaevskaya (1993) provided a description of a monorchiid (Digenea) from *Polymetme corythaeola* from the eastern mid–Atlantic Ocean. Gartner and Zwerner (1989) found only cestode larvae in the 2 sternoptychids they examined. Klimpel et al. (2004, 2007) found parasite communities similar to ours, but they found 2 digenean species and the ascaridoid species *Anisakis simplex* (sensu stricto) and *Hystero-*

thylacium aduncum. We did not find *Anisakis simplex* (sensu stricto) in any of the fish we examined, but Cavallero et al. (2011) did find individuals in stranded delphinids, *Kogia breviceps*, and *Mesoplodon europaeus*. Cavallero et al. (2011) also found five additional species of *Anisakis* plus *Pseudoterranova ceticola*; therefore, some of the additional species of *Anisakis* they identified but were not collected by us likely occur in the nGOM.

Our results must also be accompanied with a few caveats. The first of which is that the midwater fishes treated in our study were collected incidentally with a bottom trawl. We do not believe that all of these fishes were collected near the bottom, but Gartner et al. (2008) reported large numbers of *Maurolicus weitzmani* and *Polypinus clarus* associated with the benthic boundary layer. This may explain why we were able to attain a sample size greater than 100 for *Polypinus clarus*. Our sample sizes were also relatively small for most species examined (only *Polypinus clarus* and *Polymetme corythaeola* had n > 50); therefore, we elected to pool parasitological data for species across the nGOM rather than comparing infections by locations. Ross et al. (2010) found a homogenous mesopelagic fish assemblage across the nGOM that would support our consideration. However, based on diet data for some sternoptychid species in the eGOM, the species composition of available prey at lower taxonomic levels spatially varies slightly (e.g., Hopkins and Baird 1985). The stomachs of most of the fishes we examined were either inverted, empty, or contained unrecognizable (digested) prey, and could not be used to reliably compare diets. To generate a more concise picture of the parasite communities of sternoptychids and phosicthyids and to generate a better understanding of the life—cycles of such parasites, fishes collected by midwater trawls should be examined.

Acknowledgements

We thank the National Marine Fisheries Service Laboratory in Pascagoula, MS, for making sampling possible and continuing a productive collaboration. We are especially grateful to M. Grace, A. Hamilton, M. Hendon, N. Hopkins, W. Ingram, L. Jones, A. Pollack, K. Rademacher, and the crew of the NOAA *RV Pisces*. From the University of Southern Mississippi, we thank A. Claxton, J.A. Jovonovich, and J. Wright for their assistance with DNA extractions and sequencing reactions, and S. LeCroy for providing museum accession numbers. The material treated here is based on work supported by the National Science Foundation under grant no. 0529684, Ocean and Human Health Initiative grant no. NA08NOS4730322, US Fish and Wildlife Service/Mississippi Department of Marine Resources MSCIAP MS.R.798 Award M10AF20151, and BP Exploration & Production, Inc. (to RMO).

Literature Cited

Andres, M.J. and R.M. Overstreet. 2013. A new species of *Podocotyloides* (Digenea: Opecoelidae) from the grey conger eel, *Conger esculentus*, in the Caribbean Sea. Journal of Parasitology 99:619–623. doi: 10.1645/12—155.1

Bernal, A., M.P. Olivar, F. Maynou, and M.L. Fernández de Puelles. 2015. Diet and feeding strategies of mesopelagic fishes in the western Mediterranean. Progress in Oceanography 135:1–17. doi: 10.1016/j.pocean.2015.03.005

Bray, R.A. and A.V. Gaevskaya. 1993. *Bathymonorchis polyipni* (Reimer, 1985) n. g., n. comb. (Digenea: Monorchiidae) from bathypelagic fishes of the eastern mid—Atlantic Ocean. Systematic Parasitology 26:91–95. doi: 10.1007/BF00009216

Bush, A.O., K.D. Lafferty, J.M. Lotz, and A.W. Shostak. 1997. Parasitology meets ecology on its own terms: Margolis et al. revised. Journal of Parasitology 83:575–583. doi: 10.2307/3284227

Cavallero, S., S.A. Nadler, L. Paggi, N.B. Barros, and S. D'Amelio. 2011. Molecular characterization and phylogeny of anisakid nematodes from cetaceans from southeastern Atlantic coasts of USA, Gulf of Mexico, and Caribbean Sea. Parasitology Research 108:781–792. doi: 10.1007/s00436—010—2226—y

Choy, C.A., E. Portner, M. Iwane, and J.C. Drazen. 2013. Diets of five important predatory mesopelagic fishes of the central North Pacific. Marine Ecology Progress Series 492:169–184. doi: 10.3354/meps10518

Davis, M.P., N.I. Holcroft, E.O. Wiley, J.S. Sparks, and W.L. Smith. 2014. Species specific bioluminescence facilitates speciation in the deep sea. Marine Biology 161:1139–1148. doi: 10.1007/s00227—014—2406—x

Davis, R.W., J.G. Ortega—Ortiz, C.A. Ribic, W.E. Evans, D.C. Biggs, P.H. Ressler, R.B. Cady, R.R. Leben, K.D. Mullin, and B. Würsig. 2002. Cetacean habitat in the northern oceanic Gulf of Mexico. Deep—Sea Research I 49:121–142. doi: 10.1016/S0967—0637(01)00035—8

Deardorff, T.L. and R.M. Overstreet. 1980. Review of *Hysterothylacium* and *Iheringascaris* (both previously =*Thynnascaris*) (Nematoda: Anisakidae) from the northern Gulf of Mexico. Proceedings of the Biological Society of Washington 93:1035–1079.

Deardorff, T.L. and R.M. Overstreet. 1981. Larval *Hysterothylacium* (=*Thynnascaris*) (Nematoda: Anisakidae) from fishes and invertebrates in the Gulf of Mexico. Proceedings of the Helminthological Society of Washington 48:113–126.

DeVaney, S.C. 2008. The interrelationships of fishes of the Order Stomiiformes. Ph.D. thesis. University of Kansas, Lawrence, KS, USA. 233 p.

Fiedler, P.C., J. Barlow, and T. Gerrodette. 1998. Dolphin prey abundance determined from acoustic backscatter data in eastern Pacific surveys. Fishery Bulletin 96:237–247.

Folmer, O., M. Black, W. Hoeh, R. Lutz, and R. Vrijenhoek. 1994. DNA primers for the amplification of mitochondrial cytochrome c oxidase subunit I from diverse metazoan invertebrates. Molecular Marine Biology and Biotechnology 3:294–299.

García–Varela, M. and S.A. Nadler. 2006. Phylogenetic relationships among Syndermata inferred from nuclear and mitochondrial gene sequences. Molecular Phylogenetics and Evolution 40:61–72. doi: 10.1016/j.ympev.2006.02.010

García–Varela, M., G. Pérez–Ponce de León, F.J. Aznar, and S.A. Nadler. 2013. Phylogenetic relationship among genera of Polymorphidae (Acanthocephala), inferred from nuclear and mitochondrial gene sequences. Molecular Phylogenetics and Evolution 68:176–184. doi: 10.1016/j.ympev.2013.03.029

Gartner, J.V., Jr. and D.E. Zwerner. 1989. The parasite faunas of meso– and bathypelagic fishes of Norfolk Submarine Canyon, western North Atlantic. Journal of Fish Biology 34:79–95. doi: 10.1111/j.1095–8649.1989.tb02959.x

Gartner, J.V. Jr., K.J. Sulak, S.W. Ross, and A.M. Necaise. 2008. Persistent near–bottom aggregations of mesopelagic animals along the North Carolina and Virginia continental slopes. Marine Biology 153:825–841. doi: 10.1007/s00227–007–0855–1

Gregori, M., F.J. Aznar, E. Abollo, Á. Roura, Á.F. González, and S. Pascual. 2012. *Nyctiphanes couchii* as intermediate host for the acanthocephalan *Bolbosoma balaenae* in temperate waters of the NE Atlantic. Diseases of Aquatic Organisms 99:37–47. doi: 10.3354/dao02457

Gunter, G. and R.M. Overstreet. 1974. Cetacean notes. I. Sei and Rorqual whales on the Mississippi coast, a correction. II. A dwarf sperm whale in Mississippi Sound and its helminth parasites. Gulf Research Reports 4:479–481. doi: 10.18785/grr.0403.07

Hoberg, E.P., P.Y. Daoust, and S. McBurney. 1993. *Bolbosoma capitatum* and *Bolbosoma* sp. (Acanthocephala) from sperm whales (*Physeter macrocephalus*) stranded on Prince Edward Island, Canada. Journal of the Helminthological Society of Washington 60:205–210.

Hopkins, T.L. and T.M. Lancraft. 1984. The composition and standing stock of mesopelagic micronekton at 27°N 86°W in the eastern Gulf of Mexico. Contributions in Marine Science 27:143–158.

Iñiguez, A.M., C.P. Santos, and A.C. Paulo Vicente. 2009. Genetic characterization of *Anisakis typica* and *Anisakis physeteris* from marine mammals and fish from the Atlantic Ocean off Brazil. Veterinary Parasitology 165:350–356. doi: 10.1016/j.vetpar.2009.07.012

Katoh, K., K.–I. Kuma, H. Toh, and T. Miyata. 2005. MAFFT version 5: improvement in accuracy of multiple sequence alignment. Nucleic Acids Research 33:511–518. doi: 10.1093/nar/gki198

Klimpel, S., H.W. Palm, S. Rückert, and U. Piatkowski. 2004. The life cycle of *Anisakis simplex* in the Norwegian Deep (northern North Sea). Parasitology Research 94:1–9. doi: 10.1007/s00436–004–1154–0

Klimpel, S., H.P. Palm, M.W. Busch, E. Kellermanns, and S. Rückert. 2006. Fish parasites in the Arctic deep–sea: Poor diversity in pelagic fish species vs. heavy parasite load in a demersal fish. Deep–Sea Research I 53:1167–1181. doi: 10.1016/j.dsr.2006.05.009

Klimpel, S., E. Kellermanns, H.W. Palm, and F. Moravec. 2007. Zoogeography of fish parasites of the pearlside (*Maurolicus muelleri*), with genetic evidence of *Anisakis simplex* (*s.s.*) from the Mid–Atlantic Ridge. Marine Biology 152:725–732. doi: 10.1007/s00227–007–0727–8

Klimpel, S., E. Kellermanns, and H.W. Palm. 2008. The role of pelagic swarm fish (Myctophidae: Teleostei) in the oceanic life cycle of *Anisakis* sibling species at the Mid–Atlantic Ridge, Central Atlantic. Parasitology Research 104:43–53. doi: 10.1007/s00436–008–1157–3

Klimpel, S., M.W. Busch, T. Sutton, and H.W. Palm. 2010. Meso– and bathy–pelagic fish parasites at the Mid–Atlantic Ridge (MAR): Low host specificity and restricted parasite diversity. Deep–Sea Research I 57:596–603. doi: 10.1016/j.dsr.2010.01.002

Køie, M. 1992. Life cycle and structure of the fish digenean *Brachyphallus crenatus* (Hemiuridae). Journal of Parasitology 78:338–343. doi: 10.2307/3283485

Kuhn, T., J. García–Màrquez, and S. Klimpel. 2011. Adaptive radiation within marine anisakid nematodes: A zoogeographical modeling of cosmopolitan, zoonotic parasites. PLoS ONE 6(12):e28642. doi:10.1371/journal.pone.0028642

Jensen, K. and S.A. Bullard. 2009. Characterization of a diversity of tetraphyllidean and rhinebothriidean cestode larval types, with comments on host associations and life–cycles. International Journal of Parasitology 40:889–910. doi: 10.1016/j.ijpara.2009.11.015

Marcogliese, D.J. 1995. The role of zooplankton in the transmission of helminth parasites to fish. Reviews in Fish Biology and Fisheries 5:336–371. doi: 10.1007/BF00043006

Mateu, P., V. Nardi, N. Fraija–Fernández, S. Mattiucci, L. Gil de Sola, J.A. Raga, M. Fernández, and F.J. Aznar. 2015. The role of lantern fish (Myctophidae) in the life–cycle of cetacean parasites from western Mediterranean waters. Deep–Sea Research I 95:115–121. doi: 10.1016/j.dsr.2014.10.012

Mattiucci, S. and G. Nascetti. 2006. Molecular systematics, phylogeny and ecology of anisakid nematodes of the genus *Anisakis* Dujardin, 1845: An update. Parasite 13:99–113. doi: 2006132099

Mattiucci, S., L. Paggi, G. Nascetti, E. Abollo, S.C. Webb, S. Pascual, R. Cianchi, and L. Bullini. 2001. Genetic divergence and reproductive isolation between *Anisakis brevispiculata* and *Anisakis physeteris* (Nematoda: Anisakidae). International Journal of Parasitology 31: 9–14. doi: 10.1016/j.fishres.2007.09.032

Mattiucci, S., V. Farina, N. Campbell, K. MacKenzie, P. Ramos,

A.L. Ramos, A.L. Pinto, P. Abaunza, and G. Nascetti. 2008. *Anisakis* spp. larvae (Nematoda: Anisakidae) from Atlantic horse mackerel: Their genetic identification and use as biological tags for host stock characterization. Fisheries Research 89:146–151. doi: 10.1016/j.fishres.2007.09.032

Mattiucci, S., P. Cipriani, S.C. Webb, M. Paoletti, F. Marcer, B. Bellisario, D.I. Gibson, and G. Nascetti. 2014. Genetic and morphological approaches distinguish the three sibling species of the *Anisakis simplex* species complex, with a species designation as *Anisakis berlandi* n. sp. for *A. simplex* sp. C (Nematoda: Anisakidae). Journal of Parasitology 100:199–214. doi: 10.1645/12—120.1

McEachran, J.D. and J.D. Fechhelm. 1998. Fishes of the Gulf of Mexico Volume 1. University of Texas Press, Austin, TX, USA. 1112 p.

Mignucci—Giannoni, A.A., E.P. Hoberg, D. Siegel—Causey, and E.H. Williams, Jr. 1998. Metazoan parasites and other symbionts of cetaceans in the Caribbean. Journal of Parasitology 84:939–946. doi: 10.2307/3284625

Nadler, S.A. and D.S.S. Hudspeth. 1998. Ribosomal DNA and phylogeny of the Ascaridoidea (Nemata: Secernentea): Implications for morphological evolution and classification. Molecular Phylogenetics and Evolution 10:221–236. doi: 10.1006/mpev.1998.0514

Nadler, S.A., S. D'Amelio, H.P. Fagerholm, B. Berland, and L. Paggi. 2000. Phylogenetic relationships among species of *Contracaecum* Railliet and Henry 1912 and *Phocascaris* Høst, 1932 (Nematoda: Ascaridoidea) based on nuclear rDNA sequence data. Parasitology 121:455–463. doi: 0.1017/s0031182099006423

Noble, E.R. and S.B. Collard. 1970. The parasites of midwater fishes. In: S.F. Snieszko, ed. A Symposium on Diseases of Fishes and Shellfishes. American Fisheries Society Special Publication 5, Washington, D.C., USA. p. 57–68.

Overstreet, R.M. 1978. Marine Maladies? Worms, Germs, and Other Symbionts from the Northern Gulf of Mexico. Mississippi—Alabama Sea Grant Consortium, Ocean Springs, MS, USA. 140 p.

Overstreet, R.M. 2012. Waterborne parasitic diseases in the ocean. In: R.A. Meyers, ed. Encyclopedia of Sustainability Science and Technology, Volume 17. Springer, New York, USA. p. 12018–12062. doi: 10.1007/978—1—4419—0851—3

Overstreet, R.M., J.C. Cook, and R.W. Heard. 2009. Trematoda (Platyhelminthes) of the Gulf of Mexico. In: D.L. Felder and D.K. Camp, eds. Gulf of Mexico–Origins, Waters, and Biota. Biodiversity. Texas A&M University Press, College Station, TX, USA. p. 419–486.

Overstreet, R.M. and G.W. Meyer. 1981. Hemorrhagic lesions in stomach of *Rhesus* monkey caused by a piscine ascaridoid nematode. Journal of Parasitology 67:226–235. doi: 10.2307/3280642

Palm, H.W. and S. Klimpel. 2008. Metazoan fish parasites of *Macrourus berglax* Lacepède, 1801 and other macrourids of the North Atlantic: Invasion of the deep sea from the continental shelf. Deep—Sea Research II 55:236–242. doi:10.1016/j.dsr2.2007.09.010

Palm, H.W., I.M. Damriyasa, Linda, and I.B.M. Oka. 2008. Molecular genotyping of *Anisakis* Dujardin, 1845 (Nematoda: Ascaridoidea: Anisakidae) larvae from marine fish of Balinese and Javanese waters, Indonesia. Helminthologia 45:3–12. doi: 10.2478/s11687—008—0001—8

Pauly, D., A.W. Trites, E. Capuli, and V. Christensen. 1998. Diet composition and trophic levels of marine mammals. ICES Journal of Marine Science 55:467–481. doi: 10.1006/jmsc.1997.0280

Pusch, C., A. Beckmann, F.M. Porteiro, and H. von Westernhagen. 2004. The influence of seamounts on mesopelagic fish communities. Archive of Fishery and Marine Research 51:165–186. doi: 0944—1921/2004/51/1—3—165

R Core Team. 2012. R: A language and environment for statistical computing. R Foundation for Statistical Computing, Vienna, Austria. ISBN 3—900051—07—0, URL http://www.R—project.org/.

Raga, J.A., M. Fernández, J.A. Balbuena, and F.J. Aznar. 2009. Parasites. In: W.F. Perrin, B. Würsing, and H.G.M. Thewissen, eds. Encyclopedia of Marine Mammals, 2nd ed. Academic Press/Elsevier, Amsterdam, Netherlands. p. 821—829.

Ross, S.W., A.M. Quattrini, A.Y. Roa—Varón, and J.P. McClain. 2010. Species composition and distributions of mesopelagic fishes over the slope of the north—central Gulf of Mexico. Deep—Sea Research II 57:1926–1956. doi: 10.1016/j.dsr2.2010.05.008

Sakanari, J.A. and J.H. McKerrow. 1989. Anisakiasis. Clinical Microbiology Reviews 2:278–284. doi: 10.1128/CMR.2.3.278

Salgado—Maldonado, G. and O.M. Amin. 2009. Acanthocephala of the Gulf of Mexico. In: D.L. Felder and D.K. Camp, eds. Gulf of Mexico–Origins, Waters, and Biota. Biodiversity. Texas A&M University Press, College Station, TX, USA. p. 539–552.

Smith, J.W. and R. Wootten. 1978. *Anisakis* and anisakiasis. Advances in Parasitology 16:93–163.

Ward R.D., T.S. Zemlak, B.H. Innes, P.R. Last, and P.D.N. Hebert. 2005. DNA barcoding Australia's fish species. Philosophical Transactions of the Royal Society of London, Series B, Biological Sciences 360:1847–1857. doi: 10.1098/rstb.2005.1716

Young, J.W., B.P.V. Hunt, T.R. Cook, J.K. Llopiz, E.L. Hazen, H.R. Pethybridge, D. Ceccarelli, A. Lorrain, R.J. Olson, V. Allain, C. Menkes, T. Patterson, S. Nicol, P. Lehodey, R.J. Kloser, H. Arrizabalaga, and C.A. Choy. 2015. The trophodynamics of marine top predators: Current knowledge, recent advances and challenges. Deep—Sea Research II 113:170–187. doi: 10.1016/j.dsr2.2014.05.015

Zhu, X.Q., R.B. Gasser, M. Podolska, and N.B. Chilton. 1998. Characterisation of anisakid nematodes with zoonotic potential by nuclear ribosomal DNA sequences. International Journal of Parasitology 28:1911–1921. doi: 10.1016/S0020—7519(98)00150—7

Gulf and Caribbean Research

Volume 27 | Issue 1

2016

Spatial Biodiversity Patterns of Fish within the Aransas Bay Complex, Texas

Bridgette F. Froeschke
University of Tampa, bfroeschke@ut.edu

Megan M. Reese Robillard
Harte Research Institute for Gulf of Mexico Studies, megan.robillard@tamucc.edu

Gregory W. Stunz
Harte Research Institute for Gulf of Mexico Studies, greg.stunz@tamucc.edu

Gulf and Caribbean Research Vol 27, 21-32, 2016
DOI: 10.18785/gcr.2701.03
Manuscript received, January 4, 2016; accepted, May 3, 2016

SPATIAL BIODIVERSITY PATTERNS OF FISH WITHIN THE ARANSAS BAY COMPLEX, TEXAS

Bridgette F. Froeschke[1*], Megan M. Reese Robillard[2], and Gregory W. Stunz[2]
*[1]The University of Tampa, 401 West Kennedy Boulevard, Tampa, FL 33606; [2]Texas A&M University–Corpus Christi, Harte Research Institute for Gulf of Mexico Studies, 6300 Ocean Drive, Corpus Christi, Texas 78412–5869; *Corresponding author, email: bfroeschke@ut.edu*

ABSTRACT: The goal of this study was to consider the effects of habitat type and environmental conditions on the biodiversity of fishes within the Aransas Bay Complex, Texas and provide a management framework and an ecosystem examination of Essential Fish Habitat (EFH). A stratified, randomized experimental design was used to collect fishes from seagrass, oyster, and non–vegetated habitats within the Aransas Bay Complex from February through May 2010 over large spatial scales at the "bay–complex" level. We developed a biodiversity habitat model using Boosted Regression Trees (BRT). Fitted functions from the "best" fit BRT habitat model indicated that fish biodiversity was greatest in seagrass areas closest to the inlet (< 80 cost–distance units) during early spring, with temperatures < 18°C and dissolved oxygen levels between 7–8 mg O_2/L in shallow depths (< 0.5 m). Results from community assemblage analyses showed significant differences among habitats with highest abundance of fishes found in seagrass, followed by non–vegetated substrate, and oyster reef. The relatively high abundance of fishes at non–vegetated bottom compared to the low abundance found at the oyster reef was most likely due to the spatial location of the habitats sampled. Our results indicate that future conservation measures should focus along the eastern and southern areas of Aransas Bay to protect EFH with highest levels of biodiversity. The modeling approach developed in this study provides a framework for natural resource managers to identify habitats supporting the greatest biodiversity of juvenile fishes.

KEYWORDS: Boosted Regression Trees, estuarine nursery habitat, essential fish habitat, fish community assemblage, biodiversity–habitat model

INTRODUCTION

Estuaries are among the most productive aquatic ecosystems and are obligate habitats for many marine species. Given the proximity to human population centers and the influence of freshwater as a determinant to both physical (e.g., salinity regime) and biotic (seagrass abundance and distribution as affected by freshwater inflow and nutrient loading) components, these ecosystems provide an ideal research laboratory to investigate modern paradigms in biodiversity and conservation (Lotze et al. 2006). The Gulf of Mexico (GOM) includes over 200 estuarine systems that are impacted by human population growth (which is predicted to increase 40% by 2025; http://www.unwater.org/index.html). Current and potential threats include increased waste production and urban non–point runoff, loss of wildlife habitat, water quality decline, and reduced sediment quality. Additionally, increased demands for wastewater treatment, irrigation, energy sources, and potable water of the GOM (http://www.lme.noaa.gov/) can all have profound effects on the biodiversity of estuaries within the GOM (Worm et al. 2006).

Human populations and their demands for land, energy, and natural resources are growing exponentially, creating pressures on ecosystems that were not anticipated by conventional approaches to natural resource management (Arkema et al. 2006). Human impacts have altered the distribution, quantity, and quality of marine habitats (Pyke 2004, Lotze et al. 2006, Nobre 2011), and these impacts have contributed to the depletion of more than 90% of estuarine species, degraded water quality, accelerated species invasions, and destroyed greater than 65% of seagrass and wetland habitat among estuaries and coastal seas (Jackson et al. 2001, Lotze et al. 2006, Worm et al. 2006). These losses have decreased marine biodiversity, which impairs the estuaries' capacity to maintain ecological health (provide food, maintain water quality etc.; Worm et al. 2006, Hector and Bagchi 2007) and the provision of ecosystem services like nursery habitats (Worm et al. 2006). Thus, there is a need for increased measurement of biodiversity across estuarine landscapes and in particular for fishes.

In the United States and territories, legislative mandates have required resource managers to identify Essential Fish Habitat (EFH) for fish, and take measures to restore, protect, and preserve these areas (2007 Magnuson–Stevens Fishery Conservation and Management Act Public Law 94–265). Estuarine habitat types such as submerged aquatic vegetation (e.g., seagrasses), emergent intertidal marshes, and non–vegetated bottom have been thoroughly investigated, and their role as EFH is well documented (Waycott et al. 2009). It is assumed that there is a positive relationship between the quantity of EFH and fish abundance or productivity (Hayes et al. 1996). However, this assumption is not often tested as research on EFH has focused on density patterns within habitat types (Gallaway and Cole 1999). This information is important, but EFH extends well beyond simple habitat–density relationships and includes interactions among biotic and abiotic components of the habitat (Hayes et al. 1996).

Therefore, modeling species–environment relationships is crucial for examining EFH.

The objective of this study was to compare fish communities among estuarine habitat types (seagrass, oyster, and non–vegetated bottom) and to determine spatial biodiversity patterns by developing a biodiversity model that predicts a Shannon–Wiener index within the Aransas Bay Complex, Texas. Specifically, the relationship among abiotic factors (temperature, salinity, turbidity, dissolved oxygen, and pH), biotic factors (habitat type, depth, and organic content), and the Shannon–Wiener biodiversity index were investigated within the Aransas Bay Complex (Mission–Aransas National Estuarine Research Reserve; MANERR), Texas. We also characterized monthly community structure (February, March, April, and May) as well as examined assemblages for each habitat type (seagrass, oyster, and non–vegetated bottom). The biodiversity–habitat model and related community level analyses will provide crucial information needed to identify and describe EFH within the Aransas Bay Complex, TX.

Materials and Methods

Study site

Field collections were conducted in the estuarine waters of the northern GOM in Aransas Bay Complex (Figure 1) within the MANERR. The reserve encompasses 752 km^2 of seagrass beds (primarily *Halodule wrightii*), oyster reefs (*Crassostrea virginica*), salt marsh (*Spartina alterniflora*), and non–vegetated bottom (sediment consisting of sand with small amounts of clay and silt). Aransas Bay contains extensive coastal wetlands and submerged aquatic vegetation, while Copano Bay is the largest secondary bay connected to Aransas Bay, and freshwater inflow (mean daily inflow of 28 m^3/s) occurs primarily via the Aransas and Mission Rivers, and virtually all of the saltwater exchange occurs via the Aransas Pass tidal inlet (Figure 1).

Field collection

A stratified and randomized experimental design was used to classify fish community structure among seagrass, oyster, and non–vegetated bottom habitats within the Aransas Bay Complex from February through May 2010. Sites were selected by converting the study area into 100 m^2 grid cells. Habitat type for each cell was determined using existing habitat maps (http://www.csc.noaa.gov/digitalcoast/data/benthiccover/download.html), with the first available seagrass nearly 10 km from the inlet. Using this grid, forty 100 m^2 sites were sampled each month in 3 habitat types, seagrass (n=10), oyster (n=10), and non–vegetated bottom habitats (n=20). Sample sites were selected without replacement using a randomized selection of sites from the sampling grid.

Physical environment

Prior to sampling at each site, environmental variables were measured just above the substrate using a Hydrolab 5S Sonde. Variables measured included water temperature (°C), dissolved oxygen (DO) in mg O_2/L, pH, salinity, and depth (m). Turbidity was measured using a Secchi disk (cm). Sediment samples were taken at non–vegetated and seagrass sites using a modified Van–Veen grab. Sediment samples were not collected at oyster sites as shells prevented sediment collection. Sediment samples were placed on ice and transported back to the laboratory for dry weight analysis as an indication of organic content. Analyses were conducted by placing 25g of sediment from each sample into an oven at 104°C for 24 hours. After drying, samples were re–weighed and the dry weight was subtracted from the original wet weight, using the following formula: Percent dry weight = (Sediment after drying (g)) / (wet weight (g)).

Samples with a low percent of dry weight were considered to have a higher percentage of organic content than samples with a higher percent of dry weight. Thus, low percentage of dry weight is correlated with higher sediment quality (Froeschke et al. 2013a).

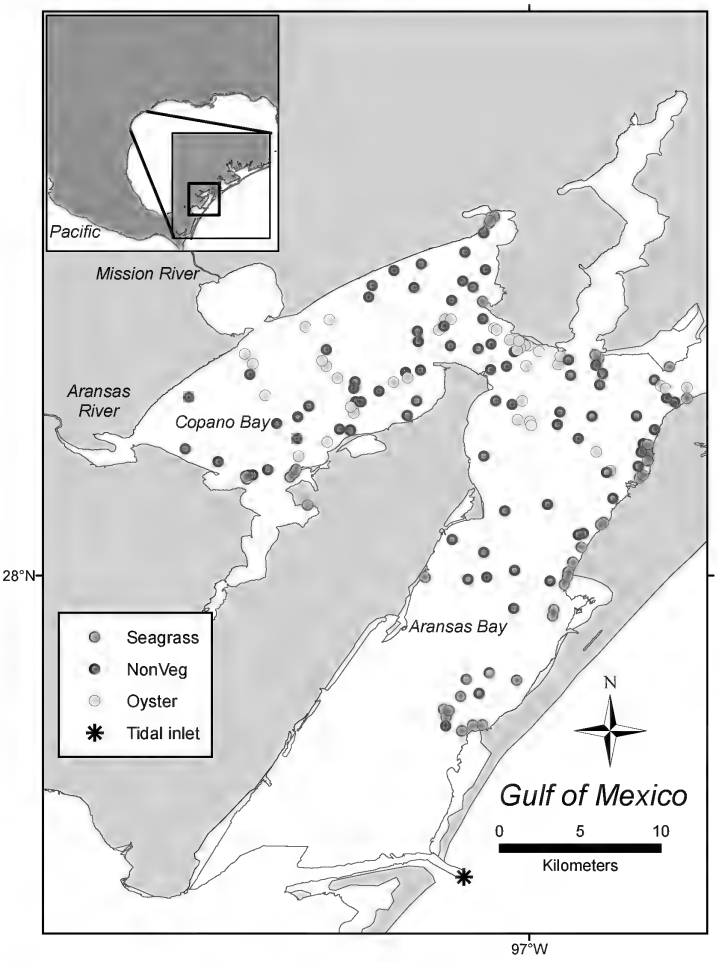

FIGURE 1. *Map of Aransas Bay Complex located along the northwestern Gulf of Mexico. Sampling locations (n = 160 sites) within the Aransas Bay Complex from February–May 2010, 80 non-vegetated bottom (NonVeg, brown circles), 40 seagrass sites (green circles), and 40 oyster sites (tan circles).*

Fish sampling

Fishes were collected using a 2 m wide beam trawl with 6 mm stretch mesh liner towed for 50 m (total area 100 m^2) at a constant speed (5 kt). Trawl samples were rough–sorted in the field to remove excessive algae, seagrass, and debris, then preserved in 10% formalin and returned to the laboratory for further processing. All fishes were identified, enumerated, and measured to the nearest mm standard length (SL).

Spatial Analyses

Saltwater and larval exchange (ingress pathway during the larval stage) occurs via the Aransas Pass tidal inlet. To examine a potential relationship between biodiversity of fishes with the connection to the GOM, the distance from the Aransas tidal inlet to each sampling location was calculated using the cost distance function in the spatial analyst extension in ArcGIS (ESRI, Redlands CA, USA), using the shoreline as a buffer (Whaley et al. 2007). The cost–distance function is used to calculate the shortest distance between 2 points that are constrained within a geographic boundary to provide more accurate relative distance estimates than Euclidian methods (Froeschke et al. 2010, 2013a, b).

Boosted Regression Trees

The relationship between Shannon–Wiener index of biodiversity of fishes and biological, physical, spatial and temporal variables were determined by developing spatially explicit distribution patterns of biodiversity of fishes. We used a forward fit, stage–wise, binomial boosted regression tree model (De'ath 2007, Elith et al. 2008), which is a powerful, yet relatively new, approach to modeling species–environment relationships. Boosted regression trees (BRT) is an ensemble method that combines statistical and machine learning techniques; it has shown to be an effective method for identifying relationships between fish distribution patterns and environmental predictors (Leathwick et al. 2006, 2008, Froeschke et al. 2010, 2013a, b, Froeschke and Froeschke 2011). Boosted regression trees: 1) accept different types of predictor variables; 2) accommodate missing values through the use of surrogates; 3) resist the effects of outliers; and 4) automatically fit interactions between predictors (Elith et al. 2006, 2008, Leathwick et al. 2006, 2008). Unlike traditional regression techniques, BRTs combine the strength of two algorithms, regression trees and boosting, to combine large numbers of relatively simple tree models instead of a single "best" model (Elith et al. 2006, 2008, Leathwick et al. 2006, 2008). Each individual model consists of a simple regression tree assembled by a rule–based classifier that partitions observations into groups having similar values for the response variable based on a series of binary splits constructed from predictor variables (Friedman 2001, Leathwick et al. 2006, Elith et al. 2008). The BRTs often have a higher predictive performance than single tree methods due to the inherent strengths of regression trees and the robustness of model averaging that improves predictive performance. Overfitting is minimized by incorporating 10–fold cross validation into the model fitting process (Elith et al. 2006, 2008, Leathwick et al. 2006, 2008).

Analyses were conducted in R (version 3.01, R Core Team 2013) using the 'gbm' library supplemented with functions from Elith et al. (2008). Initially, 10 predictors were included in the model: habitat type, organic content (%), depth (m), dissolved oxygen (mg O_2/L), temperature (°C), turbidity (cm), salinity, pH, distance to the inlet, and month (treated as a categorical variable; Figure 2). The adjustable model parameters for BRT are tree complexity (*tc*), learning rate (*lr*), and bag fraction, where *tc* controls whether interactions are fitted, *lr* determines the contribution of each tree to the growing model, and *bf* specifies the proportion of data to be selected at each step (Elith et al. 2008). Model selection was based on 2 performance metrics: 1) area under the receiver operating characteristic curve (ROC) and 2) explained deviance on cross–validated data. Selection of predictor variables was done using the gbm.simplify function from Elith et al. (2008), while the tuning parameters were optimized by cross–validation selecting a final model larger than 1,000 trees with maximum explained deviance on cross–validated data. Model validation was done by testing the null hypothesis that the slope of the trend line for

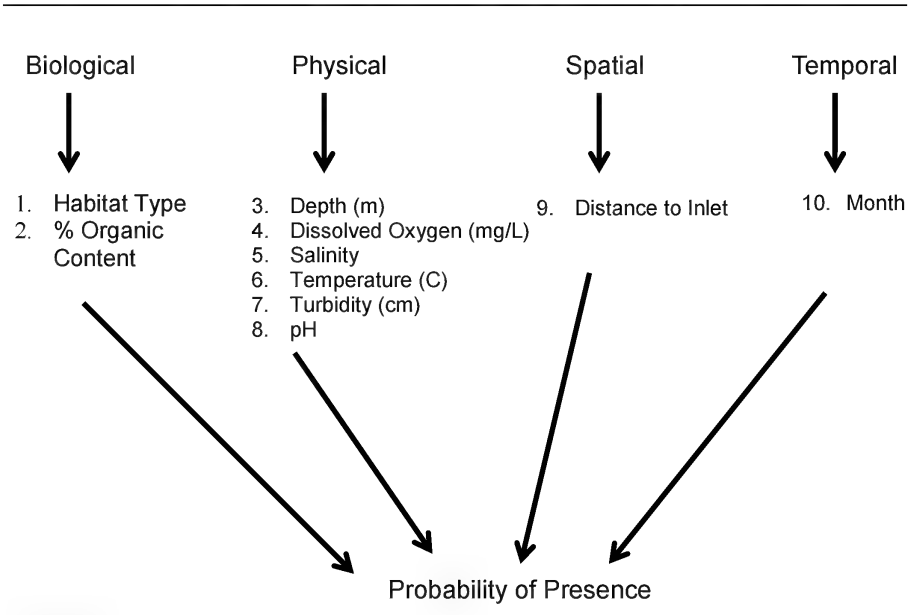

FIGURE 2. *Flowchart for Boosted Regression Trees to identify biodiversity hotspots within the Aransas Bay Complex.*

predicted biodiversity versus actual calculated biodiversity was not significantly different from one and the intercept parameter was not significantly different from zero. A least–squares linear regression was used: $Predicted_i = Intercept + C_i + Residuals_i$ where $Predicted_i$ equals predicted Shannon–Wiener index of biodiversity of fishes from the BRT model, and C_i equals the calculated Shannon–Wiener index of biodiversity of fishes from the data collected.

Community Analysis

A multivariate analysis (PRIMER v.6; Clarke and Gorley 2006) was conducted to test for significant differences in community assemblages among habitat types (Greenstreet and Hall 1996, Fisher and Frank 2002). The goal of this analysis was to test for differences in community assemblages among habitats by using several routines from PRIMER v.6 (Ludwig and Reynolds 1988, Catalán et al. 2006). The mean monthly abundance of each species collected was examined for each habitat (12 total samples). Data were 4th root transformed prior to analysis to reduce the differential effects of dominant species and differentiate among habitat types having many or few rare species (Clarke and Green 1988). The community assemblage patterns among habitat types were determined using non–metric multidimensional scaling (nMDS) based on Bray–Curtis similarity with Bray–Curtis cluster groups superimposed for interpretation (Clarke and Warwick 2001). Additionally, the SIMPER routine (similarity percentages) was used to determine the species contribution to the within group (habitat) similarity (Clarke and Warwick 2001). Along with the SIMPER routine, the BVSTEP procedure was used in the BEST routine (random selection) to identify the species that contributed the most to the whole community pattern. Using the identified species, another resemblance matrix based on Bray–Curtis similarity was created and compared to the original matrix (all species included) with the RELATE routine, with the null hypothesis that there is no relationship between the two similarity matrices, to determine if we find a similar community pattern with only the selected species (Clarke and Gorley 2006).

TABLE 1. *Mean (± se) parameter ranges by habitat from 160 sites (seagrass n = 40, oyster reef n = 40, and non-vegetated bottom n = 80) sampled from February to May 2010 within the Aransas Bay Complex.*

	Non-vegetated	Oyster	Seagrass
Water temperature (°C)	21.55 ± 2.41	21.97 ± 3.47	22.99 ± 3.64
Salinity	14.74 ± 1.65	13.13 ± 2.08	18.93 ± 2.99
Turbidity (cm)	81.12 ± 9.07	73.10 ± 11.56	56 ± 8.85
Depth (m)	3.59 ± 0.40	2.78 ± 0.44	2.15 ± 0.34
Dissolved oxygen (mg O_2/L)	7.26 ± 0.81	7.89 ± 1.25	9.03 ± 1.43
pH	8.14 ± 0.91	8.22 ± 1.30	8.44 ± 1.33
Dry weight (%)	47.83 ± 5.49	N/A	29.06 ± 4.59

Results

Abiotic and Biotic Parameters

During this study abiotic and biotic parameters varied seasonally and mean values differed among habitats (Table 1). Temperature ranged from 12.88°C (February) to 30.48°C (May), and the depth across sites ranged from 0.08 m (seagrass) to 3.54 m (non–vegetated bottom). The lowest salinity (6.22) occurred in an oyster reef in Copano Bay sampled in February, and the highest salinity (33.50) occurred in seagrass in Aransas Bay sampled in March. The lowest dissolved oxygen (2.72 mg O_2/L) occurred in April in seagrass in Copano Bay, and the highest dissolved oxygen (14.49 mg O_2/L) also occurred in April but in non–vegetated bottom in Aransas Bay. Percent dry weight was lowest (10.09%; highest organic content) in March in Copano Bay at a non–vegetated site and highest (75.58%; lowest organic content) in May in Aransas Bay at a non–vegetated site. Turbidity ranged from 20–200 cm with the lowest turbidity occurring in seagrass in February in Copano Bay, and the highest turbidity occurring in non–vegetated sites in May in Aransas Bay.

Summary of collections

A total of 5,789 fishes were collected from February to May 2010 from 160 sites (80 non–vegetated, 40 seagrass, and 40 oyster) within the Aransas Bay Complex. The fish assemblage included 35 species from 22 families. Seagrass sites supported the largest abundance of fishes (n = 3,797) and individual species (n = 27), followed by non–vegetated sites (1,487 fishes, 23 species), and then oyster reef sites (505 fishes, 16 species). The most abundant fish collected was *Micropogonias undulatus* (n = 984) comprising 17% of the fishes sampled (Table 2). *Syngnathus* sp. (mean = 18.55 ± 2.36), *Lagodon rhomboides* (mean = 16.75 ± 6.06), and *Ctenogobius boleosoma* (mean = 13.53 ± 5.41) were the most abundant fish at seagrass sites (Table 2). *Micropogonias undulatus* (mean = 8.84 ± 3.53), *Citharichthys spilopterus* (mean = 3.40 ± 0.74), and *Gobiosoma bosc* (mean = 2.30 ± 0.89) were the most abundant fish at non– vegetated sites (Table 2). *Micropogonias undulatus* (mean = 5.30 ± 2.50), and *G. bosc* (mean = 4.13 ± 1.40) were the 2 most abundant fish species at oyster sites (Table 2).

Boosted Regression Trees (Biodiversity Model)

The simplified habitat BRT model for prediction of the Shannon–Wiener Diversity Index incorporated 6 out of 10 variables and was determined as the "best" fit model (ROC = 0.87) as compared to the full model (ROC = 0.85, tree

complexity = 2, learning rate = 0.001, bag fraction = 0.5). Model validation using linear regression demonstrated an approximate 1:1 relationship between the calculated Shannon–Wiener Diversity Index values versus the predicted Shannon–Wiener Diversity Index values from the BRT (r^2 = 0.92, $F_{1,159}$ = 1,927, $p < 0.05$, Slope = 0.90; Figure 3) Within the BRT biodiversity model, habitat type explained the most deviance in the model (29.2%) followed by temperature (22.3%), distance to the nearest inlet (18.8%), month of collection (13.7%), dissolved oxygen (8.7%), and depth (7.3%; Figure 4). The fitted functions from the "best" fit

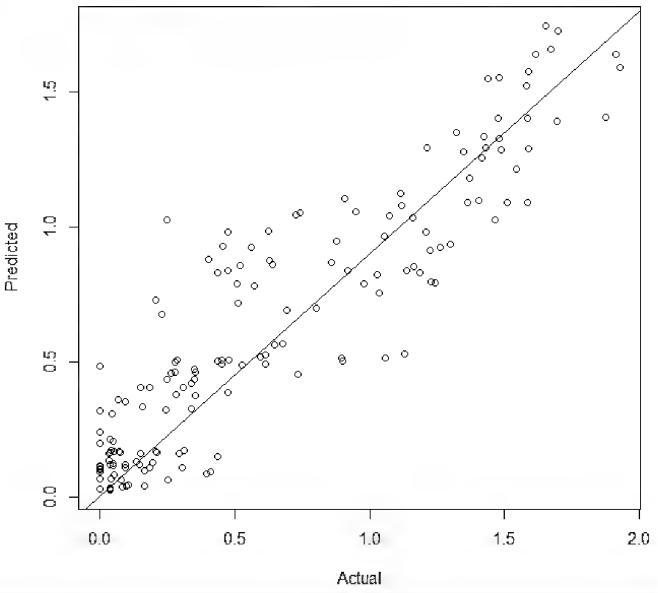

FIGURE 3. *Predicted values of biodiversity from the Boosted Regression Tree model versus the actual biodiversity values. Trend line was determined from the linear regression model (r^2 = 0.92, $F_{1,159}$ = 1,927, $p < 0.05$, Slope = 0.90).*

TABLE 2. *Overall mean abundance and standard error (SE) of all collected fishes in 3 habitat types including seagrass, oyster reef (Oyster), and non-vegetated bottom (Nonveg). The total number and relative abundance (number of individuals/total number of animals collected x 100) also are given. Species are listed in order of total and relative abundance.*

Common Name	Scientific Name	Total Number	Relative Abundance (%)	Seagrass Mean	Seagrass SE	Oyster Mean	Oyster SE	Nonveg Mean	Nonveg SE
		5,789							
Atlantic Croaker	*Micropogonias undulatus*	984	17	1.63	(0.55)	5.30	(2.50)	8.84	(3.53)
Pipefishes	*Syngnathus* sp.	800	13.8	18.55	(2.36)	0.58	(0.18)	0.44	(0.14)
Bay Whiff	*Citharichthys spilopterus*	715	12.4	10.33	(2.58)	0.75	(0.22)	3.40	(0.74)
Pinfish	*Lagodon rhomboides*	675	11.7	16.75	(6.06)	0.00	(0.00)	0.06	(0.05)
Darter Goby	*Ctenogobius boleosoma*	580	10	13.53	(5.41)	0.08	(0.06)	0.45	(0.34)
Naked Goby	*Gobiosoma bosc*	531	9.2	4.55	(2.73)	4.13	(1.40)	2.30	(0.89)
Spot	*Leiostomus xanthurus*	447	7.7	10.35	(4.01)	0.15	(0.07)	0.34	(0.10)
Code Goby	*Gobiosoma robustum*	416	7.2	7.90	(1.68)	0.65	(0.18)	0.93	(0.29)
Pigfish	*Orthopristis chrysoptera*	139	2.4	3.45	(1.36)	0.00	(0.00)	0.01	(0.01)
Blackcheek Tonguefish	*Symphurus plagiusa*	105	1.8	1.98	(0.75)	0.05	(0.03)	0.30	(0.10)
Silver Perch	*Bairdiella chrysoura*	103	1.8	2.58	(1.14)	0.00	(0.00)	0.00	(0.00)
Green Goby	*Microgobius thalassinus*	93	1.6	0.18	(0.08)	0.35	(0.13)	0.90	(0.18)
Seahorses	*Hippocampus* sp.	43	0.7	1.08	(0.27)	0.00	(0.00)	0.00	(0.00)
Southern Flounder	*Paralichthys lethostigma*	32	0.6	0.50	(0.14)	0.08	(0.06)	0.11	(0.06)
Sheepshead	*Archosargus probatocephalus*	31	0.5	0.78	(0.37)	0.00	(0.00)	0.00	(0.00)
Bay Anchovy	*Anchoa mitchilli*	24	0.4	0.08	(0.08)	0.25	(0.12)	0.14	(0.06)
Gulf Menhaden	*Brevoortia patronus*	23	0.4	0.05	(0.03)	0.15	(0.15)	0.19	(0.11)
Inshore Lizardfish	*Synodus foetens*	10	0.2	0.20	(0.11)	0.05	(0.03)	0.00	(0.00)
Gray Snapper	*Lutjanus griseus*	7	0.1	0.18	(0.11)	0.00	(0.00)	0.00	(0.00)
Gulf Toadfish	*Opsanus beta*	7	0.1	0.03	(0.03)	0.00	(0.00)	0.03	(0.02)
Inland Silverside	*Menidia beryllina*	4	0.1	0.08	(0.08)	0.00	(0.00)	0.01	(0.01)
Lined Sole	*Achirus lineatus*	3	0.1	0.00	(0.00)	0.03	(0.03)	0.03	(0.02)
Sheepshead Minnow	*Cyprinodon variegatus*	3	0.1	0.08	(0.08)	0.00	(0.00)	0.00	(0.00)
Rock Sea Bass	*Centropristis philadelphica*	2	0	0.03	(0.03)	0.00	(0.00)	0.01	(0.01)
Crested Blenny	*Hypleurochilus geminatus*	2	0	0.00	(0.00)	0.00	(0.00)	0.03	(0.03)
Shrimp Eel	*Ophichthus gomesii*	2	0	0.05	(0.05)	0.00	(0.00)	0.00	(0.00)
Ocellated Flounder	*Ancylopsetta quadrocellata*	1	0	0.03	(0.03)	0.00	(0.00)	0.00	(0.00)
Frillfin Goby	*Bathygobius soporator*	1	0	0.00	(0.00)	0.03	(0.03)	0.00	(0.00)
Striped Blenny	*Chasmodes bosquianus*	1	0	0.03	(0.03)	0.00	(0.00)	0.00	(0.00)
Striped Burrfish	*Chilomycterus schoepfii*	1	0	0.03	(0.03)	0.00	(0.00)	0.00	(0.00)
Fringed Sole	*Gymnachirus texae*	1	0	0.00	(0.00)	0.00	(0.00)	0.01	(0.01)
Skilletfish	*Gobiesox strumosus*	1	0	0.00	(0.00)	0.03	(0.03)	0.00	(0.00)
Atlantic Midshipman	*Porichthys plectrodon*	1	0	0.00	(0.00)	0.00	(0.00)	0.01	(0.01)
Least Puffer	*Sphoeroides parvus*	1	0	0.00	(0.00)	0.00	(0.00)	0.01	(0.01)

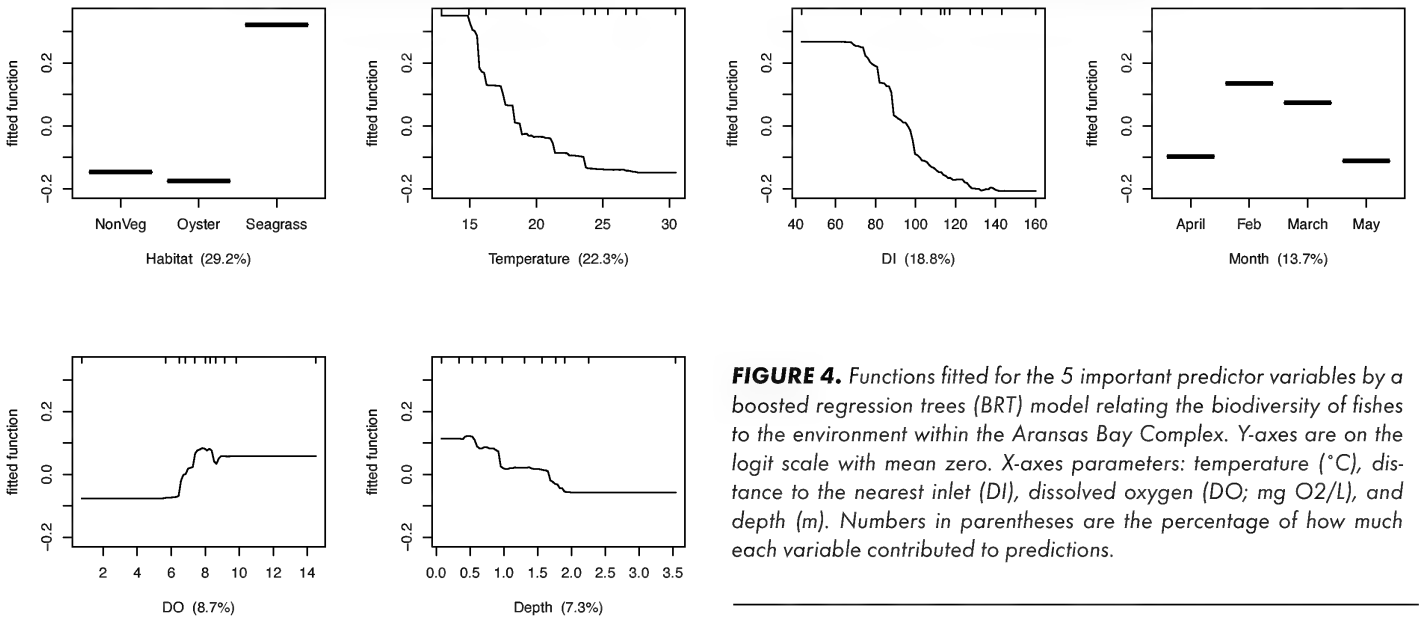

FIGURE 4. *Functions fitted for the 5 important predictor variables by a boosted regression trees (BRT) model relating the biodiversity of fishes to the environment within the Aransas Bay Complex. Y-axes are on the logit scale with mean zero. X-axes parameters: temperature (°C), distance to the nearest inlet (DI), dissolved oxygen (DO; mg O2/L), and depth (m). Numbers in parentheses are the percentage of how much each variable contributed to predictions.*

BRT habitat model indicated that the greatest biodiversity of fishes occurred in seagrass meadows closest to the inlet (< 80 cost–distance units) during the months of February and March, with temperatures < 18°C and dissolved oxygen levels between 7–8 mg O_2/L in shallow depths (< 0.5 m; Figure 4).

Spatial prediction of biodiversity of fishes from the BRT model demonstrated similar values between the calculated (Figure 5A) and predicted (Figure 5B) Shannon–Wiener Diversity Index values. Furthermore, spatial prediction indicated the highest biodiversity would occur in seagrass habitat along the eastern and southern areas of Aransas Bay (Figure 5B). Moderate biodiversity values (1.1–1.4) of fishes occurred in seagrass within Copano Bay and non–vegetated sites closest to the tidal inlet in Aransas Bay. The lowest biodiversity values (< 0.35) of fishes occurred along oyster and non–vegetation in the northern portions of Aransas and Copano Bays (Figure 5B).

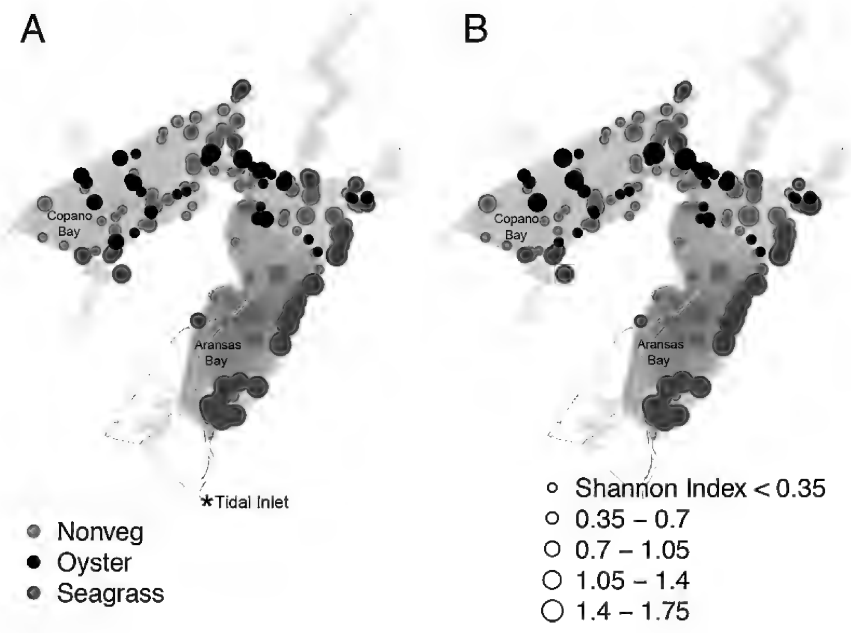

FIGURE 5. *Diversity of fishes in the Aransas Bay, TX complex. A. Calculated Shannon-Weiner Diversity Index at each site sampled. B. Spatial prediction of biodiversity of fishes from the boosted regression trees (BRT) model indicating the highest biodiversity would occur among seagrass along the east and south areas of Aransas Bay. Moderate values of biodiversity of fishes occurred in seagrass within Copano Bay and non-vegetated (Nonveg) sites closest to the tidal inlet in Aransas Bay. The lowest biodiversity values of fishes occurred along oyster and non-vegetation in the northern portions of Aransas and Copano Bay.*

Community Analysis

Our community analysis revealed differences in community assemblages both monthly and among habitats. Bray–Curtis cluster analysis found 3 groups at the 60% similarity level: 1) seagrass, 2) oyster and non–vegetated bottom, and 3) a second oyster group. The nMDS ordination indicated the same separation among habitats, but also revealed seasonal differences, which is very clear within the cluster analysis superimposed at the 60% level (Figure 6). Oyster samples collected during April and May have a different assemblage than during cooler months when they are more similar to non–vegetated bottom. Additionally, the nMDS plot reveals seasonal differences among seagrass samples with clear separation within the group from February through May. Non–vegetated bottom also reveals a similar seasonal trend with monthly differences in a similar pattern as seagrass habitat (Figure 6). The SIMPER analysis was used to determine which species were contributing to the community structure within each habitat. Estuarine–dependent species had the greatest contribution to the percent similarity among

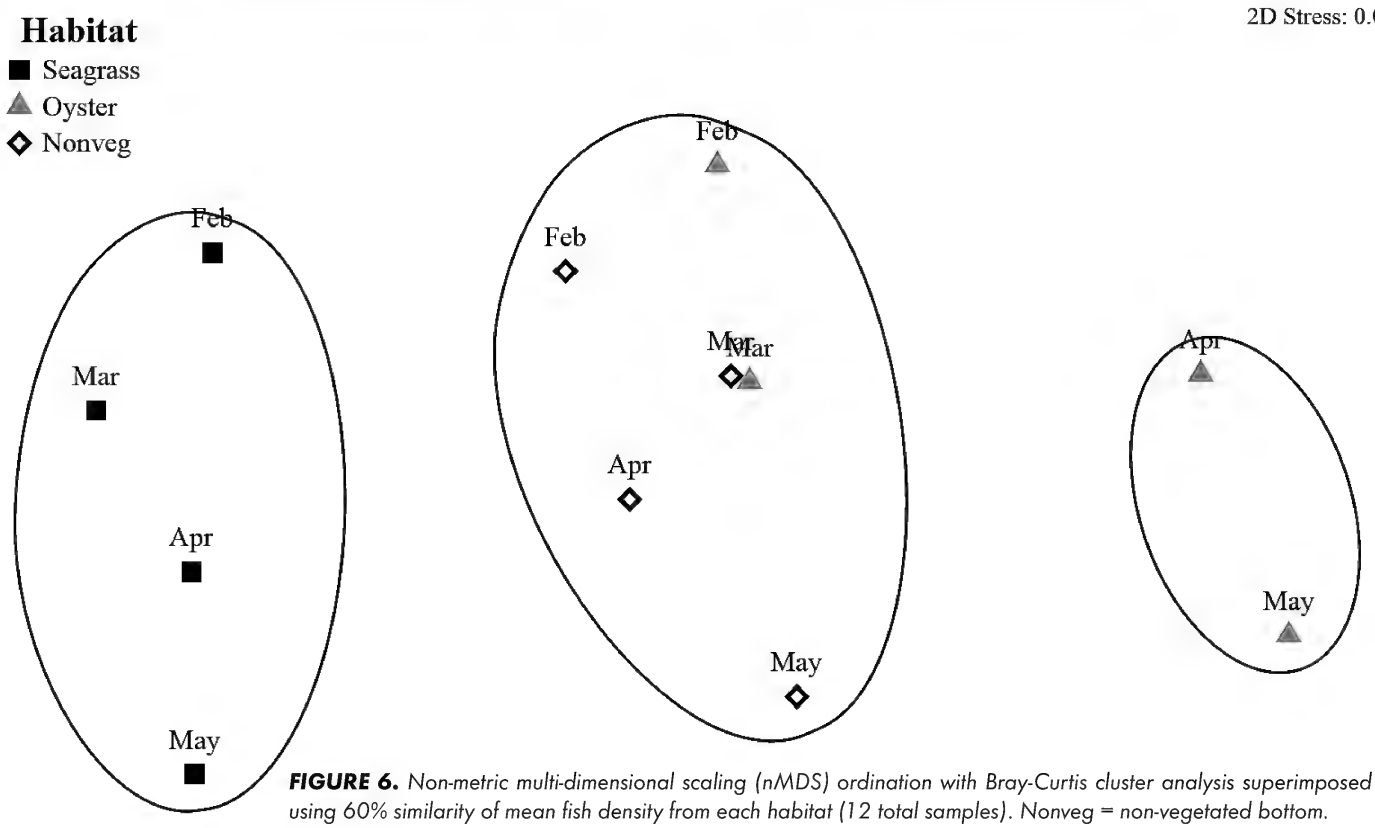

FIGURE 6. *Non-metric multi-dimensional scaling (nMDS) ordination with Bray-Curtis cluster analysis superimposed using 60% similarity of mean fish density from each habitat (12 total samples). Nonveg = non-vegetated bottom.*

habitats. In seagrass, *Syngnathus* sp., *L. rhomboides*, and *C. boleosoma* had the greatest contribution to the within–group similarity (Table 3). Whereas, in oyster reefs *G. bosc*, *Gobiosoma robustum*, and *Syngnathus* sp. had the greatest contribution to the within group similarity and in non–vegetated habitat, *C. spilopterus*, *G. bosc*, and *M. undulatus* had the greatest contribution to the within group similarity (Table 3). Using the BEST routine, we found 7 species that correlated 95.1% of the community assemblage. We also found a strong correlation between the original matrix (all species) and the BEST matrix (selected species) using the RELATE routine indicating that the matrices were similar ($r = 0.95$, $p = 0.001$). Generally, the most abundant species were identified in the BEST routine as contributing to the community

TABLE 3. *SIMPER summaries showing species that contributed to the within group average similarity for each habitat type. * denotes species that did not contribute to the within group average similarity. Nonveg = nonvegetated bottom.*

		Seagrass		Oyster		Nonveg	
		Mean Abundance	% Similarity	Mean Abundance	% Similarity	Mean Abundance	% Similarity
Pipefishes	*Syngnathus* sp.	18.55	15.93	0.58	15.31	0.44	9.23
Pinfish	*Lagodon rhomboides*	16.75	12.74	0.00	*	0.06	*
Darter Goby	*Ctenogobius boleosoma*	13.53	11.81	0.08	*	0.45	7.39
Code Goby	*Gobiosoma robustum*	7.90	11.58	0.65	16.63	0.93	9.37
Bay Whiff	*Citharichthys spilopterus*	10.33	10.31	0.75	14.61	3.40	15.66
Spot	*Leiostomus xanthurus*	10.35	7.28	0.15	8.07	0.34	8.25
Blackcheek Tonguefish	*Symphurus plagiusa*	1.98	6.85	0.05	*	0.30	7.18
Seahorses	*Hippocampus* sp.	1.08	5.49	0.00	*	0.00	*
Atlantic Croaker	*Micropogonias undulatus*	1.63	5.40	5.30	9.92	8.84	10.78
Naked Goby	*Gobiosoma bosc*	4.55	2.91	4.13	24.54	2.30	10.96
Green Goby	*Microgobius thalassinus*	0.18	*	0.35	*	0.90	10.38
Bay Anchovy	*Anchoa mitchilli*	0.08	*	0.25	6.94	0.14	3.56

assemblage (Table 3), which is similar to the SIMPER findings. *Lutjanus griseus* was the only species that had relatively low abundance and was not identified by SIMPER but was found to also contribute to the community assemblage in the BEST routine (Table 3).

Discussion

It has been hypothesized that an increase in biodiversity increases ecosystem function and services (Worm et al. 2006, Hector and Bagchi 2007) and has a direct impact on the number of viable fisheries, provision of nursery habitats, and water quality (Worm et al. 2006). This study supports these hypotheses and demonstrates the importance of incorporating biological, physical, and spatial variables to identify biodiversity hotspots. We found that biodiversity was most strongly influenced by the interaction among habitat type, water temperature, distance to the nearest inlet, month of sampling, dissolved oxygen, and depth. Results from this study also show the importance of determining which species are driving biodiversity along with spatial differences by combining diversity metrics with community assemblage techniques over a relatively large spatial scale.

Our results revealed that habitat type, specifically seagrass, was the most important predictor of biodiversity in this sub—tropical estuarine system. Given the importance of habitat on biodiversity patterns, projected habitat loss of a high biodiversity habitat (seagrass) to a lower biodiversity habitat type (non—vegetated) is concerning. Further, habitat loss due to human impacts is a primary cause of population depletion in fishes (Ruckelshaus et al. 2002, Pyke 2004, Levin and Stunz 2005, Lotze et al. 2006) and threatens the health of marine ecosystems (Pauly et al. 2002, Hilborn et al. 2003, Crowder et al. 2008, Halpern et al. 2008, Zhou et al. 2010). Water temperature was also a very important predictor of biodiversity. The relationship with temperature was most likely a result of seasonal temperature variance, which is certainly linked to annual fish recruitment patterns. For example, in the Aransas Bay Complex, occurrence of juvenile *Paralichthys lethostigma* were found in cooler water temperatures (Froeschke et al. 2013a) because their peak recruitment occurs between January and March each year (Nañez—James et al. 2009, Neahr et al. 2010).

Distance to the nearest inlet was also an important predictor of biodiversity. These results are consistent with other studies that show many estuarine species increase in abundance near inlets (Whaley et al. 2007, Reese et al. 2008, Froeschke et al. 2010, 2013b). Previous studies have identified EFH in habitats closest to the tidal inlet in the Aransas Bay Complex, TX (Nañez—James et al. 2009, Froeschke et al. 2013a, b). Moreover, our results suggest that inlet proximity remains an important feature of habitat quality across biotic habitat types. Month was the fourth most important predictor of biodiversity, with the highest biodiversity occurring in February and March. These results are most likely due to recruitment patterns of winter spawning species (*M. undulatus*, *P. lethostigma*, and *L. rhomboides*). Although decreasing biodiversity at lower salinities (greater distance from a tidal inlet) is a natural phenomenon, this is less pronounced in Texas secondary bays (e.g., Copano Bay) because they are greatly influenced by rainfall (Britton and Morton 1989). For example, during periods of drought, communities of secondary bays are characteristic of higher salinity environment (e.g., closer to the tidal inlet). Additionally, salinity was not a predictor in biodiversity, which shows that this parameter most likely did not greatly contribute to the distance pattern found.

Dissolved oxygen and depth were the least important predictors of biodiversity in this study. While dissolved oxygen levels can influence the distribution, abundance, and diversity of organisms (Breitburg 2002, Vaquer—Sunyer and Duarte 2008, Montagna and Froeschke 2009), this primarily occurs at much lower oxygen levels (i.e., < 2 mg O_2/L) (Froeschke and Stunz 2012) than observed in this study. In this study, few samples were collected in low dissolved oxygen conditions, however, low dissolved oxygen events (e.g., hypoxia) are increasing in frequency and spatial extent in Texas estuaries (Applebaum et al. 2005, Montagna and Froeschke 2009). These data suggest that oxygen levels could influence the distribution and abundance of biodiversity and that dissolved oxygen should be included as a variable in future studies. While depth may be important, these are relatively shallow estuarine well—mixed systems where depth likely has little effect.

Using community analyses we were able to determine what species were contributing to the differences in biodiversity among habitats and over time by the BRT model. Overall, both resident species (*Syngnathus* sp., *C. spilopterus* and several goby species) as well as estuarine—dependent species (*M. undulatus, L. rhomboides, Leiostomus xanthurus*) equally dominated the catch. However, the highest abundances of both of these groups of fishes were found in submerged seagrass vegetation, which is similar to many other studies (Day et al. 1989, Beck et al. 2001, Stunz et al. 2002, 2010, Reese Robillard et al. 2010). We found a low biodiversity of fishes on oyster reefs, which contrasts with numerous studies finding that structurally complex oyster reef systems support high density, biomass, and richness of estuarine nekton (Coen et al. 1999, Coen and Grizzle 2007, Stunz et al. 2010). The comparatively low biodiversity we observed could be a result of the spatial distribution of oyster reefs in the Aransas Bay Complex because the majority of oyster reefs are located in areas furthest away from the inlet in the northern portion of Aransas Bay and the northern and east portions of Copano Bay. Many estuarine species increase in abundance near inlets (Whaley et al. 2007, Froeschke et al. 2010), and Froeschke et al. (2013a) reported an in-

creased probability of flatfish occurrence closest to the inlet in the Aransas—Bay Complex, TX. The other reason for a low number of fish collected from oyster reefs could be because the reefs sampled were subtidal. Reese Robillard et al. (2010) showed similar results with deep subtidal reefs having much lower densities of nekton than shallow estuarine habitats, which may be due to lower vertical relief because these reefs are commercially fished. This similar study concluded that deep reefs may not be as important habitat for newly recruiting estuarine fishes, but are very important for resident oyster—reef species, as well as important foraging grounds for large transient fishes. It should also be noted that there could be a gear effect of using a towed gear over these complex habitats, which may also have caused the low biodiversity found. However, distance from a tidal inlet is an important factor as many estuarine—dependent species may not be able to access these habitats, thus lowering the overall biodiversity.

Despite the strengths of using BRT modeling approach, there are some inherent limitations. Cross—validated model evaluation indicated good performance of the BRT for biodiversity of fishes. It is possible other factors affecting biodiversity of fishes may not have been incorporated into the model, such as biotic components: spawning location, prey and predator density. However, we were able to examine several variables simultaneously that were related to habitat suitability, providing timely information for conservation and management of biodiversity within the Aransas Bay Complex. Furthermore, results from the BRT model were supported by the multivariate community analysis. Nonetheless, future studies of biodiversity should incorporate these abiotic parameters into the models when possible.

Although we collected the fewest number of fishes from oyster reefs, we found they had a similar community assemblage to non—vegetated bottom during February and March. *Micropogonias undulatus* was one of the most abundant species collected among all 3 habitats during this time, particularly in oyster and non—vegetated habitats, and its seasonal recruitment was most likely the driving factor for this community assemblage pattern (Rooker et al. 1998). The other evidence that *M. undulatus* was driving the community patterns is that their recruitment typically ends in March (Rooker et al. 1998), and the April and May oyster community assemblages were no longer similar to non—vegetated habitats. Seagrass samples were the most different from the other habitats among all months sampled. However, they were more closely related to non—vegetated bottom than oyster reefs, which could be because fish abundance was high at the non—vegetated sites closest to the inlet and adjacent to seagrass beds, highlighting the importance of the spatial arrangement of habitat types within ecosystems (Reese Robillard 2010). Finally, we did not directly assess the predation fields among these habitat types, and there is potential that very different trophic dynamics may exist in different habitats that may affect community structure and abundance (Grabowski 2004, Grabowski and Powers 2004). Several studies have demonstrated that different trophic linkages and connectivity between different estuarine habitats can affect nekton assemblage, density, prey mortality, and growth (Irlandi and Crawford 1997, Micheli and Peterson 1999, Grabowski et al. 2005).

A positive linkage among biodiversity, productivity, and stability across trophic levels in marine ecosystems has been demonstrated (Worm et al. 2006). Therefore, it is critical to maintain/increase the biodiversity of fishes. This study demonstrated the importance of incorporating environmental and biological variables into species biodiversity habitat models to identify areas suitable for EFH designation. The modeling approach, combined with community analyses developed in this study, provide a framework for natural resource managers to identify habitats supporting the greatest biodiversity of juvenile fishes, and to identify which species are contributing to the diversity among habitats. Marine biodiversity loss is increasingly impairing the ocean's capacity to provide food, maintain water quality, and recover from perturbations; therefore, we must understand the importance of these changes to develop a more management approaches to better maintain fish biodiversity.

Acknowledgements

We thank the Mission—Aransas National Estuarine Research Reserve Fellowship Program, and the Fisheries and Ocean Health Laboratory at the Harte Research Institute for the Gulf of Mexico Studies for funding and support of this work. In addition, we thank J. Slocum, L. Payne, R. Brewton, B. Blomberg, and J. Williams for all of their hard work in the field. We thank J. Froeschke for his insightful reviews of earlier drafts of this manuscript.

Literature Cited

Applebaum, S., P.A. Montagna, and C. Ritter. 2005. Status and trends of dissolved oxygen in Corpus Christi Bay, Texas, U.S.A. Environmental Monitoring and Assessment 107:297–311.

Arkema, K.K., S.C. Abramson, and B.M. Dewsbury. 2006. Marine ecosystem–based management: from characterization to implementation. Frontiers in Ecology and the Environment 4:525–532. doi: 10.1890/15409295(2006)4[525:MEMFCT]2.0.CO;2

Beck, M.W., K.L. Heck, K.W. Able, D.L. Childers, D.B. Eggleston, B.M. Gillanders, B. Halpern, C.G. Hays, K. Hoshino, T.J. Minello, R.J. Orth, P.F. Sheridan, and M.P. Weinstein. 2001. The identification, conservation, and management of estuarine and marine nurseries for fish and invertebrates. Bioscience 51:633–641. doi: 10.1641/0006–3568(2001)051[0633:TICAMO]2.0.CO;2

Breitburg, D. 2002. Effects of hypoxia, and the balance between hypoxia and enrichment, on coastal fishes and fisheries. Estuaries 25:767–781. doi:10.1007/BF02804904

Britton, J.C. and B. Morton. 1989. Shore ecology of the Gulf of Mexico, 3rd edition. University of Texas Press, Austin, TX, USA, 387 p.

Catalán, I.A., M.T. Jiménez, J.I. Alconchel, L. Prieto, and J.L. Muñoz. 2006. Spatial and temporal changes of coastal demersal assemblages in the Gulf of Cadiz (SW Spain) in relation to environmental conditions. Deep–Sea Res Part II 53:1402–1419. doi: 10.1016/j.dsr2.2006.04.005

Clarke, K.R. and R.N. Gorley. 2006. PRIMER v6: user manual/tutorial. PRIMER–E, Plymouth, UK, 190 p.

Clarke, K.R. and R.H. Green. 1988. Statistical design and analysis for a 'biological effects' study. Marine Ecology Progress Series 46:213–226.

Clarke, K.R. and R.M. Warwick. 2001. Change in marine communities: an approach to statistical analysis and interpretation, 2nd edition. PRIMER–E, Plymouth, UK.

Coen, L.D. and R. Grizzle. 2007. The importance of habitat created by molluscan shellfish to managed species along the Atlantic Coast of the United States. Habitat Management Series no.8. Atlantic States Marine Fisheries Commission, Washington DC, USA, 108 p.

Coen, L.D., M.W. Luckenbach, and D.L. Breitburg. 1999. The role of oyster reefs as essential fish habitat: A review of current knowledge and some new perspectives. American Fisheries Society Symposium 22:438–454.

Crowder, L.B., E.L. Hazen, N. Avissar, R. Bjorkland, C. Latanich, and M.B. Ogburn. 2008. The impacts of fisheries on marine ecosystems and the transition to ecosystem–based management. Annual Review of Ecology, Evolution and Systematics 39:259–278. doi: 10.1146/annurev.ecolsys.39.110707.173406.

Day, J.W., C.A.S. Hall, W.M. Kemp, and A. Yannez–Arancibia. 1989. Estuarine Ecology. John Wiley and Sons, New York, NY, USA, 558 p.

De'ath, G. 2007. Boosted trees for ecological modeling and prediction. Ecology 88: 243–251. doi: 10.1890/0012–9658(2007)88[243:BTFEMA]2.0.CO;2

Elith, J., C.H. Graham, and R.P. Anderson. 2006. Novel methods improve prediction of species' distributions from occurrence data. Ecography 29:129–151. doi: 10.1111/j.2006.0906–7590.04596.x

Elith, J., J.R. Leathwick, and T. Hastie. 2008. A working guide to boosted regression trees. Journal of Animal Ecology 77:802–813. doi: 10.1111/j.1365–2656.2008.01390.x

Fisher, J.A.D. and K.T. Frank. 2002. Changes in finfish community structure associated with an offshore fishery closed area on the Scotian Shelf. Marine Ecology Progress Series 240:249–265. doi: 10.3354/meps240249

Friedman, J.H. 2001. Greedy function approximation: a gradient boosting machine. The Annals of Statistics 29:1189–1232.

Froeschke, J.T. and B.F. Froeschke. 2011. Spatio–temporal predictive model based on environmental factors for juvenile spotted seatrout in Texas estuaries using boosted regression trees. Fisheries Research 111:131–138. doi: 10.1016/j.fishres.2011.07.008

Froeschke, J.T. and G.W. Stunz. 2012. Hierarchical and interactive habitat selection in response to abiotic and biotic factors: The effect of hypoxia on habitat selection of juvenile estuarine fishes. Environmental Biology of Fishes 93:31–41. doi: 10.1007/s10641–011–9887–y

Froeschke, J.T., G.W. Stunz, and M.L. Wildhaber. 2010. Environmental influences on the occurrence of coastal sharks in estuarine waters. Marine Ecology Progress Series 401:279–292. doi: 10.3354/meps08546

Froeschke, B.F., G.W. Stunz, M.R. Reese Robillard, J. Williams, and J.T. Froeschke. 2013a. A modeling and field approach to identify essential fish habitat for juvenile bay whiff (*Citharichthys spilopterus*) and southern flounder (*Paralichthys lethostigma*) within the Aransas Bay Complex, TX. Estuaries and Coasts 36:881–892. doi: 10.1007/s12237–013–9600–9

Froeschke, B.F., P. Tissot, G.W. Stunz, and J.T. Froeschke. 2013b. Spatiotemporal predictive models for juvenile southern flounder in Texas estuaries. North American Journals of Fisheries Management 33:817–828. doi: 10.1080/02755947.2013.811129

Gallaway, B.J. and J.G. Cole. 1999. Delineation of essential habitat for juvenile red snapper in the northwestern Gulf of Mexico. Transactions of the American Fisheries Society 128:713–726. doi: 10.1577/1548–8659(1999)128<0713:DOEHFJ>2.0.CO;2

Grabowski, J.H. 2004. Habitat complexity disrupts predator–prey interactions but not the trophic cascade on oyster reefs. Ecology 85:995–1004. doi: 10.1890/03–0067

Grabowski, J.H. and S.P. Powers. 2004. Habitat complexity mitigates trophic transfer on oyster reefs. Marine Ecology Progress Series 277:291–295. doi: 10.3354/meps277291

Grabowski, J.H., A.R. Hughes, D.L. Kimbro, and M.A. Dolan. 2005. How habitat setting influences restored oyster reef communities. Ecology 86:1926–1935. doi: 10.1890/04–0690

Greenstreet, S.P.R. and S.J. Hall. 1996. Fishing and the ground–fish assemblage structure in the north–western North Sea: An analysis of long–term and spatial trends. Journal of Animal Ecology 65:577–598. doi: 10.2307/5738

Halpern, B.S., S. Walbridge, K.A. Selkoe, C.V. Kappel, F. Micheli, C. D'Agrosa, J.F. Bruno, K.S. Casey, C. Ebert, H.E. Fox, R. Fujita, D. Heinemann, H.S. Lenihan, E.M.P. Madin, M.T. Perry, E.R. Selig, M. Spalding, R. Steneck, and R. Watson. 2008. A global map of human impact on marine ecosystems. Science 319:948–952. doi: 10.1126/science.1149345

Hayes, D.B., C.P. Ferreri, and W.W. Taylor. 1996. Linking fish habitat to their population dynamics. Canadian Journal of Fisheries and Aquatic Science 53(Suppl. 1):383–390. doi: 10.1007/s11160–009–9103–8

Hector, A. and R. Bagchi. 2007. Biodiversity and ecosystem multifunctionality. Nature 448:188–190. doi: 10.1038/nature05947

Hilborn, R., T.A. Branch, B. Ernst, A. Magnussum, C.V. Minte–Vera, M.D. Scheurell, and J.L. Valero. 2003. State of the world's fisheries. Annual Review of Environmental Resources 28:359–399.

Irlandi, E.A. and M.K. Crawford. 1997. Habitat linkages: the effect of intertidal saltmarshes and adjacent subtidal habitats on abundance, movement, and growth of an estuarine fish. Oecologia 110:222–230. doi: 10.1007/s004420050154

Jackson, J.B.C., M.X. Kirby, W.H. Berger, K.A. Bjorndal, L.W. Botsford, B.J. Bourque, R.H. Bradbury, R. Cooke, J. Erlandson, J.A. Estes, T.P. Hughes, S. Kidwell, C.B. Lange, H.S. Lenihan, J.M. Pandolfi, C.H. Peterson, R.S. Steneck, M.J. Tegner, and R.R. Warner. 2001. Historical overfishing and the recent collapse of coastal ecosystems. Science 293:629–638. doi: 10.1126/science.1059199

Leathwick, J.R., J. Elith, M.P. Francis, T. Hastie, and P. Taylor. 2006. Variation in demersal fish species richness in the oceans surrounding New Zealand: An analysis using boosted regression trees. Marine Ecology Progress Series 321:267–281. doi: 10.3354/meps321267

Leathwick, J.R., J. Elith, W.L. Chadderton, D. Rowe, and T. Hastie. 2008. Dispersal, disturbance, and the contrasting biogeographies of New Zealand's diadromous and non–diadromous fish species. Journal Biogeography 35:1481–1497. doi: 10.1111/j.1365–2699.2008.01887.x

Levin, P.S. and G.W. Stunz. 2005. Habitat triage for exploited fishes: Can we identify essential "Essential Fish Habitat?". Estuarine, Coastal and Shelf Science 64:70–78. doi: 10.1016/j.ecss.2005.02.007

Lotze, H.K., H.S. Lenihan, B.J. Bourque, R.H. Bradbury, R.G. Cooke, M.C. Kay, S.M. Kidwell, M.X. Kirby, C.H. Peterson, and J.B.C. Jackson. 2006. Depletion, degradation, and recovery potential of estuaries and coastal seas. Science 312:1806–1809. doi: 10.1126/science.1128035

Ludwig, J.A. and J.F. Reynolds. 1988. Statistical Ecology. A Primer on Methods and Computing. John Wiley and Sons, New York, NY, USA, 202 p.

Micheli, F. and C.H. Peterson. 1999. Estuarine vegetated habitats as corridors for predator movements. Conservation Biology 13:869–881. doi: 10.1046/j.1523–1739.1999.98233.x

Montagna, P.A. and J.T. Froeschke. 2009. Long–term biological effects of coastal hypoxia in Corpus Christi Bay, Texas, USA. Journal of Experimental Marine Biology and Ecology 381:S21–S30. doi: 10.1016/j.jembe.2009.07.006

Nañez–James, S.E., G.W. Stunz, and S. Holt. 2009. Habitat use patterns of newly settled Southern Flounder, *Paralichthys lethostigma*, in Aransas–Copano Bay, Texas. Estuaries and Coasts 32:350–359. doi: 10.1007/s12237–008–9107–y

Neahr, T.A., G.W. Stunz, and T.J. Minello. 2010. Habitat use patterns of newly–settled spotted seatrout in estuaries of the north–western Gulf of Mexico. Fisheries Management and Ecology 17:404–413. doi: 10.1111/j.1365–2400.2010.00733.x

Nobre, A.M. 2011. Scientific approaches to address challenges in coastal management. Marine Ecology Progress Series 434:279–289. doi: 10.3354/meps09250

Pauly, D., V. Christensen, S. Guènette, T.J. Pitcher, U.R. Sumaila, C.J. Walters, R. Watson, and D. Zeller. 2002. Towards sustainability in world fisheries. Nature 418:689–695. doi: 10.1038/nature01017

Pyke, C.R. 2004. Habitat loss confounds climate change impacts. Frontiers in Ecology and the Environment 2:178–182. doi: 10.1890/1540–9295(2004)002[0178:HLCCCI]2.0.CO;2

R Core Team. 2013. R: A language and environment for statistical computing. R Foundation for Statistical Computing, Vienna, Austria. URL http://www.R–project.org/.

Reese, M.M., G.W. Stunz, and A.M. Bushon. 2008. Recruitment of estuarine–dependent nekton through a new tidal inlet: The opening of Packery Channel in Corpus Christi, TX, USA. Estuaries and Coasts 32:350–359. doi: 10.1007/s12237–008–9096–x

Reese Robillard, M.M., G.W. Stunz, and J. Simons. 2010. Relative value of deep subtidal oyster reefs to other estuarine habitat types using a novel sampling method. Journal of Shellfish Research 29:291–302. doi:10.2983/035.029.0203

Rooker, J.R., S.A. Holt, M.A. Soto, and G.J. Holt. 1998. Post-settlement patterns of habitat use by sciaenid fishes in subtropical seagrass meadows. Estuaries 21:318–327. doi: 10.2307/1352478

Ruckelshaus, M.H., P.S. Levin, J.B. Johnson, and P.M. Kareiva. 2002. The Pacific salmon wars: What science brings to the challenge of recovering species. Annual Review of Ecological Systems 33:665–706. doi: 10.1146/annurev.ecolsys.33.010802.150504

Stunz, G.W., T.J. Minello, and P.S. Levin. 2002. A comparison of early juvenile red drum densities among various habitat types in Galveston Bay, Texas. Estuaries 25:76–85. doi: 10.1007/BF02696051

Stunz, G.W., T.J. Minello, and L.P. Rozas. 2010. Relative value of oyster reef as habitat for estuarine nekton in Galveston Bay, Texas. Marine Ecology Progress Series 406:147–159. doi: 10.3354/meps08556

Vaquer–Sunyer, R. and C.M. Duarte. 2008. Thresholds of hypoxia for marine biodiversity. Proceedings of the National Academy of Sciences 105:15452–15457. doi: 10.1073/pnas.0803833105

Waycott, M., C.M.M. Duarte, T.J.B. Carruthers, R.J. Orth, W.C. Dennison, S. Olyarnik, A. Calladine, J.W. Fourgurean, K.L. Heck Jr, A.R. Hughes, G.A. Kendrick, W.J. Kenworthy, F.T. Short, and S.L. Williams. 2009. Accelerating loss of seagrass across the globe threatens coastal ecosystems. Proceedings of the National Academy of Sciences 106:12377–12381. doi: 10.1073/pnas.0905620106

Whaley, S.D., J.J. Burd, and B.A. Robertson BA. 2007. Using estuarine landscape structure to model distribution patterns in nekton communities and in juveniles of fishery species. Marine Ecology Progress Series 330:83–99. doi: 10.3354/meps330083

Worm, B., E.B. Barbier, N. Beaumont, E. Duffy, C. Folke, B.S. Halpern, J.B.C. Jackson, H.K. Lotze, F. Micheli, S.R. Palumbi, E. Sala, K.A. Selkoe, J.J. Stachowicz, and R. Watson. 2006. Impacts of biodiversity loss on ocean ecosystem services. Science 314:787–790. doi: 10.1126/science.1132294

Zhou, S., A.D.M. Smith, A.E. Punt, A.J. Richardson, M. Gibbs, E.A. Fulton, S. Pascoe, C. Bulman, P. Bayliss, and K. Sainsbury. 2010. Ecosystem–based fisheries management requires a change to the selective fishing philosophy. Proceedings of the National Academy of Sciences 107:9485–9489. doi: 10.1073/pnas.0912771107

Gulf and Caribbean Research

Volume 27 | Issue 1

2016

Identification Of Compounds Of Allelopathic Extracts From Two Species Of *Metapeyssonnelia* (Rhodophyta) Growing On The Hydrocoral, *Millepora complanata*, In Puerto Rico

Maria I. Reyes-Contreras
University of Bern, mi.reyescontreras@gmail.com

Aniuska Kazandjian
Simon Bolivar University, akazandj@gmail.com

David L. Ballantine
University of Puerto Rico, Smithsonian Institution, david.ballantine@upr.edu

Gulf and Caribbean Research Vol 27, 33-41, 2016
DOI: 10.18785/gcr.2701.04

Manuscript received, October 27, 2015; accepted, May 18, 2016

IDENTIFICATION OF COMPOUNDS OF ALLELOPATHIC EXTRACTS FROM TWO SPECIES OF *METAPEYSSONNELIA* (RHODOPHYTA) GROWING ON THE HYDROCORAL, *MILLEPORA COMPLANATA*, IN PUERTO RICO

Maria Reyes–Contreras[1*], Aniuzka Kazandjián[1], and David L. Ballantine[2,3]

*[1]Laboratorio de Sistemática Molecular, Centro de Biodiversidad Marina, Simón Bolívar University, Caracas, Venezuela; [2]Department of Marine Sciences, University of Puerto Rico, Mayagüez, Puerto Rico 00681; [3]Department of Botany, NHB166, P.O. Box 37012, National Museum of Natural History, Smithsonian Institution, Washington, D.C. 20013; *Corresponding author, email: mi.reyescontreras@gmail.com*

ABSTRACT: Two Puerto Rican species of the encrusting red alga *Metapeyssonnelia* are known to overgrow and kill the hydrocoral *Millepora complanata*. The overgrowth is accompanied by bleaching or tissue lightening regions surrounding the growing margin of the algae on the coral tissue. Lipophilic and hydrophilic extracts from *Metapeyssonnelia corallepida* and *M. milleporoides* were obtained and analyzed by GC–MS. The following compounds were identified from *M. corallepida:* squalene and 5–(hydroxymethyl)–2–(dimethoxymethyl)–furan3–methoxycarbonyl–1,1–diethyl–2–buten–4–olide and from *M. milleporoides:* 2,4–dit–butyl phenol, 2(3H)–furanone and dihydro–4,4–dimethyl–(CAS), terpenes, furanones and phenol. Aliquots of crude extracts of both *Metapeyssonnelia* species applied to coral fragments resulted in visible changes to the coral tissue as well as unexpected change in numbers of zooxanthellae. The highest concentration of *M. corallepida* lipophilic extracts assayed generated bleaching halos, death of coral tissue and a reduction of the zooxanthellae number while the two lower concentrations of lipophilic extracts of *M. milleporoides* resulted in obvious tissue lightening, but without decline in zooxanthellae number.

KEYWORDS: algal extracts, allelopathy, overgrowth, furanone, necrosis

INTRODUCTION

Coral reef health has been threatened as the result of a complex combination of anthropogenic and biological factors including overfishing (McManus and Polsenberg 2004; Aronson and Precht 2006; Mora 2008), increased water temperature (Baker et. al. 2008; Strychar and Sammarco 2009), anthropogenic nutrient enrichment (Lapointe 1997; D'Angelo and Wiedenmann 2014), ocean acidification (Baker et al. 2008; Veron et al. 2009; Pandolfi et al. 2011) and coral diseases (Sutherland et al. 2004; Weil et al. 2006; Schutte et al. 2010). Those factors which are detrimental for corals and advantageous for algal proliferation have led to "phase shifts" on coral reefs (Hughes 1994; Ruiz and Ballantine 2009; Diaz–Pulido et al. 2011; Anthony et al. 2011; Barott et al. 2012). The process of "phase shifts" results in increased proximity of algae and corals leading to an increased arena for interaction. With a greater opportunity for algal contact with coral, negative effects on corals due to interactions with algae are increasingly being documented. Reports of negative interactions involving simple contact between algae (without overgrowth) include inhibition of *Porites lutea* Quoy & Gaimard by the cyanophyte *Lyngbya bouillonii* L.Hoffmann & V.Demoulin (Titlyanov et al. 2007); negative effect on *Porites* sp. by the rhodophyte *Anotrichium tenue* (C.Agardh) Nägeli (Jompa and McCook 2003a); and killing live *Porites* spp. tissue by contact with the red alga *Corallophila huysmansii* (Weber–van Bosse) R.E.Norris (Jompa and McCook 2003b). Bonaldo and Hay (2014) further reported tissue bleaching in several coral species due to contact with multiple algal species. These authors all invoked algal allelopathy as the likely cause of coral damage. While evidence was only correlative, these suggestions are probably correct.

To our knowledge, only two published accounts have experimentally demonstrated coral inhibition by allelopathic chemical extracts from macroalgae. de Nys et al. (1991) reported that compounds produced by *Plocamiun hamatum* J. Agardh (Rhodophyta) generated tissue lesions on the coral *Sinularia cruciata* Tixier–Durivault, and Rasher and Hay (2010) reported that metabolites produced by *Ochtodes secundaramea* (Montagne) M. A. Howe (Rhodophyta) also generated bleaching spots on *Porites porites* (Pallas).

Algal epizooism impacting coral well–being has been reported for several encrusting rhodophyte species. Overgrowth of coral by coralline red alga *Pneophyllum conicum* (E. Y. Dawson) Keats, Y. M. Chamberlain et M. Baba was reported by Antonius (2001). Another encrusting rhodophyte, *Ramicrusta textilis*, was later described and reported to overgrow and kill those coral species on which it grows (Pueschel and Saunders 2009). Ballantine and Ruiz (2013) reported on the extent (about 18,000 m^2) of coral overgrowth by *Ramicrusta* in Puerto Rico at a shallow–water coral reef environment. Another alga species which overgrows corals, *Metapeyssonnelia corallepida* Verlaque et al. (2000), described from the Caribbean, was reported to be responsible for killing the hydrocoral *Millepora* beneath the algal crust (Antonius and Ballesteros 1998; Antonius 1999). Subsequently, Ballantine and Ruiz (2011) described another coral killing species of the genus, *M. milleporoides* D. L. Ballantine & H.

Ruiz, from Puerto Rico. Vieira et al. (2015) reported that *Lobophora hederacea* C.W. Vieira, De Clerck & Payri (Phaeophyceae) overgrew and killed the Pocilloporidae coral *Seriatopora caliendrum* Ehrenberg. Coral bleaching at the *Lobophora* margin strongly suggested allelopathic mechanisms to the authors. Chadwick and Morrow (2011) review other negative interactions between macro algae and corals.

Metapeyssonnelia corallepida and *M. milleporoides* belong to the Rhodophyta family Peyssonneliaceae Denizot (1968) (Verlaque et al. 2000, Ballantine and Ruiz 2011). The genus is characterized by having a prostrate crustose habit, orbicular shape, dorsiventral thallus with a distinct hypothallus and perithallus, and being attached to the substratum by unicellular rhizoids and suprabasal calcification. In shallow water coral reef environments in southwest Puerto Rico both *Metapeyssonnelia* species have been observed overgrowing the hydrozoan coral *Millepora complanata* Lamarck and the scleractinian *Porites* sp., leaving no living coral tissue beneath the algal crust (Ballantine et al. 2004; Ballantine and Ruiz 2011) at La Parguera, Puerto Rico. The algal (Peyssonneliales) epizootic overgrowth of coral as exhibited by *M. corallepida* has been termed "PEY" by Antonius (1999), who referred to the phenomena as a disease condition. By extension, coral overgrowth by *M. milleporoides* would also be considered a coral disease condition. This overgrowth pattern is characterized by the presence of an unmistakable bleaching halo on coral tissue just beyond the growing edge of both *M. corallepida* and *M. milleporoides* thalli (Figure 1). Both species of *Metapeyssonnelia* in Puerto Rico have been found growing over entire *Millepora* colonies and the two *Metapeyssonnelia* species have been observed to grow sympatrically (Ballantine and Ruiz 2011).

The presence of a bleached halo just beyond the growing edges of *M. corallepida* and *M. milleporoides* on the coral *M. complanata* suggested to us that the algae produce secondary metabolic compounds with an allelopathic effect on the coral. The objectives of this study were to identify secondary metabolic compounds produced by *Metapeyssonnelia corallepida* and *M. milleporoides* that may affect tissue and/or zooxanthellae of *Millepora complanata* and to demonstrate allelopathic activity against *Millepora* by crude *Metapeyssonnelia* extracts.

Materials and Methods

Collection

Fragments of *Millepora complanata* with and without overgrowth of *Metapeyssonnelia corallepida* or *M. milleporoides* were collected by snorkeling at the reef crest area in the vicinity of Atravesado Reef in La Parguera, Lajas (southwest), Puerto Rico. Samples, in plastic bags with seawater, were placed in an insulated cooler, returned to the laboratory, and placed in running seawater within an hour of collection.

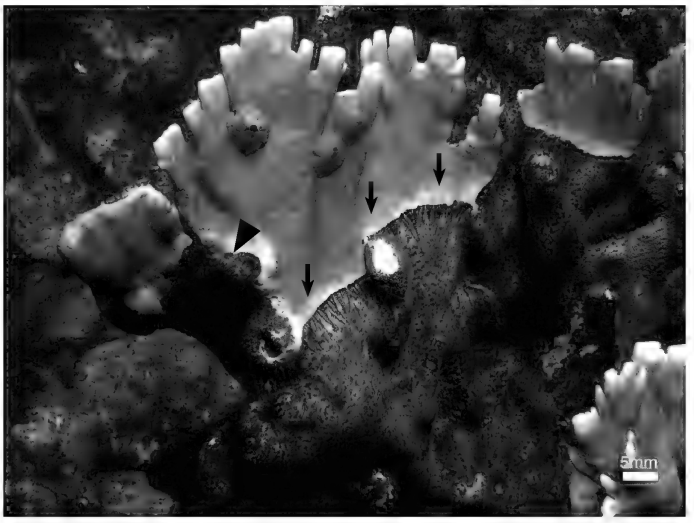

FIGURE 1. In situ *photograph of* Metapeyssonnelia milleporoides *(arrowhead) growing over* Millepora complanata. *The halo or lightened coral tissue beyond the growing edge is indicated by arrows.*

Extraction

Metapeyssonnelia corallepida and *M. milleporoides* on coral fragments were scraped off the coral with a razor blade from the algal growing edge to 2 cm behind with care that no coral tissue was included. The scrapings were distributed in vials that were frozen at –20°C for 12 hours to break algal cells through water crystal formation. To avoid enzymatic degradation, extracts were then freeze dried using a Virtis Freeze mobile® Model 25SL (Scientific Products Industries, Warminster, Pa). The lyophilized material was kept frozen until use.

Lipophilic extracts were obtained using a solvent mixture of chloroform: methanol in a 2:1 proportion (Folch et al. 1956; Bligh and Dyer 1959; Cronin et al. 1995). Extraction solvent (40 ml) was added to the freeze–dried algal scrapings and refluxed at 30°C for 30 min. The extraction solvent was decanted and the process was repeated to obtain a total of 80 ml of extract. Following 60 min in a separatory funnel, the chloroform fraction with lipophilic non–polar compounds, and the methanolic fraction with lipophilic–polar compounds were separated. The chloroform fraction was recovered with a Büchi Rotavapor® Model RE–111 (BÜCHI Corporation, New Castle, DE) at 50°C prior to being dried under a stream of nitrogen and stored at –20°C until use.

Hydrophilic extracts were obtained using methanol, a strong polar solvent used to obtain polar and hydrophilic–polar compounds from algal thalli (de Nys et al. 1998; Rasher et al. 2011; Saha et al. 2012). Algae were extracted with 50 ml of methanol for 48 h at room temperature. The methanol was then evaporated at 50°C utilizing the Buchi Rotavapor®. The dried extract was stored under nitrogen until use.

Gas Chromatography and Mass Spectrometry

Lipophilic and hydrophilic extracts of the 2 *Metapeyssonnelia* species were re—suspended in 1 ml of HPLC—quality hexane. Gas chromatography was performed using a Hewlett Packard (HP) 6890 series II gas chromatograph (GC; Palo Alto, CA) and the mass spectrometry (MS) was performed using a HP 5973 Mass Detector (MD) with electron impact ionization mode. The results were analyzed with the software MSD Chemstation E.01.00.237 (Agilent GEt Technologies Inc., Santa Clara, CA) and the compounds in each sample were identified using 2 libraries: (i) Wiley 275 and (ii) NIST Mass spectral search program, version 2.0 d, 2005.

Laboratory Assays

Assays utilizing the crude extracts on *Millepora complanata* were conducted on coral fragments that were previously acclimatized in an outdoor, shaded water table in individual glass dishes with constant seawater flow for 4 days. The crude lipophilic and hydrophilic extracts from M. *corallepida* and M. *milleporoides* were re—suspended in HPLC—grade hexane. Hexane was chosen principally as it was previously demonstrated that it could be applied to *Millepora* tissue without visual effect.

For each *Metapeyssonnelia* species, lipophilic extracts at 3 concentrations for M. *corallepida* (0.06 mg/µl, 0.04 mg/µl, and 0.02 mg/µl), and M. *milleporoides* (0.11 mg/µl, 0.07 mg/µl, and 0.03 mg/µl) were applied to 4 areas on each of 6 fragments of *Millepora corallepida*. Hydrophilic extracts from both species were also spotted onto 6 *Millepora* fragments. Thus for each species and each concentration, 4 spots were applied to a single coral fragment. As a control, 4 applications of hexane without extract were applied to one coral fragment. For all assays, 3µl of extract was applied with a 5µl micropipette, avoiding tip contact with the coral surface. Each application was mapped with transparent paper in order to observe subsequent changes in coral response at the application sites. To qualitatively assess the extract effect on coral tissue, application responses were monitored daily for 7 days and a daily photographic record was made of each coral fragment.

Zooxanthellae number

Loss of coral pigmentation or bleaching in the *Metapeyssonnelia* halo zone is presumably due to stress leading to a decrease in zooxanthellae numbers (Hoegh—Guldberg and Smith 1989, Jones 1997) or tissue death. In instances in which the treatment caused visible lightening of coral tissue, and after 7 days following extract application, zooxanthellae were enumerated at the site of extract application and at 10 mm away. Zooxanthellae counts followed removal from coral tissue utilizing a pressurized water stream (Water Pick®, Fort Collins, CO) filled with filtered seawater. To standardize zooxanthellae removal, a flexible plastic template with a 25 mm^2 cut—out was placed on top of the sampled area to limit the area of zooxanthellae removal. The water used to remove the zooxanthellae was collected in a vial and centrifuged at 3000 rpm for 4 min. The seawater was discarded carefully and the pellet was re—suspended in 1 ml of filtered seawater. Zooxanthellae number was counted in a hemocytometer. The total number of zooxanthellae is expressed as per 25 mm^2.

Results

Gas Chromatography and Mass Spectrometry

The secondary metabolic compounds identified in lipophilic and hydrophilic extracts of *Metapeyssonnelia corallepida* and M. *milleporoides* include 20 secondary metabolic products (Table 1). Products from M. *corallepida* and not shared between species were pentanoic acid (methyl ester), squalene (terpene), and 5—(hydroxymethyl)—2—(dimethoxymethyl) furan 3—methoxycarbonyl—1,1—diethyl—2—buten—4—olide (furanone). Compounds from M. *milleporoides* and not shared between species were unidentified 10 carbon compounds with chains of 23 to 32 carbon atoms, 2,4—dit—butyl phenol isobutyl ester (stearic acid) and 2(3H)—furanone, dihydro—4, 4—dimethyl—(CAS) (furanone). Lipophilic secondary metabolic products common to both species were oleic acid, stearic acid, and eicosatetraenoic acid. Among hydrophilic compounds, only the terpene, phytol, was common to both species.

Effect of extracts on *Millepora*

The highest lipophilic extract concentration from M. *milleporoides* (0.11 mg/µl) did not generate a visible effect on M. *complanata* tissue. However, the application of diluted extract (0.07 mg/µl) generated 3 bleaching areas (Figure 2A) and application of 0.03 mg/µl extract resulted in 2 bleaching responses (Figure 2B). The bleaching areas were similar in appearance and measured between 2 and 3 mm in extent. The number of zooxanthellae (Table 2) counted within each bleaching region for both concentrations did not show reduction in the number of zooxanthellae compared to an area 10 mm away. However, for the 0.03 mg/µl application, there was a reduction in zooxanthellae number on the affected areas (0.72×10^6 Zoox/25mm^2) compared with 10 mm away from the lesion (4.14×10^6 Zoox/25mm^2).

Application of lipophilic *Metapeyssonnelia corallepida* extracts (0.06 mg/µl) generated 2 different visible effects on the coral tissue (Table 2). One resulted in a lesion of necrotic tissue approximately 3 mm in diameter with a surrounding bleaching halo (Figure 3A); the other resulted in a bleaching area, approximately 5 mm in diameter but without any tissue necrosis (Figure 3B). The number of zooxanthellae in the bleaching halo surrounding the necrotic area was reduced (0.49×10^6 Zoox/25mm^2, Table 2) compared with an area 10 mm away from the lesion

TABLE 1. *Secondary metabolic compounds found in lipophilic and hydrophilic extracts of* Metapeyssonnelia corallepida *and* M. milleporoides.

Compound class (compound ID)	M. *corallepida*	M. *milleporoides*	Compound/Secondary Metabolic products previously reported in algae	Biological effects	References
Lipophilic Compounds					
Eicosatetradeconoic acid	x	x	*Murraryella periclados* (Rhodophyta)	Eicosanoids in general with molecular signaling and inflammation response in mammals	Gerwick and Bernart 1993 Hariz et al. 2008
Oleic acid	x	x	*Corallina granifera* (Rhodophyta)	Antibacterial	De Rosa et al. 2003 Venkatesalu et al. 2004
2,4–dit–buthyl phenol		x	Phenol: *Corallina mediterranea* (Rhodophyta)	Not reported	De Rosa et al. 2003
Pentadecanoic acid	x		*Corallina granifera* *Centroceras clavatum* (Rhodophyta)	Not reported	De Rosa et al. 2003 Rocha et al. 2011
Stearic acid	x	x	*Corallina granifera* (Rhodophyta) *Chondrus crispus* (Rhodophyta)	Antibacterial	Tasende 2000 McGaw et al. 2002 Seidel et al. 2004
Cholesterol	x	x	*Corallina granifera* (Rhodophyta) *Corallina mediterranea* (Rhodophyta) *Centroceras clavulatum* (Rhodophyta)	Not reported	De Rosa et al. 2003 Rocha et al. 2011
Hydrophilic compounds					
Furarone: [5–(hydroxymethyl)–2–(dimethoxymethyl) furan 3–methoxycarbonyl–1,1–diethyl–2–buten–4–olide]	x		Rhodophyta	Halogenated furanones Antibacterial	Maximilien et al. 1998; de Nys and Steinberg 2002; Bhadury and Wright 2004
Furarone: [2(3H)–furanone, dihydro–4,4–dimethyl–(CAS)]		x	Rhodophyta	Halogenated furanones Antibacterial	Maximilien et al. 1998 de Nys and Steinberg 2002 Bhadury and Wright 2004
Phytol	x	x	*Corallina granifera* *Corallina mediterranea* (Rhodophyta)	Antimicrobial, antineoplastic	De Rosa et al. 2003 Kendel et al. 2012
			Grateloupia turuturu (Rhodophyta)	Without effect in other organisms	Kendel et al. 2012
Squalene	x		Diterpenes pachydictyol A and dictyol E: *Dictyota menstrualis* (Phaeophyta)	Inhibit settlement of *Bugula neretina* larvae	Schmitt et al. 1995

(1.18×10^6 Zoox/25mm^2). In other applications in which there was a bleaching response, zooxanthellae number decreased away from the bleaching area. The hydrophilic crude extracts from both *Metapeyssonnelia* species had no effect on the coral tissue assayed. Application of the control (hexane) also did not result in obvious coral lightening but was, however, accompanied by a reduction in zooxanthellae number (Table 2, Figure 4).

Discussion

Antonius (1999) referred to Peyssonneliaceae overgrowth (PEY) as a disease condition experienced by the coral; however, that usage must certainly be regarded as a misnomer as the phenomena is the result of a competitive interaction as seen in both *Metapeyssonnelia corallepida* and *M. milleporoides*. Lipophilic extracts of *M. corallepida* and *M. milleporoides* elicited tissue lightening response by *Millepora complanata* that is indistinguishable from tissue lightening in the field

in proximity to *Metapeyssonnelia*. The strongest responses by concentrated lipophilic extracts on *M. corallepida* were necrotic tissue at the site of extract application with a lightened halo surrounding the necrotic area. Other less concentrated extract applications of both species elicited either a lightening or no obvious damage of coral tissue. The necrotic tissue lesion found in this report was similar to a lesion observed by de Nys et al. (1991) in a bioassay where a lipophilic compound, cloromertensene, of *Plocamium hamatum* (Rhodophyta) was added to coral fragments.

All of the 20 secondary compounds identified from *M. corallepida* and *M. milleporoides* have been previously reported for other Rhodophyta and Phaeophyceae species (Rosell and Srivastava 1987, Maximilien et al. 1998, de Nys and Steinberg 2002, De Rosa et al. 2003, Kendel et al. 2012). Thus no compounds unique to *Metapeyssonnelia* were resolved. A number of the *Metapeyssonnelia* secondary products are known to possess inhibitory activity against other organisms. Of these, tetradecanoic acid possesses antibacterial properties (Rosell and Srivastava 1987, Kendel et al. 2012). Terpenes (Schmitt et al. 1995, Kendel et al. 2012) and furanones (Maximilien et al. 1998, Bhadury and Wright 2004) have also been reported to have allelopathic properties including antibacterial (de Nys et al 1998, Da Gama et al. 2002) and antifouling activity against macroinvertebrates (Takahashi et al. 2002) including coral (Rasher et al. 2011). The terpene derivates squalene and phytol were common to both *Metapeyssonnelia* species. Additionally, 2 specific furanones were found in *M. corallepida* (5—(Hydroxymethyl)—2—(dimethoxymethyl) furan 3— methoxycarbonyl—1,1—diethyl—2—buten—4—olide) and another in *M. milleporoides* (2(3H)—furanone, dihydro—4,4—dimethyl)—(CAS)) extracts. Furanones are also compounds that have been reported as having inhibitory activity against fouling organisms (Dworjanyn et al. 2006).

While the purified secondary products were not assayed against *Millepora*, the application of crude *Metapeyssonnelia* extracts did elicit response by *Millepora*. At best this is a crude approximation of what occurs in nature. We do not know the concentration of compounds released by the algae in contact with the coral nor how long those compounds are active following release. Furthermore, the alga is probably

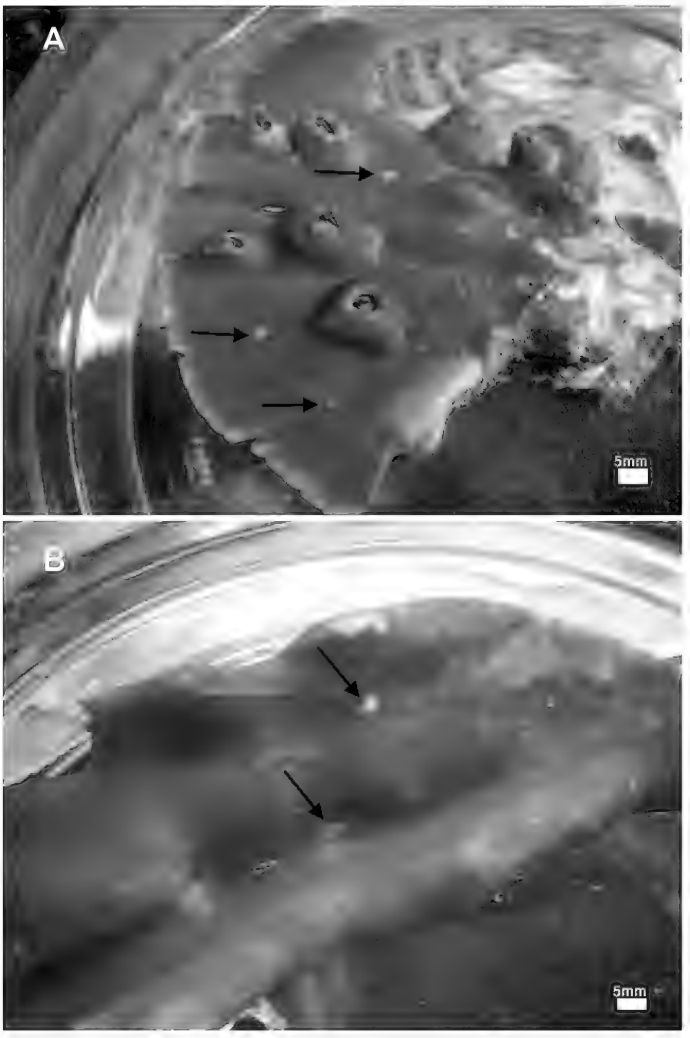

FIGURE 2. *Bleaching of* Millepora complanata *after application of lipophilic extract of* Metapeyssonnelia milleporoides. *A. 0.07 mg/µl lipophilic extract. Arrows indicate bleaching areas generated in 3 of 4 applications. B. 0.03 mg/µl lipophilic extract. Arrows indicate bleaching areas generated in 2 of 4 applications.*

TABLE 2. *Response to application of lipophilic extracts of* Metapeyssonnelia corallipeda *and* M. milleporoides *lipohilic extracts on* Millepora complanata. *Zooxanthellae counts were not made if experimental extract application did not have a tissue lightening response. Zoox = zoozanthellae*

Species	Concentration	Number of positive reactions	Zoox/25mm² x 10⁶	Zoox/25mm² x 10⁶ (10 mm away from affected area)
M. corrallepida	0.06	2	0.49	1.18
	0.04	0	–	–
	0.02	0	–	–
M. milleporoides	0.11	0	–	–
	0.07	3	2.62 ± 0.21	2.44 ± 0.56
	0.03	2	4.14 ± 1.10	0.72 ± 0.28
Hexane Control		0	0.34 – 0.80	–

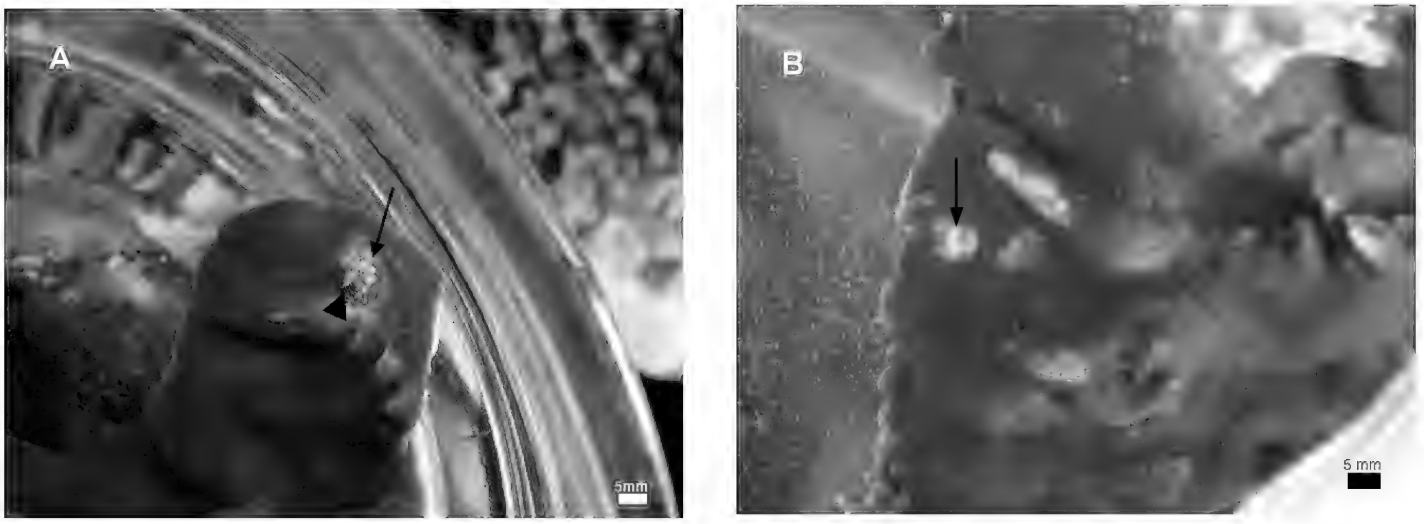

FIGURE 3. *Application of 0.06 mg/µl lipophilic extract of* Metapeyssonnelia corallepida *to* Millepora complanata. *A. Necrotic tissue (arrowhead) and bleaching halo (arrow) generated in 2 of 4 applications. B. Bleaching area (arrow).*

releasing small amounts of active chemicals continuously over time. This can easily be envisioned as having a stronger effect than the single application that we employed. Killing or weakening coral tissue by the production of allelopathic substances may abet subsequent overgrowth.

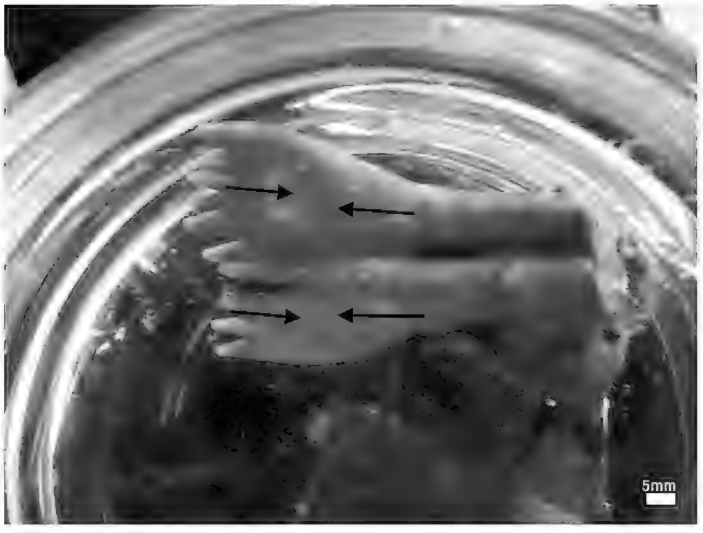

FIGURE 4. Millepora complanata *fragment used as control and inoculated with 4 applications of hexane without extract.*

At the outset, we assumed that tissue lightening following application of crude *Metapeyssonnelia* extracts could be quantified by zooxanthellae number. Lightening without decrease in zooxanthellae numbers may also occur with loss of pigmentation by zooxanthellae (Hoegh–Guldberg and Smith 1989) or sharp retraction of coral tissue into the coral skeleton (Brown et al. 1994). Even though changes in the number of zooxanthellae as a result of tissue lightening were not as expected, it is clear that lipophilic extracts of *Metapeyssonnelia corallepida* and *M. milleporoides* did cause lightening of *Millepora complanata* tissue in the areas where the extracts were applied, similar to that seen in the field. We believe that one or more of the secondary metabolites identified in this study, possibly acting synergistically, were responsible for these results.

The release of allelopathic compounds has been invoked as an explanation of tissue damage of corals in direct contact with macroalgae. While probably correct for all cases, the evidence for allelopathy is mostly correlative. We feel that the response by *Millepora* tissue to *Metapeyssonnelia* extracts provides further experimental evidence that allelopathy is the underlying cause for these interactions and that chemical interactions are an important process in coral reef algal ecology.

Acknowledgements

MRC thanks the administrative and technical staff of the Department of Marine Sciences, University of Puerto Rico including A. Santiago and D. Sanabria for assistance in the field and W. Rosado for technical laboratory support. At Simon Bolivar University, MRC and AK thank F. Morales and. C. Olivero for the sample analysis with HPLC GC–MS and A. Cabrera for her supervision in compound identification. DLB gratefully acknowledges partial support for the research by NOAA (National Oceanographic and Atmospheric Administration) Coastal Ocean Programs under award #NA17OP2919 to the University of Puerto Rico, Mayagüez.

Literature Cited

Anthony, K.R., J.A. Maynard, G. Diaz–Pulido, P.J. Mumby, P.A. Marshall, L. Cao, and O. Hoegh– Guldberg. 2011. Ocean acidification and warming will lower coral reef resilience. Global Change Biology 17:1798–1808. doi: 10.1111/j.1365–2486.2010.02364.x

Antonius, A. 1999. *Metapeyssonnelia corallepida*, a new coral–killing red alga on Caribbean reefs. Coral Reefs 18:301. doi: 10.1007/s003380050200

Antonius, A. 2001. *Pneophyllum conicum*, a coralline red alga causing coral reef–death in Mauritius. Coral Reefs 19:418. doi: 10.1007/s003380000126

Antonius, A. and E. Ballesteros. 1998. Epizoism: a new threat to coral health in Caribbean reefs. Revista de Biologia Tropical 46:145–156.

Aronson, R.B. and W.F. Precht. 2006. Conservation, precaution, and Caribbean reefs. Coral Reefs 25:441–450. doi: 10.1007/s00338–006–0122–9

Baker, A.C., P.W. Glynn, and B. Riegl. 2008. Climate change and coral reef bleaching: an ecological assessment of long–term impacts, recovery trends and future outlook. Estuarine, Coastal and Shelf Science 80:435–471. doi: 10.1016/j.ecss.2008.09.003

Ballantine, D.L., H. Ruiz, and N.E. Aponte. 2004. Notes on the benthic marine algae of Puerto Rico VIII. Additions to the flora. Botanica Marina 47:335–340. doi:10.1515/BOT.2004.039

Ballantine, D.L. and H. Ruiz 2011. *Metapeyssonnelia milleporoides*, a new species of coral–killing red alga (Peyssonneliaceae) from Puerto Rico, Caribbean Sea. Botanica Marina 54:47–51. doi: 10.1515/bot.2011.003

Ballantine, D.L. and H. Ruiz. 2013. A unique red algal reef formation in Puerto Rico. Coral Reefs 32:411. doi: 10.1007/s00338–013–1016–2

Barott, K.L., G.J. Williams, M.J. Vermeij, J. Harris, J.E. Smith, F.L. Rohwer, and S.A. Sandin. 2012. Natural history of coral–algae competition across a gradient of human activity in the Line Islands. Marine Ecology Progress Series 460:1–12. doi: 10.3354/meps09874

Bhadury, P. and P.C. Wright. 2004. Exploitation of marine algae: biogenic compounds for potential antifouling applications. Planta 219:516–578. doi: 10.1007/s00425–004–1307–5

Bligh, E.G. and W.J. Dyer. 1959. A rapid method of total lipid extraction and purification. Canadian Journal of Biochemistry and Physiology 37:911–917. doi: 10.1139/bcb–2014–0150

Bonaldo, R.M. and M.E. Hay. 2014. Seaweed–coral interactions: variance in seaweed allelopathy, coral susceptibility, and potential effects on coral resilience. Plos One 9(1):e85786. doi: 10.1371/journal.pone.0085786

Brown, B.E., M.D. Le Tissier, and R.P. Dunne. 1994. Tissue retraction in the scleractinian coral *Coeloseris mayeri*, its effect upon coral pigmentation, and preliminary implications for heat balance. Marine Ecology Progress Series 105:209–218. doi: 10.3354/meps105209

Chadwick, N.E. and K.M. Morrow. 2011. Competition among sessile organisms on coral reefs. In: Z. Dubinsky and N. Stambler, eds. Coral Reefs: An Ecosystem in Transition. Springer, Netherlands, p. 347–371. doi: 10.1007/978–94–007–0114–4_20

Cronin, G., N. Lindquist, M.E. Hay, and W. Fenical. 1995. Effects of storage and extraction procedures on yields of lipophilic metabolites from the brown seaweeds *Dictyota ciliolata* and *D. menstrualis*. Marine Ecology Progress Series 119:265–273. doi: 10.3354/meps119265

D'Angelo, C. and J. Wiedenmann. 2014. Impacts of nutrient enrichment on coral reefs: new perspectives and implications for coastal management and reef survival. Current Opinion in Environmental Sustainability 7:82–93. doi: 10.1016/j.cosust.2013.11.029

Da Gama, B.A.P., R. Gama, R.C. Pereira, A.G.V. Carvalho, R. Coutinho, and Y. Yoneshigue–Valentin. 2002. The effects of seaweed secondary metabolites on biofouling. Biofouling: The Journal of Bioadhesion and Biofilm Research 18:13–20. doi: 10.1080/08927010290017680

de Nys, R. and P.D. Steinberg. 2002. Linking marine biology and biotechnology. Current Opinion in Biotechnology 13:244–248. doi: 10.1016/S0958–1669(02)00311–7

de Nys, R., J.C. Coll, and I.R. Price. 1991. Chemically mediated interactions between the red alga *Plocamium hamatum* (Rhodophyta) and the octocoral *Sinularia cruciata* (Alcyonacea). Marine Biology 108:315–320. doi: 10.1007/BF01344346

de Nys, R., S.A. Dworjanyn, and P.D. Steinberg. 1998. A new method for determining surface concentrations of marine natural products on seaweeds. Marine Ecology Progress Series 162:79–87. doi: 10.3354/meps162079

De Rosa, S., Z. Kamenarska, K. Stefanov, S. Dimitrova–Kanaklieva, C. Najdenski, I. Tzvetkova, V. Ninova, and S. Popov. 2003. Chemical composition of *Corallina mediterranea* Areschoug and *Corallina granifera* Ell. Et Soland. Zeitschrift für Naturforschung 58:325–33. doi: 10.1515/znc–2003–5–606

Diaz–Pulido, G., M. Gouezo, B. Tilbrook, S. Dove, and K.R N. Anthony. 2011. High CO_2 enhances the competitive strength of seaweeds over corals. Ecology Letters 14:156–162. doi: 10.1111/j.1461–0248.2010.01565.x

Dworjanyn, S.A., R. de Nys, and P.D. Steinberg. 2006. Chemically mediated antifouling in the red alga *Delisea pulchra*. Marine Ecology Progress Series 318:153–163. doi: 10.3354/meps318153

Folch, J., M. Lees, and G.H.S. Stanley. 1956. A simple method for the isolation and purification of total lipids from animal tissues. Journal of Biological Chemistry 226:497–509.

Gerwick, W.H. and M.W. Bernart. 1993. Eicosanoids and related compounds from marine algae. In: D.H. Attaway and M.W. Bernart, eds. Marine Biotechnology, Vol. 1 Pharmaceutical and Bioactive Natural Products, Plenum Press, New York, NY, USA, p. 101–152.

Hariz, H., J.—B. Corcuff, and N. Gualde. 2008. Arachidonic—acid—derived eicosanoids: roles in biology and immunopathology. Trends in Molecular Medicine 14:461—469. doi: 10.1016/j.molmed.2008.08.005

Hoegh—Guldberg, O. and G.J. Smith. 1989. The effects of sudden changes in light, temperature and salinity on the population density and export of zooxanthellae from the reef corals *Seriatopora hystrix* and *Stylophora pistillata*. Journal of Experimental Marine Biology and Ecology 129:279—303. doi: 10.1016/0022—0981(89)90109—3

Hughes, T.P. 1994. Catastrophes, phase shifts, and large—scale degradation of a Caribbean coral reef. Science 265:1547—1551. doi: 0.1126/science.265.5178.1547

Jompa, J. and L.J. McCook. 2003. Coral—algal competition: macroalgae with different properties have different effects on corals. Marine Ecology Progress Series. 258:87—95. doi: 10.3354/meps258087

Jones, R.J. 1997. Zooxanthellae loss as a bioassay for assessing stress in corals. Marine Ecology Progress Series 149:163—171. doi: 10.3354/meps149163

Kendel, M., A. Couzinet—Mossion, M. Viau, J. Fleurence, G. Barnathan, and G. Wielgosz—Collin. 2012. Seasonal composition of lipids, fatty acids, and sterols in the edible red alga *Grateloupia turuturu*. Journal of Applied Phycology 25:425—432. doi: 10.1007/s10811—012—9876—3

Lapointe, B.E. 1997. Nutrient thresholds for bottom—up control of macroalgal blooms on coral reefs in Jamaica and southeast Florida. Limnology and Oceanography 42:1119—1131. doi: 10.4319/lo.1997.42.5_part_2.1119

Maximilien, R., R. de Nys, C. Holmström, L. Gram, M. Givskov, K. Crass, S. Kjelleberg, and P.D. Steinberg. 1998. Chemical mediation of bacterial surface colonization by secondary metabolites from the red alga *Delisea pulchra*. Aquatic Microbial Ecology 15:233—246. doi: /10.3354/ame015233

McGaw, L.J., A.K Jäger, and J. van Staden. 2002. Isolation of antibacterial fatty acids from *Schotia brachypetala*. Fitoterapia 73:431—433. doi: 10.1016/S0367—326X(02)00120—X

McManus J.W. and Polsenberg J.F. 2004. Coral–algal phase shifts on coral reefs: ecological and environmental aspects. Progress in Oceanography 60:263—279. doi: 10.1016/j.pocean.2004.02.014

Mora, C. 2008. A clear human footprint in the coral reefs of the Caribbean. Proceedings of the Royal Society B 275:767—773. doi: 10.1098/rspb.2007.1472

Pandolfi, J.M., S.R. Connolly, D.J. Marshall, and A.L. Cohen. 2011. Projecting coral reef futures under global warming and ocean acidification. Science 333:418—422. doi: 10.1126/science.1204794

Pueschel, C.M. and G.W. Saunders. 2009. *Ramicrusta textilis* sp. nov. (Peyssonneliaceae, Rhodophyta), an anatomically complex Caribbean alga that overgrows corals. Phycologia 48:480—491. doi: 10.2216/09—04.1

Rasher, D.B. and M.E. Hay. 2010. Chemically rich seaweeds poison corals when not controlled by herbivores. Proceedings of the National Academy of Sciences 107:9683—9688. doi: 10.1073/pnas.0912095107

Rasher, D.B. and M.E. Hay. 2010. Seaweed allelopathy degrades the resilience and function of coral reefs. Communicative and Integrative Biology 3:564–566. doi: 10.4161/cib.3.6.12978

Rasher, D.B., E.P. Stout, S. Engel, J. Kubanek, and M.E. Hay. 2011. Macroalgal terpenes function as allelopathic agents against reef corals. Proceedings of the National Academy of Sciences 108:17726—17731. doi: 10.1073/pnas.1108628108

Rocha, O.P., R. De Felicio, A.H. Rodrigues, D.L. Ambrosio, R.M. Cicarelli, S. De Alburquerque, M.C. Young, and H.M. Debonsi. 2011. Chemical profile and biological potential of non—polar fractions from *Centroceras clavulatum* (C. Agardh) Montagne (Ceramiales, Rhodophyta). Molecules 16:7105—7114. doi: 10.3390/molecules16087105

Rosell, K—G. and L.M. Srivastava. 1987. Fatty acids as antimicrobial substance in brown algae. Hydrobiologia 151—152:471—475. doi: 10.1007/978—94—009—4057—4_69

Ruiz, H. and D.L. Ballantine. 2009. Dynamics of shelf edge coral reef—associated macroalgae at La Parguera, Puerto Rico. Caribbean Journal of Science 45:260—268.

Saha, M., M. Rempt, B. Gebser, J. Grueneberg, G. Pohnert, and F. Weinberger. 2012. Dimethylsulphopropionate (DMSP) and proline from the surface of the brown alga *Fucus vesiculosus* inhibit bacterial attachment. Biofouling 28:593—604. oi: 10.1080/08927014.2012.698615

Schmitt, T.M., M.E. Hay, and N. Lindquist. 1995. Constraints on chemically mediated coevolution: multiple functions for seaweed secondary metabolites. Ecology 76:107—123. doi: 10.2307/1940635

Schutte, V.G. W.E.R. Selig, and J.F. Bruno. 2010. Regional spatio—temporal trends in Caribbean coral reef benthic communities. Marine Ecology Progress Series 402:115—122. doi: 10.3354/meps08438

Seidel, V. and P.W Taylor. 2004. *In vitro* activity of extracts and constituents of *Pelagonium* against rapidly growing mycobacteria. International Journal of Antimicrobial Agents 23:613—619. doi: 10.1016/j.ijantimicag.2003.11.008

Strychar, K.B. and P.W. Sammarco. 2009. Exaptation in corals to high seawater temperatures: low concentrations of apoptotic and necrotic cells in host coral tissue under bleaching conditions. Journal of Experimental Marine Biology and Ecology 369:31—42. doi: 10.1016/j.jembe.2008.10.021

Sutherland, K.P., J.W. Porter and C. Torres. 2004. Disease and immunity in Caribbean and Indo—Pacific zooxanthellate corals. Marine Ecology Progress Series 266:273—302. doi: 10.3354/meps266273

Takahashi, Y., M. Daitoh, M. Suzuki, T. Abe, and M. Masuda. 2002. Halogenated metabolites from the New Okinawan red alga *Laurencia yonaguniensis*. Journal of Natural Products 65:395—398. doi: 10.1021/np010468v

Tasende, M.G. 2000. Fatty acid and sterol composition of gametophytes and sporophytes of *Chondrus crispus* (Gigartinaceae, Rhodophyta). Scientia Marina 64:421—426.

doi: 10.3989/scimar.2000.64n4421

Titlyanov, E.A., I.M. Yakovleva, and T.V. Titlyanova. 2007. Interaction between benthic algae (*Lyngbya bouillonii*, *Dictyota dichotoma*) and scleractinian coral *Porites lutea* in direct contact. Journal of Experimental Marine Biology and Ecology 342:282–291. doi: 10.1016/j.jembe.2006.11.007

Venkatesalu, V., P. Sundaramoorthy, M. Anantharaj, M. Gopalakrishnan, and M. Chandrasekaran. 2004. Studies on the fatty acid composition of marine algae of Rameswaram coast. Seaweed Research and Utilisation 26:83–86.

Verlaque, M., E. Ballesteros, and A. Antonius. 2000. *Metapeyssonnelia corallepida* sp. nov. (Peyssonneliaceae, Rhodophyta), an Atlantic encrusting red alga overgrowing corals. Botanica Marina 43:191–200. doi: 10.1515/BOT.2000.020

Veron, J.E.N., O. Hoegh–Guldberg, T.M. Lenton, J.M. Lough, D.O. Obura, P. Pearce–Kelly, C.R.C. Sheppard, M. Spalding, M.G. Stafford–Smith, and A.D. Rogers. 2009. The coral reef crisis: the critical importance of < 350 ppm CO2. Marine Pollution Bulletin 58:1428–1436. doi: 10.1016/j.marpolbul.2009.09.009

Vieira, C., C. Payri, and P. De C;erck. 2015. Overgrowth and killing of corals by the brown alga *Lobophora hederacea* (Dictyotales, Phaeophyceae) on healthy reefs in New Caledonia: A new case of the epizoism syndrome. Phycological Research 63:152–153. doi: 10.1111/pre.12082

Weil, E., G. Smith, and D.L. Gil–Agudelo. 2006. Status and progress in coral reef disease research. Diseases of Aquatic Organisms 69:1–7. doi: 10.3354/dao069001

Gulf and Caribbean Research

Volume 27 | Issue 1

2016

Diets of Atlantic Sharpnose Shark (*Rhizoprionodon terraenovae*) and Bonnethead (*Sphyrna tiburo*) in the northern Gulf of Mexico

Tyler Harrington
Texas A & M University - Galveston, tyler.harrington318@gmail.com

Jeff Plumlee
Texas A & M University - Galveston, jplumlee@tamu.edu

J. Marcus Drymon
University of South Alabama, Dauphin Island Sea Lab, mdrymon@disl.org

David Wells
Texas A & M University - Galveston, wellsr@tamug.edu

Gulf and Caribbean Research Vol 27, 42-51, 2016
DOI: 10.18785/gcr.2701.05
Manuscript received, November 25, 2015; accepted, June 17, 2016

DIETS OF ATLANTIC SHARPNOSE SHARK (*RHIZOPRIONODON TERRAENOVAE*) AND BONNETHEAD (*SPHYRNA TIBURO*) IN THE NORTHERN GULF OF MEXICO

Tyler Harrington[1,2*], Jeffrey D. Plumlee[1,3], J. Marcus Drymon[4,5], R. J. David Wells[1,3]

*[1]Department of Marine Biology, Texas A&M University at Galveston, 1001 Texas Clipper Road, Galveston, TX 77553; [3]Department of Wildlife and Fisheries Sciences, Texas A&M University, College Station, TX 77843; [4]Department of Marine Sciences, University of South Alabama, Mobile, AL 36688; [5]Dauphin Island Sea Lab, 101 Bienville Boulevard, Dauphin Island, AL 36528; *Corresponding author, email: tharrington@fau.edu, [2] Current address: Wildlife Epidemiology and Population Health Lab. Florida Atlantic University – Harbor Branch Oceanographic Institute, 5600 U.S. 1, Fort Pierce, FL 34946*

Abstract: Diets of two coastal sharks, Atlantic Sharpnose Shark (*Rhizoprionodon terraenovae*) and Bonnethead (*Sphyrna tiburo*), were examined along the Texas and Alabama coasts in the northern Gulf of Mexico (GOM). Atlantic Sharpnose Sharks were collected from the northwest (n= 209) and northcentral (n= 245) GOM regions while Bonnetheads were collected from two locations within the northwest GOM (Galveston, Texas, n= 164; Matagorda, Texas, n= 79). Dietary analysis was conducted using stomach contents identified to the lowest taxonomic level, which were quantified using the index of relative importance (IRI) and non–parametric statistical analyses. Atlantic Sharpnose Sharks were revealed to be primarily piscivorous, with an overall %IRI of 79.76% for teleost fishes. Bonnetheads were shown to prey primarily on crustaceans (90.94% IRI), mainly crabs (22.06% IRI). Diets for Atlantic Sharpnose Sharks and Bonnetheads were evaluated by region and ontogeny, where variations by ontogeny were examined based on length at 50% maturity (L_{50}) values, delineating mature from immature individuals. Atlantic Sharpnose Sharks and Bonnetheads showed a decrease in dietary prey species richness from juveniles to adults using %IRI. Regional dietary differences existed with Atlantic Sharpnose Sharks from the northwest GOM consuming more crustaceans than conspecifics from the northcentral GOM. Bonnetheads collected from Galveston, TX consumed more crab than Bonnetheads from Matagorda, TX, while Bonnetheads from Matagorda, TX displayed a diet with higher prey species richness. Our results highlight differences in diets of two common shark species at both local and regional spatial scales.

Keywords: stomach contents, feeding ecology, coastal sharks

Introduction

Predators play a critical role in the structure and function of marine ecosystems (Baum and Worm 2009). Removal of these predators, such as sharks, can cause negative effects on population structure and cascade to lower trophic levels throughout the food web (Heithaus 2008). Consequently, examining diets of predators can provide information about how an ecosystem functions and can potentially be affected by changing biotic and abiotic factors.

Quantification and description of diets of mesopredators can aid greatly in understanding geographical or seasonal changes in prey abundance and overall ecosystem connectivity (Cortés 1997). Spatial variability of prey abundance is common across marine ecosystems and can drive the distribution of predators (Kinney et al. 2011). However, common mesopredators that are ubiquitous throughout a system may exhibit temporal variability within their diet based on prey availability (Drymon et al. 2012). Geographic separation among populations of shark species that display regional variation in diet, such as the Atlantic Sharpnose Shark (*Rhizoprionodon terraenovae*) (Drymon et al. 2012, Delorenzo et al. 2015) and Bonnethead (*Sphyrna tiburo*) (Bethea et al. 2007), is important to consider when describing dietary preferences.

Atlantic Sharpnose Sharks and Bonnetheads are abundant mesopredators in the northern Gulf of Mexico (GOM) (Drymon et al. 2010), share similar distributions (Drymon et al. 2013), and account for a large percentage of annual small coastal shark landings (Cortes 2005, 2009). Atlantic Sharpnose Sharks range from New Brunswick, Canada in the north to the Yucatan Peninsula in the south, including the GOM (Castillo–Geniz et al. 1998, Parsons and Hoffmayer 2005). Bonnetheads also have a widespread distribution, occurring in the coastal subtropical and tropical waters of the Pacific and Atlantic oceans surrounding the Americas (Castillo–Geniz et al. 1998). Both species are widely distributed throughout the GOM and undergo seasonal migrations that vary regionally and temporally (Parsons and Hoffmayer 2005). Atlantic Sharpnose Sharks and Bonnetheads exhibit similar life history traits, including small litter sizes and slow population growth rates (Castillo–Geniz et al., 1998; Fowler et al. 2005) making them vulnerable to overfishing. While frequently caught in recreational fisheries, these species also play an important role in commercial and artisanal fisheries. Atlantic Sharpnose Sharks account for 33% and 46% of annual small coastal shark commercial landings in the southeastern United States and annual small shark artisanal landings in Mexico, respectively (Cortés 2009). Bonnetheads

share a similar commercial importance and account for 50% of annual small coastal shark commercial landings in the southeastern United States and 15% of annual small shark artisanal landings in Mexico (Cortés 2005). A recent survey found Atlantic Sharpnose Sharks and Bonnetheads were the two most–captured shark species in the southern GOM off the coasts of Tabasco, Campeche, and Yucatan, Mexico (Pérez–Jiménez and Mendez–Loeza 2015).

Dietary information can be found for both Atlantic Sharpnose Sharks and Bonnetheads, but is limited in the northwest GOM. Atlantic Sharpnose Shark diets have been reported from the northcentral and northeastern GOM and contain a mixture of crustaceans, squid, and fish with fish as the primary dietary component (Bethea et al. 2004, Bethea et al. 2006, Drymon et al. 2012, Plumlee and Wells 2016). Bonnethead diets have also been evaluated in the northeastern GOM and northern Brazil with a specialized diet dominated by crustaceans, specifically *Callinectes* spp. crabs (Lessa and Almeida 1998, Bethea et al. 2007). Plant material has been observed in Bonnethead diets throughout all life stages (Cortés et al. 1996, Lessa and Almeida 1998, Bethea et al. 2007, Haman et al. 2012) where its presence may be due to incidental ingestion during pursuit of prey (Cortés et al 1996).

Stomach content analysis is an effective tool to evaluate trophic interactions and provide snapshots of important prey items in the diets of predators (Cortés 1999). Given their ubiquity and commercial importance in the GOM, the goals of this study were to examine the feeding patterns of Atlantic Sharpnose Sharks and Bonnetheads along coastal regions of the northern GOM. The first objective was to use stomach content analysis to quantify the diets and identify the most important prey items to each species. Secondly, spatial and ontogenetic differences were examined. For Atlantic Sharpnose Sharks, diets were compared between the northwest and northcentral GOM (i.e. regional comparison) while Bonnethead diets were compared within the northwest GOM (Galveston, TX and Matagorda, TX, local comparison). Ultimately, quantifying and understanding the diets of two abundant shark species that reside in coastal waters of the northern GOM will provide a better understanding of species interactions and food web structure, which can be incorporated into ecosystem–based fisheries management plans.

Materials and Methods

Sample Collections

Atlantic Sharpnose Sharks were collected from 2 regions in the GOM: northwest (off Galveston, TX) and northcentral (off Mobile, AL; Figure 1). Bonnetheads were opportunistically collected from 2 locations within the northwest GOM (Galveston and Matagorda, TX; Figure 1). All specimens from Galveston were obtained through recreational

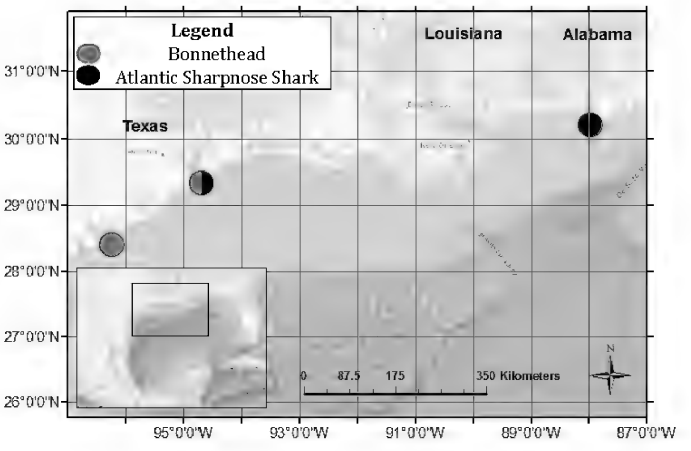

FIGURE 1. Map highlighting collection sites of Atlantic Sharpnose Shark and Bonnethead in the northern Gulf of Mexico. Dots indicate Mobile, AL, Galveston, TX, and Matagorda, TX from east to west.

headboat and private fishing vessels from April through October 2013. Shark stomach samples from Matagorda were collected from April to November 2013 through seasonal gill net sampling by the Texas Parks and Wildlife Department (TPWD). Stomach samples from the northwest GOM were removed onsite with data recorded for every specimen including total length (TL), fork length (FL), pre–caudal length (PCL), sex, and date of collection. Information such as trip time and bait type was obtained through personal correspondence with anglers and also recorded to ensure that sharks were captured within the region and that bait was not included in dietary calculations. Stomachs were transported to the laboratory where they were transferred into a 10% formalin solution for a minimum of 48 h, followed by a transfer to 70% ethanol for preservation until processing. Samples from the northcentral GOM were collected by longline surveys from 2006–2008 in the coastal waters of Alabama. A random stratified block design was used with 4 blocks, 2 west of 88° W and 2 east of 88° W, extending 37 km east to west from the shoreline to the 20 m isobaths as described in Drymon et al. (2012). Longlines were set for 1 h and sampling was replicated within each block along 3 depths: 0–5 m, 5–10 m, and 10–20 m. Six stations in one of the eastern and one of the western blocks were selected at random for monthly sampling. Measurements for samples from the northcentral GOM included weight, TL, FL, and PCL. Stomachs were removed and either frozen on the vessel or placed on ice and frozen upon return to the laboratory until processing.

Processing

Stomachs were processed in the laboratory using standard techniques. All stomachs were weighed (wet weight) to the nearest 0.1 g. Contents were then extracted with a series of 3 metal sieves with mesh sizes of 1.3 cm, 1400 μm, 500 μm, and a metal basin. Any material left in the metal basin was then run through a smaller sieve with mesh size of

50 µm and included as unidentified material. Contents in the remaining 3 sieves were placed in dissection trays to be sorted into respective groups. Stomach contents obtained from sharks caught by hook and line fishing from Galveston, TX were evaluated for hook holes and cross–referenced with information from angler interviews for identification of bait. Atlantic Mackerel was used as bait in sample collections from Mobile, AL. All contents identified as bait were not included in analysis. Prey items were identified to the lowest taxonomic level and cumulative prey curves (CPC) were developed for Atlantic Sharpnose Sharks and Bonnetheads from each region and location based on the number of prey items relative to the number of stomachs analyzed (Ferry and Cailliet 1996).

Data Analysis

Stomach contents were analyzed using standard metrics, including percent weight (%W), percent number (%N), percent frequency of occurrence (%O), and the index of relative importance (IRI) expressed as a percentage (%IRI). The IRI was determined as IRI=%O*(%N + %W) where %N is the number of items in a given stomach divided by the total number of items in that stomach, %W is the weight of a given item in a stomach divided by the total weight of the contents in that stomach, and %O is the number of stomachs that item occurred in divided by the total number of stomachs examined. To calculate IRI, the %N and %W were summed across all samples for each prey category. %IRI was then calculated as the IRI of a given prey item divided by the total IRI of all prey items. For further comparison, the %IRI data for each species was analyzed as a function of region and ontogeny. Atlantic Sharpnose Shark stomach contents were compared on a regional spatial scale between the northwest and northcentral GOM. Bonnethead data were compared on a local spatial scale within the northwest GOM (Galveston and Matagorda, TX). Changes in dietary habits with ontogeny were also investigated for each species based on length at 50% maturity (L_{50}) values to delineate immature from mature individuals (Carlson and Parsons 1997, Lombardi–Carlson et al. 2003, Fowler 2005, Hoffmayer et al. 2013, Frazier et al. 2014).

Further statistical analysis of stomach contents was accomplished using permutational analysis of variance (PERMANOVA) models. PERMANOVA models were based on a Bray–Curtis resemblance matrix and run using an unrestricted permutation of untransformed data. Stomach content analysis was accomplished by organizing the taxonomic groups found within the stomachs into higher categories. Highest level taxon was achieved at the subphylum and infraclass level (Teleostei, Crustacea, and Cephalopoda) while less common taxa were grouped into Other (Echinodermata, Bivalva, Gastropoda, indigestible material, and algae). When possible, prey items within the higher groups, Teleostei and Crustacea, were further classified using prey

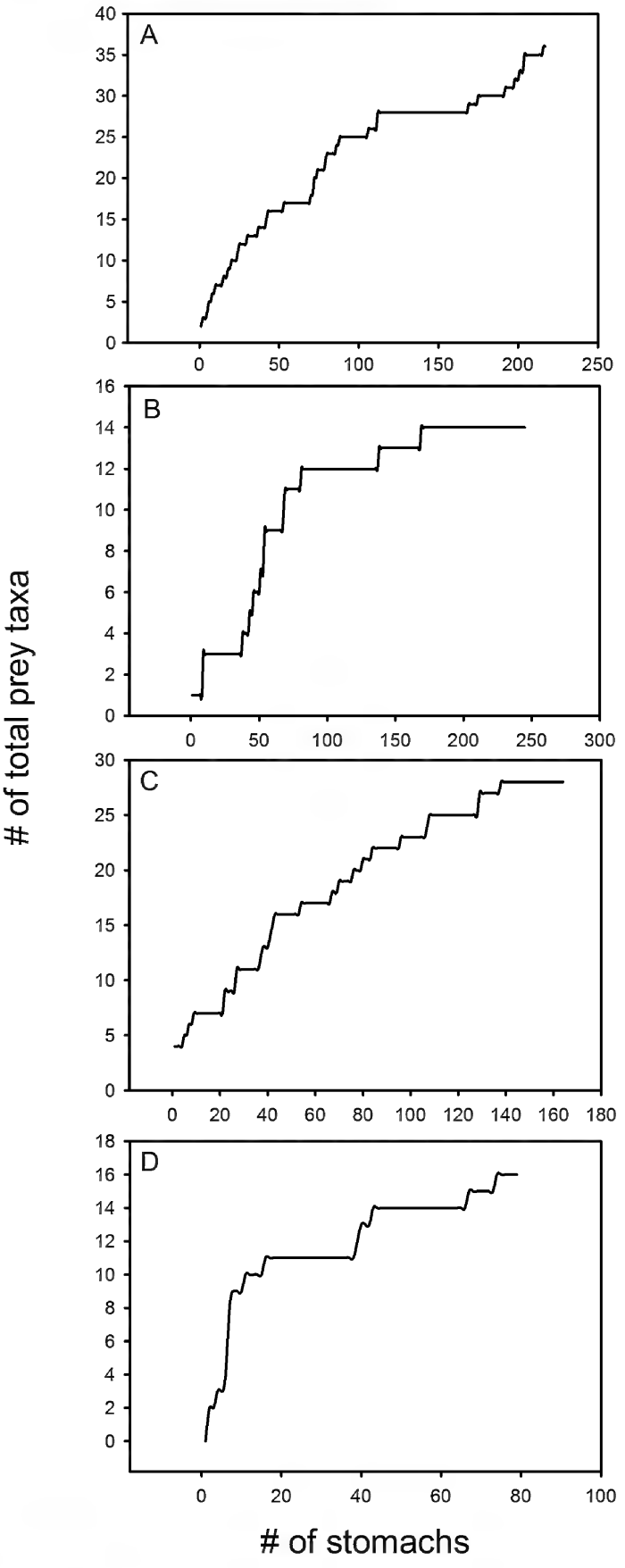

FIGURE 2. Cumulative prey curves generated for each shark species by region and location. A. Atlantic Sharpnose Shark (northwest Gulf of Mexico (GOM)). B). Atlantic Sharpnose Shark (northcentral GOM). C).Bonnethead (Galveston, TX). D. Bonnethead (Matagorda, TX).

groupings similar to those described in Bethea et al. (2004) and Bethea et al. (2007). Prey groupings included epibenthic teleost, pelagic teleost, penaeid shrimp, brachyuran, other crustaceans, cephalopods, and other (echinoderms, bivalves, gastropods, indigestible material, and algae). Unidentified material from groups Teleostei and Crustacea were removed from this analysis. Redefining the prey groupings excluded samples that had stomach contents only containing unidentified teleosts or crustaceans for both Atlantic Sharpnose Sharks (northwest GOM n = 88 and northcentral GOM n = 41) and Bonnetheads (Galveston Bay n = 135 and Matagorda Bay n = 63), yet increased taxonomic resolution of specifically important taxa to each species and region. Percent weight (%W) for each taxonomic group was used in these analyses given its significance in quantifying nutritional contribution (Rooker 1995). Similarity percentage (SIMPER) metrics were calculated to qualitatively determine differences of prey group contributions among factors. Significance was assessed at $\alpha \leq 0.05$, and all tests were run in PRIMER v.7 (Clarke and Gorley 2015).

Results

A total of 697 stomach samples throughout the northern GOM were collected during this study. For Atlantic Sharpnose Sharks (n = 454), 209 were collected from the northwest GOM and 245 were collected from the northcentral GOM. For Bonnetheads (n = 243), 164 were collected from Galveston, TX while 79 were collected from Matagorda, TX. Cumulative prey curves indicated that each species and region had CPCs trending towards or meeting defined asymptotes (Figure 2).

Both Atlantic Sharpnose Sharks and Bonnetheads were collected across a wide range of sizes. Atlantic Sharpnose Sharks ranged in size from 36.7 – 90.5 cm FL with a mean size of 71.8 ± 13.0 cm FL (Figure 3). A total of 119 juveniles and 335 adults were collected; 4 juveniles and 205 adults from the northwest GOM and 115 juveniles and 130 adults from the northcentral GOM. The mean weight of the stomach contents was 14.7 g, and 129 (18.5%) stomachs were empty. Bonnetheads had an mean length of 78.0 ± 11.9 cm FL and ranged in length from 49.0 – 102.0 cm FL (Figure 3). A total of 243 Bonnethead samples were collected; 126 adults and 38 juveniles from Galveston, TX and 23 adults and 54 juveniles from Matagorda, TX. Two individuals from Matagorda, TX lacked information on sex. Bonnetheads had a mean stomach content weight of 26.5 g, with one (0.4%) empty stomach. Among all stomach contents, 41 individual taxonomic groups were identified and 15 were identified to the species level. Atlantic Sharpnose Sharks had prey items representing 38 taxonomic groups, while Bonnetheads contained prey from 20 taxonomic groups.

Atlantic Sharpnose Shark diets consisted primarily of teleost fish (79.76% IRI) with contributions from crustaceans (8.09% IRI), cephalopods (2.58% IRI) and other material (10.61% IRI; Table 1, Figure 4). In lower taxonomic groupings, contributions came from teleost families such as Sciaenidae (0.19% IRI), Clupeidae (0.12% IRI), Engraulidae (0.08% IRI), Atherinidae (0.08% IRI), and Triglidae (0.04% IRI). Species identified included Gulf Menhaden (*Brevoortia patronus*, 0.14% IRI), Atlantic Cutlassfish (*Trichiurus lepturus*, 0.04%IRI), and Atlantic Croaker (*Micropogonias undulatus*, 0.01% IRI).

Atlantic Sharpnose Sharks from the northwest GOM had a diet primarily composed of teleost fish (77.61% IRI) and crustaceans (14.38% IRI). There were contributions from sciaenids (0.50% IRI), Gulf Menhaden (0.40% IRI), penaeid shrimp (3.05% IRI), and unidentified cephalopods (2.70% IRI). Diets of juvenile Atlantic Sharpnose Sharks

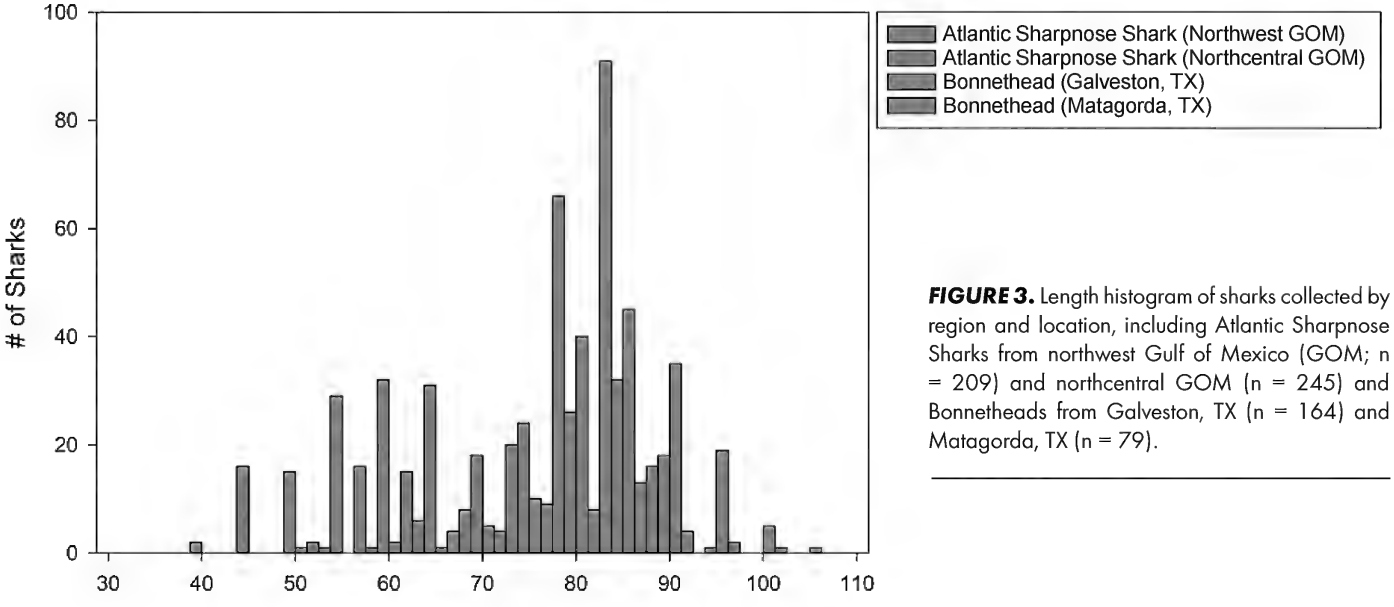

FIGURE 3. Length histogram of sharks collected by region and location, including Atlantic Sharpnose Sharks from northwest Gulf of Mexico (GOM; n = 209) and northcentral GOM (n = 245) and Bonnetheads from Galveston, TX (n = 164) and Matagorda, TX (n = 79).

TABLE 1. *Atlantic Sharpnose Shark diet content by prey species category. Data expressed as percentage of Index of Relative Importance (%IRI).*

Taxonomic Group	Identified Group	Lowest Taxonomic Group	Northcentral GOM				Northwest GOM		
			Overall %IRI	Total %IRI	Juvenile %IRI	Adult %IRI	Total %IRI	Juvenile %IRI	Adult %IRI
Teleost			79.76	78.26	74.33	79.34	77.61	26.41	78.35
	Unidentified Teleost		32.38	17.69	15.76	18.52	44.35	3.48	45.27
	Sciaenidae		0.19	0.01	-	0.01	0.50	-	0.51
		Menticirrhus spp.	<0.01	-	-	-	0.01	-	0.01
		Menticirrhus littoralis	<0.01	-	-	-	<0.01	7.07	-
		Cynoscion arenarius	<0.01	-	-	-	<0.01	-	<0.01
		Micropogonias undulatus	0.01	0.02	-	0.05	<0.01	-	<0.01
	Serranidae		<0.01	-	-	-	0.01	-	0.01
	Lutjanidae		<0.01	-	-	-	0.01	-	0.01
		Lutjanus campechanus	<0.01	0.01	0.05	-	<0.01	-	<0.01
	Scombridae		<0.01	-	-	-	<0.01	-	<0.01
	Carangidae		<0.01	-	-	-	0.01	-	0.01
		Chloroscombrus chrysurus	<0.01	-	-	-	<0.01	-	0.01
	Trichiuridae		-	-	-	-	-	-	-
		Trichiurus lepturus	0.04	-	-	-	0.12	-	0.12
	Gobiidae		-	-	-	-	-	-	-
		Gobioides broussonetii	<0.01	-	-	-	<0.01	-	<0.01
	Sparidae		-	-	-	-	-	-	-
		Archosargus probatocephalus	<0.01	-	-	-	<0.01	-	<0.01
	Paralichthyidae		<0.01	-	-		<0.01	-	<0.01
	Clupeidae		0.12	0.01	-	0.02	0.28	-	0.29
		Brevoortia patronus	0.14	-	-	-	0.40	-	0.41
	Engraulidae		0.08	0.12	0.70	<0.01	0.05	-	0.05
	Mugilidae		<0.01	-	-	-	<0.01	-	<0.01
	Ariidae		<0.01	<0.01	0.02	-	<0.01	-	<0.01
	Atherinidae		0.08	0.50	0.07	0.89	-	-	-
	Triglidae		0.04	0.18	0.03	0.31	-	-	-
		Symphurus plagiusa	<0.01	0.01	0.07	-	-	-	-
Crustacea			8.09	1.95	4.64	0.94	14.38	66.63	13.66
	Unidentified Crustacea		0.59	-	-	-	1.73	3.21	1.70
	Penaeidae		1.72	0.38	1.47	0.08	3.05	41.60	2.72
	Sicyoniidae		-	-	-	-	-	-	-
		Sicyonia brevirostris	0.01	0.04	0.07	0.02	-	-	-
	Unidentified Brachyura		0.18	0.16	0.54	0.05	0.19	-	0.20
	Portunidae		0.01	-	-	-	0.01	-	0.02
		Callinectes similis	0.01	-	-	-	0.03	-	0.03
	Xanthidae		<0.01	-	-	-	-	-	-
	Stomatopoda		0.15	0.28	0.93	0.09	0.10	5.13	0.07
		Squilla empusa	<0.01	-	-	-	<0.01	-	<0.01
Cephalopoda			1.54	0.47	2.91	0.01	2.58	5.28	2.51
	Unidentified Cephalopoda		0.02	0.19	0.96	0.01	-	-	-
	Unidentified Teuthoidea		0.91	-	-	-	2.70	5.28	2.51
		Loliginidae	<0.01	0.01	0.07	-	-	-	-
Other			10.61	19.32	18.12	19.71	5.44	1.68	5.48
	Gastropoda		<0.00	0.01	-	0.03	-	-	-
	Algae		<0.01	-	-	-	<0.01	-	<0.01

from the northwest GOM were mixed between teleost (26.41% IRI), crustaceans (66.63% IRI), and cephalopods (5.28% IRI) and adults shared the same primary components with a diet shift to a higher contribution from teleosts (78.35% IRI), and lower contributions from crustaceans (13.66% IRI) and cephalopods (2.51% IRI).

In the northcentral GOM, Atlantic Sharpnose Sharks showed a more teleost–dominated diet (78.26% IRI) with a lower contribution from crustaceans (1.95% IRI) and a larger amount of the other category (19.32% IRI). Juveniles from the northcentral GOM had contributions from teleosts (74.33% IRI), crustaceans (4.64% IRI), and other (18.12% IRI), while adults shifted primarily to teleosts (79.34% IRI) and other (19.71% IRI; Table 1). Other regional differences

included the presence of fish from families Clupeidae and Trichiuridae in the northwest GOM in contrast to fish from families Atherinidae and Triglidae present only from samples in the northcentral GOM.

Bonnethead diets were composed almost entirely of crustaceans (90.94% IRI) with a small contribution from other (8.11% IRI), primarily consisting of algae (7.44% IRI; Table 2, Figure 4). Among prey identified to lower taxonomic levels, contributions included unidentified brachyurans (22.06% IRI), blue crab (*Callinectes sapidus*) (2.19% IRI), and stomatopods (2.35% IRI). Bonnetheads from Galveston, TX showed a large dietary contribution of crustaceans (94.61 %IRI) with only algae (4.22% IRI) within the other category contributing more than 1% IRI. Between juvenile and adult Bonnetheads in Galveston, TX crustaceans remained the major contributor (96.59% IRI and 92.41% IRI, respectively) and there was a decrease in the contribution from teleosts (1.87% IRI juvenile and 0.45% IRI adult) and an increase in the contribution from other material (1.21% IRI juvenile and 6.45% IRI adults) with increasing size and age. In Matagorda, TX, crustaceans contributed most to the diet (79.67% IRI), but there was a large increase in the observed contribution of other (19.78% IRI) compared to Galveston, TX. Ontogenetically, Bonnetheads from Matagorda, TX showed an increase in the contribution of crustaceans from juveniles to adults (77.83% IRI and 81.81% IRI, respectively), while the contribution from other material decreased (21.46% IRI juveniles and 16.74% IRI adults; Table 2).

Significant differences between Atlantic Sharpnose Sharks and Bonnetheads existed using the overall prey species taxonomic groupings from all sharks combined (PERMANOVA; Pseudo–F = 320.27, permutated p–value ≤ 0.05), and prey species sub–groupings from samples that did not solely contain unidentified teleosts and crustaceans (Pseudo–F = 102.32, permutated p–value ≤ 0.05). Teleost was most important for Atlantic Sharpnose Sharks versus Bonnetheads (SIMPER; mean ± sd dissimilarity = 33.86 ± 1.59) and crustacean was most important for Bonnetheads versus Atlantic Sharpnose Sharks (SIMPER; dissimilarity = 33.70 ± 1.66 sd). Further analysis using sub–groupings (epibenthic teleost, pelagic teleost, penaeid shrimp, brachyuran, other crustaceans, cephalopods, and other) indicated that the group most differentiating Atlantic Sharpnose Sharks from Bonnetheads was pelagic teleosts (SIMPER; dissimilarity = 13.22 ± 0.63), whereas the prey category most separating Bonnetheads from Atlantic Sharpnose Sharks was crabs (SIMPER: dissimilarity = 34.23 ± 1.79).

Regional differences in Atlantic Sharpnose Shark diet were found between individuals collected in the northwest vs. the northcentral GOM using overall groupings (PERMANOVA; Pseudo–F = 3.82, permutated p–value ≤ 0.05); however, not for prey species sub–groupings (PERMANOVA; Pseudo–F = 1.83, permutated p–value > 0.05). Specifically, higher %W of teleost prey was found in the northcentral GOM compared to the northwest GOM (SIMPER; dissimilarity = 20.81 ± 0.95) and higher %W of crustaceans in the northwest GOM (SIMPER; mean abundance 29.80%) relative to the northcentral GOM (SIMPER; mean abundance 18.10%). For Bonnetheads, no significant location effect was found between sharks collected from Galveston, TX and Matagorda, TX using overall prey species groupings (PERMANOVA, Pseudo–F = 2.98, permutated p–value > 0.05); however, a significant location effect was found for sub–groupings excluding unidentified Teleost and unidentified Crustaceans (PERMANOVA, Pseudo–F =

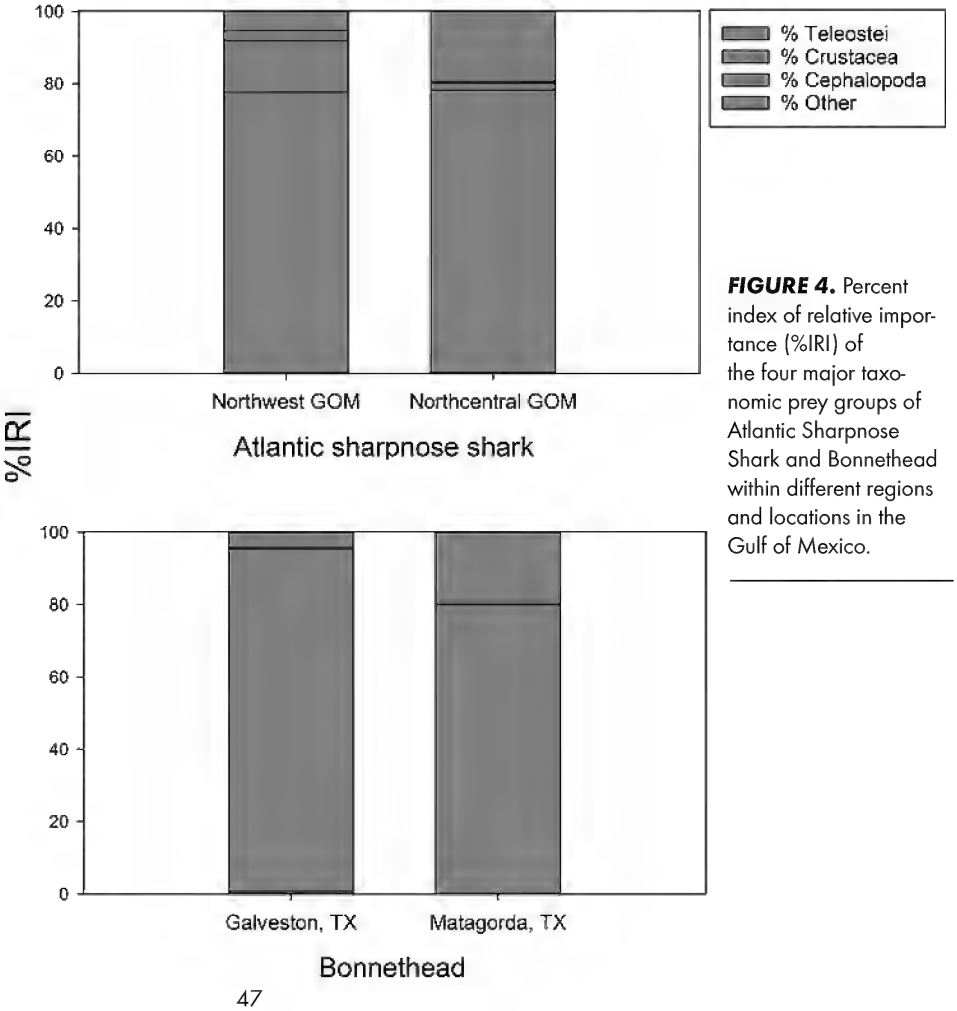

FIGURE 4. Percent index of relative importance (%IRI) of the four major taxonomic prey groups of Atlantic Sharpnose Shark and Bonnethead within different regions and locations in the Gulf of Mexico.

TABLE 2. *Bonnethead diet content by prey species category. Data expressed as percentage of Index of Relative Importance (%IRI).*

Taxonomic Group	Identified Group	Lowest Taxonomic Group		Matagorda, TX			Galveston, TX		
			Overall %IRI	Total %IRI	Juvenile %IRI	Adult %IRI	Total %IRI	Juvenile %IRI	Adult %IRI
Teleost			0.56	0.23	0.02	0.99	0.74	1.87	0.45
	Unidentified Teleost		0.35	0.24	0.02	0.84	0.41	0.50	0.35
	Sciaenidae		<0.01	-	-	-	<0.01	0.03	-
	Clupeidae		<0.01	-	-	-	<0.01	0.04	-
		Brevoortia patronus	<0.01	-	-	-	<0.01	-	0.01
	Mugilidae		<0.01	-	-	-	<0.01	0.05	-
Crustacea			90.94	79.67	77.83	81.81	94.61	96.59	92.41
	Unidentified Crustacea		6.19	4.76	4.86	-	6.73	4.78	8.40
	Penaeidae		0.10	0.03	0.11	-	0.14	0.01	0.20
		Penaeus setiferus	0.01	0.01	0.06	-	<0.01	-	0.04
	Unidentified Brachyura		22.06	16.87	11.95	29.69	24.24	18.43	25.90
	Portunidae		1.23	1.64	2.20	0.28	1.00	4.69	0.37
		Callinectes sapidus	2.19	2.02	6.49	-	2.22	3.62	1.97
		Callinectes similis	0.10	0.04	0.09	-	0.12	0.05	0.16
	Xanthidae		0.02	0.02	0.10	-	0.02	0.09	0.03
	Stomatopoda		2.35	2.41	2.56	1.96	2.27	2.58	2.47
		Squilla empusa	0.06	0.06	0.24	-	0.07	0.02	0.17
Cephalopoda			0.39	0.31	0.69	0.46	0.42	0.32	0.69
	Unidentified Cephalopoda		0.03	0.31	0.69	0.46	-	-	-
	Unidentified Teuthoidea		0.20	-	-	-	0.42	0.51	0.58
Other			8.11	19.78	21.46	16.74	4.23	1.21	6.45
	Bivalvia		<0.01	0.01	0.04	-	-	-	-
	Gastropoda		0.01	<0.01	-	-	-	-	-
	Algae		7.44	18.14	4.31	15.10	4.22	4.04	4.36

5.65, permutated p–value ≤ 0.05). The most important prey groups contributing to the differences in Bonnetheads were higher %W of crab in Galveston, TX versus Matagorda, TX (SIMPER; dissimilarity = 19.70 ±1.04) and higher %W of other in Matagorda, TX relative to Galveston, TX (SIMPER; dissimilarity = 12.65 ± 0.68).

Discussion

Differences in the diets of 2 co–occurring mesopredators were demonstrated, suggesting some degree of resource partitioning. Atlantic Sharpnose Sharks and Bonnetheads in this study displayed distinct dietary contributors, fish and crab, respectively. Atlantic Sharpnose Shark diets contained a wider range of prey items while Bonnetheads displayed a specialized diet of crustaceans, primarily consisting of crabs.

Atlantic Sharpnose Shark diets in the northwest and northcentral GOM displayed a propensity for teleost fish, but higher contributions from both crustaceans and cephalopods occurred in the northwest GOM. Previous studies have shown similar dietary variations suggesting a generalist diet for Atlantic Sharpnose Sharks with fish as the primary contributor (Gelsleichter et al. 1999, Bethea et al. 2006, Drymon et al. 2012). Further analysis of Atlantic Sharpnose Shark diets showed a reduction in dietary species richness from juveniles to adults. A large loss in the dietary contribution of crustaceans and squid in both regions suggests a refinement in diet with maturity, which is supported from previous findings (Bethea et al. 2007, Plumlee and Wells 2016). Minor differences between regions were observed at the teleost family level between the northwest and northcentral GOM. Regional variance in the dietary composition of teleost prey in Atlantic Sharpnose Sharks is frequently documented (Barry 2002, Bethea et al. 2006, Drymon et al. 2012) and likely related to the fish assemblage of a given ecosystem. Due to the high diversity of contents found in Atlantic Sharpnose Shark stomachs, our findings suggest Atlantic Sharpnose Sharks in the northwest and northcentral GOM are generalist predators, consuming a wide range of prey items that are likely dependent on the prey species composition of the region in which they are found.

Bonnetheads showed a consistent diet composed almost entirely of crustaceans with similar contributions, both geographically and ontogenetically, from Portunid crabs, xanthid crabs, and stomatopods. The results from this spatial comparison support and elucidate results from previous studies in other regions (Cortés et al. 1996, Lessa and Almeida 1998, Bethea et al. 2007) showing that blue crabs (*Callinectes* spp.) were the dominant dietary prey species for Bonnetheads. Samples collected from Galveston had a higher presence of penaeid shrimp and a lower presence in the cat-

egory other compared to samples from Matagorda, though these differences can be considered negligible. Bay systems, such as those found in Matagorda and Galveston, TX, serve as nursery grounds to many crustacean species (Beck et al. 2001, Minello et al. 2008). The slight differences observed in Bonnethead stomach contents between these 2 locations are most likely influenced by the variety of crustacean species that utilize these areas as nursery grounds. Nevertheless, the crustacean assemblages near each bay system evaluated in this study had little effect on the overall diet composition. Bonnetheads within the northwest GOM have been confirmed to be specialized predators showing little to no dietary variation beyond *Callinectes* spp. crabs.

The observed dietary differences are also driven by morphology. Many crustacean prey items found in Bonnethead stomachs in this study were comparatively large, whole, and easily identified to lower taxonomic levels. Bonnetheads have a highly modified head structure characteristic of the family Sphyrnidae (hammerhead family). The enlarged cephalofoil offers an enhanced electro–sensory system compared to sharks in the family Carcharhinidae (requiem sharks), which is used to detect concealed prey items (McComb et al. 2009). Bonnetheads also display an enlarged maximum gape but a lower maximum bite force (Wilga and Motta 2000, Mara et al. 2010, Rice et al. 2016). This, along with posterior molariform teeth, asynchronous muscle activity, tooth reorientation during biting, and prolonged jaw adductor activity patterns, allows for prey crushing and suction during feeding, making the Bonnethead an extremely efficient durophagous predator (Mara et al. 2010). Carcharhinid sharks, such as Atlantic Sharpnose, lack many of these traits, allowing Bonnetheads to exploit preferred prey items (crabs) more effectively and reduce the amount of competition from similar sized sharks.

Atlantic Sharpnose Sharks have been found to be pelagic, generalist predators with consistent, fish–dominated diets and varied contributions of taxa based upon region of collection (Drymon et al. 2012). In contrast, Bonnetheads demonstrate more benthic, specialized feeding strategies with consistent diets among various regions (Cortés et al. 1996, Lessa and Almeida 1998, Bethea et al. 2007, Bethea et al. 2011, Haman et al. 2012). This study evaluated the diets of these two species at spatial scales not previously compared and found similar results to studies conducted in singular locations. Analysis beyond traditional stomach contents (e.g., DNA barcoding) would likely increase resolution and provide insight on the prevalence of prey species in the diets of sharks, which may be dependent on ecosystem assemblages in a given region. Regional comparisons of the diets of common sharks allow for more extensive evaluations of species–wide dietary preferences. Such evaluations are important to further the understanding of the role of predators in marine ecosystems, information crucial to effective ecosystem–based fisheries management.

Acknowledgements

We thank Texas A&M University at Galveston for providing the facilities to conduct our research. We also thank Galveston Party Boats Inc. and the Galveston Yacht Basin for allowing us to conduct our surveys and collections at their facilities. Texas Parks and Wildlife Department contributed samples. We thank the reviewers who provided useful suggestions to improve the quality of this manuscript along with the volunteers who helped with sample collections and processing.

Literature Cited

Barry, K. P. 2002. Feeding habits of Blacktip Sharks, *Carcharhinus limbatus*, and Atlantic Sharpnose Sharks, *Rhizoprionodon terraenovae*, in Louisiana coastal waters. MS Thesis, Louisiana State University, Baton Rouge, LA, USA. 80 p.

Baum, J.K. and B. Worm. 2009. Cascading top–down effects of changing oceanic predator abundances. Journal of Animal Ecology 78:699–714. doi: 10.1111/j.1365–2656.2009.01531.x

Beck, M.W., K.L. Heck, K.W. Able, D.L. Childers, D.B. Eggleston, B.M. Gilanders, B. Halpern, C.G. Hays, K. Hoshino, and T.J. Minello 2001. The identification, conservation, and management of estuarine and marine nurseries for fish and invertebrates: A better understanding of the habitats that serve as nurseries for marine species and the factors that create site–specific variability in nursery quality will improve conservation and management of these areas. Bioscience 51:633–641. doi: http://dx.doi.org/10.1641/0006–3568(2001)051[0633:TICAMO]2.0.CO;2

Bethea, D.M., J.A. Buckel, and J.K. Carlson. 2004. Foraging ecology of the early life stages of four sympatric shark species. Marine Ecology Progress Series 268:245–264. doi: 10.3354/meps268245

Bethea, D.M., J.K. Carlson, J.A. Buckel, and M. Satterwhite. 2006. Ontogenetic and site–related trends in the diet of the Atlantic Sharpnose Shark *Rhizoprionodon terraenovae* from the northeast Gulf of Mexico. Bulletin of Marine Science 78:287–307.

Bethea, D.M., L. Hale, J.K. Carlson, E. Cortes, C.A. Manire, and J. Gelsleichter. 2007. Geographic and ontogenetic variation in the diet and daily ration of the Bonnethead shark, *Sphyrna tiburo*, from the eastern Gulf of Mexico. Marine Biology 152:1009–1020. doi: 10.1007/s00227–007–0728–7

Bethea, D.M., J.K. Carlson, L.D. Hollensead, Y.P. Papastamatiou, and B.S. Graham. 2011. A comparison of the foraging ecology and bioenergetics of the early life–stages of two sympatric Hammerhead Sharks. Bulletin of Marine Science 87:873–889. doi: http://dx.doi.org/10.5343/bms.2010.1047

Carlson, J.K., and G.R. Parsons. 1997. Age and growth of the Bonnethead shark, *Sphyrna tiburo*, from northwest Florida, with comments on clinal variation. Environmental Biology of Fishes 50:331–341. doi: 10.1023/A:1007342203214

Castillo–Geniz, J.L., J.F. Marquez–Farias, M.C.R. de la Cruz, E. Cortes, and A.C. del Prado. 1998. The Mexican artisanal shark fishery in the Gulf of Mexico: towards a regulated fishery. Marine and Freshwater Research 49:611–620. doi: 10.1071/MF97120

Clarke, K.R., and R.N. Gorley. 2015. PRIMER v7: user manual/tutorial. PRIMER–E, Plymouth, England.

Cortés, E. 1997. A critical review of methods of studying fish feeding based on analysis of stomach contents: application to elasmobranch fishes. Canadian Journal of Fisheries and Aquatic Sciences 54:726–738. doi: 10.1139/f96–316

Cortés, E. 1999. Standardized diet compositions and trophic levels of sharks. ICES Journal of Marine Science 56:707–717. doi: 10.1006/jmsc.1999.0489

Cortés, E. 2005. *Sphyrna tiburo*. The IUCN Red List of Threatened Species 2005: e.T39387A10193033. http://dx.doi.org/10.2305/IUCN.UK.2005.RLTS.T39387A10193033.en

Cortés, E. 2009. *Rhizoprionodon terraenovae*. The IUCN Red List of Threatened Species 2009: e.T39382A10225086. http://dx.doi.org/10.2305/IUCN.UK.2009–2.RLTS.T39382A10225086.en

Cortés, E., C.A. Manire, and R.E. Hueter. 1996. Diet, feeding habits, and diel feeding chronology of the Bonnethead shark, *Sphyrna tiburo*, in southwest Florida. Bulletin of Marine Science 58:353–367.

Delorenzo, D.M., D.M. Bethea, and J.K. Carlson. 2015. An assessment of the diet and trophic level of Atlantic Sharpnose Shark *Rhizoprionodon terraenovae*. Journal of Fish Biology 86:385–391. doi: 10.1111/jfb.12558

Drymon, J.M., S.P. Powers, J. Dindo, B. Dzwonkowski, and T.A. Henwood. 2010. Distributions of sharks across a continental shelf in the northern Gulf of Mexico. Marine and Coastal Fisheries 2:440–450. doi: 10.1577/C09–061.1

Drymon, J.M., S.P. Powers, and R.H. Carmichael. 2012. Trophic plasticity in the Atlantic Sharpnose Shark (*Rhizoprionodon terraenovae*) from the north central Gulf of Mexico. Environmental Biology of Fishes 95:21–35. doi: 10.1007/s10641–011–9922–z

Drymon, J.M., L. Carassou, S.P. Powers, M. Grace, J. Dindo, and B. Dzwonkowski. 2013. Multiscale analysis of factors that affect the distribution of sharks throughout the northern Gulf of Mexico. Fishery Bulletin 111:370–380. doi: 10.7755/FB.111.4.6

Ferry, L.A. and Cailliet, G.M. 1996. Sample size and data analysis: Are we characterizing and comparing diet properly? In: D. MacKinlay and K. Shearer, eds. Proceedings the of American Fisheries Society Symposium Gutshop '96, San Francisco, CA, USA, p. 71–80.

Fowler, S.L C., R.D. M. Camhi, G.H. Burgess, G.M. Cailliet, S.V. Fordham, C.A. Simpendorfer, and J.A. Musick. 2005. Sharks, rays and chimaeras: the status of the Chondrichthyan fishes. Status survey. IUCN/Shark Specialist Group. IUCN, Gland, Switzerland and Cambridge, UK. https://portals.iucn.org/library/efiles/html/2005–029/cover.html

Frazier, B., W. Driggers, D. Adams, C. Jones, and J. Loefer. 2014. Validated age, growth and maturity of the Bonnethead *Sphyrna tiburo* in the western North Atlantic Ocean. Journal of Fish Biology 85:688–712. doi: 10.1111/jfb.12450

Gelsleichter, J., J.A. Musick, and S. Nichols. 1999. Food habits of the smooth dogfish, *Mustelus canis*, dusky shark, *Carcharhinus obscurus*, Atlantic Sharpnose Shark, *Rhizoprionodon terraenovae*, and the sand tiger, *Carcharias taurus*, from the northwest Atlantic Ocean. Environmental Biology of Fishes 54:205–217. doi: 10.1023/A:1007527111292

Haman, K.H., T.M. Norton, A.C. Thomas, A.D.M. Dove, and F. Tseng. 2012. Baseline health parameters and species comparisons among free–ranging Atlantic Sharpnose (*Rhizoprionodon terranovae*), Bonnethead (*Sphyrna tiburo*), and Spiny Dogfish (*Squalus acanthias*) sharks in Georgia, Florida, and Washington. Journal of Wildlife Diseases 48:295–306. doi: http://dx.doi.org/10.7589/0090–3558–48.2.295

Heithaus, M.R. 2008. Predicting ecological consequences of marine top predator declines. Trends in Ecology and Evolution 23:537–537. doi: 10.1016/j.tree.2008.01.003

Hoffmayer, E.R., W.B. Driggers, L.M. Jones, J.M. Hendon, and J.A. Sulikowski. 2013. Variability in the reproductive biology of the Atlantic Sharpnose Shark in the Gulf of Mexico. Marine and Coastal Fisheries 5:139–151. doi: 10.1080/19425120.2013.783518

Kinney, M.J., N.E. Hussey, A.T. Fisk, A.J. Tobin, and C.A. Simpfendorfer. 2011. Communal or competitive? Stable isotope analysis provides evidence of resource partitioning within a communal shark nursery. Marine Ecology Progress Series 439:263–276. doi: 10.3354/meps09327

Lessa, R.P. and Z. Almeida. 1998. Feeding habits of the Bonnethead shark, *Sphyrna tiburo*, from northern Brazil. Cybium 22:383–394.

Lombardi–Carlson, L.A., E. Cortés, G.R. Parsons, and C.A. Manire. 2003. Latitudinal variation in life–history traits of Bonnethead shark, *Sphyrna tiburo*, (Carcharhiniformes: Sphyrnae) from the eastern Gulf of Mexico. Marine and Freshwater Research 54:875. doi: 10.1071/MF03023

Mara, K.R., P.J. Motta, and D.R. Huber. 2010. Bite force and performance in the durophagous Bonnethead Shark, *Sphyrna tiburo*. Journal of Experimental Zoology Part a–Ecological Genetics and Physiology 313A:95–105. doi: 10.1002/jez.576

McComb, D.M., T.C. Tricas, and S.M. Kajiura. 2009. Enhanced visual fields in hammerhead sharks. Journal of Experimental Biology 212:4010–4018. doi: 10.1242/jeb.032615

Minello, T.J., G.A. Matthews, P.A. Caldwell, and L.P. Rozas. 2008. Population and production estimates for decapod crustaceans in wetlands of Galveston Bay, Texas. Transactions of the American Fisheries Society 137:129–146. doi: 10.1577/T06–276.1

Parsons, G.R. and E.R. Hoffmayer. 2005. Seasonal changes in the distribution and relative abundance of the Atlantic Sharpnose Shark *Rhizoprionodon terraenovae* in the north central Gulf of Mexico. Copeia 2005:914–920.

Pérez–Jiménez, J.C. and I. Mendez–Loeza. 2015. The small–scale shark fisheries in the southern Gulf of Mexico: Understanding their heterogeneity to improve their management. Fisheries Research 172:96–104. doi: 10.1016/j.fishres.2015.07.004

Plumlee, J.D. and R.J.D. Wells. 2016. Feeding ecology of three coastal shark species in the northwest Gulf of Mexico. Marine Ecology Progress Series 550:163–174. doi: 10.3354/meps11723

Rice, K.W., R. Buchholz, and G.R. Parsons. 2016. Correlates of bite force in the Atlantic sharpnose shark, *Rhizoprionodon terraenovae*. Marine Biology 163:1–9. doi: 10.1007/s00227–016–2814–1

Rooker, J.R. 1995. Feeding ecology of the Schoolmaster Snapper, *Lutjanus apodus* (Walbaum), from southwestern Puerto–Rico. Bulletin of Marine Science 56:881–894.

Wilga, C.D. and P.J. Motta. 2000. Durophagy in sharks: feeding mechanics of the hammerhead *Sphyrna tiburo*. Journal of Experimental Biology 203:2781–2796.

Gulf and Caribbean Research

Volume 27 | Issue 1

2016

Hydrodynamic Variability in a Microtidal Coastal Bay Geographically Susceptible to North East Trade Winds

Israel Medina-Gómez
Centro de Investigación y de Estudios Avanzados del I.P.N. (CINVESTAV-IPN), imedgomez@gmail.com

Cecilia Enríquez
Unidad Multidisciplinaria de Docencia e Investigación (UMDI)

Björn Kjerfve
American University of Sharjah, University City, Sharjah, United Arab Emirates

Ismael Mariño
CINVESTAV-IPN

See next page for additional authors

Hydrodynamic Variability in a Microtidal Coastal Bay Geographically Susceptible to North East Trade Winds

Authors

Israel Medina-Gómez, *Centro de Investigación y de Estudios Avanzados del I.P.N. (CINVESTAV-IPN)*; Cecilia Enríquez, *Unidad Multidisciplinaria de Docencia e Investigación (UMDI)*; Björn Kjerfve, *American University of Sharjah, University City, Sharjah, United Arab Emirates*; Ismael Mariño, *CINVESTAV-IPN*; and Jorge Herrera-Silveira, *CINVESTAV-IPN*

Gulf and Caribbean Research Vol 27, 52-65, 2016
DOI: 10.18785/gcr.2701.06
Manuscript received, January 24, 2016; accepted, June 29, 2016

HYDRODYNAMIC VARIABILITY IN A MICROTIDAL COASTAL BAY GEOGRAPHICALLY SUSCEPTIBLE TO NORTH EAST TRADE WINDS

Israel Medina–Gómez[1]*, Cecilia Enríquez[2], Björn Kjerfve[3], Ismael Marino–Tapia[1], and Jorge Herrera–Silveira[1]
*[1]CINVESTAV–IPN, Km. 6 Antigua Carretera a Progreso, Cordemex, C.P. 97310, Mérida, Yucatán, México; [2]UMDI, Puerto de Abrigo s/n, Sisal Hunucmá, Yucatán, C.P. 97355; [3]American University of Sharjah, University City, Sharjah, United Arab Emirates; *Corresponding author, email: imedgomez@gmail.com*

Abstract: The ecological integrity and overall health conditions of natural coastal systems are largely based upon the balance among physical processes. The objective of this study was to assess the effects of tides and winds on the water level variability, circulation patterns, and turnover time in Bahia de la Ascension (BA), a shallow, tropical coastal bay in the Mexican Caribbean prone to the influence of Trade winds due to its geographical location. The analysis of the hydrodynamics of BA using a 2D numerical model indicates that the tidal flow in the inlets and central basin of the bay vary by tidal phase. An averaged seawater inflow through the south inlet and outflow through the north inlet is observed for every simulated case, while peak instantaneous current velocities are evident in the northern entrance. Winds play a dominant role in the water turnover from the system's interior to the main bay. The model shows an average turnover time of 45 days for the whole bay, with shorter turnover when Trade winds impart stress along the main northeast–southwest axis in the bay. Since the tidal signal is attenuated in the southwest endpoint of the bay, the relevance of winds in the transport phenomena was considered fundamental to preserve the ecological heterogeneity of BA.

Keywords: numerical model, residual flow, flushing time, Yucatan Peninsula, western Caribbean.

Introduction

The coastal oceanographic phenomena exert a main control over the hydrology of tropical estuaries, lagoons, and bays. Because of the variable open–boundary nature in these shallow ecosystems coastal hydrodynamics modulates their water exchange with the sea, and consequently, the rate and magnitude of key processes (e.g., salt and nutrient fluxes; Hench et al. 2008). The energy supplied by tides represents a salient forcing controlling the mixing and transport of materials. Even in restricted lagoons subjected to low tidal range, tidal forcing may account for up to 70% of the water level variability, driving a substantial advective, ocean–directed water transport (David and Kjerfve 1998).

However, when tidal range is small, long–term (in the order of months; *e.g.*, seasonal) and short–term (in the order of hours; e.g., winds plus heat balances) meteorological forcing may have a greater influence on the coastal environment than tides (Cavalcante et al. 2011). This non–tidal forcing can induce sea level oscillations with a period greater than a few days in the interior of coastal lagoons, altering net transport. Additionally, the balance between freshwater influx and saltwater incoming from the ocean may force gravitational circulation in estuaries and coastal lagoons, contributing to dissolved and particulate materials transport, as well as dispersion of biota across the seaward boundary (Geyer 1997, Brown et al. 2004).

Since the fluctuating hydrology in semi–enclosed systems is highly dependent on their connectivity to the adjacent shelf sea, changes in the coastal physical setting may have profound ecological implications on them (Drew 2000, Ladah et al. 2012). Thus, a proper grasp of the interplay among physical processes is of primary importance to thoroughly understand the patterns of hydrological variability and asses the overall health condition for such aquatic systems (Nixon 1988, Wolanski 1994, Umgiesser and Neves 2005).

The objective of this study is to explore the dynamic responses of water level, currents, water exchange, and circulation in response to tidal and wind forcing in a shallow, tropical coastal bay using a numerical simulation model. It is hypothesized that, given the microtidal regime in the western Caribbean, the predominant northeast trade winds rather than tidal variability more strongly influences the overall circulation patterns in this ecosystem. We are also interested in examining how the bay's turnover rates respond to the typical wind forcing experienced in the region. Furthermore, given the trend of human–driven disturbance experienced in many semi–enclosed coastal ecosystems and their intrinsic vulnerability, as well as the scarcity of analytical studies to diagnose the responses to the physical–environmental setting in developing countries, the current study is deemed both a timely and relevant effort.

Study Site

Bahia de la Ascension (BA) is a shallow coastal bay of the western Caribbean (Figure 1A), with average depth of 2.3 m and maximum depth of 6.8 m at the north inlet (Figure 1B). The bay's main axis is NE–SW and surface area is 580 km^2, with total mean water volume of 1.33 x 10^9 m^3. The tidal characteristics of this region are mixed, semi–diurnal, microtidal regime (range <0.20 m within the bay), dominated by the principal lunar (M_2) component with amplitude of

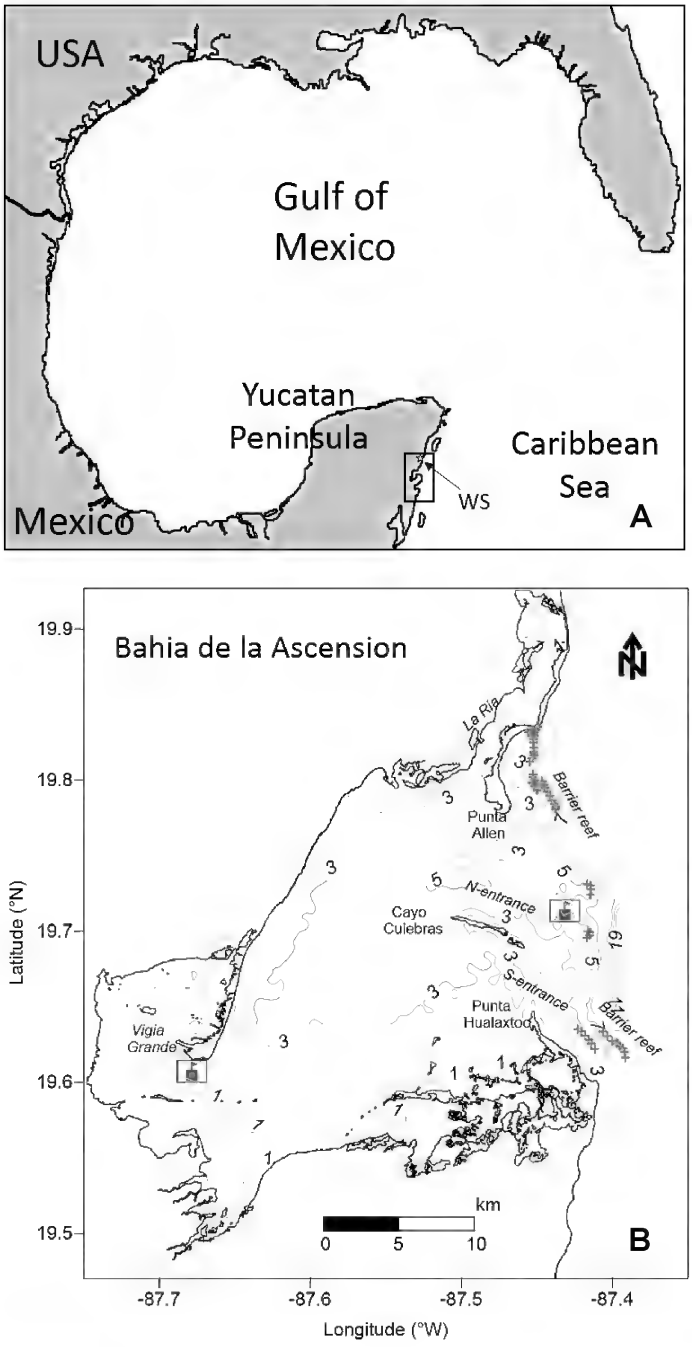

FIGURE 1. Map of the Gulf of Mexico showing Bahia de la Ascension in the Western Caribbean. A. Location of the weather stations northward from the study site (WS). B. Bahia de la Ascension with bathymetry (isobaths in meters) and seaward, discontinuous coral reef formation (x). Grey flags represent moored CTD's in the inner bay and reef lagoon.

0.074 m (Kjerfve 1981) and tidal prism of ≈105 x 10^6 m^3 per semidiurnal cycle. The bay is rimmed seaward by the Mesoamerican Barrier Reef System (MBRS), the world's second largest coral reef formation stretching across four countries (Honduras, Guatemala, Belize, and Mexico).

The ratio between buoyancy forcing (volume of freshwater per tidal cycle) and tidal forcing (tidal prism volume) in the bay is consistent with prevalent vertically homogeneous water column conditions in the inlet zone, with mild vertical stratification in the northern entrance only during peak precipitation periods and less energetic conditions associated with neap tides (Medina–Gómez et al. 2014a). The estimated water residence time in this system during dry and rainy seasons, respectively, is 1,525 days and 203 days (computed according to the freshwater fraction method; Medina–Gómez et al. 2014a). The ratio of groundwater input to tidal prism in BA is nearly 1% in the rainy season and only 0.07% during the dry season.

This system is part of the Sian Ka'an Biosphere reserve (SKBR) in the Yucatan Peninsula (19°40'32.76" N; 87°32'30.87" W), one of the largest protected coastal wetlands in Mexico and a UNESCO's World Heritage Site. The SKBR is southward from a burgeoning tourism destination, considered among one of the fastest human population growth regions in Latin America (annual growth rate within 20–25%; Meacham 2007). Because of the karstified (prone to dissolution of the carbonate rock by infiltrating rainwater) landform common to the Yucatan platform, the BA receives significant freshwater input (357 x10^6 m^3/yr) from an extensive array of fissures in the limestone draining a 1,200 km^2 hydrological basin through both diffuse and point sources (*i.e.*, submerged groundwater discharges) venting mainly into the southwest bay. Consequently, SKBR is threatened by the quick development of massive tourism occurring just a few kilometers northward, in the so–called Mayan Riviera.

Marked temporal rainfall heterogeneity rather than temperature variability controls the seasonality of the Mexican Caribbean, featuring a distinct dry season (February–May) and a distinct rainy season (June–October). In addition to the dominant northeast trade winds blowing 32% of the time (mean speed of 3.2 m/s, with strongest winds in June) and southeasterly winds (prevalent in March, with mean speed of 3.3 m/s) in the region, slight precipitation and drop in air temperature associated with boreal winds (i.e., locally known as *Nortes*) occurs from November to January.

Materials and Methods

The spatial variability of water level and currents, estimation of net water discharges across boundaries, and assessment of the time–averaged flow under tidal forcing and different wind condition scenarios were addressed in BA using a barotropic (2D) hydrodynamic model. Also, water level (WL) in the inner bay (Vigia Grande embayment, VG) and the adjacent marine environment (reef lagoon, RL) was recorded during 8 June 2007 (dry season) using an anchored Van Essen Instruments conductivity–temperature–depth recorder (CTD Diver). The WL data series collected in the RL (5 m depth) served to force the model at the ocean end during the validation stage only. On the other hand, the data series obtained in VG (1.5 m) was utilized to compare

the observed versus computed WL values, and further adjust the model parameters during the calibration–validation process. A 10 min sampling rate was set for both moored instruments during 4 days spanning the survey.

Model Setup

A depth–averaged, free–surface hydrodynamic model was implemented using the Delft 3D system (WL–Delft hydraulics) in bi–dimensional mode. The model simulates

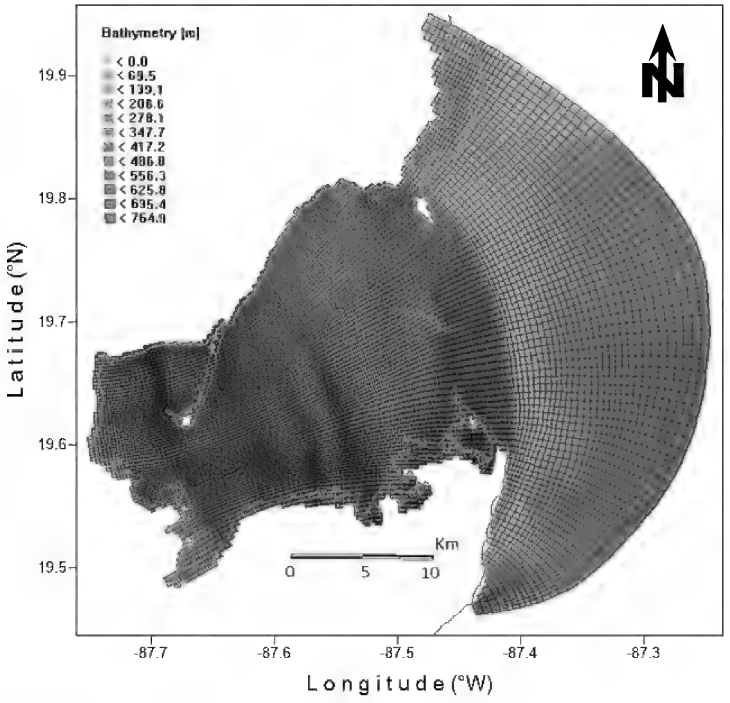

FIGURE 2. Adaptive grid of the model domain

non–steady flow resulting from tidal and meteorological forcing. The space in the computational region was partitioned using a Cartesian, curvilinear, adaptive grid–cell arrangement with 23,200 nodes with spatial resolution varying from 100 m inside the bay (the site of interest), to a coarser horizontal resolution ≈1,000 m on the shelf (Figure 2). Such a grid arrangement allows smooth spatial variation over the model domain minimizing inaccuracy errors in the finite difference operators (WL–Delft hydraulics).

The spatial discretization of the horizontal advection term was undertaken by using the cyclic method, which does not set a restriction in the time step. This flexibility enabled us to implement an alternating direction implicit (ADI) time integration (Delft3D–FLOW). Such a scheme splits one time step into 2 stages and fully solves all shallow water equations on each of such stages by taking a given term (water level gradient, advection) implicitly in time, and further taking the same term explicitly in time in the next stage (i.e., the other half–time).

Thus, from the 3 convergent solutions obtained–all of them achieving numerical stability within 2 semi–diurnal cycles as tested by the system's kinetic energy (Table 3; Medina–Gómez 2011), a Δt = 3 min was selected for the simulations, since this time–step met both numerical stability (Courant number criteria: accuracy in reproducing important spatial length scales and stability for the current barotropic model; WL–Delft hydraulics) and reasonable computational requirements.

The horizontal geometry (wet versus dry) are updated in the model domain every time a new water level is computed. This half–time steps scheme results in an overall second order accuracy in space solution for the integrated time step. The wet–dry framework is based on an algorithm that activates a switch by individually assessing depth values at the cell interfaces. Any time total water depth in a water level point is negative (i.e., dry), that horizontal cell is removed from the computation and the half–time step is repeated. Further, the initial water level at a dry cell is defined by the depth at a given water level point.

To avoid potential boundary effects, a weakly–reflective open boundary (low–pass filter using an alpha–coefficient equal to 0.2; WL–Delft hydraulics) was positioned 15 km seaward from the reef barrier. This distance was set according to the availability of bathymetric data for the region (Cetina et al. 2006).

The turbulence closure model is based on the eddy viscosity concept and defined in the Delft3D–FLOW module for 1–layer (depth–average). According to the Rossby number calculated for the system (3.4×10^{-5}), deflection of the tidal current towards the right is not negligible given the size of the model domain (e.g., prominent role of rotational processes on the flow field: Ro << 1; Tilburg et al. 2011). Thus, the latitude location of the model area on the Earth's globe was provided to take the Coriolis force into account in the simulation–default in Delft 3D.

Model Calibration and Validation

The model was calibrated by prescribing a 4 day length water level (collected in the reef lagoon; Figure 3) forcing

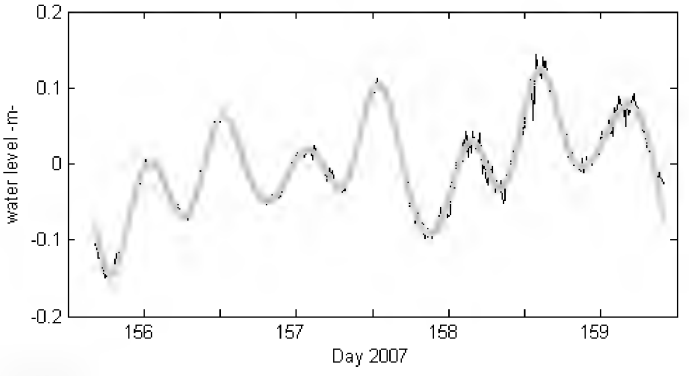

FIGURE 3. Water level in the reef lagoon site (measured, solid black lines; 6-hr low-pass, grey dotted line). High frequency oscillations were eliminated from the raw water-level data by using a discrete Fourier transform filter. This water level was specified at the ocean boundary during calibration-validation of the numeric model.

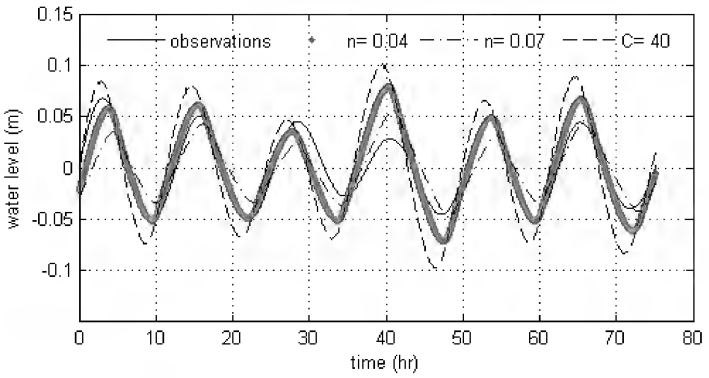

FIGURE 4. Water level at the Vigia Grande mooring (inner-most bay). Observations (demeaned time series) compared with simulated data obtained through different bottom roughness formulae: Chezy coefficient, C = 40 $m^{1/2}/s$ and two Manning coefficients, n = 0.04 and 0.07 (independent of units).

in the ocean end and further adjusting the bottom friction coefficient until reaching a water level close to that observed in the inner bay (Figure 4). We considered it appropriate to carry out the calibration–validation phase simulations using the reef lagoon and inner–bay water levels, since both time–series were obtained at the same period of time and influenced by identical background processes such as wind stress, tidal phase, and prevalent atmospheric conditions.

Since deep water is found beyond the reef crest (Figure 2), it seemed reasonable to assume a lack of shoaling on the tidal wave prescribed at the seaward boundary before stepping into the bay's edge (e.g., reef lagoon). Nonetheless, we accounted for the phase–shift presumably experienced by the water level signal across the 18 km distance (15 km from the seaward edge of the model domain to the reef crest plus 3 km from the reef crest to the mooring site within the reef lagoon) between the ocean boundary (where the forcing was prescribed) and the mooring site onto the reef lagoon (where the time series was actually recorded), by computing the phase lag of the M_2 tidal frequency (the most influential harmonic constituent in this region; Kjerve 1981) between the outer bay (Reef Lagoon) and inner–bay (Vigia Grande). The distance between the Vigia Grande and Reef Lagoon moorings is roughly 22 km, or a distance ratio between ocean boundary–reef lagoon to reef lagoon–inner bay segments equal to 0.82.

The harmonic analysis using T_TIDE showed that the M_2 tidal constituent lagged ≈1.12 h (32.24°) behind in the inner bay relative to the reef lagoon (Pawlowicz et al. 2002). By considering the distance ratio between segments, a lag of > 55 min was estimated between the ocean boundary and the reef lagoon. Consequently, a phase shift of 1 h was implemented for every modeled water level (i.e., those produced by distinct bottom roughness coefficients) before proceeding with fitting between observed and modeled water level time series.

A Chezy coefficient (default in Delft) of C = 40 $m^{1/2}/s$ and two different Manning roughness coefficients of n = 0.04 and 0.07 (independent of units) were applied in the simulations during the calibration–validation phase. Such roughness values are within those reported for macrophyte–dominated habitats (e.g., 0.03–0.30; Dawson and Robinson 1984) and have been utilized in studies to parameterize bottom friction in shallow ecosystems colonized by aquatic vegetation (e.g., 0.02–0.20; Morin et al. 2000).

After removing the first day (2 semidiurnal cycles) from startup at every simulation for stabilization reasons, the agreement between modeled and measured water level was quantified utilizing the root–mean square error (RMSE; eq. 1) and the relative mean absolute error (RMAE; eq. 2). Both statistics are widely used to evaluate accuracy of numerical models (Fernandes et al. 2001, Sousa and Dias 2007, Walstra et al. 2001):

$$\text{Eq. (1)} \quad \text{RMSE} = \sqrt{\frac{1}{N}\sum_{n=1}^{N}[x_{OBS} - x_{MOD}]^2}$$

$$\text{Eq. (2)} \quad \text{RMAE} = \frac{\frac{1}{N}\sum_{n=1}^{N}(X_{MOD} - X_{OBS})}{\frac{1}{N}\sum_{n=1}^{N}(X_{OBS})}$$

where X_{OBS} and X_{MOD} are the set of N observed and modeled values, respectively.

The minimum difference between the observed water level and that predicted by the model at the inner bay corresponded to a Manning coefficient equal to 0.04, yielding RMAE ≈ 0.17 (Table 1). According to the error categorization provided by Sutherland et al. (2004), RMAE values < 0.2 are qualified as an excellent match between predictions and observations.

TABLE 1. *Statistics summarizing the model performance. Root Mean Square Error (RMSE); Relative Mean Absolute Error (RMAE). n = 501.*

Bottom friction formulae	RMSE (m)	RMAE *
Chezy, C= 40 $m^{1/2}/s$	0.0239	0.6531
Manning, n = 0.04	0. 0228	0.1664
Manning, n = 0.07	0.0234	0.2316

*Values <0.2 correspond to an excellent agreement (Sutherland et al. 2004).

Additionally, harmonic constants of the tidal constituents for the observed and modeled water level time series were calculated for comparison. The correlation coefficients among observed versus modeled tidal constants (Table 2) differ from the statistics computed from the actual water level data series, as Chezy's is better qualified (amplitude correlation = 0.99, p ≈ 0; phase correlation = 0.86, p = 0.007) than the Manning formulae (amplitude correlation

TABLE 2. *Harmonic constants of tidal constituents (amplitude and phase) for both observed and modeled (applying distinct bottom friction coefficients) water level time-series at an observation point in the inner-most bay. Amp—amplitude; Pha—phase; Obs—observed; M04 and M07—Manning roughness coefficients of n = 0.04 and n = 0.07, respectively; Chez—Chezy modeled coefficients.*

Tide	Frequency (cph)	Amp_Obs	Pha_Obs	Amp_M04	Pha_M04	Amp_M07	Pha_M07	Amp_Chez	Pha_Chez
K1	0.0418	0.0043	141.53	0.0126	255.37	0.0105	272.74	0.0143	240.47
M2	0.0805	0.0479	108.13	0.0546	99.88	0.0353	119.77	0.0775	80.58
M3	0.1208	0.0028	2.51	0.0036	34.83	0.0026	47.88	0.0046	24.13
M4	0.1610	0.0011	155.58	0.0009	181.8	0.001	223.45	0.0004	233.7
2MK5	0.2028	0.0005	201.8	0.0009	107.68	0.0011	166.41	0.0001	206.48
M6	0.2415	0.0005	160.01	0.003	324.77	0.0024	14.42	0.0016	269.04
3MK7	0.2833	0.0002	206.52	0.0005	151.48	0.0006	203.32	0.0003	267.4
M8	0.3221	0.0003	167.28	0.0001	341	0.0002	172.29	0.0006	197.19

= 0.98, p ≈ 0; phase correlation = 0.46, p = 0.25). However, the correlation coefficient has been reported as a poor parameter quantifying accuracy of forecasts produced by numerical systems (Murphy 1988). These results led us to consider that n = 0.04 yielded the best fit between observed and simulated tidal ranges.

Hydrodynamic Simulation Scenarios

For all the numerical simulations scenarios the model was forced at the open boundary with a water level time series reconstructed from tidal components (M_2, S_2, N_2, K_1, O_1, P_1) reported for Cozumel Island, located 60 km north from BA (Kjerfve 1981). Besides applying a spatially uniform n bottom friction parameter, other predefined initial and boundary conditions were background water salinity equal to 35 and temperature of 28°C. Also, water level forcing at the offshore boundary was set to begin with the rising phase (zero—level in the water column at the start time of the simulation) of such a reconstructed signal from local tidal constituents (Kjerfve 1981). The first day of the simulation time (2 semi—diurnal cycles spin—up) was further removed from the simulation results prior to analysis (Table 1). No freshwater input was included in the set of boundary conditions of this model.

Along with a tidally forced stand—alone case, a series of simulations comprising identical tides plus 3 regionally typical wind conditions were executed: 1) Northeasterlies (Trade winds); 2) Southeasterly winds; and 3) Northwest—North winds (*Nortes*). Wind data were provided by the National Meteorological Service (SMN) from a weather station (Forest Technology Systems, Ltd.) located 9 m above the ground and 38 km northward from BA (Figure 1a), within the Sian Ka'an Biosphere Reserve (SMN 2007).

The 3 wind events were simulated using real, time—varying, spatially homogenous data with a 10 min sampling frequency rather than prescribing artificial, steady winds (Figure 5). We believe this approach allows elucidating the ecosystem's hydrodynamic response to the most prevalent local wind scenarios under real conditions as much as possible. Otherwise, using unidirectional/constant velocity wind data sets may overestimate the wind stress influence on water circulation, whilst time—varying responses of hydrodynamics in semi—enclosed ecosystems to short—term processes (e.g., seiches) might be overlooked (Staneva and Stanev 1998, Enriquez et al. 2010).

Wind events were selected by ensuring that every data series involved both a minimum direction persistence over an 8 d period and relatively high velocities according to the mean values reported for this zone. The specified duration for simulations is tied to the characteristic duration of *Nortes* (i.e., winds from the N and NW associated with polar high—pressure fronts featuring low air temperature), which are characteristically short—lived episodes in the Yucatan

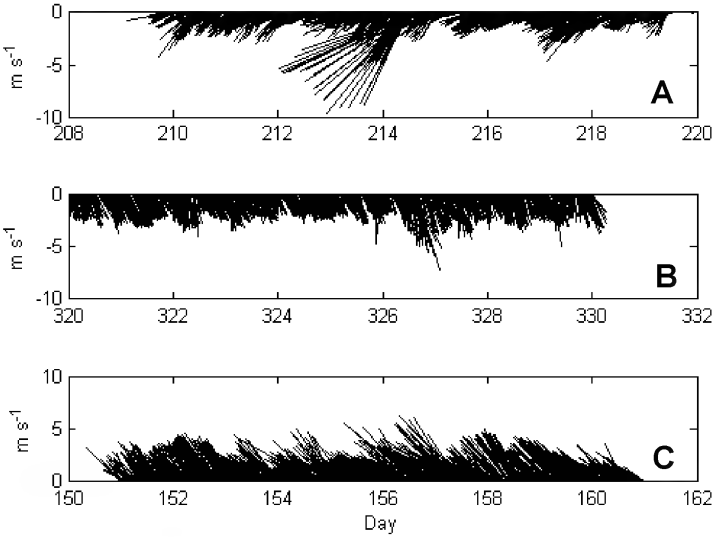

FIGURE 5. Three wind events occurring in 2007 and utilized in combination with tides to force the hydrodynamic model. A. Trade winds. B. North winds. C. Southeast winds.

TABLE 3. *Summary of the numerical simulations. ST—spring tide.*

Modeling stage	Cases	Forcing functions	Simulation time (days)	Observations
Stability tests	Kinetic energy	M_2 tide	10	Three Δt's tested: 1, 3, and 9 min
	Volume conservation	M_2 tide	30	Experiment carried out with Δt = 3 min
Reliability tests[a]	Calibration and Validation	4 day-length surface elevation observations	4	Time series collected in the reef lagoon was prescribed at the ocean end for calibration. The validation was performed by comparing bottom roughness formulae and inspecting the best fit between observed and modeled tidal ranges in a fixed point of the bay's interior
Hydrodynamic simulations[a]	Tides and winds	ST + northeasterly winds ST + southeast wind ST + "Nortes" (N-NW)	8	ST plus real winds. Wind data uniformly distributed across the model domain. Water level specified at the open boundary was a reconstructed time series from local tidal constituents recorded 60 km north of BA[b]

[a]First 24 h from startup (2 semi-diurnal cycles) were removed due to stability reasons.
[b]Kjerfve 1981.

Peninsula. It is thought that by keeping a standard simulation time, the comparison of model results obtained along distinct cases would be more duly accomplished. The tidal cycles were centered at the midpoint of each 8 d simulation run. The scenarios modeled are summarized in Table 3.

Turnover Time

The turnover time (T_t) was calculated using the rate of water exchange provided by a variety of combined scenarios: spring tides (ST) plus three typical wind events experienced in the region ("suestes", SE; trade winds, NE; "nortes", N—NW). For this purpose, the total time integral of hydrodynamic flows (e.g., the output of the Delft model "instantaneous water discharge" given in m^3/sec) through the bay—shelf boundary at both inlets (north and south entrances; Figure 1b) during one day were computed for each of the combined boundary conditions simulated (Q), and then the volume of the system (V; assumed to be constant during the simulation time and completely mixed on a time scale shorter than the turnover time; Kjerfve and Magill 1989) was divided by the integrated rate of water exchange between the bay and the ocean. T_t is given in days:

Eq. (3) $$T_t = V/Q$$

Results

The relative impact exerted by the assessed forcing functions on Bahia de la Ascension circulation is a consequence of the spatial and temporal scales under scope and the local geomorphologic features across the bay. Thus, the tidal energy input leads to strong instantaneous currents in the inlet areas and near the channel connecting the main bay with the southwestern embayment (Vigia Grande). Furthermore, sub—tidal events (e.g., Trade northeasterlies) drove a large residual, ocean—directed flow in the bay.

Instantaneous Currents

The instantaneous currents observed in BA when tidal input is the only forcing showed a seaward water motion under ebb tide through both inlets, yet stronger currents and a smoother water level transition zone were evident across the north entrance during ebbing compared to the southern inlet (Figure 6A). Also, swift currents occurred at the southern subsystems indicated a rapid emptying of these inner embayments. During low water, relatively slow incoming water masses observed in the inlets contrasted with strong water motion crossing from the SW subsystem Vigia Grande to the main bay. The contact between these opposite—directed currents defined a slight frontal zone along the mid—bay (Figure 6B).

The currents in flood tide indicated water inflow in the inlet zones that extends farther into the bay, although current velocities rapidly decelerated once they reached the central basin. Also, two contrary instantaneous currents coexisted in the channel connecting Vigia Grande and the main bay, with water flowing seaward in the northern portion of the channel and landward water motion occurring across the southern portion of this entrance (Figure 6C). A relatively strong landward current velocity replaced this lateral flow structure further during high water (Figure 6D).

When southeasterly winds were included into the model during the ebbing case, a similar pattern in terms of current direction to the ebb tide alone case was found (Figure 7A). However, the relative magnitude of instantaneous water motion is dampened at the inlets and in the south and southwest inner embayments compared to currents in the central basin, which remain almost unaffected. This variation is particularly evident in the Vigia Grande subsystem, where reduced water outflow led to a steeper water level gradient towards the landward side of the channel compared to the tides stand—alone scenario (Figures 6A and 7A). The phase

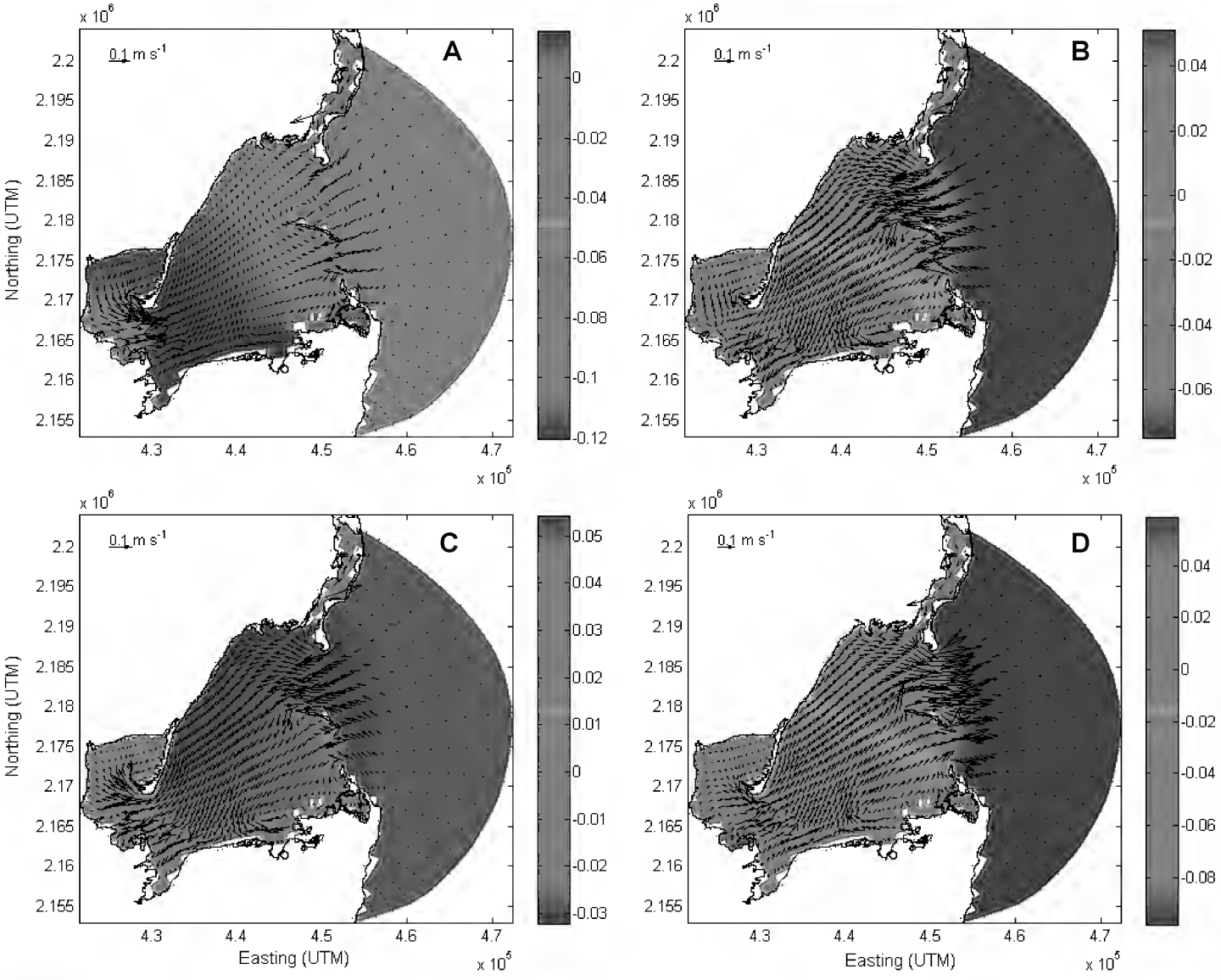

FIGURE 6. Instantaneous water level (m; vertical color bar to the right of the figure) and currents (depth averaged velocity, m/s; vectors) when the model is forced only with tides during 4 instantaneous tidal phases. A. Ebb tide. B. Low tide. C. Flood tide. D. High tide.

shift in the Vigia Grande embayment (Figure 8) reflects the attenuation of the tidal wave as it propagates from the central basin (3 m mean depth) to the shallow inner bay water column (mean depth of 0.5 m).

The circulation under "Nortes" and flood tide is similar to the lack of winds flooding scenario, although current velocities are diminished overall throughout the system, except for the northern section of the bay. The Trade winds plus spring tides case showed an intense flow emptying the SW inner embayment (e.g., towards the central bay) under low tide. During the flood tide plus Trades combined case, water motion is also comparable to the stand–alone tides scenario, with an overall even distribution of the water current velocities throughout the bay (Figures 7C and 7D).

Residual Currents

The tide averaged currents over 14 semidiurnal cycles (*i.e.*, first day removed from the 8 d simulation run for numerical stability) simulated under the effect of astronomical tides alone showed incoming flow along "Cayo Culebras" mangrove cay (CC) in the inlet zone, with strong flow in the western tip of the cay (Figure 9A). Because of the tidal energy dampening just past the channel into the VG embayment (Figure 8), the net tidal flow in the VG embayment is minor and limited to the channel between this inner subsystem and the central basin (Figure 9A).

The circulation pattern occurring under southeasterly winds plus spring tides resulted in a predominantly northward residual flow parallel to the reef barrier (mean velocity of 0.04 ± 0.02 SD m/s and 0.12 m/s maxima), which caused a bay–directed transport through the south inlet (Figure 9B). Pervasive SE wind sustained a clockwise cell (radius ≈ 5 km) flowing in the southern portion of the central basin, in front of the connecting channel with the SW embayment Vigia Grande (Figure 9B).

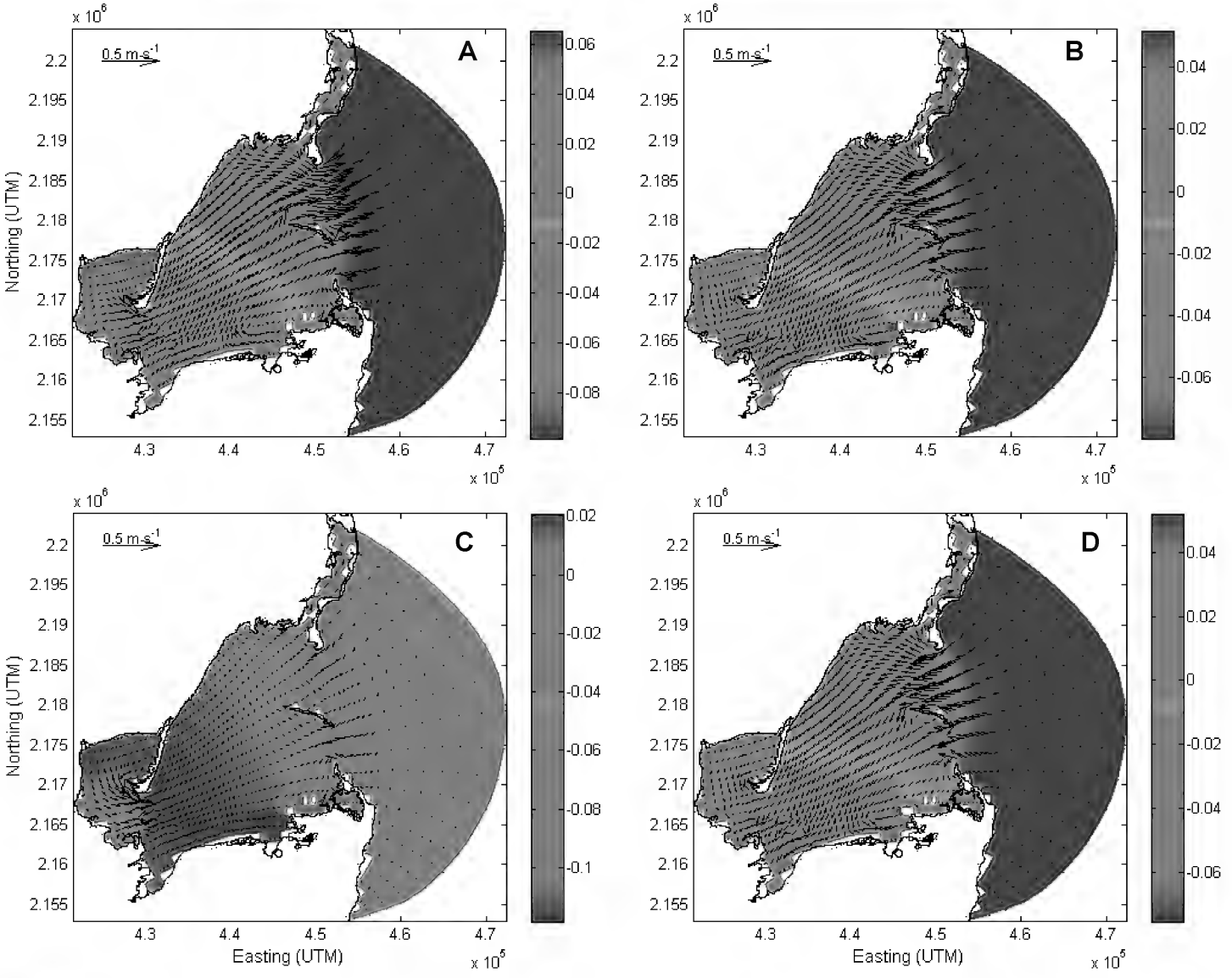

FIGURE 7. Instantaneous water level (m; vertical color bar to the right of the figure) and currents (depth averaged velocity, m/s; vectors) when the model is forced with tides plus winds. A. Southeast winds in ebb tide. B. "Nortes" winds in flood tide. C. Trade winds in low tide. D. Trade winds in flood tide.

The simulation results obtained with the combined NW–N wind field (i.e., "Nortes") and spring tide forcing exhibited an active alongshore and southward water transport with peak current velocity of 0.03 m/s. The water exited the system through the north entrance. Also, an anticlockwise cell circulation was observed close to the one occurring under SE winds (Figure 9C).

During the Trade wind event, a prevalent southward coastal flow with peak current velocity of nearly 0.05 m/s was observed. The residual current field showed a series of strong currents radiating from the CC cay towards the NW (0.013 m/s), W (0.012 m/s), and SE (0.03 m/s). Trade winds (NE) generated an average current velocity of 0.005 ± 0.003 SD m/s within the bay. A clockwise cell of shorter length scale than those established under SE and NW–N winds took place in the southeast portion of the central basin (Figure 9D). Maximum southeasterly wind–induced currents were only one half of that observed in the Trade winds case.

Both time averaged circulations involving eastern compo-

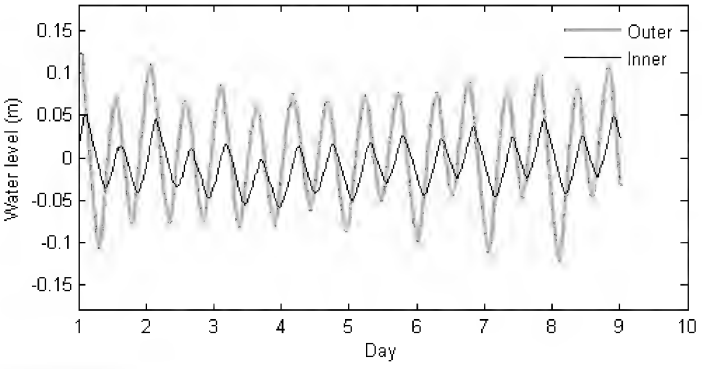

FIGURE 8. Modeled water level obtained in both sides of the channel connecting Vigia Grande embayment (Inner) with the bay's central basin (Outer) under spring tides-southeast winds combined scenario (such conditions are akin to those observed during the June survey).

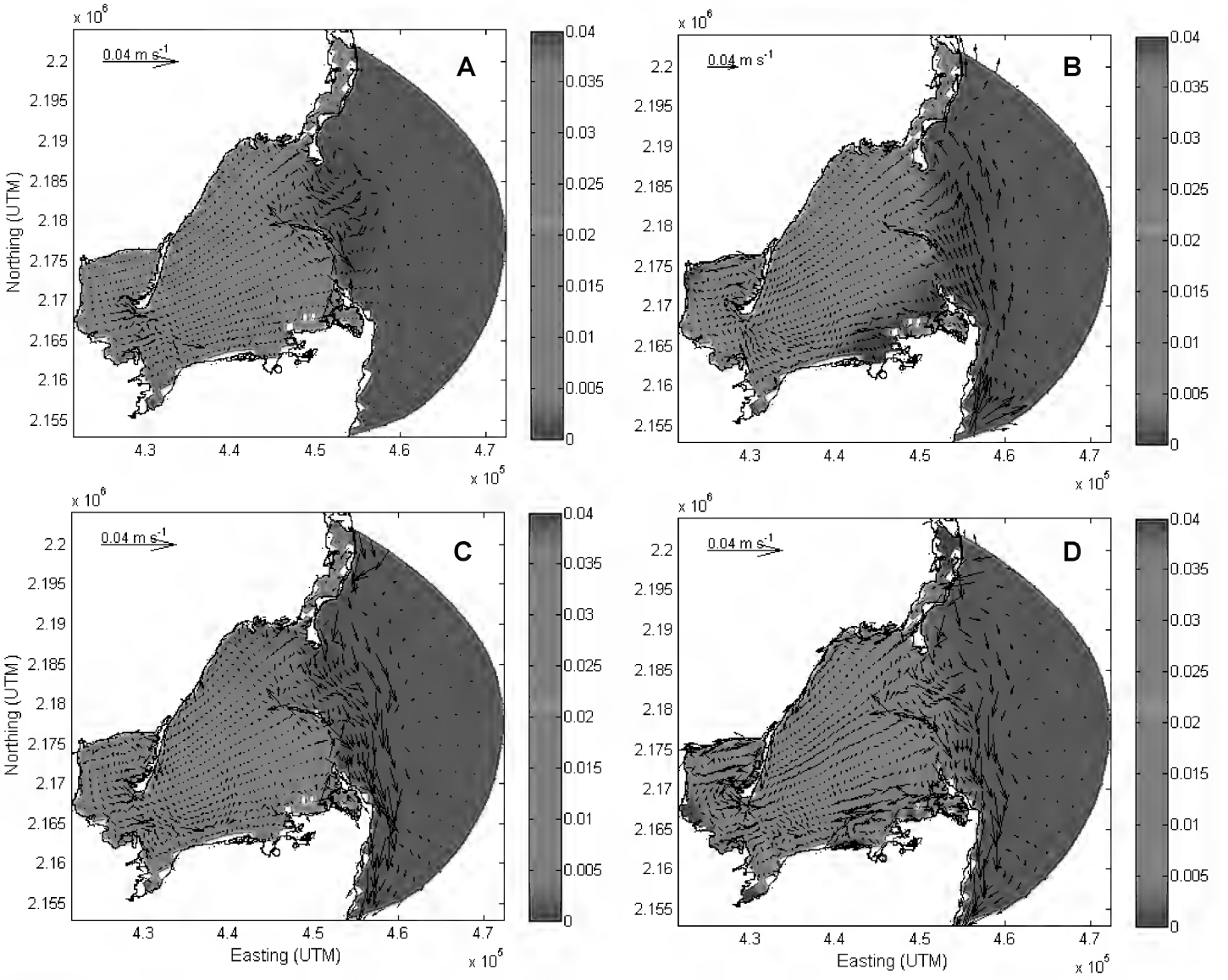

FIGURE 9. Four scenarios of 7 d average water level (m; vertical color bar to the right of the figure) and residual currents (depth averaged velocity, m/s; vectors). A. Tides alone. B. Tides plus southeast wind. C. Tides plus "Nortes" event. D. Tides plus Trade winds.

nent winds (SE wind and NE Trades combined with spring tides) induced a ≈3.5 cm water level increase in the inner–most bay. However, the water level gradient simulated under the Trade winds case showed a smoother spatial distribution along the NE–SW plane of the system than that defined by the southeasterly forcing winds (Figures 9B and 9D). The time–varying water level response within VG embayment during Trade Winds simulation exhibited a water column elevation spanning ≈ 6 hours (Figure 10).

Turnover Time

The turnover times (T_t) showed a pattern seemingly associated with the wind direction, with a mean T_t of 1.5 months for the simulated scenarios. Longer T_t in the whole bay corresponded to the spring tide (ST) stand–alone forcing, as well as under the ST plus "Nortes" event, whilst northeasterly winds (Trades) acting over the BA area drove high water volumes flushing out from the system. For instance, NE Trade winds were responsible for carrying away 387 m^3/d from the system, or nearly 6% more water than either the ST stand–alone forcing or the ST–Nortes combined simulations. As a consequence, Trade winds induced the shortest T_t of the

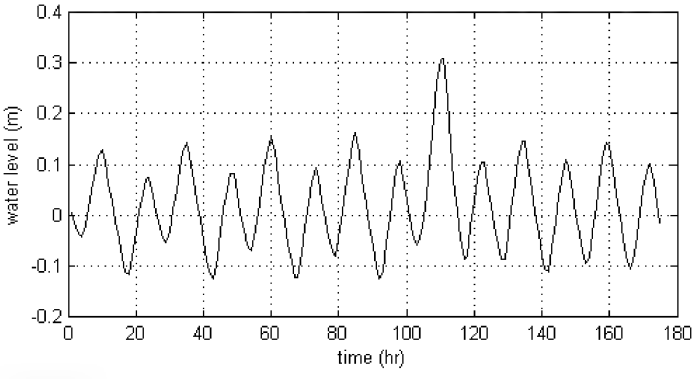

FIGURE 10. Time varying water level (m) in the inner-most bay (Vigia Grande subsystem) during Trade winds simulation.

study (≈42 days), which is 3 days shorter than any other simulated scenario.

Discussion

The simulation of the water circulation in Bahia de la Ascension under the dynamic forcing of tides and 3 typical wind conditions occurring in the Mexican Caribbean showed that, despite a microtidal regime characterizing the area, tides influence the water transport across the inlets. Strong currents with peak velocity of 0.25 m/s corresponded to the northern entrance near the seaward endpoint of the "Cayo Culebras" mangrove cay during spring tides. Nevertheless, tidally—driven effects are mostly confined to the inlet zone and partially across the main bay, as tidal currents substantially decelerate in the upper reaches of the central basin.

Wind stress alters the tidally—driven water movement in BA, as hydraulic flows often defined parallel trajectories to those of winds acting upon the system. The wind influence was more vividly illustrated at the inner—most bay (Vigia Grande embayment) when the model is forced with NE winds. The regional climatologic forcing may represent a main driver of the replenishing time of water in this inner section of the bay. Such a water exchange may be enhanced by the wind—driven setup in the northwest portion of the VG embayment (see Figure 10). However, this modeled water setup induced by the Trade winds is still lower than the 18 cm water level slope reported by Medina—Gomez et al. (2014a) in the inner bay during 5 days of sustained southeasterly winds.

The circulation—constrained SW embayment is the receiving water body of substantial freshwater and abundant materials (e.g., nutrients, dissolved organic matter) draining low—lying, well—developed mangrove forests (Medina—Gómez et al. 2014a). It seems feasible that, due to tidal energy attenuation in the inner bay (see Figure 8), a variable extent of isolation between this inner section and the main bay would occur, unless there is a mechanism controlling the water motion. The easterlies and particularly, the Trade winds, may represent such a wind—driven propagation mechanism of water properties farther into the sea—influenced central basin.

The potential of Trade winds to play a prominent role in the water transport from the bay's interior to the main bay steams from the fact that northeasterly winds act over the bay's surface in the same direction as the system's main axis (i.e., NE—SW), optimizing its forcing effect over the bay's surface and thus, on the water level field. However, this scenario might reduce, at some point, water transport from the main bay into VG during episodes of sustained NE winds, unless a return flow mechanism (e.g., through the bottom layer) is established to maintain a water exchange with the central basin (Kjerfve and Oliveira 2004). Consequently, the water level rise observed in the landward edge of VG (see Figure 9d) might be adjusted through an upwind—directed flow established at depth (Kjerfve and Magill 1989).

It is thought that, in combination with mid—term hydrometeorological process controlling the net freshwater input (Thattai et al. 2003), Trade winds would help to regulate the confinement degree in the inner—most bay and favor the connection between this mesohaline area and the central basin, as well as to spread the hydrographic properties characterizing the southwestern—most subsystem (i.e., Vigia Grande embayment) farther into the bay during episodes of persistent NE winds. If true, this wind—enhanced hydrodynamic feature has the potential to not only alter a number of physical—environmental traits in the whole system, such as thermohaline characteristics in the water column and heat fluxes, but also would lessen the average turnover time in the bay, thus contributing to avoidance of environmental impairment often experienced in locations with constrained circulation (Cavalcante et al. 2012).

The model results indicated that the *Nortes* wind (i.e., N—NW) does not play as relevant a role in the circulation pattern of this bay as in coastal ecosystems of the Yucatan north coast. The northern polar cold—fronts constitute dominant hydrometeorological processes in the northern Yucatan, inducing a remarkable marine influence on its ecosystems and longer water residence times during the winter season which features such events (Medina—Gómez and Herrera—Silveira 2009). Because *Nortes* winds show a trajectory "from the continent" in Bahia de la Ascension instead of "from the ocean" as in the Yucatan north coast, the geographic location of the bay contributes to relieving the potential effects of these events over the system.

The turnover time (T_t) during *Nortes* winds is consistent with a lessened influence on the system hydrodynamics under these events, as nearly the same T_t were calculated both under stand—alone spring tides and *Nortes* plus spring tides scenarios. Also, the mean T_t of 1.5 months calculated in this study is well below the range of previous seasonal turnover time estimations (203—1,525 days in rainy and dry seasons, respectively) carried out in BA using bulk hydro—meteorological information (Medina—Gómez et al. 2014a).

These ample differences between T_t reported elsewhere and that obtained in the current numerical study may reflect an intrinsic methodological variation due to distinct approaches utilized. The water flows of empirical—based Schreiber models (e.g., groundwater discharge, evapotranspiration) used to compute the turnover time (freshwater fraction method) by Medina—Gómez et al. (2014a) occurs at larger time—scales (e.g., seasonal) than both the unidirectional (advective) and three—dimensional (diffusive) water motion (e.g., within hours) accounted for in the processes implemented in this hydrodynamic model (Delft3D).

However, T_t values in BA were much higher than the aver-

TABLE 4. *Geomorphologic and water budget features in four coastal lagoons along the Mexican Caribbean and the Gulf of Mexico (northern and southern regions).*

System	Area (km^2)	Volume ($x\ 10^6\ m^3$)	Depth (m)	Tidal Range (m)	Freshwater Discharge ($x10^6\ m^3/yr$)	Turnover Time (days)
Lake Pontchartrain[a]	1,630	6,031	3.7	0.1	5,929	20-105
Terminos Lagoon[b]	2,500	8,750	3.5	0.4	12,600	67
Puerto Morelos (reef lagoon)	7.5	8[c]	3[c]	0.17[c]	60.2[d]	0.125[c]
Bahia de la Ascension[e]	580	1,422	2.2	0.18	870	45

[a]Kjerfve 1986.

[b]David 1999.

[c]Coronado et al. 2007.

[d]Estimated as fresh groundwater discharge (GD) using the figure provided by Hanshaw and Back (1980) for mean GD in the eastern Yucatan Peninsula equal to 8.6 x106 m3 per year per kilometer of coastline.

[e]Medina et al. 2014a. Except for the turnover time which was computed from the hydrodynamic simulations results in the current study.

age T_t value of 3 h reported for Puerto Morelos reef lagoon (PMRL), located 130 km northward from this study site (Coronado et al. 2007). The PMRL estimation corresponded to typical wave–wind conditions and background current velocity. In addition to striking geomorphologic differences between BA (juxtaposition of a wide, relatively deep and open central basin and a shallow, inner, confined subsystem in the SW extreme, with a well–developed fringing mangrove forest) and PMRL (a relatively shallow reef lagoon bounded by an almost continuous reef barrier seaward and shore coastline landward), PMRL drains relatively higher volumes from a much smaller system (volume of 8 $x10^6$ m^3 with a system transport equal to 986 m^3/s; Coronado et al. 2007) than Bahia de la Ascension (volume of 1,422 $x10^6$ m^3 and system transport of 370 m^3/s; Table 4).

The interplay between such geomorphologic water balance traits may explain the relatively high short–term sensitivity of turnover times in PMRL to a hurricane (T_t = 0.35 h, more than 8 times shorter than the average T_t under a regular physical setting; Coronado et al. 2007) compared to both seasonal (Medina–Gómez et al. 2014a) and climatologic event–driven flushing rates observed in BA. In addition to the previously mentioned return flow, the flooding pattern over adjacent wetland vegetation in BA may also offset water level rise in the landward section of VG generated either by tidal or climatic forcing.

It is thought that because of the low–lying topography in the south and southwestern part of the bay (Adame et al. 2013), even small water level increases lead to the flooding of a vast area featuring an anastomosing network of tidal creeks and sloughs within the adjacent mangrove wetland (Hsu et al. 2013). This flooding regime of the neighboring ecosystems may buffer the hydrodynamic coupling between inner and main bay, defining significant differences from other tropical coastal ecosystems, like in the reef lagoons, where hydrodynamic features are typically associated with both the complex geometry and bottom roughness of reef formations (Lambrechts et al. 2008, Taebi et al. 2011).

Such a vegetation–modulated response adds to the overall system resilience by reducing the impact that strong storms, characteristic of this region (Boose et al. 2003), may exert on the hydrographic heterogeneity and habitat diversity in BA. Flushing times in Terminos Lagoon (David 1999) and Lake Pontchartrain (Kjerve 1986), two restricted lagoons in the Gulf of Mexico significantly larger than BA, exhibited comparable T_t values to BA, despite both aquatic ecosystems being fed by rivers, as opposed to the ground freshwater input in BA (Table 4).

The openness of BA not only controls how shelf sea processes are conveyed into the bay across the inlets, but may also influence the system's sensitivity to variations in the rate and magnitude of atmospheric processes (e.g., strong storms). For instance, homogeneous salinity in Lake Pontchartrain, a brackish system associated with the Mississippi River, reflects both the prominent freshwater input and relatively restricted hydraulic exchange (Kjerfve 1986). Strong salinity changes have been documented in Lake Pontchartrain after water diversion from the Mississippi River into this system to relieve high water levels in the New Orleans rivers following extremely high precipitation (Kjerfve 1986). In contrast, a consistent estuarine gradient was observed in BA throughout the year (seasonal salinity variation < 4), and this horizontal salinity structure was maintained < 2 months after a category 5 hurricane made landfall in the region (Medina–Gómez et al. 2014a). These contrasting patterns suggest a higher vulnerability of the riverine–influenced Lake Pontchartrain than in BA under high intensity events (e.g., hurricanes).

However, the gravitational circulation brought about by

the freshwater supply in the fluvial systems (e.g., inner estuaries) surrounding the landward margin of Terminos Lagoon (Medina–Gómez et al. 2014b) may account for the comparable turnover times between this system and BA, regardless of the significant differences in geomorphologic features between both lagoons (Table 4). The marked seasonal pattern of net freshwater input may exert a mid–term control on the thermohaline circulation of the bay, particularly during the moment of wind–direction change and at the onset of neap tides.

Although only a weak vertical structure has been reported in the deepest, northern inlet of BA (Medina–Gómez et al. 2014a), this stratified water mass was recorded adjacent to the northern "Punta Allen" headland, a zone which might be characterized by improved turbulence due to jet and eddy formation (Lambrechts et al. 2008). Because a variety of hydrodynamic structures may prevent vertical stratification in that area, the mere presence of such a stratification of the water column suggests that it might actually represent a more common feature than previously considered (Medina–Gómez et al. 2014a).

It is argued that physical connectivity along the whole bay and coupling between the system and the reef barrier are influenced by processes occurring over distinct time–scales, from periodic tidal oscillations to sub–tidal variability associated with wind–field forcing and atmospheric systems (Cowen et al. 2006). The ecological processes within the system may respond to such a range of astronomical and meteorological forcing, where wind stress is a major controlling factor for fish larval habitat and thus, their variability in abundance and distribution (Chiappa–Carrara et al. 2003). Furthermore, released eggs from fish spawning aggregations are prone to enter these shallow coastal systems through wind–driven flow from reproductive sites offshore (Méndez–Jiménez et al. 2015).

Additionally, far–field forcing on coastal circulation may introduce variability in the water flow of the bay and extent of exchange with the adjacent shelf sea. The system's water level responses to the near–geostrophic nature of the coastal Yucatan current (YC; Ezer et al. 2005) may influence its flushing characteristics, since the occurrence of anticyclonic eddies detached from the YC induce a barotropic pressure gradient associated with a decrease of the bay's water level and subsequent net volume displacement. Thus, under strengthened YC episodes the appearance of mesoscale eddies and their tendency to propagate into the western Caribbean Sea (i.e., getting closer to the Caribbean coastline) may couple offshore oceanographic features with ecological traits in Bahia de la Ascension by altering the flushing rates of both biologically significant particles and potentially deleterious materials (trace metals).

The presence of recurrent mesoscale oceanographic features characterizing the regional circulation pattern (e.g., Ascension–Cozumel coastal eddy; Carrillo et al. 2015) influences the residence time of particles in front of the bay (e.g., entrainment during flooding of a portion of the water mass previously carried out from the system in the last ebb tide). Thus, the dispersion of bay–directed materials might be tied to the spatial–temporal variability of this cyclonic eddy, and its persistence may induce a longer retention of outwelled materials within the gyre before they are advected offshore or more likely, northward, according to observations on the regional circulation into the coastal flow (Carrillo et al. 2015).

Finally, the current model results not only allow a better understanding of the patterns of water movement within relatively small coastal systems indented along the MBRS, but would also, if implemented as a nested model, help to improve the grasp of regional circulation by complementing information provided in mesoscale hydrodynamic studies (Ezer et al. 2005; Carillo et al. 2015). Such a nested model approach will help to examine the role of these productive ecosystems as either buffers or a source of land–derived materials to a broader area in the MBRS. This understanding is crucial to address the threat level that such inputs represent for the health of coral reef formations and the biological communities they harbor.

Conclusions

This hydrodynamic model proved to be an appropriate tool to evaluate the circulation patterns of Bahia de la Ascension under the influence of tides and winds. Tide is an important forcing function controlling the hydrodynamics of this system, as tidal phase alters both instantaneous and time–average flow in the inlet zone and the bay's central basin. Also, Trade winds acting along the northeast–southwest main–axis of the bay enhance the ocean–directed water circulation from the system's interior.

The tidally–averaged circulation is relevant for the bay's spatial heterogeneity, as it favors water exchange between the freshwater–influenced area and the marine–influenced main bay. The wind action strongly alters water exchange in BA, and the geographic orientation of the Bay aligned with the system's main axis is crucial to sustain a significant discharge through the system. The instantaneous current velocities are higher in the deeper north inlet than in the southern one, while tidally–averaged circulation showed water inflow through the latter and outflow through the north entrance.

The turnover times (T_t) in the system reflected such residual flow scenarios. The T_t length showed a correlation with the geographic orientation of the wind field, featuring shorter T_t under northeasterly winds than in north winds occurring during winter storms (*Nortes*). The influence of Trade winds constitutes a major driving force on the circulation of an embayment placed in the inner–most bay subsystem.

Acknowledgments

The authors extend their appreciation to J. Ramírez and J. Caamal of the "Primary Production" Laboratory in CINVESTAV–Unidad Mérida for their eager assistance during the field campaigns. The Nature Conservancy (TNC) and the board and staff of Reserva de la Biósfera de Sian Ka'an (National Commission of Natural Protected Areas: CONANP) provided the funds and logistics to carry out the field surveys during this study.

Literature Cited

Adame, M.F., J.B. Kauffman, I. Medina, J.N. Gamboa, O. Torres, J.P. Caamal, M. Reza, and J. Herrera–Silveira. 2013. Carbon stocks of tropical coastal wetlands within the karstic landscape of the Mexican Caribbean. PLoS ONE 8:e56569. doi:10.1371/journal.pone.0056569

Boose, E.R., D.R. Foster, A. Barker–Plotkin, and B. Hall. 2003. Geographical and historical variation in hurricanes across the Yucatan Peninsula. In: A. Gómez–Pompa, M.F. Allen, S.L. Fedick, and J.J Jiménez, eds. Lowland Maya Area: Three Millennia at the Human–Wildland Interface. Haworth Press, New York, NY, USA, p. 495–516.

Brown, C.A., S.A. Holt, G.A. Jackson, D.A. Brooks, and G.H. Holt. 2004. Simulating larval supply to estuarine nursery areas: how important are physical processes to the supply of larvae to the Aransas Pass Inlet. Fisheries Oceanography 13:181–196.

Carrillo, L., E.M. Johns, R.H. Smith, J.T. Lamkin, and J.L. Largier. 2015. Pathways and Hydrography in the Mesoamerican Barrier Reef System Part 1: Circulation. Continental Shelf Research 109:164–176. doi:10.1016/j.csr.2015.09.014.

Cavalcante, G.H., B. Kjerfve, D.A. Feary, A.G. Bauman, and P. Usseglio. 2011. Water currents and water budget in a coastal megastructure, Palm Jumeirah Lagoon, Dubai, UAE. Journal of Coastal Research 27:384–393.

Cavalcante, G.H., B. Kjerfve, and D.A. Feary. 2012. Examination of residence time and its relevance to water quality within a coastal mega–structure: The Palm Jumeirah Lagoon. Journal of Hydrology 468–469:111–119. doi:10.1016/j.jhydrol.2012.08.027.

Cetina, P., J. Candela, J. Sheinbaum, J. Ochoa, and A. Badan. 2006. Circulation along the Mexican Caribbean coast. Journal of Geophysical Research 111:1–19. doi:10.1029/2005JC003056.

Chiappa–Carrara, X., L. Sanvicente–Añorve, A. Monreal–Gómez, D. Salas De León. 2003. Ichthyoplankton distribution as an indicator of hydrodynamic conditions of a lagoon system in the Mexican Caribbean. Journal of Plankton Research 25:687–696.

Coronado, C., J. Candela, R. Iglesias–Prieto, J. Sheinbaum, M. López, and F.J. Ocampo–Torres. 2007. On the circulation in the Puerto Morelos fringing reef lagoon. Coral Reefs 26:149–163. doi:10.1007/s00338–006–0175–9.

Cowen, R.K., C.B. Paris, and A. Srinivasan. 2006. Scaling of population connectivity in marine populations. Science 311:522–527. doi:10.1126/science.1122039.

David, L.T. 1999. LOICZ budget in Laguna de Terminos, Campeche. In: S.V. Smith, J.I. Marshall, and C.J. Crossland, eds. Mexican and Central American Coastal Lagoon Systems: Carbon, Nitrogen and Phosphorus Fluxes (Regional Workshop II), LOICZ Reports & Studies No. 13, LOICZ IPO, Texel, The Netherlands, p. 9–15.

David, L.T. and B. Kjerfve. 1998. Tides and currents in a two–inlet coastal lagoon: Laguna de Terminos, Mexico. Continental Shelf Research 18:1057–1079.

Dawson, F.H. and W.N. Robinson. 1984. Submersed macrophytes and the hydraulic roughness of a lowland chalkstream. Verhandlungen Internationale Vereinigung für Theoretische und Angewandte Limnologie 22:1944–1948.

Delft3D–FLOW. 2014. Simulation of multi–dimensional hydrodynamic flows and transport phenomena, including sediments; User Manual, Version 3.15.34158. WL|Delft Hydraulics. Deltares; Delft, The Netherlands. http://www.deltares.nl.

Drew, E.A. 2000. Ocean nutrients to sediment banks via tidal jets and *Halimeda* meadows. In: E. Wolanski, ed. Oceanographic Processes of Coral Reefs: Physical and Biological Links in the Great Barrier Reef. CRC Press, Boca Raton, FL, USA, p. 255–268.

Enriquez, C., I.J. Mariño–Tapia, and J.A. Herrera–Silveira. 2010. Dispersion in the Yucatan coastal zone: Implications for red tide events. Continental Shelf Research 30:127–137. doi:10.1016/j.csr.2009.10.005.

Ezer, T., D.V Thattai, B. Kjerfve, and W. Heyman. 2005. On the variability of the flow along the Meso–American Barrier System: a numerical model study of the influence of the Caribbean current and eddies. Ocean Dynamics 55:458–475. doi:10.1007/s10236–005–0033–2.

Fernandes, E.H.L., K.R. Dyer, and L.F.H. Niencheski. 2001. TELEMAC–2D calibration and validation to the hydrodynamics of the Patos Lagoon (Brazil). Journal of Coastal Research 34:470–488.

Geyer, W.R. 1997. Influence of wind on dynamics and flushing of shallow estuaries. Estuarine, Coastal, and Shelf Science 44:713–722.

Hanshaw, B.B. and W. Back. 1980. Chemical mass–wasting of the northern Yucatan Peninsula by groundwater dissolution. Geology 8:222–224.

Hench, J.L., J.J. Leichter, and S.G. Monismith. 2008. Episodic circulation and exchange in a wave–driven coral reef and lagoon system. Limnology and Oceanography 53:2681–2694. doi: 10.4319/lo.2008.53.6.2681.

Hsu, K., M.T. Stacey, and R.C. Holleman. 2013. Exchange between an estuary and an intertidal marsh and slough. Estuaries and Coasts 36:1137–1149. doi:10.1007/s12237–013–9631–2.

Kjerfve, B. 1981. Tides of the Caribbean Sea. Journal of Geophysical Research 86:4243–4247.

Kjerfve, B. 1986. Comparative oceanography of coastal lagoons. In: D.A. Wolfe, ed. Estuarine Variability. Academic Press, New York, NY, USA, p. 63–81.

Kjerfve, B., and K.E. Magill. 1989. Geographic and hydrodynamic characteristics of shallow coastal lagoons. Marine Geology 88:187–199.

Kjerfve, B., and A.M. Oliveira. 2004. Modelling of circulation and water exchange in a hypersaline coastal lagoon: Lagoa de Araruama, Brazil. In: L. Drude de Lacerda, R.E. Santelli, E.K. Duursma, and J.J. Abrão, eds. Environmental Geochemistry in Tropical and Subtropical Environments. Springer Berlin Heidelberg, Germany, p. 235–251. doi: 10.1007/978–3–662–07060–4_18

Ladah, L., A. Filonov, M.F. Lavín, J.J. Leichter, J.A. Zertuche–González, and D.M. Pérez–Mayorga. 2012. Cross–shelf transport of sub–thermocline nitrate by the internal tide and rapid (3–6 h) incorporation by an inshore macroalage. Continental Shelf Research 42:10–19. doi:10.1016/j.csr.2012.03.010.

Lambrechts, J., E. Hanert, E. Deleersnijder, P.E. Bernard, V. Legat, J.F. Ramacle, and E. Wolanski. 2008. A multi–scale model of the hydrodynamics of the whole Great Barrier Reef. Estuarine, Coastal, and Shelf Science 79:143–151. doi:10.1016/j.ecss.2008.03.016.

Meacham, S. 2007. Freshwater resources in the Yucatan Peninsula. In: L. Holliday, L. Marin, and H. Vaux, eds. Sustainable Management of Groundwater in Mexico. The National Academies Press, Washington D.C., USA, p. 6–12.

Medina–Gómez, I. 2011. Characterization of a karst coastal ecosystem in the Mexican Caribbean: assessing the influence of coastal hydrodynamics and submerged groundwater discharges on seagrass. Ph.D. thesis. Texas A&M University, College Station, TX, USA, 101p.

Medina–Gómez, I. and J.A. Herrera–Silveira. 2009. Seasonal responses of phytoplankton productivity to water–quality variations in a coastal karst ecosystem of the Yucatan Peninsula. Gulf of Mexico Science 27:39–51.

Medina–Gómez, I., B. Kjerfve, I. Marino–Tapia, and J.A. Herrera–Silveira. 2014a. Sources of salinity variation in a coastal lagoon in a karst landscape. Estuaries and Coasts 37:1329–1342. doi: 10.1007/s 12237–014–9774–9

Medina–Gómez, I., G. Villalobos, and J.A. Herrera–Silveira. 2014b. Spatial and temporal hydrological variations in the inner estuaries of a large coastal lagoon of the southern Gulf of Mexico. Journal of Coastal Research 31:1429–1438. doi: 10.2112/JCOASTRES–D–13–00226.1.

Méndez–Jiménez, A., W.D. Heyman, and S.F. DiMarco. 2015. Surface drifter movement indicates onshore egg transport from a reef fish spawning aggregation. Physical Geography 36:353–366. doi: 10.1080/02723646.2015.1023243

Morin, J., M. Leclerc, Y. Secretan, and P. Boudreau. 2000. Integrated two–dimensional macrophytes–hydrodynamic modeling. Journal of Hydraulic Research 38:163–172.

Murphy, A. 1988. Skill scores based on the mean square error and their relationships to the correlation coefficient. Monthly Weather Review 116:2417–2424.

Nixon, S.W. 1988. Physical energy inputs and the comparative ecology of lake and marine ecosystems. Limnology and Oceanography 33:1005–1025.

Pawlowicz, R., B. Beardsley, and S. Lentz. 2002. Classical tidal harmonic analysis including error estimates in MATLAB using T_TIDE. Computers and Geosciences 28:929–937.

SMN, 2007. Servicio Meteorológico Nacional de México (Datos históricos EMAs). http://smn.cna.gob.mx/productos/emas/emas.html. (Viewed on 11/11/2011).

Sousa, M.C. and J.M. Dias. 2007. Hydrodynamic model calibration for a mesotidal lagoon: the case of Ria de Aveiro (Portugal). Proceedings of the 9th International Coastal Symposium. Journal of Coastal Research, Special Issue No. 50:1075–1080.

Staneva, J.V. and E.V. Stanev. 1998. Oceanic response to atmospheric forcing derived from different climatic data sets. Intercomparison study for the Black Sea. Oceanologica Acta 21:393–417.

Sutherland, J., D.J.R. Walstra, T.J. Chesher, L.C. van Rijn, and H.N. Southgate. 2004. Evaluation of coastal area modelling systems at an estuary mouth. Coastal Engineering 51:119–142. doi:10.1016/j.coastaleng.2003.12.003.

Taebi, S., R.J. Lowe, C.B. Pattiaratchi, G.N. Ivey, G. Symonds, and R. Brinkman. 2011. Nearshore circulation in a tropical fringing reef system. Journal of Geophysical Research 116:C02016. doi:10.1029/2010JC006439.

Thattai, D., B. Kjerfve, and W.D. Heyman. 2003. Hydrometeorology and variability of water discharge and sediment load in the inner Gulf of Honduras, western Caribbean. Journal of Hydrometeorology 4:985–995. doi:10.1175/1525–7541(2003)004<0985:HAVOWD>2.0.CO;2.

Tilburg, C.E., S.M. Gill, S.I. Zeeman, A.E. Carlson, T.W. Arienti, J.A. Eickhorst, and P.O. Yund. 2011. Characteristics of a shallow river plume: observations from the Saco River Coastal Observing System. Estuaries and Coasts 34:785–799. doi:10.1007/s12237–011–9401–y

Umgiesser, G. and R. Neves. 2005. Physical processes. In: I.E. Gönec and J.P. Wolflin, eds. Coastal Lagoons: Ecosystem Processes and Modeling for Sustainable Use and Development. CRC Press, Boca Raton, FL, USA, p. 43–78.

Walstra, D.J.R., L.C. Van Rinj, H. Blogg, and M. Van Ormondt. 2001. Evaluation of a hydrodynamic area model based on the Coast3D Data at Teignmouth 1999. Proceedings of the Fourth Conference on Coastal Dynamics, Lund, Sweden, (11–15 June 2001), American Society of Civil Engineers, ISBN 0784405662, p. D4.1–D4.4.

Wolanski, E. 1994. Physical Oceanographic Processes of the Great Barrier Reef. CRC Press, Boca Raton, FL, USA, 194 p.

Gulf and Caribbean Research

Volume 27 | Issue 1

2016

Age, Growth and Natural Mortality of Blackfin Snapper *Lutjanus buccanella* from the Southeastern United States and U. S. Caribbean

Michael L. Burton
NOAA Southeast Fisheries Science Center, Beaufort Laboratory, michael.burton@noaa.gov

Jennifer C. Potts
NOAA Southeast Fisheries Science Center, Beaufort Laboratory, jennifer.potts@noaa.gov

Daniel R. Carr
Independent Affiliation

Gulf and Caribbean Research Vol 27, 66-73, 2016
DOI: 10.18785/gcr.2701.10

Manuscript received, May 11, 2016; accepted, November 22, 2016

AGE, GROWTH AND NATURAL MORTALITY OF BLACKFIN SNAPPER, *LUTJANUS BUCCANELLA*, FROM THE SOUTHEASTERN UNITED STATES AND U.S. CARIBBEAN.

Michael L. Burton[1*], Jennifer C. Potts[1], and Daniel R. Carr[2]
[1]National Marine Fisheries Service, Southeast Fisheries Science Center, 101 Pivers Island Rd., Beaufort NC 28516–9722; [2] 3103 Country Club Rd., Morehead City, NC 28557–3016; Corresponding author, email: michael.burton@noaa.gov

ABSTRACT: We determined ages of Blackfin Snapper (*Lutjanus buccanella* Cuvier 1828; *n* = 622) collected from the southeastern United States coast and U.S. Caribbean from 1979–2015 using sectioned sagittal otoliths. Opaque zones were determined to be annular, forming March – July (peaking in April–June). Blackfin Snapper ranged from 1–27 years and from 180–609 mm total length (TL). Body size relationships for Blackfin Snapper were: TL = 1.09 FL + 0.81 (n = 203, r^2 = 0.99); FL = 0.91 TL + 3.38 (n = 203, r^2 = 0.99); TL = 1.23 SL + 14.27 (n = 83, r^2 = 0.97); FL = 1.14 SL + 10.84 (n = 83, r^2 = 0.99); W = 7.79 x 10^{-9} $TL^{3.09}$ (n = 216); and W = 9.54 x 10^{-9} $FL^{3.11}$ (n = 228). The von Bertalanffy growth equation was: L_t = 549 (1 – $e^{-0.20\,(t\,+1.51)}$) (n = 622). Point estimate of natural mortality was *M* = 0.16, while age–specific estimates of *M* ranged from 0.65–0.21/y for ages 1–27. This study presents the first findings of life history parameters for Blackfin Snapper from the Atlantic waters off the southeastern United States and U.S. Caribbean.

KEYWORDS: Lutjanidae, Life history parameters, Fisheries management, Caribbean reef fish, data–limited species.

INTRODUCTION

Blackfin Snapper (*Lutjanus buccanella* Cuvier 1828, Family Lutjanidae) are found in the tropical western Atlantic and are capable of attaining weights of up to 14 kg but usually average < 4 kg (Grimes et al. 1977). The species is found from North Carolina throughout Bermuda and the Caribbean, including the Gulf of Mexico, and as far south as northeast Brazil (Cervigon 1966). Adults typically inhabit the continental shelf edge or live–bottom areas in depths from 9–219 m. Blackfin Snapper are of minor importance to the southeastern United States (SEUS, North Carolina to Florida Keys, including the Dry Tortugas) reef fish fishery but are more important to anglers in the U.S. Caribbean (Puerto Rico and the U.S. Virgin Islands). Estimated recreational landings of Blackfin Snapper in the SEUS averaged 1,006 kg from 1981–2014, while landings from the private/charter sector in Puerto Rico averaged 5,178 fish annually from 2000–2012 (T. Sminkey, unpublished data, NMFS, Silver Spring, MD). Commercial landings for the SEUS averaged 386 kg from 1982–2014 but were 22,750 kg annually from 2000–2014 for the U.S. Caribbean (D. Gloeckner, unpublished data, NMFS Southeast Fisheries Science Center (SEFSC), Miami, FL). Sylvester et al. (1980) reported that Blackfin Snapper was the second most commonly landed deepwater Snapper in the U.S. Virgin Islands, behind Silk Snapper (*Lutjanus vivanus*).

Blackfin Snapper is currently managed in the SEUS by the South Atlantic Fishery Management Council's Snapper–Grouper Fishery Management Plan (FMP; SAFMC 2015) with a 305 mm total length (TL, 12 inches) minimum size limit in both commercial and recreational fisheries and includes a 10 snapper per person per day bag limit (excluding Red Snapper, *Lutjanus campechanus*, and Vermilion Snapper, *Rhomboplites aurorubens)* in the recreational fishery. The species is managed in the U.S. Caribbean by the Caribbean Fishery Management Council's Reef Fish FMP with annual catch limits. The Magnuson–Stevens Fishery Conservation and Management Act requires that annual catch limits be set for all managed species (or species groups) in both the SEUS and U.S. Caribbean territories, despite the fact that many of these species may be data–poor (SERO 2015). Data–limited assessment methods currently in use require basic inputs such as natural mortality or growth parameters which, when combined with catch histories or size distributions, can be used to estimate fishery targets or limits. Even this rudimentary data is sparse or non–existent for many reef fish species in the SEUS and U.S. Caribbean, however.

We studied Blackfin Snapper from the SEUS in order to fill in data gaps in their life history in SEUS or U.S. Caribbean waters. While Claro and Lindeman (2008) published a thorough review of the biology of the family Lutjanidae from the tropical western Atlantic region, previous estimates of age–growth parameters or mortality rates of the species came from stocks outside the SEUS or U.S. Caribbean and were derived used methods other than sectioned sagittal otoliths (Thompson and Munro 1983: Jamaica, length frequency data; Espinoso and Pozo 1982: Cuba, urohyal bones). This study uses archived sagittal otolith samples collected over decades of sampling to provide the first estimates of life history parameters for Blackfin Snapper from the SEUS and U.S. Caribbean region, thereby filling in a significant data

gap and contributing to the proactive management of data–limited reef fish resources in the regions.

Materials and Methods

Age determination and timing of opaque zone formation

Blackfin Snapper (n = 505) were opportunistically obtained from fisheries landings by NMFS and state agencies' port agents sampling the recreational headboat and commercial fisheries along the SEUS coast from 1981–2015. Additional samples were collected by NMFS fishery–independent surveys from the waters of Puerto Rico and the U.S. Virgin Islands in 1979 and 2009 (n = 131). All fishery–dependent specimens were captured by conventional vertical hook and line or longline gear. Fishery–independent specimens were captured using vertical hook and line, bottom longline, or fish traps. Fork length (FL, mm) and/or TL (mm) of specimens were recorded from fishery–dependent and fishery–independent samples, and standard length (SL, mm) from fishery–independent samples. Whole weight (W, kg) was recorded for fish landed in the headboat fishery and from fishery–independent samples. Fish landed by commercial fisheries were eviscerated at sea, thus whole weights were not available. Sagittal otoliths were removed and stored dry in coin envelopes. Otoliths were mounted on glass microscope slides and sectioned using a diamond–edged wafering blade on a Buehler Isomet low speed saw following the methods of Potts and Manooch (1995). Three 0.5 mm sections were taken near the otolith core. The sections were mounted on microscope slides with thermal cement and covered with mounting medium before analysis. The sections were viewed under a dissecting microscope at 12.5X using reflected light. Each sample was assigned an opaque zone count by an experienced reader with extensive experience interpreting otolith sections (Burton 2001, 2002; Burton et al. 2012). Sections were read with no knowledge of date of capture or fish size. A randomly chosen subset of otoliths (n = 142; 23% of all otoliths) was then read by a second experienced reader and an index of average percent error (APE) was calculated following Beamish and Fournier (1981).

Timing of opaque zone formation was assessed using edge analysis. The edge type of the otolith was noted: 1 = opaque zone forming on the edge of the otolith section; 2 = narrow translucent zone on the edge, generally < 30% of the width of the previous translucent zone; 3 = moderate translucent zone on the edge, generally 30% – 60% of the width of the previous translucent zone; 4 = wide translucent zone on the edge, generally > 60% of the width of the previous translucent zone (Harris et al. 2007). Based upon edge frequency analysis, all samples were assigned a calendar age, obtained by increasing the opaque zone count by one if the fish was caught before that year's opaque zone was formed and had an edge which was a moderate to wide translucent zone (type 3 or 4). Fish caught during the time of year of opaque zone formation with an edge type of 1 or 2, as well as fish caught after opaque zone formation, were assigned a calendar age equivalent to the opaque zone count. This adjustment to opaque zone counts functionally put each fish into its correct annual cohort. Finally, while Munro et al. (1973) suggested that peak spawning of Blackfin Snapper occurred in April in Jamaica, Erdman (1976) and Boardman and Weiler (1980) reported that Blackfin Snapper spawned year–round in Puerto Rico. Therefore, we decided not to adjust the age of the fish for the time of year caught (fractional age) due to the lack of a specific discrete birth month.

Growth

Von Bertalanffy (1938) growth parameters were estimated from the observed length at calendar age data using SAS PROC NLIN, a nonlinear regression procedure using the Marquardt iterative algorithm (SAS Institute, Inc. 1987). We anticipated there would be few fish of the youngest age classes available to us, as hook–and–line gear or fishers generally selected for larger fish, and because the SAFMC size limit since January 1992 of 305 mm TL may have excluded smaller fish from the landings. Consequently, the model would be unable to depict initial growth of the youngest fish, leading to difficulty in accurately estimating size at the youngest ages. We therefore re–ran the growth model using the method of McGarvey and Fowler (2002), which adjusts for the bias imposed by minimum size limits by assuming zero probability of capture below the minimum size limit. Size–at–age data were examined using analysis of variance (ANOVA) to determine if there were differences in total length–at–age by region (SEUS vs. U.S. Caribbean) and if pooling of data for estimation of growth curves was appropriate.

Body–Size Relationships

We examined the relationships between TL–W and FL–W for Blackfin Snapper for fish collected from the headboat fishery and the fishery–independent samples with non–linear regression and examining the residuals to determine if a ln–ln transformation of the data was appropriate. Samples from commercial fisheries were eviscerated at sea and thus weights were not available. We also examined the linear relationships between FL–TL and TL–FL (n = 203) and FL–SL and TL–SL (n = 83).

Natural Mortality

We estimated the instantaneous rate of natural mortality (M) using two methods:

(1) Hewitt and Hoenig's (2005) longevity mortality relationship, $M = 4.22/t_{max}$, where t_{max} is the maximum age of the fish in the sample, and

(2) Charnov et al.'s (2013) method using life history

parameters, $M_A = (L_A/L_\infty)^{-1.5} \times K$, where M_A is natural mortality at age A, L_∞ and K are the von Bertalanffy growth equation parameters and L_A is fish length at age A. We used the midpoint between integer ages (e.g., 0.5, 1.5, 2.5, etc.) to calculate age–specific M, because the Charnov et al. (2013) method cannot mathematically calculate M for age–0. Additionally, for stock assessment purposes where the integer age is used to describe the entire year of the fish's life, the mid–point gives the median value of M for that age.

The equation of Hewitt and Hoenig (2005) uses maximum age to generate a single point estimate of mortality. The Charnov et al. (2013) method, which incorporates life history information via the growth parameters, is based upon evidence suggesting that M decreases as a power function of body size. This method generates age–specific rates of M and has recently been used in the Southeast Data Assessment and Review (SEDAR) stock assessments (E. Williams, pers. comm., NMFS Beaufort Laboratory, Beaufort, NC).

There are many methods available with which to estimate natural mortality. We choose to use Charnov et al.'s M estimator function because the equation takes into account many aspects of life history strategies of many marine fish. We feel that Charnov's equation is the more appropriate model to use versus the equation of Lorenzen (1996) for 2 reasons. First, Lorenzen's method was developed using fish species from temperate regions almost exclusively and included lake, riverine and oceanic species and focused on body weight, but not other life history strategies. The fish in our study come primarily from a subtropical regime. Secondly, the Lorenzen equation used mean weight–at–age. Because many of our samples were from the commercial fishery where the weight of the fish was not available, there would have been more uncertainty in the mean weight–at–age compared to the mean length–at–age. Given the high correlation of weight to length, the using of mean length–at–age should not be any different than using the mean weight–at–age.

TABLE 1. *Number of samples of sagittal otoliths that were used for age and growth study of Blackfin Snapper (Lutjanus buccanella) collected from 1979–2015 from fisheries landings and fishery-independent sampling along the coast of the southeastern United States and the U.S. Caribbean. Samples were collected in the following states: North Carolina (NC), South Carolina (SC), and Florida (FL), Puerto Rico, and the U.S. Virgin Islands (Caribbean).*

State	Commercial	Recreational	Fishery-Independent
NC	230	1	0
SC	93	5	0
FL	45	117	0
Caribbean	0	2	129
TOTAL	368	125	129

Results

Age determination and timing of opaque zone formation

A total of 636 otoliths from Blackfin Snapper were sectioned (Table 1); the majority came from the North Carolina and South Carolina commercial fisheries (39% and 15%, respectively). Twenty–seven percent of Blackfin Snapper sampled were from Florida, with the majority of these coming from the recreational sector. Fishery–independent samples from the Caribbean accounted for 22% of all samples. Opaque zones were counted on 622 (98%) of Blackfin Snapper sections, as 14 samples were unreadable and excluded from the analysis.

We were able to assign an edge type to all samples for our analysis of opaque zone periodicity. Blackfin Snapper otoliths exhibited opaque zones on the margin from March–July, with peaks in April and June (Figure 1). A shift to a

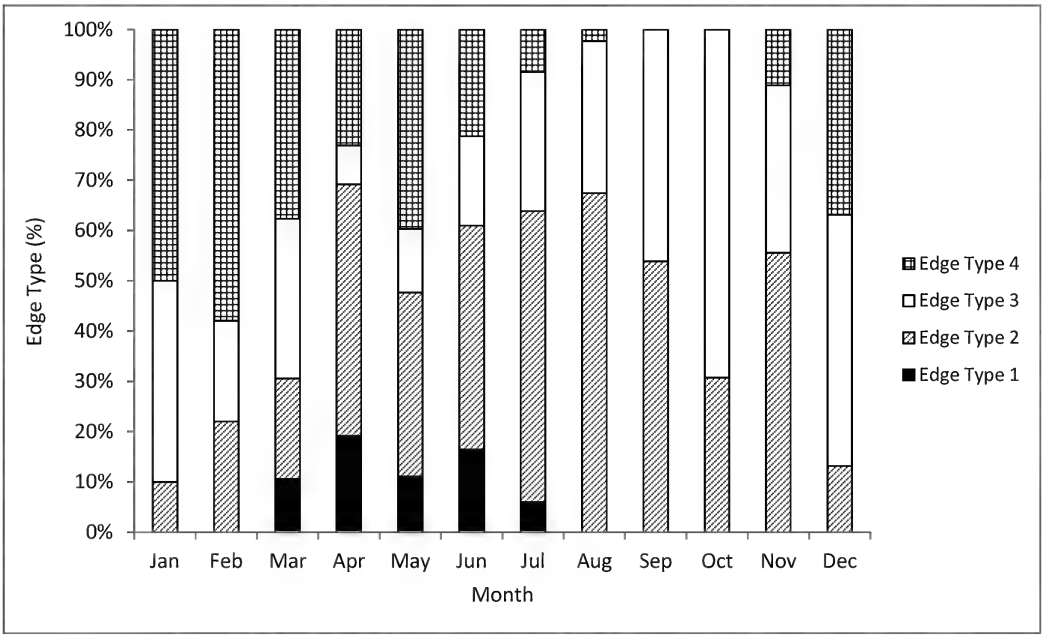

FIGURE 1. *Monthly percentages of all otolith edge types for Blackfin Snapper (Lutjanus buccanella) collected from the southeastern United States and U.S. Caribbean from 1979–2015. Edge type codes: 1=opaque zone on edge, indicating annulus formation; 2=small translucent zone, <30% of previous increment; 3=moderate translucent zone, 30–60% of previous increment; 4=wide translucent zone, >60% of previous increment.*

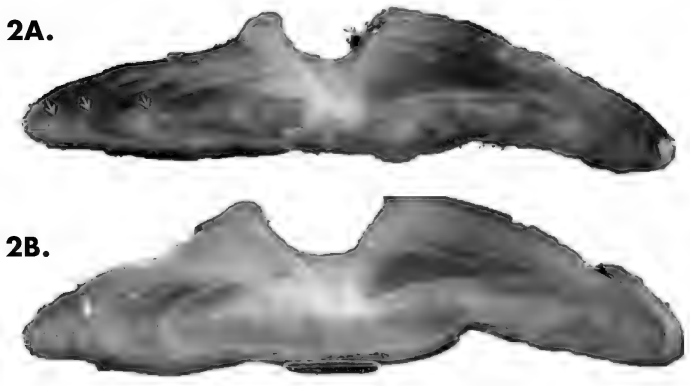

FIGURE 2. *Sections from sagittal otoliths of Blackfin Snapper (Lutjanus buccanella). A. 415 mm TL, age 3, edge-type 3; B. 425 mm, age 6, edge-type 2. Age was determined by counting opaque increments (indicated by arrows) along the ventral axis and sulcus using transmitted light at 12.5 X magnification. Brackets indicate marginal increment.*

narrow translucent edge was observed during July–September and November. Blackfin Snapper otoliths were without an opaque zone on the edge from August through February. Moderate to wide translucent edge was found December–March, and the widest translucent edge was found in February, prior to opaque zone formation beginning in March. We concluded that opaque zones in Blackfin Snapper otoliths formed annually. Finally, calendar ages were assigned as follows: for fish caught January through July and having an edge type of 3 or 4, the annuli count was increased by one; for fish caught in that same time period with an edge type of 1 or 2 and for fish caught from August to December, the calendar age was equivalent to the annuli count.

Blackfin Snapper sagittae (Figure 2) were clear and easy to interpret, resulting in an APE of 6.9% (n = 142) for opaque zone count agreement between the two readers. Direct agreement between readings was 55%, and this agreement increased to 97% when ± 1 year was used. An age bias plot indicates good agreement between readers for ages 1–15, with no apparent systematic tendency for the second reader to under– or overestimate ages in comparison with the first reader (Figure 3). The mean difference between readers for ages 1–27 was only 0.34 years. The largest difference between readers was 2 years.

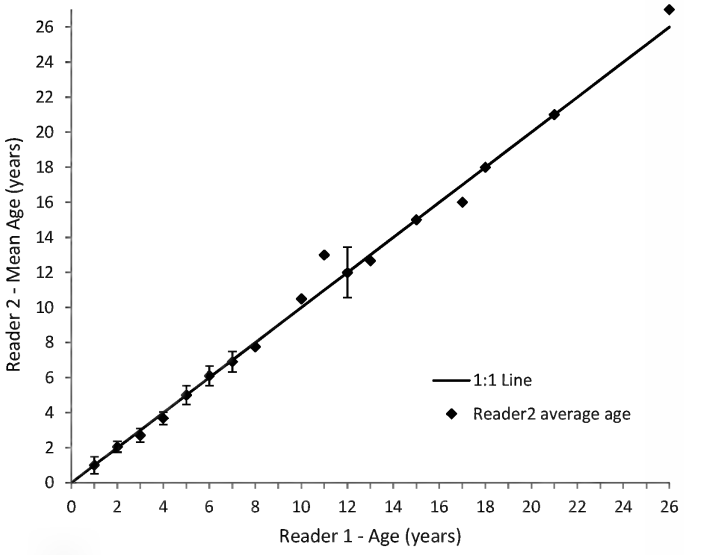

FIGURE 3. *Age bias plot for 143 Blackfin Snapper sampled from the southeastern United States from 1979–2015 and aged by 2 primary readers. The first reader's age estimates (X-axis) are plotted against the second reader's mean age estimates for the same-aged fish (Y-axis). Error bars are 95% confidence intervals.*

Growth

Blackfin Snapper in this study ranged from 180–609 mm TL and ages 1–27 but only 8 fish were estimated to be >15 years old (Table 2). ANOVA results show that mean TL–at–age was not significantly different by geographic re-

TABLE 2. *Observed and predicted mean total length (TL, mm) from the freely estimated growth model and natural mortality at age (M, Charnov et al. 2013) for Blackfin Snapper (Lutjanus buccanella) collected from 1979–2015 along the coast of the southeastern United States and U.S. Caribbean. Standard errors of the mean (SE) are provided in parentheses.*

				Predicted	
Age	**n**	**TL (mean ± SE)**	**TL range**	**TL**	**M/y**
1	1	237	-	217	0.65
2	70	285 (5)	180 - 389	277	0.49
3	152	326 (4)	211 - 448	327	0.40
4	113	372 (5)	249 - 492	367	0.34
5	85	405 (7)	245 - 497	400	0.31
6	69	439 (6)	292 - 524	427	0.28
7	33	473 (10)	335 - 609	449	0.27
8	44	460 (8)	293 - 568	467	0.25
9	15	455 (16)	304 - 565	482	0.24
10	9	478 (37)	296 - 600	494	0.23
11	9	518 (17)	398 - 561	504	0.23
12	5	538 (20)	465 - 577	512	0.22
13	4	475 (39)	382 - 565	519	0.22
14	2	485 (27)	459- 512	524	0.22
15	3	553 (35)	483 - 595	529	0.21
16	3	553 (11)	540 - 574	532	0.21
17	2	579 (14)	565 - 593	535	0.21
18	-	-	-	538	0.21
19	1	582	-	540	0.21
20	1	580	-	542	0.21
21	-	-	-	543	0.21
22	-	-	-	544	0.21
23	-	-	-	545	0.21
24	-	-	-	546	0.21
25	-	-	-	546	0.21
26	-	-	-	547	0.21
27	1	512	-	547	0.21

TABLE 3. *von Bertalanffy growth parameters and standard errors (SE) from Blackfin Snapper (Lutjanus buccanella) from the southeastern United States and the U.S. Caribbean based on various model runs. Size-at-age was not significantly different by sex or by region (ANOVA: $F_{(2,620)} = 1.61$, $p = 0.11$). All lengths are TL (mm). All model runs were unweighted and not corrected for size-limit bias unless stated otherwise.*

Model Run	n	L_∞ (SE)	K (SE)	t_0 (SE)
Unweighted, freely estimated, all data combined	622	549 (15)	0.20 (0.02)	-1.51 (0.33)
Bias-corrected, all data combined	587	532 (9)	0.28 (0.01)	-0.04 (1.90)
Florida-Caribbean region	293	579 (23)	0.16 (0.02)	-1.60 (0.43)
North Carolina-South Carolina region	329	526 (21)	0.27 (0.05)	-0.99 (0.46)
Females	91	584 (62)	0.12 (0.04)	-2.26 (1.03)
Males	85	579 (37)	0.17 (0.04)	-1.17 (0.72)

gion (Florida–Caribbean: n = 293; Carolinas: n = 329; $F_{2,620} = 1.61$, p = 0.11). We then pooled all data and the resulting estimated von Bertalanffy equation was: $L_t = 549\ (1 - e^{-0.20\ (t+1.51)})$ (n = 622; Figure 4, Table 3).

There were few fish < age–2 available to us, no doubt because hook–and–line gear or fishers generally select for larger fish. Also, in 1992 the SAFMC enacted a 305 mm TL (12 inch) minimum size limit on the species in the South Atlantic jurisdiction. Consequently, the model was unable to depict initial growth of the youngest fish, thus explaining the slightly negative estimate of t_0. We therefore re–ran the growth model using the method of McGarvey and Fowler (2002), which adjusts for the bias imposed by minimum size limits by assuming zero probability of capture below the minimum size limit. The resulting von Bertalanffy growth equation was: $L_t = 532\ (1 - e^{-0.28(t+0.00)})$ (n = 587; Figure 4).

While the bias–corrected von Bertalanffy model better estimated size at the youngest ages than the uncorrected

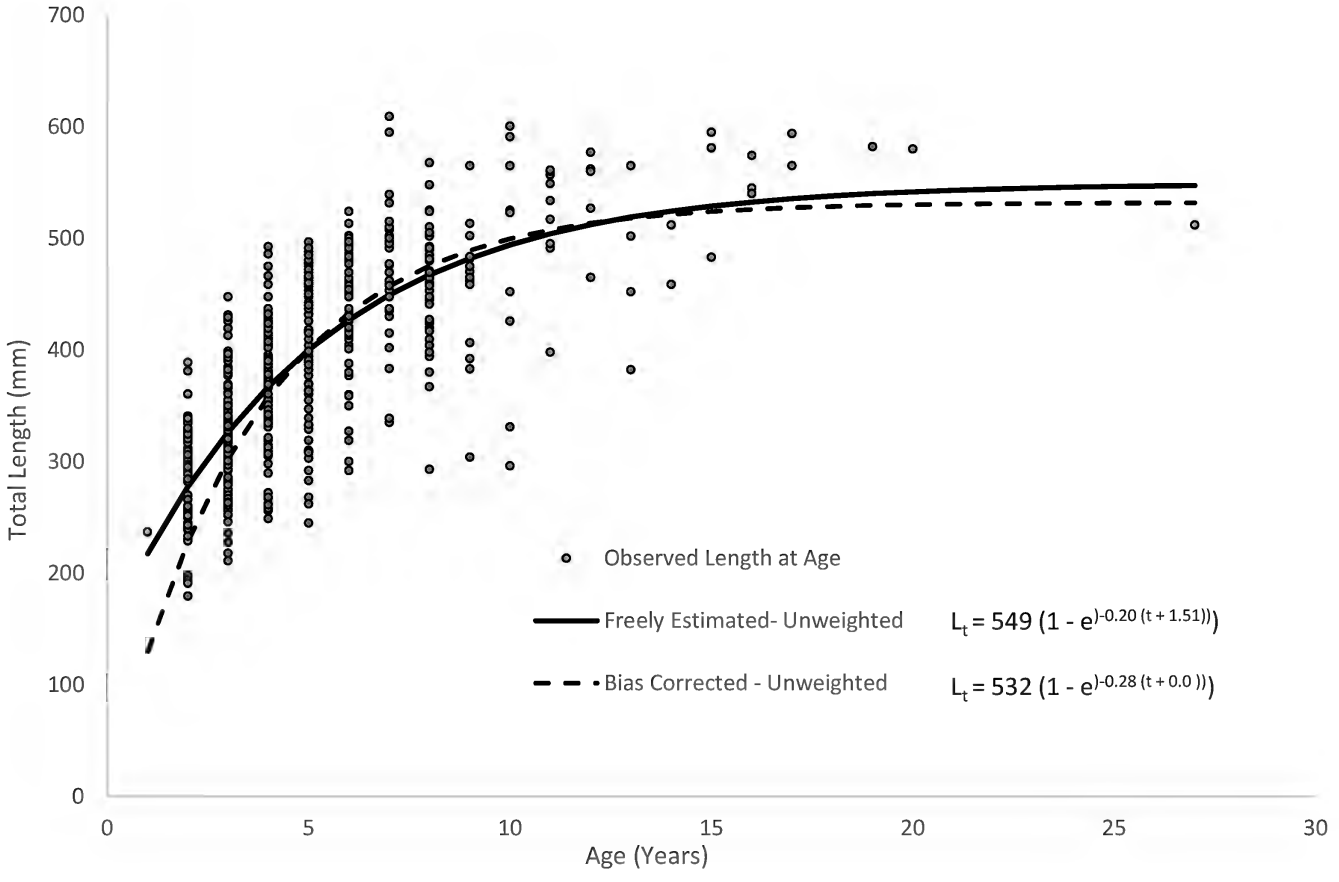

FIGURE 4. *Comparison of southeastern United States - U.S. Caribbean Blackfin Snapper observed size at age to von Bertalanffy growth curves for freely estimated (unweighted) and size limit bias-corrected model runs (models follow McGarvey and Fowler 2002).*

model (e.g., 130 mm TL vs. 217 mm TL for age–1), there was negligible difference in predicted sizes for most ages. By age–8 the curves converge and were nearly identical, with there being only 15 mm difference in predicted size at age–27, the oldest age in our sample (Figure 4). Our freely estimated growth curve fit the observed data very well, given the moderate range in length–at–age.

Body–size relationships

Body size relationships for Blackfin Snapper are shown in Table 4. The W–TL and W–FL relationships both exhibited additive variance in the residuals (variance not increasing with size), therefore we concluded that the direct non–linear fit was appropriate.

Natural mortality

Natural mortality (M) was estimated to be 0.15/y for Blackfin Snapper when integrating all ages into a single point estimate and using the maximum age from our study of 27 years. Age–specific estimates of M ranged from 0.65 to 0.21/y for ages 1–27 (Table 2).

TABLE 4. *Body-size relationships and associated statistics for Blackfin Snapper (Lutjanus buccanella) collected from 1979-2015 from the southeastern United States and the U.S. Caribean.*

Relationship	n	r^2	a (SE)	b (SE)
TL = bFL + a	203	0.99	0.81 (3.00)	1.09 (0.01)
FL = bTL + a	203	0.99	3.38 (2.74)	0.91 (0.01)
TL = bSL + a	83	0.97	14.27 (6.24)	1.23 (0.02)
FL = bSL + a	89	0.99	10.84 (2.84)	1.14 (0.01)
$W = aTL^b$	216	–	7.79×10^{-9} (4.47×10^{-9})	3.09 (0.09)
$W = aFL^b$	228	–	9.54×10^{-9} (4.95×10^{-9})	3.11 (0.08)

When considering the cumulative estimate of survivorship to the oldest age, the Hewitt and Hoenig method estimates 2.3% survivorship, while the Charnov estimate is 0.3%. Few of the fish in our samples were older than 12 years (17 of 622) and only 2 were 20 years or older (0.3%). Our age frequency suggests that the chance of survivorship to the oldest age may be as low as 0.3%. There is no evidence that the selectivity function of hook and line gear is dome shaped, thus our study had a chance of collecting the largest and oldest fish in the population. These observations give weight to the argument to use Charnov's estimate of M at age.

Discussion

This study fills important gaps in basic life history information for Blackfin Snapper in the SEUS and U.S. Caribbean. We have shown that sagittal otoliths are a suitable structure for ageing, with agreement between readers close to Campana's (2001) acceptable standard of 5% APE between readers for species of moderate longevity and reading complexity. One opaque zone was deposited per year from March–July. These results are similar to timing of annulus formation for other members of the family Lutjanidae in the SEUS (June for Gray Snapper (*Lutjanus griseus*), Burton 2001; May for Mutton Snapper (*Lutjanus analis*), Burton 2002). We present the first description of growth of Blackfin Snapper in SEUS waters. The species grows fast, attaining a mean observed length of 372 mm TL by age–4. Growth of fish in our study slowed after reaching a mean observed length of 473 mm TL at age–7. Mean observed size–at–age fluctuated for older ages, probably due to a combination of small sample sizes at the oldest ages as well as variability in size–at–age. Our study contained 17 fish older than age–12, ranging from 382–595 mm TL, but our largest fish was a 609 mm TL individual that was only age–7.

The maximum age of Blackfin Snapper in this study, 27 years, is substantially larger than Espinozo and Pozo's (1982) finding of a maximum age of nine years for Blackfin Snapper from the southeastern coast of Cuba, using urohyal bones, but is comparable to other *Lutjanus* spp. from the SEUS. The observed maximum age of Gray Snapper, a close congener, is 25 years (Burton 2001). Other large snappers have observed maximum ages recorded in the 40s (Mutton Snapper, SEDAR 2015) and 50s (Red Snapper, McInerny 2007; Cubera Snapper (*Lutjanus cyanopterus*), ML Burton unpublished data). Smaller lutjanids such as Lane Snapper (*Lutjanus synagris*) and Mahogany Snapper (*Lutjanus mahogoni*), have maximum ages of just 11 to 18 years, respectively (Brennan 2004; ML Burton, unpublished data). Schoolmaster (*Lutjanus apodus*), a small to medium snapper found in coastal habitats in the Florida Keys, was found to have a maximum age of 42 years (Potts et al. 2016). The maximum age of Blackfin Snapper from this study should be not be considered a true maximum age since, with increased sampling, a new maximum could be encountered.

The fact that there were no significant differences in mean TL–at–age between the northern sampled area (North Carolina–South Carolina) and the southern sampled area (Florida–U.S. Caribbean) allowed us to pool our data to generate a combined growth curve. This result may be useful to managers in areas with less resources available to conduct studies to generate life history information. These vital life history data could be combined with catch data using data–limited assessment methodologies to generate annual catch limits.

Natural mortality (M) of wild populations of fish is difficult to estimate but is an important input variable into stock assessments. A point estimate of M, such as that obtained using the method of Hewitt and Hoenig (2005), for the entire life span of a fish seems relatively uninformative, because as fish grow they become less vulnerable to preda-

tion. The estimate of M derived from the maximum age was a reasonable estimate for the fully recruited ages in our study but is an insufficient estimate of M for all ages. The age—varying M calculated using Charnov et al. (2013) is a more appropriate estimator for the younger ages. The initial Charnov estimates of M starting with the fully recruited age of 4 are slightly more than double the Hewitt and Hoenig estimate, reflecting higher natural mortality at younger ages. The age—specific estimates of M for the older ages continue to decrease until stabilizing at 0.21 at age—15.

When we compare estimates of M from this study with estimates from other lutjanids, we need to be cognizant of differences in both maximum size and longevity, two factors that influence estimates of M. Potts et al. (2016) estimated M = 0.47–0.12 for Schoolmaster for ages 1–42. Schoolmaster is a slightly smaller—sized fish than Blackfin Snapper but it has a higher maximum age (42 years vs. 27 years). Cubera Snapper, the largest lutjanid in the SEUS, is both larger and longer—lived than Blackfin Snapper (maximum size 1422 mm TL, maximum age 55 years; ML Burton, unpublished data), but the range of estimated values for M was similar, 0.50– 0.05 for ages 1–55. Survivorship to the oldest age is similar between these three lutjanids, with Schoolmaster survivorship estimated at 0.3% (Potts et al. 2016) and Cubera Snapper survivorship estimated at 0.2% (ML Burton, unpublished data).

One limitation of many age—growth studies is the lack of fish in smaller size classes, due to the fishery—dependent nature of the samples as well as the selectivity of fishing gear. We included fishery—independent samples to help overcome this problem, but only 11% of our samples were age—2 or younger, no doubt because the majority of our fishery—independent samples were still collected with gear (hook—and—line) that was selective for larger fish. One potential way to address this problem in future studies would be to structure fishery—independent sampling to include gear types that did not select only for larger fish (e.g., trawl, spear).

The data in this study were collected over a protracted period of time (36 years). While one could argue that this approach would be beneficial in capturing natural variability, it is true that population parameters can vary inter—annually for various reasons (e. g., variable recruitment, environmental variability, changes in fishing pressure), and it is likely that parameter estimates based on samples collected over a long time period would have increased variability. Reducing this variability may be possible by increasing the sample sizes or adding consistency to the temporal spread of samples. Species such as Blackfin Snapper are harvested frequently enough from SEUS waters that obtaining adequate biological samples for age and reproduction studies should not be problematic. With a minimal increase in resources, more gaps in information for data—poor and data—limited species, in both the SEUS and U.S. Caribbean, should be eliminated.

Acknowledgments

We gratefully acknowledge the many NMFS headboat and commercial port samplers and the scientific personnel of the NOAA R/V Oregon II whose efforts made this study possible. Rob Cheshire, D. Meyer, T. Kellison, E. Williams and two anonymous reviewers provided reviews which greatly improved the manuscript. Mention of trade names or commercial companies is for identification purposes only and does not imply endorsement by the National Marine Fisheries Service, NOAA.

Literature Cited

Beamish, R.J. and D.A. Fournier. 1981. A method for comparing the precision of a set of age determinations. Canadian Journal of Fisheries and Aquatic Science 38:982—983.

Boardman, C. and D. Weiler. 1980. Aspects of the life history of three deep water snappers around Puerto Rico. Proceedings of the Gulf and Caribbean Fisheries Institute 32:158—172.

Brennan, K.J. 2004. Age, growth and mortality of lane snapper, *Lutjanus synagris*, from the east coast of Florida. M.S. Thesis. East Carolina University, Greenville, NC, USA, 59 p.

Burton, M.L. 2001. Age, growth, and mortality of gray snapper from the east coast of Florida. Fishery Bulletin 99:245—256.

Burton, M.L. 2002. Age, growth and mortality of mutton snapper, *Lutjanus analis*, from the east coast of Florida, with a brief discussion of management implications. Fisheries Research 59:31—41.

Burton, M.L., J.C. Potts, and D.R. Carr. 2012. Age, growth and natural mortality of rock hind, *Epinephelus adscencionis*, from the Gulf of Mexico. Bulletin of Marine Science 88:903—917. doi: 10.5343/bms.2011.1102

Campana, S.E. 2001. Accuracy, precision and quality control in age determination, including a review of the use and abuse of age validation methods. Journal of Fish Biology 59:197–242. doi: 10.1111/j.1095–8649.2001.tb00127.x

Cervigon, F. 1966. Los peces marinos de Venezuela. Estación de Investigaciones Marinas de Margarita. Fundación La Salle de Ciencias Naturales, Caracas, Venezuela. 951 p.

Charnov, E.L., H. Gislason, and J.G. Pope. 2013. Evolutionary assembly rules for fish life histories. Fish and Fisheries 14:212–224. doi: 10.1111/j.1467–2979.2012.00467.x/epdf

Claro, R. and K.C. Lindeman. 2008. Biología y manejo de los pargos (Lutjanidae) en el Atlántico occidental. Instituto de Oceanología, CITMA, La Habana, Cuba, 472 p.

Erdman, D.S. 1976. Spawning patterns of fishes from the northeastern Caribbean. Puerto Rico Department of Agriculture, Commonwealth of Puerto Rico, Area of Special Services, Commercial Fisheries Laboratory, Agricultural and Fisheries Contributions, Official Publication in the Area of Special Services 8:1–36.

Espinoso, L. and E. Pozo. 1982. Edad y crecimiento del sesi (*Lutjanus buccanella* Cuvier 1828) en la plataforma suroriental de Cuba. Revista Cubana de Investigaciones Pesqueras 7:80–100.

Grimes, C.B., C.S. Manooch III, G.R. Huntsman, and R.L. Dixon. 1977. Red snappers of the Carolina coast. Marine Fisheries Review 39:12–15.

Harris, P.J., D.M. Wyanski, D.B. White, P.P. Mikell, and P.B. Eyo. 2007. Age, growth, and reproduction of greater amberjack off the southeastern U.S. Atlantic coast. Transactions of the American Fisheries Society 136:1534–1545. doi: 10.1577/T06–113.1

Hewitt, D.A. and J.M Hoenig. 2005. Comparison of two approaches for estimating natural mortality based on longevity. Fishery Bulletin 103:433–437.

Lorenzen, K. 1996. The relationship between body weight and natural mortality in juvenile and adult fish: a comparison of natural ecosystems and aquaculture. Journal of Fish Biology 49:627–647.

McGarvey, R. and A.J. Fowler. 2002. Seasonal growth of King George whiting (*Sillaginodes punctata*) estimated from length–at–age samples of the legal–size harvest. Fishery Bulletin 100:545–558.

McInerny, S.A. 2007. Age and growth of Red Snapper, *Lutjanus campechanus*, from the southeastern United States. M.S. Thesis, University of North Carolina–Wilmington, Wilmington, N.C. 96 p.

Munro, J.L., V.C. Gaut, R. Thompson, and P.H. Reeson. 1973. The spawning seasons of Caribbean reef fishes. Journal of Fish Biology 5:69–84.

Potts, J.C. and C.S. Manooch III. 1995. Age and growth of red hind and rock hind collected from North Carolina through the Dry Tortugas, Florida. Bulletin of Marine Science 56:784–794.

Potts, J.C., M.L. Burton, and A.R. Myers. 2016. Age, growth, and natural mortality of schoolmaster, (*Lutjanus apodus*) from the southeastern United States. PeerJ 4:e2543. doi: 10.7717/peerj.2543

South Atlantic Fisheries Management Council (SAFMC). 2015. Blackfin Snapper: Fish ID and Regs: Regulations by Species. Available: http://safmc.net/regulations/regulations–by–species/blackfin–snapper/. (viewed on 11/30/2016).

SAS Institute, Inc. 1987. SAS/STAT guide for personal computers, version 6 edition. SAS Institute, Cary, NC, USA 1028 p.

SEDAR. 2015. SEDAR 15A DW 15. Life History of *Lutjanus analis* inhabiting Florida waters. http://sedarweb.org/sedar–15a–dw15–life–history–lutjanus–analis–inhabiting–florida–waters (viewed on 11/30/2016).

SERO. 2015. Summary of commercial and recreational fishing regulations for the U.S. Caribbean Exclusive Economic Zone for species managed by the Caribbean Fishery Management Council. http://sero.nmfs.noaa.gov/sustainable_fisheries/caribbean/documents/pdfs/regs_booklet.pdf. (viewed on 11/30/2016).

Sylvester, J.R., D.W. Drew, and A.E Damann. 1980. Selective life history of silk and blackfin snapper from the Virgin Islands. Caribbean Journal of Science 15:41–48.

Thompson, R. and J.L. Munro. 1983. The biology, ecology and bionomics of the snappers, Lutjanidae. In: J. L. Munro., ed. Caribbean Coral Reef Fishery Resources Volume 17. ICLARM Studies and Reviews Manila, Phillipines, p. 94–109.

von Bertalanffy, L. 1938. A quantitative theory of organic growth. Human Biology 10:181–243.

Gulf and Caribbean Research

Volume 27 | Issue 1

2016

Parasites from the Red Lionfish, *Pterois volitans* from the Gulf of Mexico

Alexander Q. Fogg
Florida Fish and Wildlife Conservation Commission, fogg.alex@gmail.com

Carlos F. Ruiz
Auburn University, cfr0006@tigermail.auburn.edu

Stephen S. Curran
The University of Southern Mississippi, stephen.curran@usm.edu

Stephen A. Bullard
Auburn University, sab0019@auburn.edu

Recommended Citation

Fogg, A. Q., C. F. Ruiz, S. S. Curran and S. A. Bullard. 2016. Parasites from the Red Lionfish, *Pterois volitans* from the Gulf of Mexico. Gulf and Caribbean Research 27 (1): SC1-SC5.
Retrieved from https://aquila.usm.edu/gcr/vol27/iss1/7
DOI: https://doi.org/10.18785/gcr.2701.07

Gulf and Caribbean Research Vol 27, SC1-5, 2016
DOI: 10.18785/gcr.2701.07

Manuscript received, May 19, 2016; accepted, July 28, 2016

SHORT COMMUNICATION

PARASITES FROM THE RED LIONFISH, *PTEROIS VOLITANS*, FROM THE GULF OF MEXICO

Alexander Q. Fogg[1, 2], Carlos F. Ruiz[3], Stephen S. Curran[2,4], and Stephen A. Bullard[3]

[1]Florida Fish and Wildlife Conservation Commission, 620 South Meridian Street, Box 4B2, Tallahassee, FL 32399; [2]Division of Coastal Sciences, School of Ocean Science and Technology, The University of Southern Mississippi, 703 East Beach Drive, Ocean Springs, Mississippi 39564; [3]Department of Fisheries, Aquaculture, and Aquatic Sciences, Auburn University, 203 Swingle Hall, Auburn, Alabama 36849; [4]Corresponding author, email:stephen.curran@usm.edu

KEY WORDS: Ectoparasite, endoparasite, host–parasite association, taxonomy, invasive

INTRODUCTION

Invasion of lionfish from the Indo–Pacific Ocean into the western Atlantic Ocean has recently become the subject for ecological investigation directed at exploring concepts pertaining to host–parasite ecology (Sikkel et al. 2014, Sellers et al. 2015). The potential impact that host–parasite interactions may have on the relative success of lionfish in their new habitat is of particular interest. The value of data analyzed in such ecological investigations is dependent on accurate identification of parasite species, which in turn is dependent on the ability to verify parasite identification with vouchered museum specimens and sequence data. Studies identifying parasites of invasive lionfish in the western Atlantic Ocean that are supported by museum vouchered specimens or published sequence data are limited to 4 reports (Ruiz–Carus et al. 2006, Bullard et al. 2011, Ramos–Ascherl et al. 2015, Claxton et al. 2017), so there is a need to improve the current state of knowledge of parasites of invasive lionfish. This study reports and vouchers some parasites from invasive Red Lionfish from the northern Gulf of Mexico.

MATERIALS AND METHODS

Red Lionfish (*Pterois volitans* [Linnaeus, 1758]) were collected from the Gulf of Mexico between 29 March 2013 and 13 October 2014 (see Table 1). Fish were collected and identified following methods described in Fogg et al. (2013, 2014). Forty–nine fish from a separate life history study of Red Lionfish were opportunistically examined for external parasites (skin, fins, mouth and gills). Twenty–four of the 49 fish were placed on ice after initial external examination and further examined for internal parasites (from the heart and digestive tract) between 12 and 24 h after capture.

Leeches were cold–shocked or recently dead and therefore not relaxed prior to preservation in 70% ethanol. Arthropods were preserved in 70% ethanol. Digeneans and a nematode were removed, fixed using hot water, and preserved in 70% ethanol. Digeneans were stained using aqueous Meyer's hematoxylin, dehydrated through an alcohol series, cleared in methyl salicylate, and mounted in Damar gum.

TABLE 1. *Collections of Red Lionfish,* Pterois volitans, *examined for parasites.*

Collection date	Latitude	Longitude	Bottom habitat	Depth (m)	Number of fish examined	
					External only (n=25)	Internal and external (n=24)
3/29/2013	30.31	-86.60	Artificial	26	1	
6/12/2013	26.68	-83.73	Natural	74	1	
6/13/2013	25.84	-83.61	Natural	70	1	
6/13/2013	25.98	-83.70	Natural	86	1	
6/14/2013	24.65	-83.43	Natural	61	1	
6/15/2013	25.53	-83.18	Natural	59	1	
6/22/2013	28.34	-91.18	Artificial	30	1	
7/1/2013	30.32	-86.58	Natural	26	1	
9/21/2013	27.26	-83.01	Natural	26	1	
10/1/2013	29.69	-87.40	Natural	32	1	
10/13/2013	30.19	-86.43	Natural	30	1	
12/3/2013	29.97	-87.21	Artificial	34	3	
2/25/2014	30.15	-86.94	Natural	35		6
3/21/2014	30.18	-86.86	Natural	36	1	5
4/12/2014	27.45	-83.27	Artificial	34		5
4/22/2014	30.04	-87.56	Artificial	32	1	8
4/26/2014	29.59	-88.05	Artificial	44	1	
5/2/2014	30.08	-87.20	Artificial	27	1	
6/10/2014	30.11	-87.25	Artificial	34	3	
6/10/2014	28.71	-84.49	Natural	41	1	
6/18/2014	27.13	-83.31	Natural	42	1	
9/7/2014	29.61	-88.10	Artificial	40	1	
10/13/2014	30.13	-86.04	Natural	28	1	

The nematode was cleared and mounted in warm glycerin jelly for microscopic examination. Arthropods and leeches were directly examined in ethanol and temporarily cleared and examined using lactic acid. Identification of leeches was based on Ingram (1957) and Meyer (1965). Identification of arthropods was based on Richardson (1905), Wilson (1911, 1917), Brusca (1981), Kensley and Schotte (1989), and Williams and Bunkley–Williams (1996).

Two ecological parameters, prevalence and mean intensity of infection (with standard deviation), were calculated for each species of parasite when appropriate. Parasite prevalence is the percentage of fish examined that are infected with a particular parasite species; mean intensity is the mean number of a particular parasite species per individual infected host (Bush et al. 1997). Ecological data were pooled for the entire study area due to the small number of fish examined. Reef habitat type was noted as natural or artificial for each captured fish and its associated parasites. Representative voucher specimens of each species of parasite are deposited in the United States National Museum in the Smithsonian Institution, Washington, D.C., and in the Gulf Coast Research Laboratory Museum, Ocean Springs, Mississippi (Table 2).

Results and Discussion

We collected 9 species of parasites during the study. Four of the 9 taxa are reported from the Red Lionfish for the first time (Table 2).

Annelida

A single species of marine leech, *Trachelobdella lubrica* (Grube, 1840) Ingram, 1957, infested the mouth or inner operculum of 10 of 49 fish (Prevalence = 20.4%, Mean intensity = 1.2 ± 0.63). The leech occurred at both natural and artificial reefs. *Trachelobdella lubrica* is known to occur in clear, high–salinity habitats, and infests a wide variety of teleosts over much of the warm Atlantic Ocean, Mediterranean Sea, and Red Sea (Sawyer, 1986). Meyer (1965) redescribed the species based on material from an unidentified serranid fish from western Africa, providing the best available taxonomic description for the species. Williams et al. (1994) reported *T. lubrica* from fishes from the orders Elopiformes, Myctophormes and Perciformes in the Caribbean Sea, and Saglam et al. (2003) and Sanver–Celik and Aydin (2006) reported *T. lubrica* from the Black Scorpionfish, *Scorpaena porcus* Linnaeus, 1758, and the Red Scorpionfish, *Scorpaena scrofa* Linnaeus, 1758, in the Dardanelles of the Aegean Sea. *Trachelobdella lubrica* was reported from lionfish from near Jacksonville, Florida (see Ruiz–Carus et al. 2006, Bullard et al. 2011), and Puerto Rico (Ramos–Ascherl et al. 2015). *Trachelobdella lubrica* is known to infest *P. volitans* in the Red Sea (see Paperna, 1976); consequently, *T. lubrica* is the only known parasite that invasive lionfish share with fish from their native range.

Arthropoda

Three isopod species and 2 copepod species were collected. In all cases, infested fish had a single arthropod parasite. The isopods *Rocinela signata* Schiödte and Meinert, 1879 and *Nerocila acuminata* Schiödte and Meinert, 1881 each infested 4 of 49 fish examined (Prevalences = 8.2%). *Rocinela signata* occurred only on natural reefs (near Sarasota and Pensacola, Florida) while *N. acuminata* occurred

TABLE 2. *Parasites of the Red Lionfish,* Pterois volitans, *from the northern Gulf of Mexico. The location of the parasite on the host and museum accession numbers for representative vouchers are indicted. *Represents a new host record for the parasite. USNM–United States National Museum, Smithsonian Institute, Washington, D.C.; GCRLM–Gulf Coast Research Laboratory Museum, Ocean Springs, MS.*

Parasite Phylum Class/Subclass Order Family Species	**Site on/in host**	**Museum accession #**
Annelida		
Clitellata/Hirudinea		
Rhynchobdellida		
Piscicolidae		
Trachelobdella lubrica	Gill chamber, operculum	USNM 1420607-1420614
Arthropoda		
Malacostraca/Eumalacostraca		
Isopoda		
Aegidae		
Rocinela signata	Mouth, gills, pectoral fin	GCRLM 06577-80
Corallanidae		
*Alcirona krebsii**	External surface, gills	GCRLM 06581-2
Cymothoidae		
*Nerocila acuminata**	Fins, external surface	GCRLM 06573-6
Maxillipoda/Copepoda		
Siphonostomatoida		
Caligidae		
*Caligus lobodes**	External surface	USNM 1420615
Pennellidae		
*Lernaeenicus cf. polyceraus**	Tongue, operculum, mandible muscles	USNM 1420616-7, GCRLM 06583
Nematoda		
Chromadorea/Chromadoria		
Rhabditida		
Raphidascarididae		
Raphidascaris sp.	Intestine	Not deposited
Platyhelminthes		
Trematoda/Digenea		
Plagiorchiida		
Didymozoidae		
Unidentified adult	Inner operculum	USNM 1420618
Hemiuridae		
Lecithochirium floridense	Stomach	GCRLM 06569-72

on a natural reef (near Sarasota, Florida) and artificial reefs (near Mississippi and Alabama). Both of these isopod species are known to be generalist parasites of various fishes in the Gulf of Mexico (Kensley and Schotte 1989). A third isopod species, *Alcirona krebsii* Hansen, 1890, infested the gills of a fish and the external surface of another, both at natural reef sites (near Destin, Florida and near Sarasota, Florida; Prevalence = 4.0%). *Alcirona krebsii* is typically a free–living associate of sponges and corals and is not normally a parasite on fishes; however, Richardson (1905) reported that 2 individuals infested a "Hamlet Grouper" in the Atlantic. The infestation we observed on the Red Lionfish may or may not represent an accidental association. Similarly, Poole (2011) reported that another corallanid isopod specimen belonging in *Excorallana* Stebbing, 1904 infested the gills of *P. volitans* from the Caribbean Sea but members of that genus are also free–living and not normally parasites on fish. Of the 3 isopod species collected, only *R. signata* had been previously reported to infest *P. volitans* in Puerto Rico (Ramos–Ascherl et al. 2015) and Panama (Sellers et al. 2015).

A single adult specimen of the copepod *Caligus lobodes* (Wilson, 1911) Kabata, 1979 infested the skin of a fish from a natural reef near Sarasota, Florida. This copepod was originally described from an infestation from the head of the Great Barracuda, *Sphyraena barracuda* Walbaum, 1792, from the Dry Tortugas, Florida. *Caligus lobodes* is well–known from Great Barracuda in the Caribbean Sea and Gulf of Mexico (see Williams and Bunkley–Williams 1996), and was also reported from *Sphyraena* sp. from the Indian Ocean (Lewis et al. 1969). This represents the first global report of C. *lobodes* from a Red Lionfish. Five specimens of the copepod *Lernaeenicus* cf. *polyceraus* Wilson, 1917 were found embedded in the tongue or musculature associated with the dentary on 5 fish (Prevalence = 10.2%) collected from both natural and artificial reefs (Figure 1). The specimens conform closely to the description of *L. polyceraus* by Wilson (1917), but certain elements of the cephalothorax of each specimen were damaged or removed during collection. Observation of number and size of all swimming legs, which represent key generic features for *Lernaeenicus* Le Sueur, 1824, was not possible, rendering the identification of this species reasonable but tentative. *Lernaeenicus polyceraus* is infrequently reported but known to occur on a variety of fishes in the western Atlantic Ocean. Wilson (1917) described the species on the basis of the holotype from the Atlantic Tomcod, *Microgadus tomcod* (Walbaum, 1792) at Woods Hole, Massachusetts and two paratypes from Red Goatfish (as *Upeneus maculatus*, a junior subjective synonym of the Spotted Goatfish, *Pseudupeneus maculatus* (Bloch, 1793), (see page 992 of Eschmeyer 1998, Eschmeyer and Fong 2016) at Beaufort, North Carolina. Pearse (1947) reported *L. polyceraus* from the Bay Anchovy, *Anchoa mitchilli* (Valenciennes, 1848), the American Eel, *Anguilla rostrata* (Le Sueur, 1817)

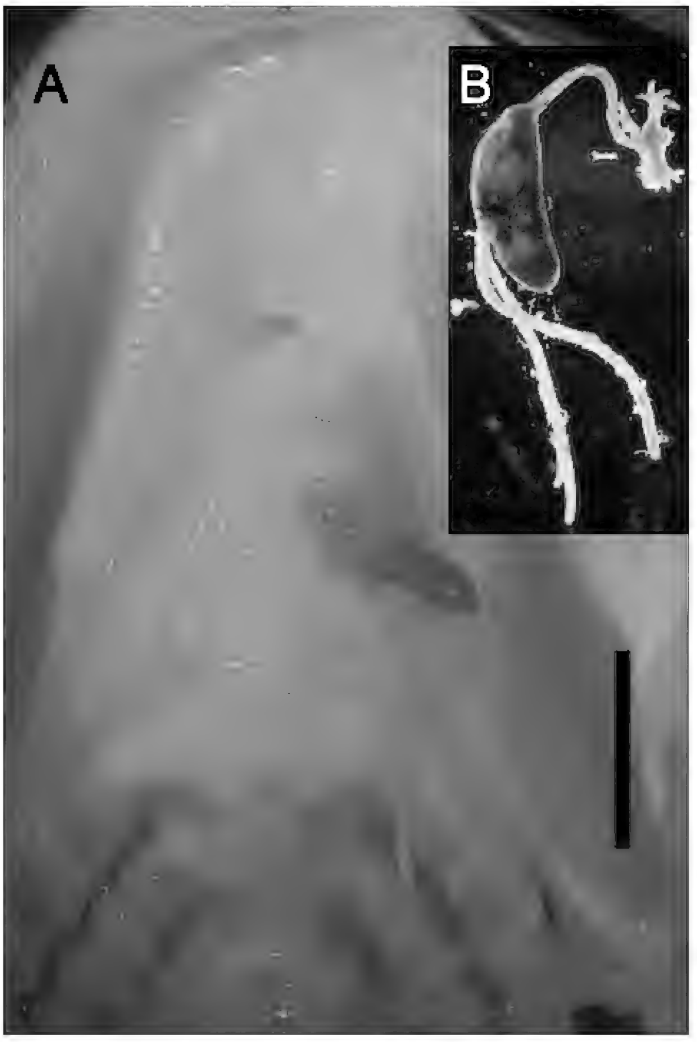

FIGURE 1. Lernaeenicus cf. polyceraus *from the Red Lionfish,* Pterois volitans*, from the northern Gulf of Mexico near Destin, Florida. A. Adult female specimen anchored on the ventral side of tongue. B. Specimen removed from tongue revealing anchored anterior end. Scale bar = 5 mm.*

and the Naked Goby, *Gobiosoma bosc* (Lacepède, 1800), all from Beaufort, North Carolina. Skinner (1978) reported *L. polyceraus* from the Vermilion Snapper, *Rhomboplites aurorubens* (Cuvier, 1829), from near Panama City, Florida. This represents the first global report of *L. polyceraus* from a Red Lionfish.

Nematoda

A single mature female specimen of *Raphidascaris* sp. infected the intestine of 1 fish from a natural reef near Destin, Florida; however, after preliminary identification the specimen was lost. Observed features consistent with *Raphidascaris* Railliet and Henry, 1915 according to Hartwich (1974) were: spines absent on cuticular rings, and an appendix emanated from a ventriculus. The position of the excretory pore was not noted. Ramos–Ascherl et al. (2015) reported adult *Raphidascaris* sp. from the stomach of *P. volitans* in the vicinity of Puerto Rico.

Platyhelminthes

Two species of Platyhelminthes, both adult digeneans,

were collected. One was represented by a single specimen belonging in the Didymozoidae Monticelli, 1888 that was embedded beneath the epidermis of the inner opercle of a fish from a natural reef near Sarasota, Florida. The anterior extremity was not intact preventing further identification. Neotorticaecum—type didymozoid metacercaria were reported from the stomach of *P. volitans* in Puerto Rico (see Ramos—Ascherl et al. 2015), but it is not clear if the adult reported herein is conspecific with the larval stage from Puerto Rico. The other digenean species, *Lecithochirium floridense* (Manter, 1934) Crowcroft, 1946, was the most common parasite encountered during the present study. *Lecithochirium floridense* infected the stomachs of 13 of 24 fish (Prevalence = 54.2%, Mean intensity = 7.7 ± 5.92), from both natural and artificial reefs. *Lecithochirium floridense* is a common generalist stomach parasite of teleosts in the western Atlantic Ocean, where it is known to infect perhaps as many as 60 species of pelagic and reef—oriented fishes, including the Red Lionfish (Bullard et al. 2011). Based on high prevalence of *L. floridense* reported in this and recent studies of invasive lionfish parasites, *L. floridense* represents the most successful parasite colonizer of Red Lionfish in the western Atlantic Ocean (Bullard et al. 2011; Ramos—Ascherl et al. 2015; Sellers et al. 2015; Claxton et al. 2017). The present study confirms what common sense would predict: only generalist parasites are found in invasive Red Lionfish in the Gulf of Mexico and no exotic parasites have been detected thus far.

Acknowledgements

We thank: Coast Watch Alliance, Perdido Key Chamber of Commerce, Mississippi Gulf Fishing Backs Inc., Mississippi Chapter of American Fisheries Society, National Oceanic and Atmospheric Administration, Florida Fish and Wildlife Conservation Commission, Alabama Department of Marine Resources, Gulf Coast Lionfish Coalition, Dauphin Island Sea Lab, Zookeeper LLC, Lytle Scholarship, Tom McIllwain Scholarship, Reef Pirate Emerald Coast Reef Association, Florida Skin Divers Association, Sarasota Underwater Club, Tampa Bay Spearfishing Club, Louisiana Council of Underwater Dive Clubs, and Canyon Coolers for their generous financial and logistical support in the acquisition of lionfish samples. We also thank the undergraduate interns at GCRL (Charles Duffie, Cody Jones, Jennifer Gross, Eileen Gibson, Judith Gonnello, Alicia Monroe, Megan McKenzie, and Aimee Rust) for laboratory assistance in processing lionfish.

Literature Cited

Brusca, R.C. 1981. A monograph on the isopoda Cymothoidae (Crustacea) of the eastern Pacific. Zoological Journal of the Linnean Society 73:117—199. doi: 10.1111/j.1096—3642.1981.tb01592.x.

Bush, A.O., K.D. Lafferty, J.M. Lotz, and A.W. Shostak. 1997. Parasitology meets ecology on its own terms: Margolis et al. revisited. Journal of Parasitology 83:575—583. doi: 10.2307/3284227.

Bullard, S.A., A.M. Barse, S.S. Curran, and J.A. Morris, Jr. 2011. First record of a digenean from invasive lionfish, *Pterois cf. volitans*, (Scorpaeniformes: Scorpaenidae) in the northwestern Atlantic Ocean. Journal of Parasitology 97:833—837. doi: 10.1645/GE—2746.1.

Claxton, A.T., A.D. Fuehring, M.J. Andres, T.D. Moncrief, and S.S. Curran. 2017. Parasites of the Vermilion Snapper, *Rhomboplites aurorubens* (Cuvier), from the western Atlantic Ocean. Comparative Parasitology 84(1):in press.

Eschmeyer, W.N., editor. 1998. Catalog of Fishes. Special Publication No. 1 of the Center for Biodiversity Research and Information. Volume 2, Species of Fishes (M—Z). California Academy of Sciences, San Francisco, CA, USA, p. 960—1,820.

Eschmeyer, W.N. and J.D. Fong. 2015. Species of Fishes by family/subfamily. http://research.calacademy.org/research/ichthyology/catalog/SpeciesByFamily.asp. (viewed on 2/3/2015)

Fogg, A.Q., E.R. Hoffmayer, W.B. Driggers III, M.D. Campbell, G.J. Pellegrin, and W. Stein. 2013. Distribution and length frequency of invasive lionfish (*Pterois* sp.) in the northern Gulf of Mexico. Gulf and Caribbean Research 25:111—115. doi: 10.18785/gcr.2501.08.

Fogg, A.Q., M.S. Peterson, and N.J. Brown—Peterson. 2014. Northern Gulf of Mexico lionfish: Distribution and reproductive life history trajectories. Proceedings of the Gulf and Caribbean Fisheries Institute 66:206—207.

Hartwich, G. 1974. No. 2. Keys to Genera of the Ascaridoidea. In: R.C. Anderson, A.G. Chabaud, and S. Willmott, eds. CIH Keys to the Nematode Parasites of Vertebrates. Commonwealth Agricultural Bureaux International, Wallingford, UK, 15 p. doi: 10.1186/1756—3305—2—42.

Ingram, D.M. 1957. Some Tasmanian Hirudinea. Papers and Proceedings of the Royal Society of Tasmania 91:191—232.

Kensley, B. and M. Schotte. 1989. Guide to the marine isopod crustaceans of the Caribbean. Smithsonian Institution

Press, Washington, D.C., USA, 308pp. doi: http://dx.doi.org/10.5962/bhl.title.10375.

Lewis, A.G., J. Dean, and E. Gilfillan, III. 1969. Taxonomy and host associations of some parasitic copepods (Crustacea) from pelagic teleost fishes. Pacific Science 23:414—437.

Meyer, M.C. 1965. Fish leeches (Hirudinea) from tropical West Africa. Scientific results of the Danish expedition to the coasts of tropical West Africa. Atlantide Report 8:237—245.

Paperna, I. 1976. Parasitological survey of fishes of the Red Sea and the Indian Ocean. In: Z. Reiss and I. Paperna, eds. Fifth report of the H. Steinitz Marine Biology Laboratory, H. Steinitz Marine Biology Laboratory, Elat, Israel, 69 p.

Pearse, A.S. 1947. Parasitic copepods from Beaufort, North Carolina. Journal of the Elisha Mitchell Scientific Society 63:1—16.

Poole, T. 2011. The sensitivity of the invasive lionfish, *Pterois volitans*, to parasitism in Bonaire, Dutch Caribbean. Physis Journal of Marine Sciences 9:44—49.

Ramos—Ascherl, Z., E.H. Williams, Jr., L. Bunkley—Williams, L.J. Tuttle, P.C. Sikkel, and M.A. Hixon. 2015. Parasitism in *Pterois volitans* (Scorpaenidae) from coastal waters of Puerto Rico, the Cayman Islands, and the Bahamas. Journal of Parasitology 101:50—56. doi: 10.1645/13—422.1.

Richardson, H. 1905. A monograph on the isopods of North America. Bulletin of the United States National Museum 54:727 pp. doi: 10.5479/si.03629236.54.i.

Ruiz—Carus, R., R.E. Matheson, D.R. Roberts, and P.E. Whitfield. 2006. The western Pacific red lionfish, *Pterois volitans* (Scorpaenidae), in Florida: Evidence for reproduction and parasitism in the first exotic marine fish established in state waters. Biological Conservation 128:384—390. doi: 10.1016/j.biocon.2005.10.012.

Saglam, N., M. Cemal—Oguz, E. Sanver—Celik, S. Ali—Doyuk, and A. Usta. 2003. *Pontobdella muricata* and *Trachelobdella lubrica* (Hirudinea: Piscicolidae) on some marine fish in the Dardanelles, Turkey. Journal of the Marine Biological Association of the UK 83:1315— 1316. doi: 10.1017/S0025315403008749.

Sanver—Celik, E. and S. Aydin. 2006. Effect of *Trachelobdella lubrica* (Hirudinea: Piscicolidae) on biochemical and haematological characteristics of black scorpion fish (*Scorpaena porucs*, Linnaeus 1758). Fish Physiology and Biochemistry 32:255—260. doi: 10.1007/s10695—006—9003—y.

Sawyer, R. T. 1986. Leech biology and behavior, volumes I—III. Oxford University Press, Oxford, U. K., 1065 p.

Sellers, A.J., G.M. Ruiz, B. Leung, and M.E. Torchin. 2015. Regional variation in parasite species richness and abundance in the introduced range of the invasive lionfish, *Pterois volitans*. PloS ONE 10(6):e0131075. doi: 10.1371/journal.pone.0131075.

Sikkel, P.C., L.J. Tuttle, K. Cure, A.M. Coile and M.A. Hixon. 2014. Low susceptibility of invasive red lionfish (*Pterois volitans*) to a generalist ectoparasite in both its introduced and native ranges. PloS ONE 9(5):e95854. doi: 10.1371/journal.pone.0095854.

Skinner, R. H. 1978. Some external parasites of Florida fishes. Bulletin of Marine Science 28:590—595.

Williams, Jr., E.H. and L. Bunkley—Williams. 1996. Parasites of offshore big game fishes of Puerto Rico and the western Atlantic. Puerto Rico Department of Natural and Environmental Resources, San Juan, PR, and the University of Puerto Rico, Mayaguez, PR. 382 p.

Williams, Jr., E.H., L. Bunkley—Williams, and E.M. Burreson. 1994. Some new records of marine and freshwater leeches from Caribbean, southeastern U.S.A., eastern Pacific, and Okinawan animals. Journal of the Helminthological Society of Washington 61:133—138.

Wilson, C.B. 1911. North American parasitic copepods. Descriptions of new genera and species. Proceedings of the United States National Museum 39:625—634. doi: 10.5479/si.00963801.39—1805.625.

Wilson, C.B. 1917. North American parasitic copepods belonging to the Lernaeidae with revision of the entire family. Proceedings of the United States National Museum 53:1— 150. doi: 10.5479/si.00963801.53—2194.1.

Gulf and Caribbean Research

Volume 27 | Issue 1

2016

Pelagic *Sargassum* in the Tropical North Atlantic

James S. Franks
USM-GCRL-Center for Fisheries R&D, jim.franks@usm.edu

Donald R. Johnson
USM-GCRL-Center for Fisheries R&D, donald.r.johnson@usm.edu

Dong S. Ko
US Naval Research Laboratory, ko@nrlssc.navy.mil

Gulf and Caribbean Research Vol 27, SC6-11, 2016
DOI: 10.18785/gcr.2701.08

Manuscript received, May 11, 2016; accepted, September 20, 2016

SHORT COMMUNICATION

PELAGIC *SARGASSUM* IN THE TROPICAL NORTH ATLANTIC

James S. Franks[1*], Donald R. Johnson[1], and Dong S. Ko[2]
*[1]Center for Fisheries Research and Development, Gulf Coast Research Laboratory, School of Ocean Science and Technology, The University of Southern Mississippi, Ocean Springs, Mississippi, 39564; [2]Oceanography Division, Naval Research Laboratory, Stennis Space Center, Mississippi, 39522; *Corresponding author, email: jim.franks@usm.edu*

KEY WORDS: Marine macroalgae, *Sargassum* blooms, Caribbean, West Africa, Equatorial currents

INTRODUCTION

Pelagic *Sargassum*, a complex of two co—occurring species of floating marine brown macroalgae (*Sargassum natans, Sargassum fluitans*; Class Phaeophyceae), is commonly found in surface waters of the Sargasso Sea and the northwestern Gulf of Mexico (GOM) (Lapointe 1995, Gower and King 2008), areas where ocean eddies tend to retain and consolidate deployed surface drifters. Winds and ocean currents aggregate the *Sargassum* into large neustonic rafts tens of meters wide (Marmorino et al. 2011) and weed lines (windrows) that extend across the ocean surface for tens of kilometers (Butler et al. 1983, Hu et al. 2105, Hu et al. 2016). These *Sargassum* features provide habitat for a large and diverse assemblage of marine organisms (Coston—Clements et al. 1991, Wells and Rooker 2004, Hoffmayer et al. 2005, Hallett, 2011, Huffard et al. 2014) but may also raft invasive species.

Beginning in boreal spring and summer of 2011, massive quantities of pelagic *Sargassum* have intermittently washed ashore along the coastlines of eastern Caribbean islands and West Africa (Franks et al. 2011; Supplemental Figure S1A—F). Pelagic *Sargassum* was also spotted by aircraft offshore of northeastern Brazil where not previously observed (de Széchy et al. 2012). The quantity and the frequency of occurrence of pelagic *Sargassum* in the beach stranding events created immediate problems for fishery and tourism industries of nations on both sides of the tropical Atlantic, and ecological impacts remain largely unknown.

Pelagic *Sargassum* that appeared in the eastern Caribbean events was first suspected to come from the Sargasso Sea (Webster and Linton 2013) and later thought to originate off northeastern Brazil (Gower et al. 2013). However, when the first massive incursions in 2011 were reported online to the Gulf and Caribbean Fisheries Institute (gcfinet@listserv.gcfi.org), it became clear that this was a broad scaled, complex event. A web site was established for documenting locations and dates of mass strandings (gcrl.usm.edu/sargassum).

Following the 2011 strandings, extensive pelagic *Sargassum* lines were observed far offshore by color satellite (Gower et al. 2013), and beach strandings were documented over a broad area of the tropical North Atlantic, including west Africa from Sierra Leone to the Gulf of Guinea (Oyesiku and Egunyomi 2014) and South America from northeast Brazil to the Caribbean (Gower et al. 2013, Smetacek and Zingone 2013). Although pelagic *Sargassum* was previously reported in the tropical North Atlantic (Taylor 1960), it had never been observed in such large quantities as occurred in 2011 (Franks et al. 2011). Since there were no documented reports of pelagic *Sargassum* being transported in large quantities on currents from the North Atlantic Gyre into the tropical Atlantic, and lacking evidence to the contrary from either *in situ* observations or satellite imagery, indications were strong that the *Sargassum* bloomed (Schell et al. 2015) in an area we identified as the North Equatorial Recirculation Region (NERR, Franks et al. 2011; Figure 1). The NERR is substantially larger than could be expected to produce *Sargassum* blooms via coastal eutrophication (Smetacek and Zingone 2013). Our previous work to determine the source of the pelagic *Sargassum* that stranded in the eastern Caribbean demonstrated that it most likely passed through the Guiana Current/North Brazilian Current system (Franks et al. 2011; see Supplemental Figure S2A). This low—latitude limb of the North Atlantic western boundary current originates in equatorial currents (Johns et al. 2002).

The nature of its origin and reasons for its unusual bloom in recent years will require knowledge of pelagic *Sargassum* growth rates in the NERR, genetic associations and understanding of climate changes in tropical ecosystems (including equatorial ocean dynamics) which would enable a massive broad—scale bloom and regional consolidations to occur. Historical tropical Atlantic circulation patterns (Philander 2001) suggest that pelagic *Sargassum* in the NERR can be retained during summer months (July—September) when the North Equatorial Counter Current (NECC; Supplemental Figure S2A) is established. From January through May, however, the NECC breaks down and surface flow is westward (Supplemental Figure S2B) in the western tropical Atlantic. Our long term interest is in the balance between growth of pelagic *Sargassum* mats within the NERR and export from the NERR. In this short communication we isolate and address the issues of historical recirculation/consolidation dynamics in the NERR and transport pathways as a first step

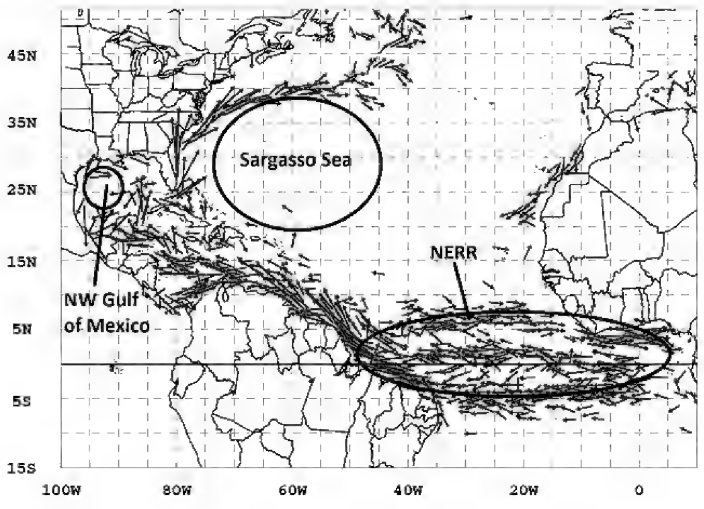

FIGURE 1. *Locations of pelagic Sargassum. Two regions where pelagic Sargassum is commonly found in abundance (northwest Gulf of Mexico and the Sargasso Sea) and a new area, the North Equatorial Recirculation Region (NERR), proposed in Franks et al. (2011). Current vectors are calculated from mixed layer satellite tracked drifters and plotted where the current speed averaged ≥ 0.25 m/s between June-September. This limit shows persistent currents, important for long distance transport, connecting the NERR with the northwest Gulf of Mexico and Sargasso Sea, but little connection from the Sargasso Sea back to the NERR.*

in understanding the timing of the bloom and the coastal incursion.

Materials and Methods

Model

In the present study, movements of pelagic *Sargassum* were backtracked for a period of one year from reported stranding sites in the eastern Caribbean, Brazil and West Africa (Supplemental Table S1) to possible source regions using archived surface currents from the global Hybrid Coordinate Ocean Model (HYCOM; Bleck 2002). The model has 1/12° longitude/latitude resolution and complete coverage of the tropical Atlantic domain of interest. The model uses hybrid vertical coordinates consisting of sigma—coordinates in the upper layer and z—coordinates in the lower layer. Surface boundary conditions (wind stress, heat flux, and salt flux) are supplied by the Navy Operational Global Atmospheric Prediction System (NOGAPS), and climatological river input is included for major rivers. In addition, data assimilation of satellite derived sea surface height and sea surface temperature through the Navy Coupled Ocean Data Assimilation (NCODA) system tends to phase lock the model into real events.

Reverse—time trajectory tracking is a simple process done with a field of finite—difference modeled currents by calculating successive positions of a parcel of water over small time increments: $\delta x(t+\delta t) = U(x+\delta x/2, t+\delta t/2)\ \delta t$, where x and t are the initial position and time, U is the current vector located midway in space and time, dt is the time step and dx is the distance traced by the parcel during the time step. The equation for dx was solved explicitly by iteration, and Akima cubic spline (Akima 1970) was used to interpolate gridded model currents to the time and location. The time step was set to 15 min. To accommodate the effects of sub—grid scale motion, 5 parcels were released at each position with a Gaussian (mean of zero, standard deviation of one) addition of 1 km/d to the current vector and center—of—mass averaged for a new position. The process was continued for 365 days from locations of pelagic *Sargassum* stranding events in 2011.

Drifting Buoys

In order to isolate transport pathways that can demonstrate recirculation and consolidation in the NERR together with reported stranding's on both sides of the Atlantic, designed experiments were conducted using selected drifting buoys. Satellite tracked drifting buoys have been deployed globally as part of the World Ocean Circulation Experiment, with records starting in 1979 and archived at NOAA'S Atlantic Oceanographic and Meteorological Office (http://www.aoml.noaa.gov/phod/dac/index.php). Buoys are drogued to reduce wind slippage and hence are reasonable simulators of surface drifting pelagic *Sargassum*. Buoy tracks are interpolated to 6 hourly positions, with currents calculated from successive positions. The data are quality controlled, archived and made available for general use (Lumpkin and Pazos 2007). In order to simulate transport pathways of the surface drifting *Sargassum* both into and within the NERR, boxes were created at strategic locations and the pathways of satellite tracked buoys which passed through the boxes were studied.

Results and Discussion

Backtracking pelagic *Sargassum* movements from stranding sites lead to the equatorial region (Supplemental Figure S3). Prior to the incursion into the eastern Caribbean, consolidation of the *Sargassum* off NE Brazil is apparent from the density of tracks in the model run and in local cycling of a validation buoy. The West Africa strandings were also traced, first to the interior of the NERR and then to the equatorial region where the tracks joined the eastern Caribbean tracks. To check these findings, back traces calculated for a few strandings that occurred in early 2014 (Supplemental Figure S4) in the eastern Caribbean confirmed the connection with the equatorial region.

Transport connections between the Sargasso Sea/North Atlantic and the NERR (Figure 1) are a major issue for deciphering if the *Sargassum* incursions into the Tropical Atlantic arrived *en masse* or bloomed in the area from seedings. This issue can be addressed using historical drifting buoys. A virtual box (Figure 2A) was created across the Atlantic from 13.9°N to 16°N, where *Sargassum* from the Sargasso Sea would have to cross to reach the NERR (≤ 7.5°N latitude). Buoy identification numbers were obtained for all

drifting buoys deployed within the box (regardless of year or season) and only those buoy tracks which led into the NERR were plotted (Figure 2A, orange lines). Our results show the only historical connection between the North Atlantic surface gyre and the NERR is along an intermittent, narrow coastal current off West Africa. Of the 305 buoys that were deployed in the 13.9°N to 16°N area (1992–2014), only 6 (~2%) entered the eastern NERR via this coastal current where they cycled for an average of 18 months until they died or grounded. None of the buoys lived long enough to enter the NERR along the African boundary and subsequently reach the eastern Antilles. This exercise demonstrates that historical transport pathways show limited connection between the NERR and the Subtropical North Atlantic, and that drifter retention in the eastern NERR for periods longer than a year is possible.

A second buoy experiment was conducted in order to address surface circulation and resulting *Sargassum* distribution throughout the NERR along with connections among areas of retention/consolidation within the NERR where *Sargassum* growth could occur. This was done with another virtual box experiment in the Gulf of Guinea (Figure 2B). The tracks of all buoys (170 total) that passed through this box showed 2 patterns of particular interest. One path connects the Gulf of Guinea with the recycling area in the eastern NERR found in the above experiment. After spending considerable time in the eastern NERR, many of these buoys grounded along the African coast from Sierra Leone to the Gulf of Guinea. The second path went westward in the South Equatorial Current (SEC; Supplemental Figure S2B) to the coast of northeast Brazil and then into either the Caribbean, or back to the eastern NERR via the NECC during boreal summer. In both pathways, the dominant transport pattern is clockwise.

In order to isolate the 2 patterns and determine potential consolidation areas, buoys that went through the Gulf of Guinea virtual box were further separated into those that also drifted west of 45°W (Figure 2C, red lines) and those that remained east of 30°W (Figure 2D, yellow lines). Fifteen of the buoys were entrained in the SEC in January/February, arriving along the coast of northeast Brazil in the North Brazil Current (NBC) the following boreal spring (Figure 2C). Some of these grounded along the coast of northeast Brazil, some entered the Caribbean and some returned eastward in the North Brazil Current Retroflection (NBCR), crossing the entire Atlantic to the Gulf of Guinea. A total of 111 other buoys cycled between the Gulf of Guinea and the eastern NERR (Figure 2D), many eventually

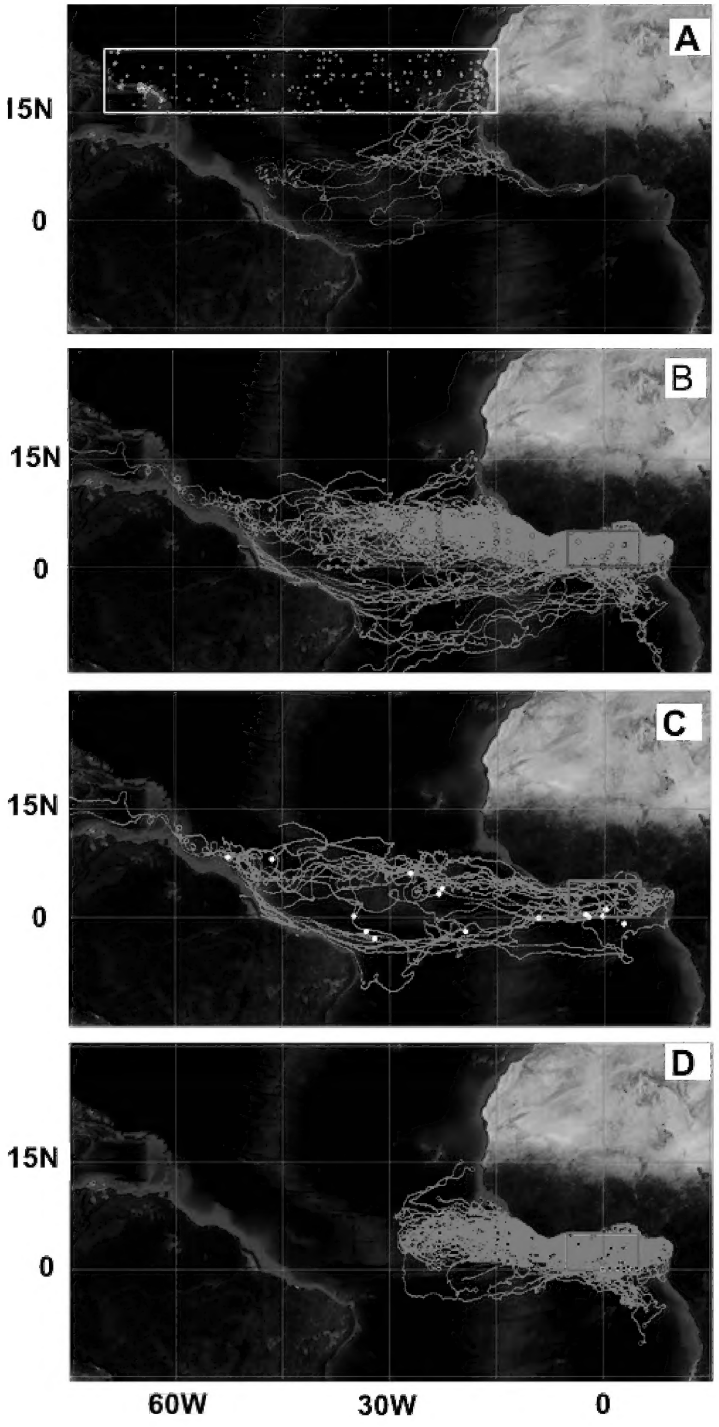

FIGURE 2. *(A) Experiment using satellite tracked mixed-layer drifting buoys to determine level of connection between the North Equatorial Recirculation Region (NERR) and the North Atlantic gyre (and the Sargasso Sea). Blue dots are locations of first-calculated currents (near deployment location). Only 6 of the 305 buoys entered the NERR in a narrow band along the coast of Africa. Orange dots indicate tracks of these 6 buoys. B. Experiment using satellite tracked mixed-layer drifting buoys to determine potential pelagic* Sargassum *consolidation areas and area connections. Identification numbers of all drifting buoys that passed through the virtual blue box in the Gulf of Guinea were obtained and the entire track of these buoys plotted from locations of first-calculated currents (red dots) to last report. C. Separation of all drifting buoys from the above experiment (Figure 2B) that passed through the Gulf of Guinea virtual box and also passed west of 45°W. White dots are locations of first-calculated currents. This demonstrates entrainment (in January and February) into the South Equatorial Current in the Gulf of Guinea and westward transport to the northeast coast of Brazil. D. Separation of all drifting buoys from the above experiment (Figure 2B) that passed through the Gulf of Guinea virtual box, but remained east of 30°W. Black dots are locations of first-calculated currents.*

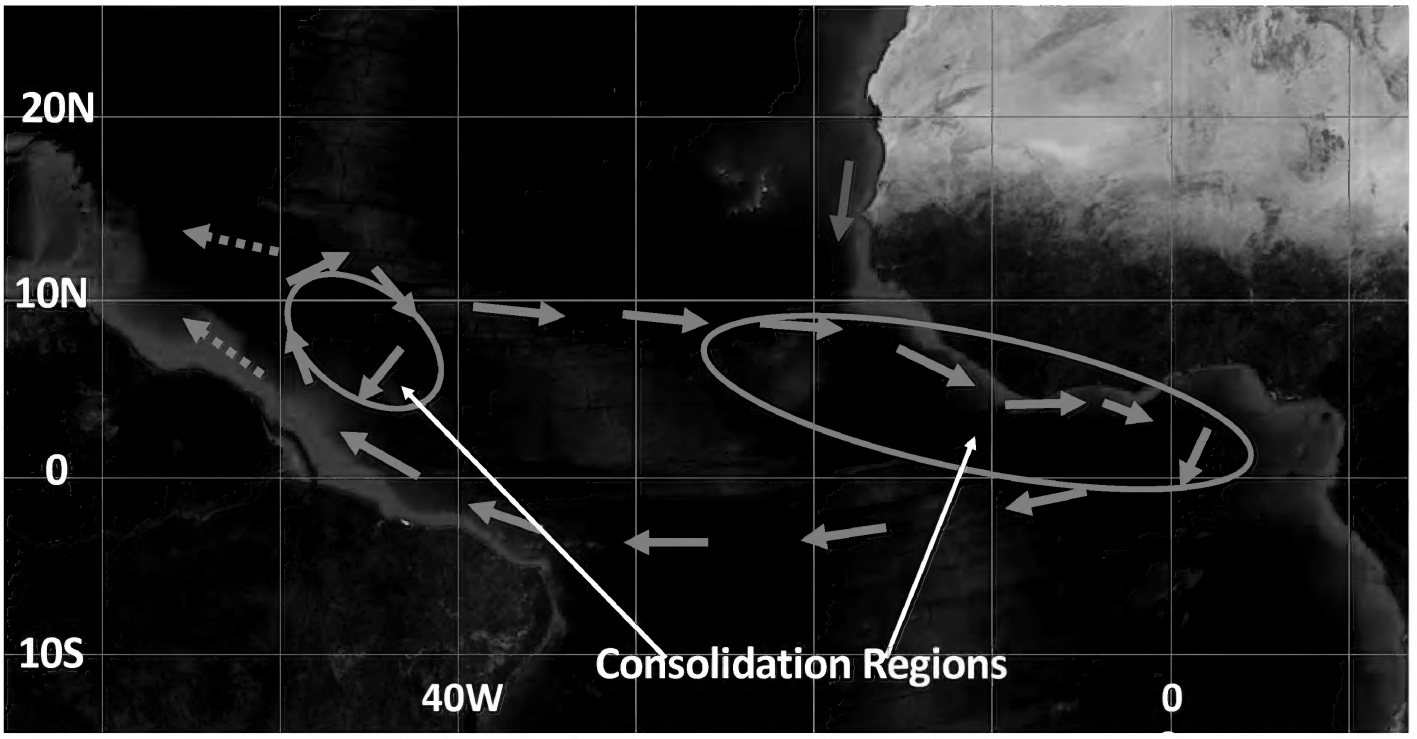

FIGURE 3. *Schematic of proposed pelagic* Sargassum *transport pathways in the North Equatorial Recirculation Region (NERR). From the drifting buoy experiments, there are 2 buoy consolidation regions: in the eastern NERR (large red ellipse) which includes the Gulf of Guinea and in the western NERR (small red ellipse) which includes the North Brazil Current Retroflection (NBCR). The 2 areas are connected by the South Equatorial Current (SEC) and the North Equatorial Counter Current (NECC) (yellow arrows). Buoy transports to the Caribbean occur in spring/summer through the North Brazil Current/ Guiana Current (NBC/GC) and NBCR rings, and in the winter through the North Equatorial Current (NEC). Connections to the subtropical North Atlantic are weak with an intermittent flow to the NERR by a coastal current along West Africa (green arrow).*

grounding along the coast of Africa. Other buoys (Figure 2B) were spread between the eastern NERR and the coast of northeast Brazil. These latter buoys are in position for winter transport to the eastern Caribbean when the NECC breaks down and the transport is predominantly westward throughout the North Tropical Atlantic. Within the NERR, consolidation areas where the buoys cycle for extensive periods were apparent.

A summary of the isolated circulation patterns is schematically presented in Figure 3. From the drifter experiments, there appear to be 2 consolidation regions within the NERR; one on the eastern side of the tropical Atlantic, associated with the Gulf of Guinea but broadly extending westward into the central NERR, and one on the western side associated with the NBCR. The large path conforms to climatological summer clockwise circulation around the NERR where flow is westward along the equator in the SEC, turning northwest along the northeast coast of South America and returning to the Gulf of Guinea via the NECC.

Timing associated with the schematic pattern can be summarized as follows: during January–February, entrainment occurs from the Gulf of Guinea into the SEC where drifters travel westward and ground off northeast Brazil in the early spring. In the following months, buoy groundings take place progressively further north along the northeast coast of South America until late spring/early summer when most drifters continue along the coast until they reach the southern Lesser Antilles.

It is worth pointing out that discharge from the Amazon River reaches its peak in June/July (Filizola and Guyot 2004), pushing drifters further off the coast of Brazil where they are less likely to ground. Furthermore, the NBCR forms at about the same time which shunts drifters into the NECC. Drifters can reach the Lesser Antilles in summer either through a narrow coastal current (Guiana Current) or via rings which break off from the NBCR and drift northwestward to the Caribbean (Johns et al. 2014). A ring break–off occurred in the first pelagic *Sargassum* incursion events of the Lesser Antilles in 2011 (Franks et al. 2011), creating uncertainty in direction of incursion until model backtracking revealed its path. During summer and fall, drifters that have been caught in the NBCR drift eastward in the NECC until they reach the eastern consolidation region with spreading along the coast of West Africa. This eastward drift is confirmed in satellite images (Gower et al. 2013). In winter, drifters can be caught in westward transport to the Caribbean as the NECC breaks down. This provides 3 generic ways that pelagic *Sargassum* incursion events in the Caribbean can occur: (1) into the southern Lesser Antilles via the Guiana

Current in late spring and summer, (2) into the northern Lesser Antilles in winter via the North Equatorial Current (NEC; Supplemental Figure S2B) and (3) intermittently in summer due to formation of an NBCR ring.

In the spring of 2016, incursion events again took place in both the Lesser Antilles and Sierra Leone, West Africa. The first appearance in satellite images (Supplemental Figure S5) was recognized on 24 May 2016 in the area of the NBCR. Our efforts at predicting arrival in the Lesser Antilles using archived model data suggested that *Sargassum* would begin stranding in late July 2016. Subsequent images and on–ground sightings showed that it arrived in mid–July 2016. Both forward tracking (Supplemental Figure S5) and back-tracking tended to confirm the transport patterns identified in our 2011 study (Franks et al. 2011).

It is expected that prolonged time spent in recirculation within the higher nutrient, warmer NERR (Franks et al. 2016) can significantly increase the biomass of *Sargassum*. LaPointe et al. (2014) found different growth rates of pelagic *Sargassum* between nutrient poor waters (oceanic) and nutrient richer waters (neritic) in the GOM and the western North Atlantic. In oceanic waters the mass was found to double in ~50 days for both *Sargassum fluitans* and *Sargassum natans*, whereas in neritic waters the mass doubled in ~11 days. This means that over one year of growth with poor nutrients, and without reference to mortality, one ton of pelagic *Sargassum* could grow to ~158 tons. However, in higher nutrient waters one ton could grow to ~10 billion tons in one year. Modeling pelagic *Sargassum* blooms in the NERR will require growth rates, mortality rates, and finding the balance between a better understanding of recycling in the NERR and export from the NERR.

Acknowledgments

We express our deep gratitude to the Guy Harvey Ocean Foundation (GHOF) for providing financial support for this study. We thank Caribbean fisheries officers and fisherfolk, Caribbean regional scientists, NGOs, GCFI colleague Emma Doyle, and others for reporting pelagic *Sargassum* beach strandings. Jean-Philippe Maréchal processed and provided satellite imagery acquired from Chuanmin Hu (http://optics.marine.usf.edu) for use in Figure S5. We appreciate the helpful comments provided by 3 anonymous reviewers. Diana Reid is acknowledged for her assistance with the graphics.

Literature Cited

Akima, H. 1970. A new method of interpolation and smooth curve fitting based on local Procedures. Journal of the Association for Computing Machinery 17:589–602.

Bleck, R. 2002. An oceanic general circulation model framed in hybrid isopycnic–Cartesian coordinates. Ocean Modelling 37:55–88. doi: 10.1145/321607.321609

Butler, J.N., B.F. Morris, J. Cadwallader, and A.W. Stoner. 1983. Studies of *Sargassum* and the *Sargassum* community. Bermuda Biological Station Special Publication 22:1–307.

Coston–Clements L., L.R. Settle, D.E. Hoss, and F.A. Cross. 1991. Utilization of the *Sargassum* habitat by marine invertebrates and vertebrates: A review. NOAA Technical Memorandum NMFS–SEFSC–296. Beaufort, NC, USA, 32 p.

de Széchy, M.T.M., P.M. Guedes, M.H. Baeta–Neves, and E.N. Olivera. 2012. Verification of *Sargassum natans* (Linnaeus) Gaillon (Heterokontophyta: Phaeophyceae) from the Sargasso Sea off the coast of Brazil, western Atlantic Ocean. Check List 8:638–642. http://www.checklist.org.br/getpdf?NGD002–12

Filizola, N. and J.L. Guyot. 2004. The use of Doppler technology for suspended sediment discharge determinations in the River Amazon. Hydrological Sciences Journal 49:143–153. doi: 10.1623/hysj.49.1.143.53990

Franks, J.S., D.R. Johnson, D.S. Ko, G. Sanchez–Rubio, J.R. Hendon, and M. Lay. 2011. Unprecedented influx of pelagic *Sargassum* along Caribbean island coastlines during summer 2011. Proceedings of the Gulf and Caribbean Fisheries Institute 64:6–8.

Franks, J.S., D.R. Johnson, and D.S. Ko. 2016. Mass strandings of pelagic *Sargassum* along Caribbean and West Africa Coastlines: Understanding and prediction. Proceedings of the Gulf and Caribbean Fisheries Institute 68:402–408.

Gower, J. and S. King. 2008. Satellite images show the movement of floating *Sargassum* in the Gulf of Mexico and Atlantic Ocean. Nature Proceedings. http//precedings.nature.com/documents/1894/version11 (accessed 11/8/2016).

Gower, J., Young E., and S. King. 2013. Satellite images suggest a new *Sargassum* source region in 2011. Remote Sensing Letters 4:764–773. doi: 10.1080/2150704X.2013.796433

Hallett, J. 2011. The importance of the Sargasso Sea and the offshore waters of the Bermudian Exclusive Economic Zone to Bermuda and its people. Sargasso Sea Alliance Science Report Series No. 4, Hamilton, Bermuda, 18 p.

Hoffmayer, E.R., J.S. Franks, B.H. Comyns, J.R. Hendon, and R.S. Waller. 2005. Larval and juvenile fishes associated with pelagic *Sargassum* in the northcentral Gulf of Mexico. Proceedings of the Gulf and Caribbean Fisheries Institute 58:259–269.

Hu, C., L. Feng, R.F. Hardy, and E.J. Hochberg. 2015. Spectral and spatial requirements of remote measurements of pelagic *Sargassum* macroalgae. Remote Sensing of Environment 167:229–246. doi: 10.1016/j.rse.2015.05.022

Hu, C., B. Murch, B.B. Barnes, M. Wang, J–P Maréchal, J. Franks, D. Johnson, B. Lapointe, D.S. Goodwin, J.M. Schell, and A.N.S. Suida. 2016. *Sargassum* watch warns of incoming seaweed. Eos 97: In press doi:10.1029/2016EO058355

Huffard, C.L, S. von Thun, A.D. Sherman, K. Sealey, and K.L. Smith Jr. 2014. Pelagic *Sargassum* community change over a 40–year period: Temporal and spatial variability. Marine Biology 161:2735–2751. doi: 10.1007/s00227–014–2539–y

Johns, W.E., T.L. Townsend, D.M. Fratantoni, and W.D. Wilson. 2002. On the Atlantic inflow into the Caribbean Sea. Deep–Sea Research 49:211–243. doi: 10.1016/S0967–637(01)00041–3

Johns, E.M., B.A. Muhling, R.C. Perez, F.E. Muler–Karger, N. Melo, R.H. Smith, J.T. Lamkin, T.L. Gerard, and E. Malca. 2014. Amazon River water in the northeastern Caribbean Sea and its effect on larval reef fish assemblages during April 2009. Fisheries Oceanography 23:472–494. doi:10.1111/fog.12082

Lapointe, B.E. 1995. A comparison of nutrient–limited productivity in *Sargassum natans* from neritic vs. oceanic waters of the western North Atlantic Ocean. Limnology and Oceanography 40:625–633.

Lapointe, B.E., L.E. West, T.T. Sutton, and C. Hu. 2014. Ryther revisited: nutrient excretions by fishes enhance productivity of pelagic *Sargassum* in the western North Atlantic Ocean. Journal of Experimental Marine Biology and Ecology 458:46–56. doi:10.1016/j/jembe.2014.05.002

Lumpkin, R. and M. Pazos. 2007. Measuring surface currents with Surface Velocity Program drifters: the instrument, its data, and some recent results. In: A. Griffa, A.D. Kirwan, A. Mariano, T. Ozgokmen, and T. Rossby, eds. Lagrangian Analysis and Prediction of Coastal and Ocean Dynamics. Cambridge University Press, New York, NY, USA, p. 39–57. doi: 10.1017/CBO9780511535901.003

Marmorino, G.O., W.D. Miller, G.B. Smith, and J.H. Bowles. 2011. Airborne imagery of a disintegrating *Sargassum* drift line. Deep–Sea Research 58:316–321. doi:10.1016/j.dsr.2011.01.001

Oyesiku, O.O. and A. Egunyomi. 2014. Identification and chemical studies of pelagic masses of *Sargassum natans* (Linnaeus) Gaillon and *S. fluitans* (Borgessen) Borgesen (brown algae) found offshore in Ondo State, Nigeria. African Journal of Biotechnology 13:1188–1193. doi: 10.5897/AJB2013.12335

Philander, S.G. 2001. Atlantic Ocean equatorial currents. In: J.H. Steele, S.A. Thorpe, and K.K. Turekian, eds. Encyclopedia of Ocean Sciences. Academic Press, Cambridge, MA, USA, p. 188–191.

Schell, J.M., D.S. Goodwind, and A.N.S. Siuda. 2015. Recent *Sargassum* inundation events in the Caribbean: Shipboard observations reveal dominance of a previously rare form. Oceanography 28:8–10. doi: 10.5670/oceanog.2015.70

Smetacek, V. and A. Zingone. 2013. Green and golden seaweed tides on the rise. Nature 504:84–88. doi: 10.1038/nature1286

Taylor, W.R. 1960. Marine Algae of the Eastern Tropical and Subtropical Coasts of the Americas. The University of Michigan Press, Ann Arbor, MI, USA. 870 p. doi:10.1073/pnas.1207514109

Webster R.K. and T. Linton 2013. Development and implementation of *Sargassum* early advisory system (SEAS). Shore and Beach 81:1–6.

Wells, R.J.D. and J.R. Rooker. 2004. Spatial and temporal habitat use by fishes associated with *Sargassum* mats in the NW Gulf of Mexico. Bulletin of Marine Science 74:81–99.